
Theses and Dissertations

Summer 2011

Metabolism, enzymology, and genetic characterization of caffeine degradation by pseudomonas putida CBB5

Ryan Michael Summers
University of Iowa

Follow this and additional works at: <https://ir.uiowa.edu/etd>

 Part of the [Chemical Engineering Commons](#)


Copyright 2011 Ryan M. Summers

This dissertation is available at Iowa Research Online: <https://ir.uiowa.edu/etd/3389>

Recommended Citation

Summers, Ryan Michael. "Metabolism, enzymology, and genetic characterization of caffeine degradation by pseudomonas putida CBB5." PhD (Doctor of Philosophy) thesis, University of Iowa, 2011.
<https://doi.org/10.17077/etd.qto8ggr4>

Follow this and additional works at: <https://ir.uiowa.edu/etd>

 Part of the [Chemical Engineering Commons](#)

METABOLISM, ENZYMOLOGY, AND GENETIC CHARACTERIZATION OF
CAFFEINE DEGRADATION BY *PSEUDOMONAS PUTIDA* CBB5

by
Ryan Michael Summers

An Abstract

Of a thesis submitted in partial fulfillment
of the requirements for the Doctor of
Philosophy degree in Chemical and Biochemical Engineering
in the Graduate College of
The University of Iowa

July 2011

Thesis Supervisor: Professor Mani Subramanian

ABSTRACT

A novel caffeine-degrading bacterium, *Pseudomonas putida* CBB5, was isolated from the soil by an enrichment procedure using caffeine as the sole source of carbon and nitrogen. CBB5 grew not only on caffeine, theobromine, paraxanthine, and 7-methylxanthine as sole carbon and nitrogen sources, but also on theophylline and 3-methylxanthine. Analyses of metabolites in spent media, resting cell suspensions, and crude cell extracts confirmed that CBB5 degraded caffeine *via* *N*-demethylation to theobromine (major metabolite) and paraxanthine (minor metabolite). These dimethylxanthines were further *N*-demethylated to xanthine *via* 7-methylxanthine. A previously unreported pathway for *N*-demethylation of theophylline to 1- and 3-methylxanthines, followed by further *N*-demethylation to xanthine, was also discovered in CBB5.

A 240 kDa, Fe²⁺-dependent *N*-demethylase (Ndm) was purified from CBB5 by traditional chromatographic techniques. Ndm was composed of NdmA (40 kDa) and NdmB (35 kDa), which could not be resolved further. Ndm was active only in the presence of a partially purified protein which exhibited cytochrome *c* reductase activity (Ccr). Ccr transferred reducing equivalents from NAD(P)H to Ndm, which catalyzed an oxygen-dependent *N*-demethylation of methylxanthines to xanthine, formaldehyde and water. Ndm displayed *N*-demethylation activity toward all substrates in the caffeine and theophylline metabolic pathways. Ndm was deduced to be a Rieske [2Fe-2S]-domain-containing non-heme iron oxygenase based on its distinct absorption spectrum and significant identity of NdmA and NdmB sequences to those of other Rieske non-heme iron proteins.

The *ndmA* and *ndmB* gene sequences were determined and cloned individually into the pET32a expression vector as C-terminal His-tagged proteins. Both NdmA-His and NdmB-His proteins were purified using a Ni-NTA column. NdmA-His, in

conjunction with Ccr, was capable of *N*-demethylating caffeine, theophylline, paraxanthine, and 1-methylxanthine to theobromine, 3-methylxanthine, 7-methylxanthine, and xanthine, respectively, suggesting that NdmA-His is a specific *N*-1-demethylase. Similarly, NdmB-His was determined to be a specific *N*-3-demethylase, as it was capable of *N*-demethylating caffeine, theophylline, theobromine, and 3-methylxanthine to paraxanthine, 1-methylxanthine, 7-methylxanthine, and xanthine, respectively. *N*-demethylation activity of 7-methylxanthine to xanthine (putative NdmC) co-eluted with the partially purified Ccr fraction. This report describes the first purification and cloning of multiple, highly positional-specific, Rieske, non-heme iron *N*-demethylase enzymes for bacterial metabolism of purine alkaloids.

Abstract Approved: _____
Thesis Supervisor

Title and Department

Date

METABOLISM, ENZYMOLOGY, AND GENETIC CHARACTERIZATION OF
CAFFEINE DEGRADATION BY *PSEUDOMONAS PUTIDA* CBB5

by
Ryan Michael Summers

A thesis submitted in partial fulfillment
of the requirements for the Doctor of
Philosophy degree in Chemical and Biochemical Engineering
in the Graduate College of
The University of Iowa

July 2011

Thesis Supervisor: Professor Mani Subramanian

Graduate College
The University of Iowa
Iowa City, Iowa

CERTIFICATE OF APPROVAL

PH.D. THESIS

This is to certify that the Ph.D. thesis of

Ryan Michael Summers

has been approved by the Examining Committee
for the thesis requirement for the Doctor of Philosophy
degree in Chemical and Biochemical Engineering at the July 2011 graduation.

Thesis Committee: _____
Mani Subramanian, Thesis Supervisor

David Murhammer

Tonya Peeples

Tim Mattes

David Weiss

To my girls, Emmie, Jane, and most especially Rachel, for their support throughout this entire process and for the joy they bring to my life.

ACKNOWLEDGMENTS

Obviously, a work of this magnitude requires assistance from many people. I am deeply grateful to all of those listed here and to anybody that I might have forgotten. First and foremost, I would like to thank my thesis advisor, Dr. Mani Subramanian, for accepting me into his lab. His industry-style approach and constant lab meetings helped me to focus, stay on track, and not get distracted as I worked on this research. I always wanted to have some good news whenever he asked the question, “Anything interesting?” His knowledge of microbiology, biochemistry, and molecular biology was a vast resource from which I was able to draw ideas countless times over the last four years- from his suggestion to add iron to the *N*-demethylase activity assay to his plan to clone the *ndmA* and *ndmB* genes separately, and everything in between.

There are many talented people in our research group who contributed greatly to this project. Dr. Chi Li Yu isolated CBB5 from the soil and performed many of the studies to determine its metabolism of caffeine and theophylline. She was also my mentor on enzyme purification, teaching me how to equilibrate columns, load and elute proteins, assay for activity, and many other procedures. Dr. Michael Louie both performed research and served as my mentor for all of the molecular biology work performed here. He constructed the gDNA libraries, suggested and performed many of the techniques used to sequence and clone the *ndmA* and *ndmB* genes, and answered more questions in four years than anybody should have to answer. I’ve received a lot of credit for the research described herein, but these two people have also put a lot of work and brainpower into the project.

Katelynn Louie also helped with the molecular biology work and continuously kept me supplied with HPLC vials, filters, and inserts in order to get all of the kinetic assays done. Bhavita Bhatt has continued to keep the supplies in stock. Dr. Shuvendu Das has served as a resource for questions regarding HPLC and LCMS. Fellow graduate

students Jimmy Glenn and Yogesh Kale, who paved the way before me and gave me an example to emulate, and Sujit Mohanty, who has been here for the past three years, have all been good friends and helped keep me sane while in the lab. All members of the Subramanian lab have contributed key ideas and suggestions throughout the course of this project, and I'm sure they will continue to do so.

I would also like to thank the staff at the Center for Biocatalysis and Bioprocessing for letting me use the equipment there at times. Dr. Sridhar Gopishetty has a vast knowledge of caffeine-metabolizing bacteria and was a great resource of ideas. Kevin Erpelding helped in setting up FPLC columns and showing me how to run the Unicorn software. Wensheng Liu has managed to help me stay positive throughout my time here. Secretaries Kay Spidle at the CBB and Linda Wheatley and Natalie Potter in the CBE office were willing to answer a question, help with submitting an order, complete necessary paperwork, and much more, and always with a smile.

I am thankful to my thesis committee members, Dr. Tim Mattes, Dr. David Murhammer, Dr. Tonya Peoples, and Dr. David Weiss, for listening to my presentations, reading my research proposal, editing this document, and offering key suggestions during committee meetings.

Finally, I would like to express my appreciation to my family for their support. My mother and father instilled in me a love of learning and taught me to always do my best work. My mother- and father-in-law entrusted me with their baby. My girls, Jane and Emmie, are willing to lend their father to the lab every day and always greet my arrival home with a smile. My wonderful wife, Rachel, let me drag her out here to Iowa just after we were married and has never once complained. She has been my support for the last four years and I am looking forward to spending the rest of eternity with her. Thank you to all who have helped me get to this point. It has certainly been worth the effort.

TABLE OF CONTENTS

LIST OF TABLES	ix
LIST OF FIGURES	xi
CHAPTER 1 INTRODUCTION	1
Purine Alkaloids	1
Natural Distribution of Purine Alkaloids.....	2
Biosynthesis of Purine Alkaloid	3
Uses and Applications of Methylxanthines	6
Foods and Beverages.....	6
Health and Beauty	6
Catabolism of Methylxanthines in Plants.....	9
Mammalian Metabolism of Methylxanthines.....	10
Microbial Metabolism of Methylxanthines	12
Bacterial C-8 Oxidation of Methylxanthines	12
Bacterial <i>N</i> -demethylation of Methylxanthines.....	15
Biotechnological Applications of Microbial Methylxanthine Degradation.....	18
Pharmaceutical Production.....	18
Bioremediation and Treatment of Wastes	19
Decaffeination of Coffee and Tea	20
Biosensor Development.....	21
Synthetic Biology.....	22
Previous Research.....	23
Objectives	24
CHAPTER 2 MATERIALS AND METHODS	26
Chemicals	26
Culture Conditions.....	27
Culture of CBB5.....	27
Culture of <i>E. coli</i> Cells.....	27
Whole-Cell Degradation Assays.....	28
Growth Media Studies	28
Resting Cell Assays.....	28
Harvesting of Cells for Enzyme Purification.....	29
Cell Extract Preparation.....	29
Enzyme Purification	29
Partial Purification of Xanthine-Oxidizing Enzymes.....	30
Purification of <i>N</i> -Demethylase Enzymes	30
Electrophoresis	31
Protein Gel Electrophoresis.....	31
Protein Blotting	32
Agarose Gel Electrophoresis	32
Acrylamide Gel Electrophoresis of DNA.....	33
Quantification of DNA concentration	33
Enzyme Activity Assays.....	33
Xanthine-Oxidizing Assay	33
CCR Activity Assay	34

<i>N</i> -demethylation Assay	34
Characterization of <i>Ndm</i>	35
Molecular mass estimation.....	35
Determination of pH and Temperature Optima.....	36
Determination of Kinetic Parameters	36
Determination of Oxygen Requirement	37
Formaldehyde Determination	38
Analytical Procedures	38
Molecular Biology Kits	40
Gel Purification	40
PCR Cleanup	40
Plasmid extraction	40
TA cloning.....	41
Electroporation	41
PCR.....	42
Colony/Culture PCR.....	43
Location of <i>ndmA</i> and <i>ndmB</i> Relative to Each Other.....	46
Sequencing of <i>ndmA</i> and its Flanking Regions.....	46
Sequencing of <i>ndmB</i> and its Flanking Regions.....	47
Cloning	50
Cloning of <i>ndmA</i>	50
Cloning of <i>ndmA-His</i>	51
Cloning of <i>ndmB</i>	52
Cloning of <i>ndmB-His</i>	53
Functional Expression	54
Purification of His-Tagged Proteins	55

CHAPTER 3 METABOLISM OF CAFFEINE, THEOPHYLLINE, AND RELATED METHYLXANTHINES BY <i>PSEUDOMONAS PUTIDA</i> CBB5	56
Introduction.....	56
Growth and Degradation of Caffeine and Theophylline by CBB5	57
Identification of Metabolites Produced from Caffeine Degradation	59
Catabolism of Caffeine and Related Methylxanthines by Caffeine- Grown CBB5 Resting Cells.....	61
Catabolism of Theophylline and 3-Methylxanthine by Caffeine-Grown CBB5	63
Metabolism of Theophylline by Theophylline-Grown CBB5.....	64
Growth and Metabolism of 3-Methylxanthine by CBB5	68
Co-expression of Theophylline and Caffeine Metabolism in CBB5.....	68
Origin of 1,3-Dimethyluric Acid and 1- and 3-Methyluric Acids from Theophylline	71
Discussion.....	74
Caffeine and Theophylline are Metabolized <i>via N</i> -Demethylation by <i>Pseudomonas putida</i> CBB5.....	74
Broad-Substrate-Range Xanthine Dehydrogenases Oxidize Theophylline and its Metabolites to Methyluric Acids	77
Multiple <i>N</i> -Demethylases Might be Involved in Metabolism of Caffeine and Theophylline by CBB5	78
Both Caffeine and Theophylline Metabolic Pathways are Co- Expressed in CBB5.....	80
Summary.....	81

CHAPTER 4	PURIFICATION AND CHARACTERIZATION OF A BROAD-SPECIFICITY METHYLXANTHINE <i>N</i> -DEMETHYLASE.....	83
	Introduction.....	83
	<i>N</i> -Demethylase Activity of CBB5 in Cell Extracts.....	85
	Purification of Ndm.....	86
	Biochemical Characterization of Ndm.....	89
	Optimal pH and Temperature of the <i>N</i> -demethylation reaction.....	94
	Oxygen Requirement and Stoichiometric Analysis of Ndm Reaction.....	95
	Substrate Specificity of Ndm.....	97
	Reductase Requirement of Ndm.....	99
	Discussion.....	100
	Ndm is a Broad-Specificity Methylxanthine <i>N</i> -Demethylase.....	100
	Ndm Appears to be a Rieske [2Fe-2S] Non-Heme Iron Oxygenase.....	101
	Ndm Receives Electrons from a Specific Reductase.....	103
	The Number of <i>N</i> -demethylases in <i>P. putida</i> CBB5 is Still Unknown.....	104
	Summary.....	106
CHAPTER 5	CLONING, HETEROLOGOUS EXPRESSION, AND ACTIVITY OF NDMA AND NDMB.....	108
	Introduction.....	108
	Previous Work.....	110
	Determination of 5'-Sequences of <i>ndmA</i> and <i>ndmB</i>	110
	Further Sequencing of <i>ndmA</i> and <i>ndmB</i>	114
	Isolation of the Complete <i>ndmA</i> Gene.....	118
	Isolation of the Complete <i>ndmB</i> Gene.....	120
	Sequencing of the Regions Flanking <i>ndmA</i> and <i>ndmB</i>	122
	Cloning of <i>ndmA</i> into the pET32a Expression Vector.....	129
	Cloning of <i>ndmA</i>	129
	Mutagenesis of <i>ndmA</i> to Produce <i>ndmA-His</i>	130
	Cloning of <i>ndmB</i> into the pET32a Expression Vector.....	130
	Cloning of <i>ndmB</i>	131
	Cloning of <i>ndmB-His</i>	132
	Functional Expression and of NdmA and NdmB.....	133
	Expression of NdmA.....	133
	Expression and Purification of NdmA-His.....	134
	Expression of NdmB.....	136
	Expression and Purification of NdmB-His.....	137
	Activity Assay of NdmA-His and NdmB-His.....	138
	Percent Identity of NdmA and NdmB to Other Enzymes.....	141
	Discussion.....	143
	Summary.....	146
CHAPTER 6	SUMMARY OF COMPLETED RESEARCH AND SUGGESTIONS FOR FUTURE WORK.....	147
APPENDIX A	PRIMERS USED IN THIS STUDY.....	152
APPENDIX B	DNA AND PROTEIN SEQUENCES.....	155
	DNA sequence.....	155
	Peptide Sequences.....	160

APPENDIX C SEQUENCES USED TO CREATE THE RADIAL PHYLOGRAM	164
APPENDIX D PUBLICATIONS AND PRESENTATIONS	168
Publications.....	168
Presentations	168
REFERENCES	171

LIST OF TABLES

Table 1.1. Distribution of purine alkaloids in plants.	3
Table 1.2. Concentration of caffeine in various common beverages and drugs.	7
Table 1.3. Comparison of different caffeine and xanthine oxidizing enzymes.	14
Table 2.1. Temperatures and times of each step and the number of cycles performed in the different PCR reactions used in this study.	42
Table 2.2. A comprehensive list of all PCR reactions, and the templates, primers, and time programs used in each reaction, excluding colony/culture screening.	44
Table 3.1. Growth of CBB5 on caffeine, with or without nitrogen supplementation.	58
Table 3.2. UV absorption spectra and ESI mass spectral properties of metabolites formed from degradation of caffeine, theophylline, and 3-methylxanthine by <i>P. putida</i> CBB5.	60
Table 4.1. Purification of methylxanthine <i>N</i> -demethylase from <i>Pseudomonas</i> <i>putida</i> CBB5.	87
Table 4.2. Iron is required for <i>N</i> -demethylation of paraxanthine by Ndm.	93
Table 4.3. Substrate preference of Ndm towards methylxanthines, relative to paraxanthine.	99
Table 5.1. PCR set-up to determine if <i>ndmA</i> and <i>ndmB</i> were near each other on the genome using degenerate primers derived from the N-terminal amino acid sequences of NdmA and NdmB.	111
Table 5.2. PCR set-up to amplify approximately 250 bp of <i>ndmA</i> and <i>ndmB</i> using degenerate primers derived from the N-terminal amino acid sequences of NdmA and NdmB.	112
Table 5.3. PCR set-up to amplify <i>ndmA</i> and <i>ndmB</i> using the cdm-R1 reverse primer.	115
Table 5.4. PCR set-up to amplify <i>ndmB</i> using the cdm-R2 and cdm-R3 reverse primers.	116
Table 5.5 Primers and templates used to amplify the <i>ndmA</i> DNA from gDNA libraries using a nested PCR approach.	119
Table 5.6. Primers and templates used in the site directed mutagenesis and nested PCR approaches used to isolate <i>ndmB</i>	121
Table 5.7. Primers and templates used to amplify the region 5' to <i>ndmA</i> for sequencing.	123

Table 5.8. Primers and templates used during the nested PCR approach to sequence the regions both 5' and 3' to <i>ndmB</i> .	125
Table 5.9. Genes containing the highest identity to ORFs 1-10 as determined by BLASTP search.	128
Table 5.10. OD600 of <i>E. coli</i> BL21(DE3) containing either pET32a/ <i>ndmA</i> or pET32a empty plasmid induced at 30 °C for 4.5 h.	133
Table 5.11. OD600 of <i>E. coli</i> BL23(DE3) containing pET32a/ <i>ndmA-His</i> induced at 30 or 23 °C with IPTG concentrations from 0.1-0.4 mM.	134
Table 5.12. Growth and induction of BL21(DE3) cells containing pET32a/ <i>ndmB</i> .	136
Table 5.13. Growth and induction of BL21(DE3) cells containing pET32a/ <i>ndmB-His</i> .	137
Table 5.14. Substrate specificity of NdmA-His plus Ccr.	139
Table 5.15. Substrate specificity of NdmB-His plus Ccr.	140
Table 5.16. Percent Identity of NdmA, NdmB, Cdm, and <i>mma_0224</i> peptide sequences.	141
Table A1. A complete list of primers used in this study and their sequences.	152
Table C1. Names and accession numbers of the genes used to create the radial phylogram in Figure 5.18.	164

LIST OF FIGURES

Figure 1.1. Caffeine, theophylline, theobromine, and paraxanthine are naturally occurring purine alkaloids comprised of a xanthine ring with methyl groups substituted at the 1, 3, and/or 7-positions.	1
Figure 1.2. Theacrine, methylxanthine, and liberine are naturally occurring methyluric acids derived from catabolism of caffeine in certain species of coffee.	2
Figure 1.3. Structure of AMP, GMP, IMP, and XMP, the four precursors for purine alkaloid biosynthesis. AMP: R ₁ = H, R ₂ = NH ₂ ; GMP: R ₁ = NH ₂ , R ₂ = O; IMP: R ₁ = H, R ₂ = O; XMP: R ₁ = R ₂ = O.	4
Figure 1.4. Biosynthesis of caffeine in plants. Solid lines indicate the major biosynthetic route, while dashed lines represent alternative steps.....	5
Figure 1.5. Pentoxifylline, enprofylline, and doxofylline are three synthetic xanthine derivatives used in pharmaceutical treatments.....	8
Figure 1.6. Catabolism of caffeine in coffee and tea plants. Solid lines indicate the major degradative route, while dashed lines represent alternative degradation steps.	9
Figure 1.7. Catabolism of caffeine and related methylxanthines in humans. Bold arrows represent the major metabolic pathway. Other solid arrows show minor <i>N</i> -demethylation steps, and dashed arrows indicate C-8 oxidation of methylxanthines.	11
Figure 1.8. C-8 oxidation of caffeine to 1,3,7-trimethyluric acid. Bacterial C-8 oxidation has also been observed with theophylline, theobromine, paraxanthine, 1-methylxanthine, 3-methylxanthine, 7-methylxanthine, and xanthine to form 1,3-, 3,7-, and 1,7-dimethyluric acids, 1-, 3-, and 7-methyluric acids, and uric acid, respectively.....	13
Figure 1.9. Bacterial <i>N</i> -demethylation of caffeine to paraxanthine and theobromine. These two metabolites are sequentially <i>N</i> -demethylated to 7-methylxanthine and xanthine. The xanthine is then oxidized at the C-8 position to form uric acid.....	15
Figure 1.10. Hypothetical process to produce pentoxifylline from caffeine. Here, an <i>N</i> -1 demethylase could be used to convert caffeine to theobromine. The 5-oxohexyl group could then be selectively added to the <i>N</i> -1 atom of theobromine to form pentoxifylline.....	18
Figure 3.1. Growth curves of <i>P. putida</i> CBB5 in soytone-free (closed symbol) and soytone supplemented (open symbol) M9 media with caffeine (◆, ◇) or theophylline (■, □) as carbon and nitrogen sources. Concentration of caffeine in soytone-free and soytone supplemented media was 2.5 g·L ⁻¹ . Concentration of theophylline in soytone-free media was 1 g·L ⁻¹ ; 2.5 g·L ⁻¹ was used in soytone supplemented media.	57

- Figure 3.2. HPLC of spent medium of *P. putida* CBB5 grown in soytone-supplemented M9-caffeine medium. A sample was collected 20 h post-inoculation. The identities of the metabolites are as follows: metabolite I, paraxanthine; metabolite II, theobromine; metabolite III, 7-methylxanthine; metabolite IV, xanthine; and metabolite V, uric acid. Physical characteristics of these metabolites are shown in Table 3.2.....59
- Figure 3.3. HPLC analyses of metabolites produced by *P. putida* CBB5 resting cell suspensions. CBB5 was cultivated in soytone-supplemented M9-medium. The cells were washed and resuspended at an OD₆₀₀ of 4.0. The following compounds (1 mM) were then added to cell suspensions: (A) caffeine, (B) theobromine, (C) 7-methylxanthine, (D) paraxanthine, (E) theophylline, and (F) 3-methylxanthine; metabolite IV, xanthine; metabolite V, uric acid; metabolite VI, 1,3-dimethyluric acid; metabolite VII, 1-methyluric acid; and metabolite VIII, 3-methyluric acid. Physical characteristics of these metabolites are shown in Table 3.2.62
- Figure 3.4. Determination of theophylline metabolites. (A) HPLC analyses of metabolites produced from theophylline by a resting cell suspension of *P. putida* CBB5 grown in soytone-free M9-theophylline medium. The identities of metabolites are shown in Table 3.2. (B) Degradation of theophylline and various metabolites by a resting cell suspension of *P. putida* CBB5 grown in soytone-free M9-theophylline medium. Symbols: ◆, theophylline; ○, 1-methylxanthine; ▲, 3-methylxanthine; ×, xanthine; *, 1,3-dimethyluric acid; ▲, 1-methyluric acid; □, 3-methyluric acid; and ◇, uric acid.....66
- Figure 3.5. Production of 1-methylxanthine (◆) and 3-methylxanthine (×) from theophylline by cell extracts prepared from *P. putida* CBB5 grown in soytone-supplemented M9-theophylline medium. At 5 h, 0.15 mM NADH was added to the enzyme reaction mixture (indicated by the arrow), resulting in increased production of 1- and 3-methylxanthine.67
- Figure 3.6. Relative degradation rates of caffeine and other methylxanthines (y-axis) by CBB5 resting cells prepared from cultures that were grown in soytone supplemented M9 medium containing 2.5 g·L⁻¹ caffeine, 2.5 g·L⁻¹ theophylline, 1.0 g·L⁻¹ 3-methylxanthine, or without caffeine and any methylxanthines (x-axis). Bars represent degradation of 1 mM of the following substrates in resting cell: (■) caffeine, (■) theobromine, (≡) 7-methylxanthine, (■) paraxanthine, (□) theophylline, and (▨) 3-methylxanthine. Degradation rates of these substrates by resting cells prepared from caffeine grown CBB5 culture were designated as 100%. Resting cells prepared from CBB5 grown on theobromine, paraxanthine, and 7-methylxanthine degraded the test substrates at rates similar to resting cells prepared from CBB5 grown on caffeine.....69
- Figure 3.7. Native PAGE gels of crude extracts (lane 1) and partially purified xanthine dehydrogenase (lane 2) prepared from *P. putida* CBB5 cells grown on soytone supplemented M9-theophylline medium were stained by a substrate-dependent nitro blue tetrazolium reduction activity. Substrates used in this staining were (A) xanthine and (B) theophylline. Bio-Rad precision plus protein standards (Kaleidoscope, lane M) were used to monitor progress of electrophoresis. No stained bands were observed in either lane when caffeine, theobromine, and 3-methylxanthine were used as substrates.72

- Figure 3.8. Elution profile of CE separated on Phenyl Sepharose. Blue line, A_{280} (mAU, left axis); Brown line, conductivity (mS/cm, right axis). Elution of fractions A, B, and C are indicated by the green, blue, and red arrows, respectively.73
- Figure 3.9. Proposed pathway for degradation of (A) caffeine and (B) theophylline by *P. putida* CBB5. The dashed arrows indicate oxidation of theophylline and 1- and 3-methylxanthine to their respective methyluric acids, which were not metabolized further.75
- Figure 4.1. Degradation of paraxanthine (■), theobromine (□), caffeine (○), and theophylline (●) by cell extracts prepared from *P. putida* CBB5 grown in soytone-supplemented M9-caffeine medium. All reactions contained 0.5 mM substrate, 0.5 mM NADH, and 7.2 mg·mL⁻¹ protein. This experiment was repeated three times and similar patterns were observed in all replicates.86
- Figure 4.2. Elution profile of CE separated on DEAE Sepharose. Blue line, A_{280} (mAU, left axis); Brown line, conductivity (mS/cm, right axis). Elution of Ccr and Ndm is indicated by the black arrow.87
- Figure 4.3. Elution profile of DEAE Sepharose-purified Ccr and Ndm separated on Phenyl Sepharose. Blue line, A_{280} (mAU, left axis); Brown line, conductivity (mS/cm, right axis). Elution of Ccr is indicated by the grey arrow, while elution of Ndm is indicated by the black arrow.88
- Figure 4.4. Elution profile of Phenyl Sepharose-separated Ndm on Q Sepharose. Blue line, A_{280} (mAU, left axis); Brown line, conductivity (mS/cm, right axis). Elution of Ndm is indicated by the black arrow.89
- Figure 4.5. SDS-PAGE analysis of *P. putida* CBB5 N-demethylase, Ndm, during the purification process. Molecular masses of markers (in kDa) are shown on the left and right (lanes M). Ndm is composed of two subunits with apparent molecular masses of 40 kDa (NdmA) and 35 kDa (NdmB). Lane 1, cell extracts of CBB5 grown on soytone alone; lane 2, cell extracts of CBB5 grown on soytone plus caffeine; lane 3, DEAE Sepharose eluant; lane 4, Phenyl Sepharose eluant; lane 5, Q Sepharose eluant.90
- Figure 4.6. Elution profile of purified Ndm on Sephacryl. Blue line, A_{280} (mAU, left axis). Ndm eluted as a single, symmetrical peak with a calculated native molecular weight of 240 kDa, indicating that it is a hexameric enzyme.91
- Figure 4.7. NdmA and NdmB are similar to other predicted Rieske, non-heme iron proteins. (a) Multiple sequence alignment of the N-terminal protein sequences of NdmA and NdmB with the first 25 amino acid residues of caffeine demethylase (Cdm) of *P. putida* IF-3 and the hypothetical protein mma_0224 in *Janthinobacterium* sp. Marseille. (b) Consensus sequences of the Rieske [2Fe-2S] domain (CXHX16CX2H, highlighted in black) and the mononuclear ferrous iron domain [(D/E)X3DX2HX4H, highlighted in grey] are identified in Cdm and mma_0224.92
- Figure 4.8. UV/visible spectrum of purified Ndm (1.7 mg·mL⁻¹) eluted from Q Sepharose. Ndm exhibited three peaks of maximum absorbance, at 318, 440, and 438 nm, characteristic of proteins with Rieske-type [2Fe-2S] clusters.93

Figure 4.9. Relative activity of <i>N</i> -demethylation of paraxanthine by Ndm at different temperature (A) and pH (B). Values are reported as the percent of activity relative to those at which Ndm was most active, which were 30 °C and a pH of 7.5.....	94
Figure 4.10. Oxygen is required for <i>N</i> -demethylation. (A) Degradation of 400 μM paraxanthine under aerobic (○) and anaerobic (●) conditions. After one hour, the anaerobic enzyme reaction mixture was exposed to ambient air (indicated by arrow), and paraxanthine was rapidly degraded. This experiment was repeated twice and a similar pattern was observed in both replicates. (B) Oxygen consumption by Ndm plus Ccr with (●) or without (○) 100 μM paraxanthine in the reaction mixture. The reactions were carried out in air-saturated buffer and equilibrated at 30 °C for 3.3 min before addition of Ndm plus partially purified Ccr to initial the reactions (indicated by the arrow). The oxygen concentrations reported are means of four replicates with standard deviations (error bars).	96
Figure 4.11. Stoichiometric <i>N</i> -demethylation of paraxanthine (○), via 7-methylxanthine (●) to xanthine (□) by purified Ndm with concomitant production of formaldehyde (■). The concentrations reported are means of triplicates with standard deviations (error bars).	97
Figure 4.12. Rate of <i>N</i> -demethylation of 7-methylxanthine (A) and paraxanthine (B) by Ndm at concentrations of 20 μM to 500 μM substrate for determination of apparent K_M and k_{cat}	98
Figure 4.13. Proposed reaction scheme for paraxanthine <i>N</i> -demethylation by the <i>P. putida</i> CBB5 two-component <i>N</i> -demethylase. Reducing equivalents are transferred from NAD(P)H to the two-subunit <i>N</i> -demethylase component (Ndm) by a specific reductase (Ccr). One mole of paraxanthine (PX) is <i>N</i> -demethylated to xanthine (Xan) through 7-methylxanthine (7MX) as an intermediate (dashed arrow).	104
Figure 5.1. The four potential arrangements for <i>ndmA</i> and <i>ndmB</i> where both are proximal on the genome of CBB5. The <i>ndmA</i> and <i>ndmB</i> genes could be in the same direction as each other with either <i>ndmA</i> 5'-to <i>ndmB</i> (A) or <i>ndmB</i> 5'-to <i>ndmA</i> (B). The genes could also be in opposite directions, with their respective 3' ends (C) or 5' ends (D) nearest each other. Degenerate forward (A-F and B-F) and reverse (A-R and B-R) primers designed from the <i>N</i> -terminal amino acid sequences of NdmA and NdmB are also depicted.....	109
Figure 5.2. Agarose gel electrophoresis of reactions 1A, 1B, 1C, 1D, and their controls to determine the orientation of <i>ndmA</i> and <i>ndmB</i> relative to each other. M, kb marker; AF, A-degF primer only; AR, A-degR primer only; BF, B-degF primer only; BR- B-degR primer only; 1A _T , 1B _T , 1C _T , 1D _T , no template controls of reactions 1A, 1B, 1C, and 1D, respectively.....	112
Figure 5.3. Acrylamide gel electrophoresis of reactions A1, A2, B1, B2, and their controls. M, kb marker; XY _F , forward primer only controls; C _R , reverse primer only control; XY _T , no template controls. A product of approximately 250 bp was amplified in each reaction, but was not observed in the control reactions.	113

Figure 5.4. Screening of JM109 colonies containing the TA-ligated 250 bp PCR product from reactions A1, A2, B1, and B2. Five colonies of each ligation were screened. Inserts of approximately the correct size were found in all lanes.	114
Figure 5.5. PCR of <i>ndmA</i> and <i>ndmB</i> using the <i>cdm-R1</i> reverse primer. (A) An approximately 1-kb <i>ndmA</i> product was amplified in each reaction (A1 ₁ -A1 ₄) and not observed in the control reactions (A1 _F , forward only primer; A1 _R , reverse only primer; A1 _T , no template). (B) Products observed in reaction B1-1 (B1 ₁) were due to non-specific amplification from the B-degF1 primer (B1 _F). No specific <i>ndmB</i> products were amplified with the <i>cdm-R1</i> primer.	116
Figure 5.6. PCR of <i>ndmB</i> using the <i>cdm-R2</i> and <i>cdm-R3</i> reverse primers. (A) About 500 bp <i>ndmB</i> were amplified using <i>cdm-R3</i> reverse primer (B3 ₁ -B3 ₄). No specific products were observed using <i>cdm-R2</i> primer (B2 ₁ -B2 ₄). (B) The 500 bp product in reaction B3-1 (B3 ₁) was not produced in the forward primer only (B3 _F), reverse primer only (B3 _R), and no template (B3 _T) controls.	117
Figure 5.7. Scheme for a nested PCR approach to amplify <i>ndmA</i> from a CBB5 gDNA library. E, restriction enzyme site; V1, pUC19R primer, V2, Marcy primer; A1, A-speF2 primer; A2, A-speF3 primer.	118
Figure 5.8. A 3-kb PCR product containing the 3' end of <i>ndmA</i> was observed in the nested PCR reaction E1-2 (E1 ₂). No other dominant PCR products were amplified using the PCR approach.	120
Figure 5.9. A combination of site-directed mutagenesis and nested PCR approaches was used to sequence the complete <i>ndmB</i> gene. (A) Amplification of DNA containing <i>ndmB</i> resulted in a 1.1-kb product in reaction B2-2 (B2 ₂). (B) The 1.1-kb product was not amplified in the forward primer only (B2 _F), reverse primer only (B2 _R), or no template (B2 _T) controls.	121
Figure 5.10. A 3-kb PCR product was amplified in the nested PCR reaction A5'-2 (A5' ₂) which was not observed in the forward primer only (A5' _F), reverse primer only (A5' _R), or no template (A5' _T) controls.	123
Figure 5.11. Arrangement and orientation of <i>ndmA</i> , <i>ndmB</i> , and the genes surrounding them on the genome of <i>P. putida</i> CBB5.	126
Figure 5.12. The 1.1-kb <i>ndmB</i> gene product amplified with B-degF and B-R-XhoI primers (lane 1) was not produced in the negative controls. M, kb marker; 2, forward primer only control; 3, reverse primer only control; 4, no template control.	131
Figure 5.13. A soluble, 40-kDa NdmA was expressed in BL21(DE3) cells. Lanes 1 and 2, lysate and soluble fraction of empty pET32a vector control; M, molecular weight marker; 3, lysate containing expressed NdmA; 4, soluble fraction containing soluble NdmA; 5, insoluble fraction containing insoluble NdmA.	134

- Figure 5.14. The lysate, soluble, and insoluble fractions of ndmA-His induced at 0.4 mM IPTG, 30 °C (lanes 1-3); 0.2 mM IPTG, 30 °C (lanes 4-6); 0.1 mM IPTG, 23 °C (lanes 7-9A); lane M, MW marker. The induction at 0.1 mM IPTG and 23 °C provided the highest ratio of soluble:insoluble NdmA-His.135
- Figure 5.15. NdmA-His and NdmB-His were purified to about 95-99% purity with a nickel column. Lane M, molecular weight marker; 1, NdmA-His lysate; 2, purified NdmA-His; 3, purified Ndm; 4, purified NdmB-His; 5, NdmB-His lysate. A slight increase in molecular weight was observed for the histidine-tagged subunits (lanes 2 and 4) compared with their native molecular weight (lane 3).135
- Figure 5.16. SDS-PAGE analysis of expressed NdmB. Lane M, molecular weight marker; lanes 1-2, insoluble fraction of 18 °C-induced cells; 3 and 4, soluble fraction and lysate of 18 °C induced cells; 5, purified Ndm.137
- Figure 5.17. SDS-PAGE analysis of expressed NdmB-His induced at 18 °C (lanes 1-4) and 25 °C (lanes 5-8). Lanes 1 and 5, lysate; 2 and 6, soluble fraction; 3, 4, 7, and 8, insoluble fraction.....138
- Figure 5.18. Radial phylogram showing the similarity of NdmA and NdmB to the catalytic subunits of 75 other well-characterized Rieske [2Fe-2S] oxygenases. Phylogenetic analyses were conducted using *MEGA* version 4.0.2 (Tamura *et al.*, 2007). The evolutionary history was inferred using the Neighbor-Joining method with bootstrap values of 5,000. The tree is drawn to scale, and distance correlates to the number of amino acids substituted per site.142

CHAPTER 1 INTRODUCTION

Purine Alkaloids

Methylxanthines and methyluric acids comprise a class of compounds commonly referred to as purine alkaloids. These compounds are secondary metabolites derived from purine nucleotides (Anaya *et al.*, 2006) and have been reported to be present in at least 80 species of plants (Ashihara and Crozier, 1999). Structurally, alkylxanthines are comprised of a xanthine ring with varying R-groups attached, primarily at the 1-, 3-, and 7-positions (Figure 1.1).

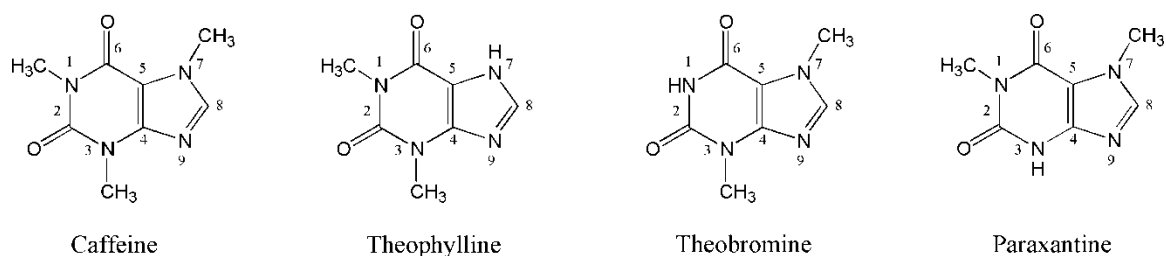


Figure 1.1. Caffeine, theophylline, theobromine, and paraxanthine are naturally occurring purine alkaloids comprised of a xanthine ring with methyl groups substituted at the 1, 3, and/or 7-positions.

The most common among the naturally occurring alkyl purines is caffeine (1,3,7-trimethylxanthine), followed by theobromine (3,7-dimethylxanthine). Other intermediates of caffeine biosynthesis and/or catabolism that can also be found in nature, albeit at low levels, include theophylline (1,3-dimethylxanthine), paraxanthine (1,7-dimethylxanthine), 1-methylxanthine, 3-methylxanthine, 7-methylxanthine, and 7-methylxanthosine (Ashihara and Suzuki., 2004).

Methyluric acids are formed as metabolites of caffeine in plants (Peterman and Baumann, 1983), animals (Grant *et al.*, 1983), and bacteria (Madyastha and Sridhar,

1998; Yamaoka-Yano and Mazzafera, 1999; Yu *et al.*, 2008). In mammals and microorganisms, these compounds are formed from oxidation at the C-8 position of methylxanthines to form mono-, di-, and trimethyluric acids. In certain species of coffee, caffeine is metabolized to the methyluric acids theacrine (1,3,7,9-methyluric acid), methyllyberine (*O*(2),1,7,9-tetramethyluric acid), and liberine (*O*(2),1,9-trimethyluric acid) (Petermann and Baumann, 1983) (Figure 1.2).

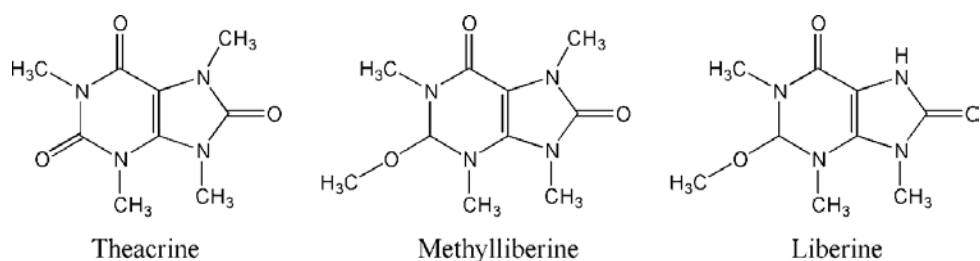


Figure 1.2. Theacrine, methyllyberine, and liberine are naturally occurring methyluric acids derived from catabolism of caffeine in certain species of coffee.

Natural Distribution of Purine Alkaloids

Purine alkaloids are found naturally in many plants from many geographical regions of the world. These plants include coffee (*Coffea* species), tea (*Camellia* species), maté (*Ilex paraguariensis*), cocoa (*Theobroma cacao*), cupuaçu (*Theobroma grandiflorum*), and guaraná (*Paullinia cupana*) (Ashihara and Crozier, 1999). Caffeine is the most abundant purine alkaloid encountered in these plants, although theobromine, theophylline, theacrine, and liberine are also present in certain species (Table 1.1).

Two hypotheses concerning the reason for natural production of purine alkaloids have been postulated. The “chemical defense theory” suggests that caffeine is synthesized at high concentrations in new tissues of plants, such as young leaves, flower buds, and fruits, as protection from insect larvae and other predators (Nathanson, 1984; Hollingsworth *et al.*, 2002). A second hypothesis is the “allelopathic or autotoxic

theory,” which theorizes that caffeine is released into the soil through degradation of seed coats and other plant matter and inhibits the germination of other seeds (Rizvi *et al.*, 1981; Suzuki and Waller, 1987; Waller, 1989).

Table 1.1. Distribution of purine alkaloids in plants.

Latin Name	Family Name	Common Name	Major Alkaloid
<i>Coffea arabica</i>	Rubiaceae	Arabica coffee	Caffeine
<i>Coffea canephora</i>	Rubiaceae	Robusta coffee	Caffeine
<i>Coffea liberica</i>	Rubiaceae		Theacrine, liberine
<i>Coffea dewevrei</i>	Rubiaceae		Theacrine, liberine
<i>Camellia sinensis</i>	Theaceae	Tea	Caffeine
<i>Camellia assamica</i>	Theaceae	Assam tea	Caffeine
<i>Camellia assamica</i> var <i>Kucha</i>	Theaceae	Kucha	Theacrine
<i>Camellia taliensis</i>	Theaceae		Caffeine
<i>Camellia irrawadiensis</i>	Theaceae		Theobromine
<i>Camellia ptilophylla</i>	Theaceae	Cocoa tea	Theobromine
<i>Theobroma cacao</i>	Sterculiaceae	Cacao (cocoa)	Theobromine
<i>Theobroma grandiflorum</i>	Sterculiaceae	Cupu	Liberine
<i>Paulinia cupana</i>	Sapindaceae	Guaraná	Caffeine
<i>Cola</i> sp.	Sterculiaceae	Cola	Caffeine
<i>Citrus</i> sp.	Rutaceae		Caffeine
<i>Ilex paraguariensis</i>	Aquifoliaceae	Yerba mate	Caffeine

Source: Anaya, A. L., Cruz-Ortega, R., & Waller, G. R. (2006). Metabolism and ecology of purine alkaloids. *Frontiers in Bioscience* **11**: 2354-2370.

Biosynthesis of Purine Alkaloid

Purine alkaloids are synthesized from purine nucleotides, which also serve as the precursors for nucleic acids, universal sources of energy, components of major co-enzymes, activated intermediates in a number of biosynthetic pathways, and metabolic regulators (Henderson and Paterson, 1973; Stryer, 1995; Ashihara and Crozier, 1999). Cellular sources of purine nucleotides include *de novo* biosynthesis and purine salvage

(Ashihara and Crozier, 1999). Purine nucleotides are synthesized *de novo* on a ribose phosphate molecule by assimilating parts of several small molecules, including aspartate (the *N*-1 atom), glycine (C-4, C-5, and *N*-7), glutamine (*N*-3 and *N*-9), a single carbon unit from *N*¹⁰-formyltetrahydrofolate (C-2 and C-8), and CO₂ (C-6) (Shemin and Rittenberg, 1947; Buchanan *et al.*, 1948; Anderson and Gibbs, 1962; Proiser and Serenikov, 1963 ; Stryer, 1995). Inosine 5'-monophosphate (IMP, Figure 1.3) is the “true end product” (Henderson and Paterson, 1973) of *de novo* purine nucleotide synthesis, and is the precursor for adenosine, guanosine, and xanthosine 5'-monophosphates (AMP, GMP, and XMP, respectively). These four compounds are the initial compounds used in the biosynthesis of purine alkaloids (Figure 1.3).

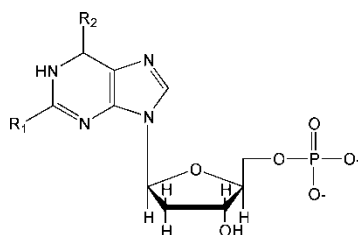


Figure 1.3. Structure of AMP, GMP, IMP, and XMP, the four precursors for purine alkaloid biosynthesis. AMP: R₁ = H, R₂ = NH₂; GMP: R₁ = NH₂, R₂ = O; IMP: R₁ = H, R₂ = O; XMP: R₁ = R₂ = O.

The pathways for purine alkaloid biosynthesis are shown in Figure 1.4. The first committed step in biosynthesis of methylxanthines is conversion of AMP, IMP, XMP, and GMP to xanthosine. Under the major caffeine biosynthetic pathway in both coffee and tea, xanthosine is converted to caffeine through a series of *N*-methylation steps. Each methyl group is donated from S-adenosyl-L-methionine by *N*-methyltransferase enzymes.

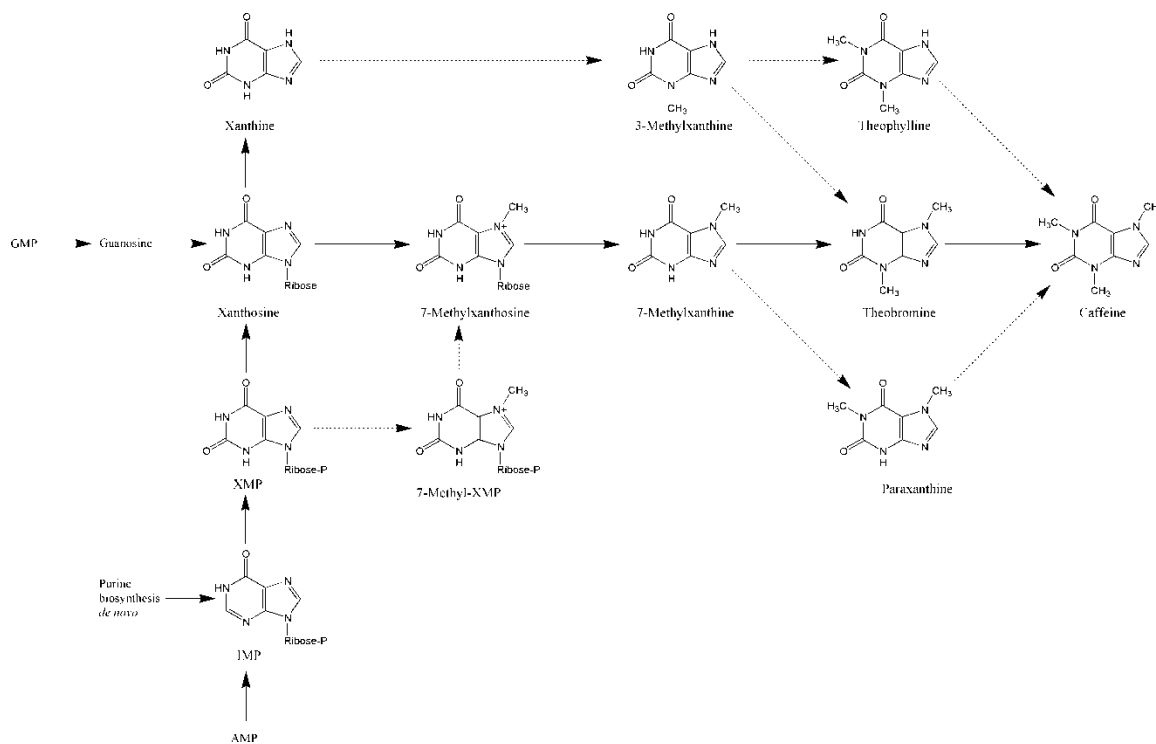


Figure 1.4. Biosynthesis of caffeine in plants. Solid lines indicate the major biosynthetic route, while dashed lines represent alternative steps.

Image adapted from Ashihara and Crozier, 1999.

Xanthosine is converted to 7-methylxanthosine by 7-methylxanthine synthase, a specific *N*-methyltransferase (Negishi *et al.*, 1985; Mizuno *et al.*, 2003). Following hydrolytic cleavage of the purine ring from ribose by methylxanthine nucleosidase (Negishi, *et al.*, 1988), 7-methylxanthine is further *N*-methylated at the *N*-3 position to form theobromine. Caffeine is produced by a final *N*-1 methylation step (Suzuki and Takahashi, 1975; Roberts and Wallert, 1979; Baumann *et al.*, 1983; Fujimori *et al.*, 1991). Some minor routes of caffeine production have also been detected. These routes include the transient formation of 7-methyl-XMP, paraxanthine, xanthine, 3-methylxanthine, and theophylline (Ashihara and Crozier, 1999).

Uses and Applications of Methylxanthines

Foods and Beverages

Caffeine is a major human dietary component and can be found in common food and beverage products such as coffee, tea, soft drinks, and chocolates. Theobromine (chocolates, some teas), theophylline (tea), and the methyluric acids theacrine and liberine (some teas and coffees) are also present in certain foods (Ashihara and Crozier, 1999; Anaya *et al.*, 2006, Dash and Gummadi, 2006). The caffeine content of many popular foods, beverages, and drugs is listed in Table 1.2.

Health and Beauty

Purine alkaloids are often referred to as xanthine derivatives when used as pharmaceuticals. These compounds, both synthetic and natural, act as antagonists at the A₁ and A₂ adenosine receptors to either inhibit or stimulate adenylate cyclase activity, serve as non-selective phosphodiesterase inhibitors, and have been used in pharmaceutical preparations for a variety of effects (Daly *et al.*; 1983; Schwabe *et al.*, 1985; Essayan, 2001; Juliano and Griffiths, 2005).

Caffeine has been described as “the most widely used mood-altering drug in the world” (Juliano and Griffiths, 2005). It is often used as a neurological, cardiac, and respiratory stimulant (Gokulakrishnan *et al.*, 2005; Dash and Gummadi, 2006), as well as an analgesic enhancer in cold, cough, headache, and asthma medicines (Daly, 2007; Stavric 1988b). Theophylline, a potent bronchodilator, is used to treat neonatal apnea, control asthma, and relieve bronchial spasms (Mazzafera, 2002; Stavric, 1988a). Because the physiological reactions of theobromine are not as severe as those of caffeine, theobromine is used primarily as a diuretic, myocardial stimulant, or vasodilator (Stavric 1988c). 7-Methylxanthine has been shown to improve the quality of sclera collagen, and has been suggested for treatment and/or prevention of axial myopia, glaucoma, and

Table 1.2. Concentration of caffeine in various common beverages and drugs.

Source of Caffeine	mg/serving	mg/oz
Coffee		
Decaffeinated (10 oz)	4-15	0.4-1.5
Instant (10 oz)	9-216	0.9-21.6
Plain, brewed (10 oz)	128-250	12.8-25
Espresso (5 oz)	150-450	30-90
Tea		
Tea, brewed (10 oz)	80-120	8-12
Iced Tea (12 oz)	65-75	5.4-6.3
Green (8 oz)	30-50	3.8-6.3
Black (8 oz)	25-110	3.1-13.8
Yerba Mate (8 oz)	65-130	8-16
Chocolate		
Hot cocoa (5 oz)	4	0.8
Chocolate milk (6 oz)	4	0.7
Milk chocolate (1.5 oz)	9	6
Chocolate bar (1.5 oz)	30	20
Soft Drinks		
Coca Cola (12 oz)	35	2.9
Pepsi (12 oz)	40	3.3
Dr. Pepper (12 oz)	40	3.3
Mountain Dew (12 oz)	55	4.6
Energy Drinks		
Monster (16 oz)	160	10
Rockstar (16 oz)	160	10
Red Bull (8.3 oz)	80	9.6
Amp (8.3 oz)	75	8.9
Drugs		
Anacin (2 tablets)	32	N/A
Exedrin (1 tablet)	65	N/A

Source: Table adapted from Barone and Roberts, 1996; Carillo and Benitez, 2000; McCusker *et al.*, 2006; Reissig *et al.*, 2009; Heckman *et al.*, 2010; and Gopishetty *et al.*, 2011.

macular degeneration (Trier, 1999). Uric acid and methyluric acids are used in obesity-treating pharmaceuticals, skin cosmetics, and anti-dandruff preparations (Madyastha and Sridhar, 1999). Theacrine exhibits sedative, analgesic, and anti-inflammatory properties (Wang *et al.*, 2010). Also, 1-methylxanthine, 1-methyluric acid, and uric acid have been investigated for their antioxidant properties (Lee, 2000).

A mixture of $15 \text{ g}\cdot\text{L}^{-1}$ caffeine, $0.07 \text{ g}\cdot\text{L}^{-1}$ paraxanthine, $1.4 \text{ g}\cdot\text{L}^{-1}$ theobromine, and $0.6 \text{ g}\cdot\text{L}^{-1}$ 7-methylxanthine known as SveltamTM is currently being marketed as a natural skincare and slimming agent (Libragen, 2011). This methylxanthine blend inhibits glyceraldehyde-3-phosphate dehydrogenase activity and accumulation of lipids while stimulating production of cAMP, glycerol, and free fatty acids from adipocytes.

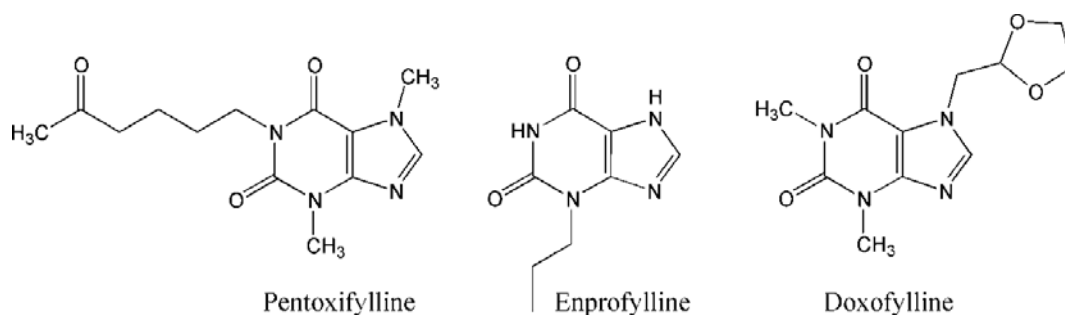


Figure 1.5. Pentoxifylline, enprofylline, and doxofylline are three synthetic xanthine derivatives used in pharmaceutical treatments.

Many synthetic xanthine derivatives, produced by addition of varying R-groups to the xanthine molecule, are also used in pharmaceutical treatments (Figure 1.5).

Doxofylline (7-(1,3-dioxolan-2-ylmethyl)-1,3-dimethylxanthine), sold commercially as AnsimarTM, has been studied as a bronchodilator (Sankar, 2008). Enprofylline (3-propylxanthine) also initiates a bronchodilation response without the stimulation and diuretic effects of theophylline (Lunell *et al.*, 1982). Pentoxifylline (1-(5-oxohexyl)-3,7-dimethylxanthine) has been used to treat peripheral and cerebrovascular disease (Ward

and Clissold, 1987). Other xanthine derivatives have been designed and synthesized as diuretics, as pulmonary and cardiac stimulants (Zavialov *et al.*, 2004), and for the treatment of male erectile dysfunction (Wang *et al.*, 2002). Also, the 8-oxo derivatives of these synthetic xanthine derivatives have shown high antioxidant and anti-inflammatory properties (Bhat and Madyastha, 2001).

Catabolism of Methylxanthines in Plants

Caffeine is degraded in plants primarily through *N*-demethylation (Figure 1.6); however, oxidation to methyluric acids has been observed in a few species (Peterman and Baumann, 1983; Suzuki and Waller, 1984; Ashihara *et al.*, 1996).

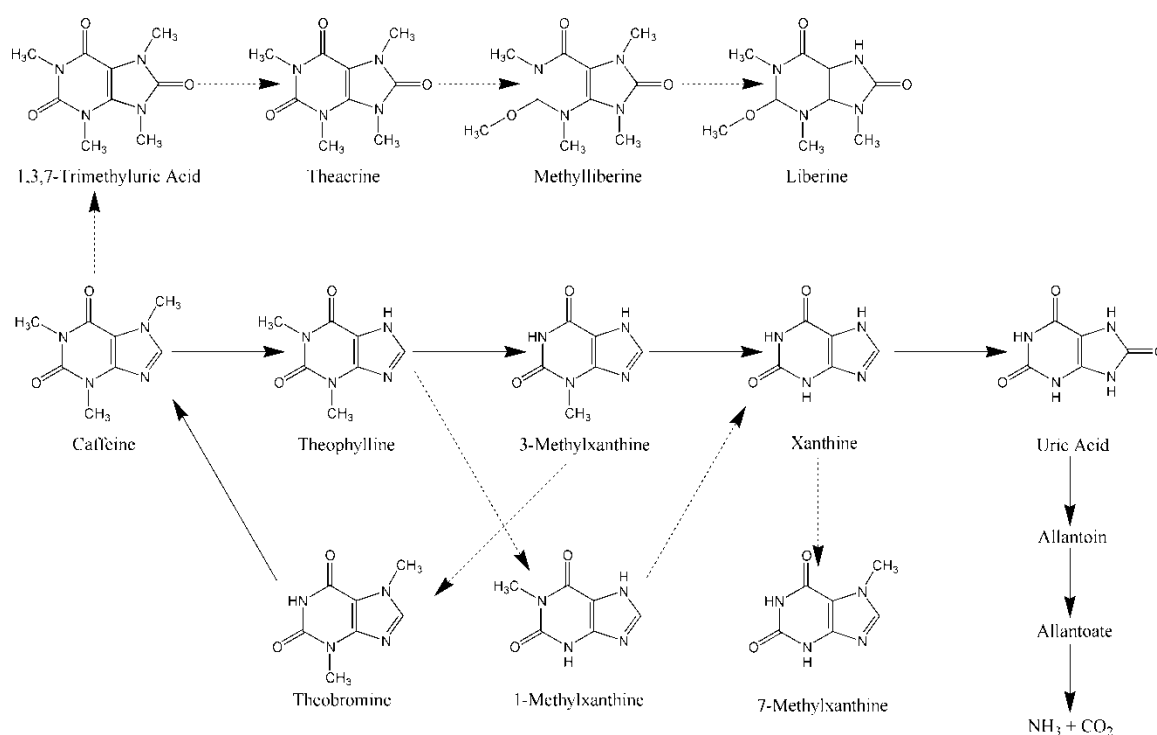


Figure 1.6. Catabolism of caffeine in coffee and tea plants. Solid lines indicate the major degradative route, while dashed lines represent alternative degradation steps.

Image adapted from Anaya *et al.*, 2006 and Mazzafera, 2004.

In young tissues of coffee and tea, caffeine accumulates primarily because conversion of caffeine to its first metabolite, theophylline, is the rate-limiting step (Ashihara and Crozier, 1999). Following *N*-7 demethylation of caffeine to theophylline, an *N*-1 demethylation occurs to form 3-methylxanthine, which is further *N*-demethylated to xanthine (Anaya *et al.*, 2006). Xanthine is oxidized to uric acid, which enters the normal purine catabolic pathway to form allantoin, allantoic acid, and ultimately CO₂ and NH₃. In older leaves of *Cof. dewevrei*, *Cof. liberica*, and *Cof. abeokutae*, caffeine is converted to theacrine via 1,3,7-trimethyluric acid (TMU), which is further converted to methylxanthines and liberine (Petermann and Baumann, 1983).

Mammalian Metabolism of Methylxanthines

More than 25 metabolites of caffeine have been identified in humans (Carrillo and Benitez, 2000). Caffeine degradation is catalyzed by a number of cytochrome P450 enzymes (Grant *et al.*, 1987; Campbell *et al.*, 1987; Butler *et al.*, 1989; Berthou *et al.*, 1991; Eugster *et al.*, 1993; Tassaneeyakul *et al.*, 1994). Although CYP1A1 and CYP1A2 are the major enzymes involved in metabolism of caffeine and related methylxanthines, other P450 isoforms- such as CYP2E1 and CYP2A6- also catalyze *N*-demethylation (Carrillo and Benitez, 2000). Following ingestion by humans, caffeine is converted to paraxanthine (80%), theobromine (10%), and theophylline (4%), with the remaining 6% leaving the body as either TMU, 6-amino-5-[*N*-formylmethylamino]-1,3-dimethyluracil, or unchanged caffeine (Lelo *et al.*, 1986). While paraxanthine is the major metabolite in humans and rabbits, *N*-7 demethylation to form theophylline is the major pathway for caffeine metabolism in monkeys, and all three dimethylxanthines are produced at similar rates in mice and rats (Berthou *et al.*, 1992).

The major metabolic pathway of caffeine in humans (Figure 1.7) occurs through two *N*-demethylation steps, *N*-3 demethylation of caffeine to paraxanthine, followed by *N*-7 demethylation to 1-methylxanthine, which is oxidized to 1-methyluric acid (Lelo *et*

al., 1986; Carrillo and Benitez, 2000). Other routes of caffeine metabolism include *N*-demethylation of paraxanthine to 7-methylxanthine, theophylline to 1- and 3-methylxanthines, and theobromine to 3- and 7-methylxanthines. Furthermore, all of the methylxanthines can be oxidized to their corresponding methyluric acids or *N*-acetylated to their corresponding methyluracils (Tang *et al.*, 1983; Grant *et al.*, 1983; Lelo *et al.*, 1986).

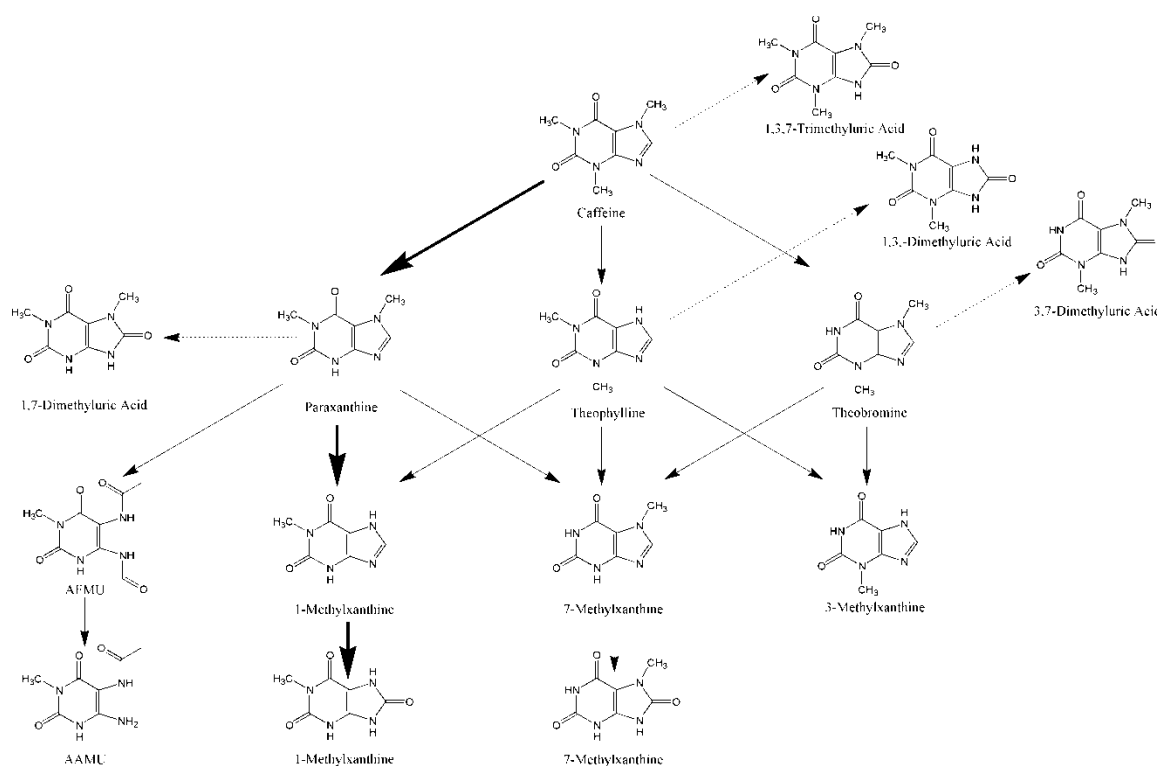


Figure 1.7. Catabolism of caffeine and related methylxanthines in humans. Bold arrows represent the major metabolic pathway. Other solid arrows show minor *N*-demethylation steps, and dashed arrows indicate C-8 oxidation of methylxanthines.

Image adapted from Lelo *et al.*, 1986 and Carrillo and Benitez, 2000.

Microbial Metabolism of Methylxanthines

Because caffeine and related methylxanthines have such a wide use, it should come as no surprise that some caffeine-degrading microorganisms have been isolated from the environment. Similar to degradation of caffeine in humans, yeast cells use P450 enzymes to *N*-demethylate caffeine (Sauer *et al.*, 1982). Little is known concerning the enzymology of caffeine metabolism in other fungi. However, theophylline has been reported as the first metabolite, suggesting an *N*-7-demethylation route (Schwimmer *et al.*, 1971; Hakil *et al.*, 1998). Hakil *et al.* (1998) reported on seven strains of filamentous fungi that could grow on caffeine as the sole nitrogen source. Metabolism in all strains was the same, with caffeine being degraded to theophylline, which was further converted to 3-methylxanthine. Theobromine was also *N*-demethylated to 3-methylxanthine, while paraxanthine could be *N*-demethylated at either position to form 1- and 7-methylxanthines. Metabolism of the monomethylxanthines was not reported, and no methyluric acids were detected.

A number of bacteria have also been isolated due to their ability to degrade caffeine. These species are primarily from the genus *Pseudomonas*, although *Serratia*, *Klebsiella*, and *Rhodococcus* species have also been isolated (Woolfolk, 1975; Mazzafera *et al.*, 1996; Madyastha *et al.*, 1999; Dash and Gummadi, 2006; Yu *et al.*, 2008). Bacteria that can metabolize caffeine and related methylxanthines do so by breaking open the ring structure in order to assimilate the carbon and nitrogen contained therein. Prior to ring cleavage, however, there are one or more preliminary steps that must occur. These steps proceed *via* one of two pathways: C-8 oxidation and *N*-demethylation (Dash and Gummadi, 2006).

Bacterial C-8 Oxidation of Methylxanthines

During C-8 oxidation of xanthine and its alkylated derivatives, the molecule is oxidized at the C-8 position, as shown in Figure 1.8. After oxidation, the ring structure is

oxidation of theophylline, 3-methylxanthine, 7-methylxanthine, and xanthine by activity staining of native PAGE with nitroblue tetrazolium (NBT). The xanthine oxidase was also active at low levels on paraxanthine and theobromine, but was not active on caffeine. Many other xanthine oxidase and xanthine dehydrogenase enzymes have been studied previously (Dickstein *et al.*, 1957; Woolfolk and Downard, 1977; Woolfolk, 1985; Hille and Nishino, 1995). These enzymes belong to the family of molybdenum hydroxylases, and usually contain molybdopterin, flavin adenine dinucleotide, and [2Fe-2S] clusters as cofactors. Caffeine has not yet been reported as a substrate for any xanthine oxidase or xanthine dehydrogenase (Yu *et al.*, 2008).

Table 1.3. Comparison of different caffeine and xanthine oxidizing enzymes.

Properties	Caffeine Oxidase	Caffeine Oxidase	Caffeine Dehydrogenase	Xanthine Oxidase
Organism	<i>Rhodococcus</i> sp./ <i>Klebsiella</i> sp.	<i>Alcaligenes</i> sp.	<i>Pseudomonas</i> sp. CBB1	<i>Pseudomonas putida</i> L
M.W. (kDa)	85	65	158	198
Subunit M.W. (kDa)	85	65	α : 90 β : 34 γ : 20	α : 71 β : 66 γ : 62
Subunit Structure	α	α	$\alpha\beta\gamma$	$\alpha\beta\gamma$
Electron Acceptors	Cyt. C, O ₂	DCPIP, O ₂	Coenzyme Q ₀	O ₂ , NBT
Substrates	Caffeine	Caffeine	Caffeine	Xanthine
Product	TMU	N/A	TMU	Uric acid

Source: Table adapted from Gopishetty, S. R., Louie, T. M., Yu, C. L., & Subramanian, M. V. (2011). Microbial degradation of caffeine, methylxanthines, and its biotechnological applications. Narosa Publishing House, *In Press*.

Pseudomonas sp. CBB1 cells use a novel caffeine dehydrogenase enzyme to degrade caffeine to TMU (Yu *et al.*, 2008). This enzyme was shown to be a heterotrimer

with subunits approximately 90, 40, and 20 kDa in size. Caffeine dehydrogenase was also active on theobromine and theophylline (46 and 0.6% activity, respectively), but did not oxidize 3-methylxanthine, 7-methylxanthine, or xanthine. Oxidation of methylxanthines to methyluric acids was stoichiometric and hydrolytic. Water is the source of oxygen, and coenzyme Q_0 was the preferred electron acceptor. A comparison of different methylxanthine-oxidizing enzymes is shown in Table 1.3.

Bacterial *N*-demethylation of Methylxanthines

Based on literature survey, *N*-demethylation of caffeine seems to occur more frequently in bacteria than does C-8 oxidation (Mazzafera, 2004; Dash and Gummadi, 2006). During this process, the methyl groups are sequentially removed from caffeine to form xanthine (Figure 1.9).

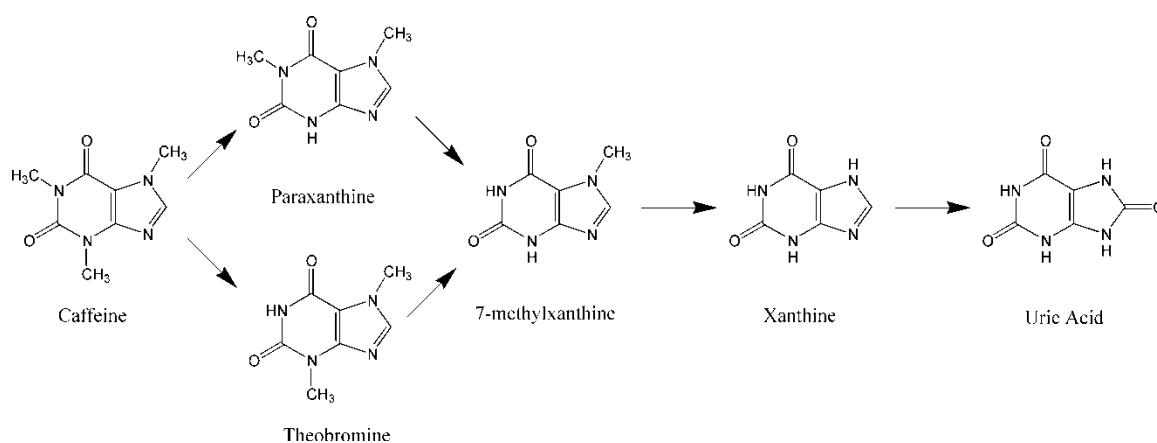


Figure 1.9. Bacterial *N*-demethylation of caffeine to paraxanthine and theobromine. These two metabolites are sequentially *N*-demethylated to 7-methylxanthine and xanthine. The xanthine is then oxidized at the C-8 position to form uric acid.

The first *N*-demethylation step in caffeine metabolism yields theobromine and/or paraxanthine. Theophylline, the major caffeine metabolite in plants and fungi, has not

been reported as a product of bacterial caffeine degradation. Theobromine and paraxanthine are subsequently converted into 7-methylxanthine before a final *N*-demethylation step to yield xanthine. Xanthine is oxidized to uric acid by xanthine oxidase/dehydrogenase, which then enters the normal purine catabolic pathway to form CO₂ and NH₄ (Woolfolk and Downward, 1977). In some bacteria, metabolites of caffeine undergo both *N*-demethylation and C8-oxidation, however, the methyluric acids formed are not metabolized further (Blecher and Lingens, 1977; Yamaoka-Yano and Mazzafera, 1999).

The number and nature of enzymes involved in *N*-demethylations has yet to be determined due to poor enzyme stability (Sideso *et al.*, 2001; Gokulakrishnan *et al.*, 2005; Beltrán *et al.*, 2006). Woolfolk (1975) originally reported that caffeine was degraded by a single hydrolytic enzyme in *P. putida* strain 40 capable of removing all three methyl groups to form methanol and xanthine. More recent studies, however, indicate that multiple monooxygenase enzymes might actually be involved in caffeine degradation (Asano *et al.*, 1994; Sideso *et al.*, 2001; Dash and Gumadi, 2007). Blecher and Lingens (1977) observed formation of formaldehyde, not methanol, during *N*-demethylation of caffeine by *Pseudomonas putida* C1, indicating that *N*-demethylation was catalyzed by a monooxygenase. Further work showed that caffeine *N*-demethylation was dependent on oxidation of NAD(P)H to NAD(P)⁺ (Hohnloser *et al.*, 1980).

Two proteins of molecular weights 43.5 and 36.6 kDa were observed in *P. putida* KD6 cultured on caffeine (Sideso *et al.*, 2001). In another strain of *Pseudomonas* sp., Co²⁺, Mn²⁺, and Ni²⁺ did not affect caffeine degradation, but did strongly inhibit theobromine degradation (Dash and Gummadi, 2007). A recent study by Dash and Gummadi (2008) showed that caffeine and theobromine *N*-demethylases are inducible in *Pseudomonas* sp. strain NCIM5235. The *N*-demethylase activity on caffeine was 10-fold lower in theobromine-grown cells than in caffeine-grown cells, indicating that different *N*-demethylases might be responsible for *N*-demethylation of caffeine and theobromine.

A caffeine *N*-demethylase (size undetermined) and a theobromine *N*-demethylase comprised of six identical subunits 41 kDa in size were reported in *P. putida* No. 352 (Asano *et al.*, 1994). The theobromine *N*-demethylase was purified to homogeneity and characterized by substrate specificity and inhibition by Zn^{2+} ; this divalent ion did not inhibit caffeine *N*-demethylation to theobromine. The enzyme was believed to contain iron in either heme or non-heme form, but this was not substantiated. NAD(P)H was required as a cofactor for the *N*-demethylase activity. Although it now appears that caffeine is degraded by more than one enzyme, purification of the enzymes and/or isolation of the gene sequence for those enzymes are needed in order to confirm this hypothesis.

As with the enzymology, very little is known regarding the genes coding for bacterial *N*-demethylases. A search in the UniProt protein database (UniProt, 2001) returned only one known bacterial *N*-demethylase, *N*-methylproline demethylase (StcD) of *Sinorhizobium meliloti*, which is involved in stachydrine catabolism (Phillips *et al.*, 1998). The sequence of a caffeine *N*-demethylase gene was also found in the GenBank database. This deduced protein sequence showed a high degree of similarity with Rieske [2Fe-2S] domain-containing oxygenase subunits of many putative vanillate *O*-demethylases, putative phenylpropionate dioxygenases, and HpxD of *Klebsiella pneumoniae*, which is involved in the oxidation of hypoxanthine to uric acid (de la Riva *et al.*, 2008). Many *O*-demethylases are multicomponent systems that contain an oxygenase, reductase, and possibly a ferredoxin (Wang *et al.*, 1997). Similarly, the dioxygenases involved in degradation of many xenobiotic compounds have one or two electron transfer proteins that precede the terminal oxygenase (Gibson and Parales, 2000). Hence, a multicomponent system must be considered during purification of a caffeine *N*-demethylase.

In this case, a gene encoding an *N*-1 caffeine demethylase would be cloned into *E. coli* or *S. cerevisiae* in order to perform the biotransformation of caffeine to theobromine. The *N*-3 and *N*-7 atoms would be blocked from addition of the 5-oxohexyl group, leaving only the *N*-1 atom available. Similarly, many other xanthine derivatives may be produced from caffeine if the genes coding for caffeine-degrading enzymes can be isolated and heterologously expressed.

Bioremediation and Treatment of Wastes

Another potential biotechnological aspect to microbial caffeine degradation is bioremediation and treatment of industrial wastes. Millions of tons of coffee and tea plant matter are processed every year, with an average caffeine content of 1% in the waste pulp (Brand *et al.*, 2000; Gopishetty *et al.*, 2011). The waste pulp is unsuitable for use as animal feed due to its caffeine content (Mazzafera, 2002). Biodecaffeination of wastes may render them suitable for use as animal feed or crop fertilizers. Treatment of liquid effluents from these plants with caffeine-degrading bacteria may also reduce the amount of caffeine being released into the local water supply.

Coffee and tea fields contain high concentrations of caffeine in the soil due to degradation of plant matter. Also, the high consumption of methylxanthines in food, beverages, and pharmaceuticals can lead to high levels of these compounds as contaminants in surface and ground water (Mohapatra *et al.*, 2006). Caffeine has also been suggested as a pesticide (Nathanson, 1984; Hollingsworth *et al.*, 2002) and herbicide (Rizvi *et al.*, 1981). However, once in the soil caffeine serves as a sterilant, inhibiting seed germination and growth of seedlings (Smyth, 1992).

Because caffeine and related methylxanthines are widely used in food and pharmaceutical industries, they can enter the soil and groundwater through human waste streams, as well. Although xanthine derivatives are used in a variety of medical preparations, some detrimental health effects have been observed. These side effects may

include headache, nausea, vomiting, anorexia, cardiac arrhythmia, depression, seizures, tremors, insomnia, obesity, osteoporosis, reproductive disorders and many more (Stavric, 1988a-c; Carrillo and Benitez, 2000; Ressig *et al.*, 2009; Heckman *et al.*, 2010).

Environmental contamination of methylxanthines is so prevalent in surface and ground water that caffeine has been suggested as an anthropogenic marker for wastewater pollution of drinking water (Buerge *et al.*, 2003; Ogunseitan, 1996; Seiler *et al.*, 1999). 8-Chlorocaffeine, which is produced during the chlorination of drinking water, can cause DNA damage and has genotoxic properties (Lumb *et al.*, 1968; White and Rasmussen, 1998; Mohapatra *et al.*, 2006). Therefore, care must be taken to remove these compounds from human waste products before they can enter into potable water treatment facilities. This might be done by using bacteria to degrade caffeine and other xanthine derivatives in sewage before it undergoes further processing (Ogunseitan, 1996). Thus, there are many potential applications for use of caffeine-degrading microbes in bioremediation.

Decaffeination of Coffee and Tea

Due to the adverse physiological effects to which caffeine may contribute, many people prefer to consume coffee in its decaffeinated form. Caffeine is removed from coffee and tea by solvent extraction, water diffusion, and supercritical CO₂ extraction (Feldman and Katz, 1976; Udayasankar *et al.*, 1986; Coulate, 2009). Under the first method, water is first added to bring the moisture content to about 40%. Caffeine is then extracted in a counter-current system between 50 and 120 °C with methylene chloride. Coffee beans and tea leaves are steam stripped to remove residual solvent, and the decaffeinated product is dried (Coulate, 2009). Caffeine is also extracted from coffee beans by water diffusion, in which coffee beans are passed counter-currently through water containing 15% solids other than caffeine. The water extract removes approximately 98% of the caffeine, and the beans are then air dried (Berry and Waters,

1943; Feldman and Katz, 1976). Alternatively, supercritical carbon dioxide can be used to extract caffeine from coffee and tea (Udayasankar *et al.*, 1986). Supercritical CO₂ is extremely selective for caffeine, and can be used as a non-toxic extraction agent. Unfortunately, the process requires a large energy input, as the CO₂ must be compressed to 120 to 180 atm.

Due to the high temperatures and/or pressures at which the above methods must run, they often have high energy and operational costs (Mohapatra *et al.*, 2006). Methods such as solvent extraction use toxic compounds that might not be completely removed, and the flavor may be altered. Therefore, a “green” method to decaffeination has garnered public interest (Gokulakrishan *et al.*, 2005; Dash and Gummadi, 2006; Gopishetty *et al.*, 2011). Decaffeination by either whole cells or enzymes has been proposed; however, there is no current process using microbial cells or enzymes for commercial decaffeination of coffee and tea. Cloning of a caffeine-degrading enzyme into a host that is Generally Regarded as Safe, such as *Saccharomyces cerevisiae* may enable for biodecaffeination to occur at an industrial scale (Gopishetty *et al.*, 2011).

Biosensor Development

There is increasing interest in development of an easy, portable, and rapid diagnostic test for concentration of caffeine, such as a “dipstick” assay similar to pH strips and home pregnancy tests (Ladenson *et al.*, 2006; Gopishetty *et al.*, 2011). Such a test could be of use in detecting approximate caffeine concentrations in a cup of decaffeinated coffee at a restaurant, a mother’s breast milk prior to feeding an infant, or an environmental sample. Currently, caffeine is routinely measured by high performance liquid chromatography, thin layer chromatography, gas chromatography, ultraviolet spectroscopy, and capillary electrophoresis, none of which would serve the above purposes.

An enzymatic method to determine approximate caffeine concentration has been developed with the caffeine dehydrogenase (Cdh) from *Pseudomonas putida* CBB1 (Gopishetty *et al.*, 2011). Caffeine levels from 0 to 12 mg·L⁻¹ in buffer and whole milk were detected by coupling oxidation of caffeine by Cdh to reduction of several tetrazolium salts in a 96-well plate. The tetrazolium salts change color when reduced, thus allowing for rapid determination of caffeine concentration. A second approach to develop a caffeine diagnostic kit has focused on antibody recognition of caffeine (Ladenson *et al.*, 2006). Future research on bacterial metabolism of caffeine may lead to more enzymes and/or more methods for easy, rapid caffeine biosensors.

Synthetic Biology

Caffeine-degrading enzymes might also be of interest in the nascent field of synthetic biology. Synthetic riboswitches have been designed that contain RNA sequences which selectively bind caffeine, theophylline, or 3-methylxanthine (Desai and Gallivan, 2004). The riboswitch undergoes a conformational change when bound to the methylxanthine, which either enables or represses translation of the targeted gene. These riboswitches have been used to detect the presence of an endogenous small molecule, perform genetic screening (Desai and Gallivan, 2004), and control regulation of exogenous genes used in metabolic engineering purposes (Bayer and Smolke, 2005). Use of an *N*-1 demethylase in a system containing both theophylline and 3-methylxanthine riboswitches may be used to control expression of two different enzymes. In this hypothetical system, theophylline would be converted to 3-methylxanthine, which would inactivate the theophylline riboswitch while simultaneously activating the 3-methylxanthine riboswitch. Translation of the target genes for both riboswitches could then be expressed or inhibited in different combinations, depending on the properties of the riboswitches.

The discovery of new enzymes which will allow for the production of natural products in heterologous biosynthetic pathways is also important in metabolic engineering research. Thus, purification of novel caffeine-degrading enzymes and determination of the genes that encode them may also be of import in the exciting new field of synthetic biology.

Previous Research

In order to better study bacterial *N*-demethylation, a bacterial strain capable of degrading caffeine by such a mechanism was required. Therefore, an enrichment procedure to isolate a colony capable of *N*-demethylation was designed and carried out as described below.

Enrichment of caffeine-degrading bacteria was performed by adding soil samples obtained from Coralville, IA to M9 mineral salts medium (Sambrook, 1989) containing $2.5 \text{ g} \cdot \text{L}^{-1}$ caffeine as the sole carbon and nitrogen source (Yu *et al.*, 2009). Cultures were incubated at $29 \text{ }^{\circ}\text{C}$ with rotary shaking at 200 rpm. Aliquots were periodically removed from the enrichment culture for analysis of caffeine utilization by HPLC. Growth of the enrichment culture was monitored by measuring the optical density at 600 nm (OD_{600}). After eight days, the $2.5 \text{ g} \cdot \text{L}^{-1}$ caffeine present in the medium was completely consumed. This culture was further enriched by three subcultures in M9-caffeine medium, following which an aliquot of the third subculture was serially diluted and plated on M9-caffeine agar. The plates were incubated at $29 \text{ }^{\circ}\text{C}$, and morphologically different colonies were isolated and screened for the ability to degrade caffeine.

Four colonies of different morphology were isolated from M9-caffeine agar plates. These colonies, designated strains CBB1, CBB3, CBB5, and CES, were submitted to MIDI Inc. (Newark, DE) for identification. Phylogenetic analysis based on the 16S rRNA gene sequence indicated that all four strains were members of the genus *Pseudomonas*. The closest phylogenetic relative to strain CBB5 was *P. putida* strain AJ

(GenBank accession no. AY391278, 99% identity). Also, fatty acid methyl ester analysis identified CBB5 as *Pseudomonas putida* biotype B with a similarity index of 0.81. Based on these results, CBB5 was identified as a strain of *P. putida*. The remaining three strains were characterized as *Pseudomonas* sp. CBB1, *Pseudomonas nitroreducens* CBB3, and *Pseudomonas* sp. CES.

Strain CBB1 was shown to degrade caffeine *via* C-8 oxidation to TMU by a novel caffeine dehydrogenase (Yu *et al.*, 2008). The mechanism of caffeine degradation in strains CBB3 and CES, however, has yet to be determined. HPLC analysis of growth media showed that when caffeine was metabolized by CBB5 cells, theobromine, 7-methylxanthine, xanthine, and uric acid were produced. Surprisingly, CBB5 was also capable of growth on theophylline. Degradation of theophylline in growth medium by CBB5 resulted concomitant formation of 1,3-dimethyluric acid, 3-methyluric acid, and uric acid. These results indicated that both C-8 oxidizing and *N*-demethylating enzymes are present in CBB5.

Objectives

While some work has been performed on the bacterial degradation of caffeine and theobromine, there is still much work to be done in order to completely understand the process. Due to poor stability, the enzyme(s) that catalyze *N*-demethylation have yet to be purified and characterized, nor has the gene sequence for this (these) enzyme(s) been elucidated. Because of this, the number of bacterial enzymes that catalyze *N*-demethylations and their substrate specificities are yet unclear. Also, bacterial growth on, and metabolism of, theophylline has not been reported previously. The distinct caffeine and theophylline degradation pathways exhibited by CBB5 led to the hypothesis that these two compounds and their respective metabolites are *N*-demethylated by different enzymes. In order to test the hypothesis, four research objectives were developed:

1. Determine the metabolic pathway,
2. Purify and characterize the proteins responsible for methylxanthine metabolism,
3. Isolate the genes coding for the above proteins, and
4. Express the recombinant proteins and characterize their substrate specificities.

Under the first task, growth media, resting cell suspensions, and cell extract assays were used to determine all metabolites of caffeine and theophylline down to uric acid. The second task focused on the purification of *N*-demethylase(s) in CBB5. These purified enzymes were then assayed to determine if caffeine, theophylline, and their metabolites were *N*-demethylated by the same enzyme. Under the third task, the genes involved in *N*-demethylation were isolated and characterized using degenerate primers designed from the N-terminal sequences of *N*-demethylase subunits and the conserved Rieske [2Fe-2S] domain of bacterial oxygenases. Finally, the number of *N*-demethylases present in CBB5 was determined by cloning and expressing the *N*-demethylase genes and characterizing their substrate specificity. Completion of these tasks has provided a better understanding of the number and nature of the *N*-demethylase enzymes expressed in CBB5, the genes that code for them, and their role in the metabolism of various methylxanthines.

CHAPTER 2: MATERIALS AND METHODS

Chemicals

Caffeine, theophylline, theobromine, paraxanthine, 1-methylxanthine, 3-methylxanthine, 7-methylxanthine, xanthine, uric acid, 1-methyluric acid, 1,3-dimethyluric acid, DNase I from bovine pancreas, ammonium acetate, acetic acid, 2,4-pentanedione, spinach ferredoxin, and spinach ferredoxin reductase were purchased from Sigma-Aldrich (St. Louis, MO). Reductase and ferredoxin of *Pseudomonas* sp. 9816 naphthalene dioxygenase were kindly provided by Dr. David T. Gibson, University of Iowa. Soytone, tryptone, yeast extract, and agar were obtained from Becton, Dickinson and Company (Sparks, MD), and yeast nitrogen base without amino acids and without ammonium sulfate (YNB) was purchased from ForMedium (Norfolk, United Kingdom). High-pressure liquid chromatography (HPLC)-grade methanol (J.T. Baker, Phillipsberg, NJ) was used in chromatographic studies.

Isopropyl- β -D-thiogalactopyranoside (IPTG), 5-bromo-4-chloro-3-indolyl- β -D-galactopyranoside (X-gal), and Tris Base were obtained from RPI Corp. (Mt. Prospect, IL). Agarose was purchased from Invitrogen (Carlsbad, CA). Taq DNA polymerase, restriction enzymes AseI, DpnI, NdeI, and XhoI, 10x Taq polymerase buffer, 10 mM dNTP mixture, NEB buffers 2, 3, and 4, Antarctic Phosphatase enzyme and buffer, 10x BSA, and pUC19 and pET32 plasmids were obtained from New England Biolabs (Ipswich, MA). Pfu polymerase and buffer were purchased from Stratgene (Santa Clara, CA). Phusion HF polymerase and buffer were purchased from Finnzymes (Espoo, Finland). Ethidium bromide was obtained from Bio-Rad (Hercules, CA). Dithiothreitol (DTT), glacial acetic acid, and ethylenediaminetetraacetic acid (EDTA) were purchased from Fischer Scientific (Waltham, MA).

Culture Conditions

Culture of CBB5

In order to determine the metabolic pathway of CBB5 on caffeine, theophylline, and related methylxanthines, a pure culture was grown in the M9 mineral salts medium (Sambrook, 1989) containing $2.5 \text{ g}\cdot\text{L}^{-1}$ caffeine (medium C), which was the same medium used for enrichment. Cultures were incubated at $30 \text{ }^{\circ}\text{C}$ and 200 rpm rotary shaking. In addition, CBB5 was grown in M9 containing $1.0 \text{ g}\cdot\text{L}^{-1}$ theobromine, theophylline (medium T), paraxanthine, 7-methylxanthine, or 3-methylxanthine. When indicated, $4.0 \text{ g}\cdot\text{L}^{-1}$ soytone or YNB was added to M9 medium. For enzyme purification, CBB5 was grown in M9 medium containing $4.0 \text{ g}\cdot\text{L}^{-1}$ soytone and $2.5 \text{ g}\cdot\text{L}^{-1}$ caffeine (medium CS) or theophylline (medium TS).

Culture of *E. coli* Cells

Electrocompetent *Escherichia coli* strains JM109 (Yanisch-Perron *et al.*, 1985; ATCC, Manassas, VA), BL21(DE3) (Novagen, San Diego, CA), ElectroMAX DH10B (Invitrogen), and *E. coli* 10G (Lucigen, Middleton, WI) were rescued following electroporation (described below) in SOC medium containing 2% (w/v) tryptone, 0.5% (w/v) yeast extract, 10 mM NaCl, 2.5 mM KCl, 20 mM glucose, 10 mM MgCl_2 , and 10 mM MgSO_4 . Rescued cells were grown in LB medium containing $10 \text{ g}\cdot\text{L}^{-1}$ tryptone, $5 \text{ g}\cdot\text{L}^{-1}$ yeast extract, and $5 \text{ g}\cdot\text{L}^{-1}$ NaCl at $37 \text{ }^{\circ}\text{C}$. LB agar plates were prepared by adding $14 \text{ g}\cdot\text{L}^{-1}$ agar. Ampicillin was added to LB broth and LB agar to a final concentration of $100 \text{ }\mu\text{g}/\text{mL}$ (LBA broth and LBA agar, respectively). Blue/white screening of transformants was carried out on LBA agar containing $80 \text{ }\mu\text{g}/\text{mL}$ X-gal and 0.5 mM IPTG (LBAXI agar).

Whole-Cell Degradation Assays

Growth Media Studies

Degradation of caffeine and related methylxanthines by CBB5 was investigated by adding these compounds to M9 medium as growth substrates. A seed culture of CBB5 was first grown in CS medium to an OD₆₀₀ of 2.0. The seed culture was harvested by centrifugation (8,000 × g for 15 min at 4 °C) and washed twice with M9 medium containing neither caffeine nor soytone. The cells were then suspended in M9 medium and inoculated into 50 mL soytone-free or soytone-supplemented M9 medium containing a test compound to an OD₆₀₀ of approximately 0.01-0.02. All cultures were incubated at 29 °C with rotary shaking at 200 rpm. Growth of CBB5 on the test compounds was monitored by periodically measuring the OD₆₀₀ of each culture. Concomitant degradation of the test compounds and accumulation of metabolites in the media (spent media) were monitored by liquid chromatography and mass spectrometry (LCMS). Identities of the metabolites were established by comparing the metabolites' retention times (Rts), absorption spectra, and electrospray ionization (ESI) mass spectra with those of authentic standards.

Resting Cell Assays

Degradation of caffeine and related methylxanthines by CBB5 was also demonstrated by performing resting cell assays. CBB5 grown in soytone-supplemented M9 medium containing either caffeine or a related methylxanthine was harvested by centrifugation (8,000 × g for 15 min at 4 °C) when the OD₆₀₀ reached 2.0 to 2.4. The cells were washed once with 50 mM potassium phosphate (KP_i) buffer (pH 7.5) and suspended in 5 mL KP_i buffer at a final OD₆₀₀ of 4.0. Caffeine and related methylxanthines were added to the cell suspensions at a final concentration of 1 mM. The resting cell suspensions were incubated at 29 °C with shaking at 200 rpm. Aliquots

were removed from the cell suspensions periodically to monitor the degradation of test compounds and the formation of metabolites by HPLC.

Harvesting of Cells for Enzyme Purification

CBB5 was grown in either TS (C-8 oxidizing enzymes) or CS (*N*-demethylase and reductase enzymes) media for enzyme purification studies. Upon reaching an OD₆₀₀ between 2.0 and 2.5, cells were harvested by centrifugation (10,000 × *g* for 10 min at 4 °C) and washed twice in 50 mM potassium phosphate (KP_i) buffer (pH 7.5). About 3.9 g (wet weight) of pelleted cells grown in TS medium were suspended in 10 mL 50 mM KP_i buffer. For CBB5 grown in CS medium, 16 g pelleted cells were suspended in 35 mL 50 mM KP_i buffer containing 5% (v/v) glycerol and 1 mM DTT (KPGD buffer). Both sets of cells were stored at -80 °C prior to lysis and enzyme purification.

Cell Extract Preparation

Cell extracts of CBB5 grown in either CS or TS media were prepared in the same manner, regardless of the growth medium. Frozen cells were removed from -80 °C and allowed to thaw on ice. DNase I was then added to the cell suspension to a final concentration of 10 µg·mL⁻¹. Cells were broken by passage through a chilled French press cell twice at 138 MPa. Unbroken cells and cell debris were removed from the lysate by centrifugation (16,000 × *g* for 20 min at 4 °C), and the supernatant was designated the cell extract (CE).

Enzyme Purification

All purification procedures were performed at 4 °C using an automated fast protein liquid chromatography system (ÄKTA Purifier, Amersham Pharmacia Biotech, Piscataway, NJ). After each chromatographic step, eluant fractions were assayed for xanthine oxidizing, *N*-demethylase (Ndm), or cytochrome *c* reductase (Ccr) activities as described below. Fractions with activities were concentrated by centrifugation (4,000 × *g*

for 30 min at 4 °C) using Amicon ultrafiltration units (Millipore, Billerica, MA) with 10,000 molecular weight cut-off (MWCO).

Partial Purification of Xanthine-Oxidizing Enzymes

A 4.0 M solution of ammonium sulfate was added drop-wise to CE from CBB5 grown in TS medium to a final concentration of 0.5 M. After incubation with shaking on ice for 20 min, the mixture was centrifuged at $16,000 \times g$ for 15 min to remove precipitated proteins. The supernatant was loaded onto a 120-mL (bed volume) Phenyl Sepharose High Performance column (Amersham) preequilibrated with 50 mM KP_i buffer (pH 7.5) containing 0.5 M ammonium sulfate. Unbound proteins were washed from the column with 120 mL 50 mM KP_i buffer containing 0.5 M ammonium sulfate. Bound proteins were eluted from the column with a 360-mL reverse gradient of ammonium sulfate (0.5 to 0 M in KP_i buffer) at a flow rate of $1 \text{ mL} \cdot \text{min}^{-1}$. The column was then washed with 120 mL KP_i buffer at the same flow rate. Finally, hydrophobic proteins tightly bound to the column were eluted with 120 mL deionized water. Fractions containing xanthine-oxidizing enzyme activities were identified by a spectrophotometric enzyme activity assay.

Purification of *N*-Demethylase Enzymes

Cell extract from CBB5 grown in CS medium was loaded onto a 160-mL (bed volume) DEAE Sepharose column (GE Healthcare, Waukesha, WI) pre-equilibrated in KPGD buffer. After washing unbound proteins from the column with 160 mL KPGD buffer at a flow rate of $1.5 \text{ mL} \cdot \text{min}^{-1}$, the bound proteins were eluted from the column with a 540-mL linear gradient of KCl (0 to 0.4 M) in KPGD buffer. Fractions with Ndm activity were pooled and concentrated.

A 4.0 M ammonium sulfate solution was added to the Ndm-activity-containing fractions from DEAE Sepharose to a final concentration of 0.25 M ammonium sulfate with constant stirring. After 20 min, the mixture was centrifuged ($16,000 \times g$ for 20

min), and the supernatant was loaded onto a 30-mL (bed volume) Phenyl Sepharose High Performance column (Amersham) pre-equilibrated in KPGD buffer containing 0.25 M ammonium sulfate. Unbound proteins were eluted from the column with 60 mL KPGD buffer containing 0.25 M ammonium sulfate. Bound proteins were eluted with a 30-mL reverse linear gradient of ammonium sulfate (0.25 to 0 M in KPGD buffer) at a flow rate of 1 mL·min⁻¹. The column was then washed with 45 mL KPGD buffer, followed by 60 mL deionized water containing 1 mM DTT and 5% (v/v) glycerol.

Phenyl Sepharose eluants with *N*-demethylase activity were pooled, concentrated to 2 mL, and loaded onto a 5-mL (bed volume) Q Sepharose column (GE Healthcare) pre-equilibrated in KPGD buffer containing 0.2 M KCl. After washing unbound proteins from the column with 10 mL equilibration buffer, bound proteins were eluted from the column using a 120-mL linear gradient of KCl (0.2 to 0.4 M) in KPGD buffer with a flow rate of 1 mL·min⁻¹. Ndm was eluted from the Q Sepharose column as a single peak around 0.29 M KCl.

Electrophoresis

Protein Gel Electrophoresis

After each chromatographic step, purity of protein in active fractions was determined using native and denaturing PAGE. For native PAGE analysis, fractions were mixed 1:2 (v/v) with Native Sample Buffer (Bio-Rad), loaded onto 4-15% Tris-HCl gels (Bio-Rad), and electrophoresed for 60 min at a constant 100 V. For denaturing PAGE analysis, fractions were mixed with 4X LDS loading buffer (Invitrogen) and 1 M DTT (70:25:5, v/v) and loaded onto 10% Bis-Tris gels. Gels were subjected to a constant 200 V for 80 min. Upon completion of PAGE, gels were washed three times in 100 mL deionized water and stained with GelCode Blue Safe Protein Stain (ThermoFisher Scientific).

Protein Blotting

Proteins were transferred to a 0.2 μm Sequi-blot PVDF membrane (Bio-Rad) by electroblotting (Burnette, 1981) prior to submitting for N-terminal amino acid sequencing. Protein samples were separated on 10% Bis-Tris gels as described above. Following SDS-PAGE, the gel was placed in a western blotting assembly next to a PVDF membrane and subjected to a constant 30 V for 1 h in NuPAGE Transfer Buffer (Invitrogen). Following transfer, the membrane was removed, washed twice for 1 min with H_2O , and stained for 30 min with GelCode Blue Safe Protein Stain. The membrane was destained by washing 15 s in 100% MeOH, rinsed 3 times in H_2O , and air dried overnight. Blots were stored at $-20\text{ }^\circ\text{C}$ until they were submitted for N-terminal amino acid sequencing.

Agarose Gel Electrophoresis

Agarose gel electrophoresis was used to fractionate DNA fragments of different sizes and to estimate the concentration of DNA in samples. A 0.5x concentration of Tris-Acetate-EDTA (TAE) buffer, pH 8.0, consisting of 20 mM Tris Base, 10 mM glacial acetic acid, and 5 mM EDTA, was used as running buffer during electrophoresis of agarose gels. DNA loading buffer (6x concentration) was prepared with 1.7 mM bromophenol blue, 6 mM EDTA, 30% glycerol, and 60 mM Tris-HCl. Agarose gels were prepared by adding 0.21 or 0.36 g agarose (0.7% or 1.2%, v/v, respectively) to 30 mL 0.5x TAE buffer. After addition of 0.5 μL ethidium bromide, the mixture was heated until the agarose was completely melted (about 45 seconds in a microwave on HIGH setting) and poured into the gel mold. Gels were allowed to cure at least 30 min at $4\text{ }^\circ\text{C}$ prior to electrophoresis. After the gel had set and the well comb was removed, 0.5 to 5 μL DNA sample were added to 0.5x TAE plus 1 μL 6x DNA loading buffer to a final volume of 6 μL and loaded into the gel wells. Gels were electrophoresed at 100 V constant voltage for 30-40 min in 0.5x TAE buffer and imaged with UV illumination at

302 nm in a Gel Doc XR (BioRad) equipped with a CCD camera and Quantity One software (BioRad).

Acrylamide Gel Electrophoresis of DNA

DNA fragments less than 500 bp were resolved on 8% acrylamide gels. Up to 5 μ L DNA sample was mixed with 1 μ L 6x DNA loading buffer and loaded onto the gel. Gels were electrophoresed at a constant 100 V for 30 min and visualized by UV illumination as described above.

Quantification of DNA concentration

Concentration of DNA was estimated by comparing the intensity of DNA bands in an agarose gel under UV illumination as described above. A 1 kb DNA ladder stock (Invitrogen) was diluted in 0.5x TAE buffer and 6x DNA loading buffer (100:167:733 v/v/v) so that the 1.6-kb band was at a concentration of 10 ng/ μ L. Both ladder (1-5 μ L) and an appropriate amount of DNA sample were loaded onto an agarose gel and electrophoresed as described above. The concentration of DNA was then estimated by comparing the intensity of the DNA band with that of the 1.6-kb band in the DNA ladder and calculated according to Equation 2.1:

$$[\text{DNA}] = \left(\frac{V_S}{V_L} \right) * 10 \frac{\text{ng}}{\mu\text{L}}, \quad (2.1)$$

where [DNA] is the concentration of DNA in the sample and V_S and V_L are the volume of sample and ladder, respectively, which contain bands displaying similar intensity under UV imaging.

Enzyme Activity Assays

Xanthine-Oxidizing Assay

To determine xanthine-oxidizing activity, a 1-mL reaction mixture consisting of 50 mM KP_i buffer (pH 7.5), an appropriate amount of partially purified enzyme, 0.5 mM

xanthine, and either 0.5 mM nitroblue tetrazolium (NBT) or 0.5 mM NAD^+ as the electron acceptor was incubated at 30 °C. When NBT was used, enzyme activity was determined by monitoring the increase in absorbance at 566 nm ($\Delta\epsilon_{566} = 15,500 \text{ M}^{-1}\text{cm}^{-1}$), due to formazan production, with a UV-visible spectrophotometer (Shimadzu UV-2450). When NAD^+ was used, enzyme activity was determined by monitoring the increase in absorbance at 340 nm ($\Delta\epsilon_{340} = 6,220 \text{ M}^{-1}\text{cm}^{-1}$) due to NADH production. Substrate preference was tested by replacing xanthine with 0.5 mM caffeine, theophylline, theobromine, or 3-methylxanthine.

CCR Activity Assay

NADH:cytochrome *c* oxidoreductase (cytochrome *c* reductase, Ccr) activity was determined as described by Ueda *et al.* (1972). A typical 1-mL reaction contained 300 μM NADH, 87 μM bovine cytochrome *c* (type III; Sigma), and 1-20 μg CBB5 protein (depending on purity) in 50 mM KPi buffer. The activity was determined by monitoring the increase in absorbance at 550 nm due to reduction of cytochrome *c* at 30 °C. An extinction coefficient of $21,000 \text{ M}^{-1}\text{cm}^{-1}$ for reduced minus oxidized cytochrome *c* was used for quantitating the activity. One unit of activity was defined as one μmol of cytochrome *c* reduced per min.

N-demethylation Assay

Theophylline *N*-demethylase activity in cell extracts prepared from theophylline-grown CBB5 cells was assayed in order to determine the metabolic products of theophylline by CBB5 (Chapter 3). A typical 2-mL reaction mixture containing 50 mM KPi buffer (pH 7.5), an appropriate amount of cell extract, and 0.5 mM theophylline was incubated at 30 °C. Aliquots were removed from the reaction mixture periodically and added 1:1 (v/v) with acetonitrile to monitor consumption of theophylline and formation of metabolites by HPLC.

All other *N*-demethylase activity assays were performed using enzyme from CBB5 grown in CS medium used during purification of Ndm. Methylxanthine *N*-demethylase activity assay contained, in 1 mL total volume, 0.5 mM methylxanthine, 1 mM NADH, 50 μ M Fe(NH₄)₂(SO₄)₂, and an appropriate amount of Ndm (0.08-7.5 mg protein, depending on purity of the protein) in 50 mM KP_i buffer. Approximately 4 U of partially purified Ccr was added to reaction mixture when assaying Ndm in Phenyl Sepharose and Q Sepharose eluant-fractions (Ccr was not added to the enzyme reaction mixture when assaying Ndm activity in DEAE Sepharose eluant-fractions because Ccr co-eluted with Ndm). The reaction mixture was incubated at 30°C with 300 rpm shaking on an incubating microplate shaker (VWR, Radnor, PA). Periodically, a small aliquot was sampled from the reaction mixture and mixed with an equal volume of acetonitrile for quantifying concentrations of methylxanthines and *N*-demethylated products by HPLC. One unit of *N*-demethylase activity was defined as the consumption of one μ mol methylxanthine per minute. When Ndm was coupled with the reductase and ferredoxin components of naphthalene dioxygenase of *Pseudomonas sp.* strain 9816 (Haigler & Gibson, 1990a; Haigler & Gibson, 1990b), 30 and 100 μ g of the respective proteins were used. Spinach ferredoxin reductase and ferredoxin were also substituted for Ccr as described by Subramanian *et al.* (1979).

Characterization of Ndm

Molecular mass estimation

The molecular masses of the Ndm subunits were estimated under denaturing conditions by PAGE on 10% Bis-Tris gels with MOPS running buffer containing SDS (Invitrogen). Native molecular mass of Ndm was determined by gel filtration chromatography using an 80-mL (V_c , geometrical volume) Sephacryl S-300 HR column (Amersham) equilibrated with 0.1 M KCl in 50 mM KP_i buffer at 1 mL·min⁻¹. The void volume (V_o) of the column was determined by measuring the elution volume (V_e) of a 1

mg·mL⁻¹ solution of blue dextran 2000 (GE Healthcare). The column was calibrated with ferritin (440 kDa), catalase (232 kDa), adolase (158 kDa), and conalbumin (75 kDa). The V_e of each standard protein was measured, from which the respective K_{av} value was calculated according to Equation 2.2:

$$K_{av} = \frac{V_e - V_o}{V_c - V_o}, \quad (2.2)$$

where K_{av} is the partition coefficient related to the size of a molecule, v_e is the elution volume of the protein, v_o is the void volume of the column, and v_c is the geometrical volume of the column. A standard curve of K_{av} values against the logarithmic molecular masses of the standard proteins was then used to determine the native molecular mass of Ndm.

Determination of pH and Temperature Optima

To determine pH optimum, Ndm activity was measured as described above at various pH values within the range of 6.0 to 8.0 by using 50 mM KPi buffer. The temperature optimum for Ndm activity in 50 mM KPi (pH 7.5) buffer was determined by incubating the enzyme reactions at 25 to 40 °C and monitoring *N*-demethylation of paraxanthine by HPLC.

Determination of Kinetic Parameters

Apparent kinetic parameters of Ndm were determined by measuring the initial rate of disappearance (v_o) of paraxanthine or 7-methylxanthine in 50 mM KPi buffer (pH 7.5) at 30 °C. The paraxanthine and 7-methylxanthine concentrations ($[S]$) used in these experiments were from 20 to 500 μM. Substrates were incubated with Ndm and Ccr under standard conditions for 15 min. At 1, 5, 10, and 15 min, samples were removed from the reaction mixtures to quantitate substrate concentrations by HPLC. Plots of substrate concentrations against time were used to determine the initial rates of disappearance of substrates, which were linear over 15 min.

The apparent kinetic parameters were determined from Michaelis-Menten plots of v_o against $[S]$ fitted with the Michaelis-Menten equation, Equation 2.3:

$$v_o = \frac{k_{cat}[E_T][S]}{K_M + [S]}, \quad (2.3)$$

where $[E_T]$ is the concentration of enzyme in the reaction, v_o is the initial rate of substrate disappearance, $[S]$ is the initial substrate concentration, K_M is the substrate concentration at one-half maximum velocity, v_{max} , and k_{cat} is the specific maximum activity, v_{max}/E_T . All of the experiments were performed in triplicate and the data were analyzed by using GraFit 5.0 software (Erithacus Software Limited, Surrey, UK).

Determination of Oxygen Requirement

Purified Ndm and partially purified Ccr were mixed in a sealed cuvette, while a second sealed cuvette contained paraxanthine, NADH, and $\text{Fe}(\text{NH}_4)_2(\text{SO}_4)_2$. Both solutions were then flushed with N_2 for 15 min to remove oxygen. Ndm reaction was started by combining the contents of the two cuvettes anaerobically. After 1 h of anaerobic incubation at 30°C , the cuvette was exposed to ambient air and incubation of the mixture continued at 30°C for another hour. During the 2-hour incubation, samples were periodically drawn from the cuvette for determination of paraxanthine concentration by HPLC. A parallel reaction was conducted under aerobic conditions.

Oxygen consumption by Ndm during *N*-demethylation of paraxanthine was determined in a closed reaction vessel equipped with a Clarke-type oxygen electrode (Digital Model 10, Rank Brothers Ltd., Cambridge, England). The electrode was calibrated by using glucose oxidase (Sigma) and glucose to quantitatively determine consumed oxygen. Ndm activity assay was performed at 30°C in a total volume of 1 mL of air-saturated 50 mM KPi buffer (pH 7.5) with 100 μM paraxanthine, 200 μM NADH, 50 μM $\text{Fe}(\text{NH}_4)_2(\text{SO}_4)_2$, 0.2 mg purified Ndm, and 4 U partially purified Ccr. The reaction was initiated by adding Ndm and partially purified Ccr after equilibration of all other reaction components for 3.3 min. After 13 min, a 100- μL aliquot was withdrawn

from the reaction, immediately mixed with an equal volume of acetonitrile to stop the enzyme reaction, and analyzed for *N*-demethylation product by HPLC. Background oxygen consumption, possibly due to NADH oxidase enzyme activity in the partially purified Ccr, was quantitated in control reactions containing all reaction components except paraxanthine.

Formaldehyde Determination

Production of formaldehyde during *N*-demethylation of paraxanthine was determined by derivatizing formaldehyde with Nash reagent prepared by the method of Jones *et al.* (1999). Twenty μL Nash reagent was added to 50 μL Ndm reaction sample plus 50 μL acetonitrile. This mixture was incubated at 51°C for 12 min. After cooling to room temperature, the 3,5-diacetyl-1,4-dihydrolutidine formed from formaldehyde and Nash reagent was analyzed at 412 nm by a HPLC equipped with a photodiode array detector. Standards were prepared with known concentrations of formaldehyde added to control Ndm enzyme reaction mixtures without paraxanthine.

Analytical Procedures

Identification and quantification of caffeine and related methylxanthines and their metabolites were conducted with a Shimadzu LC-10AD HPLC system equipped with a photodiode array detector and a Shimadzu LCMS-2010EV single-stage quadrupole mass analyzer. Compounds were separated on a Hypersil BDS C18 column (4.6 by 125 mm). Methanol-water-acetic acid (25:75:0.5, vol/vol/vol) was used as the mobile phase with a flow rate of 0.5 mL·min⁻¹. For analysis of theophylline metabolites, the mobile phase was changed to methanol-water-acetic acid (7.5:92.5:0.5, vol/vol/vol) for better resolution. The metabolites resolved by the C₁₈ column first passed through the photodiode array detector, during which UV-visible absorption spectra were recorded. Then molecules were ionized by ESI in positive-ion mode. The following selected ions corresponding to the M+1 molecular ions of compounds were monitored: caffeine, *m/z*

195; theobromine, theophylline, and paraxanthine, m/z 181; 1-methylxanthine, 3-methylxanthine, and 7-methylxanthine, m/z 167; 1,3-dimethyluric acid, m/z 197; 1-methyluric acid and 3-methyluric acid, m/z 183; uric acid, m/z 169; and xanthine, m/z 153.

During purification of Ndm, identification and quantification of methylxanthines and their metabolites were conducted with a Shimadzu LC-20AT HPLC system equipped with a SPD-M20A photodiode array detector and a Hypersil BDS C₁₈ column (4.6 by 125 mm) as described above. For analysis of 3,5-diacetyl-1,4-dihydrolutidine, methanol-water-acetic acid (30:20:0.5, v/v/v) was used as an isocratic mobile phase at a flow rate of 0.5 mL·min⁻¹.

Protein concentration was determined by the Bradford method (Bradford, 1976) using bovine serum albumin as the standard with a dye reagent purchased from Bio-Rad. The N-terminal amino acid sequences of both Ndm subunits were determined by Edman degradation (Edman, 1950) with a Model 494 Procise protein/peptide sequencer (Perkin Elmer Applied Biosystems, Waltham, MA) at the Protein Facility, Iowa State University, Ames, Iowa. Iron content in Ndm was determined by ICP-MS. An aliquot of purified Ndm was mixed with an equal volume of trace metal-free, ultrapure concentrated nitric acid. The mixture was heated at 160 °C for 1 h to breakdown all organic materials. The acid digest was then diluted appropriately with ultrapure water for quantification of iron by a Thermo X-series II ICP-MS system at the Department of Geosciences, University of Iowa. The ICP-MS system was calibrated with high-purity iron standard solution. Bovine cytochrome *c* was used as a positive control. DNA sequences were determined at the DNA core facility, College of Medicine, University of Iowa.

Molecular Biology Kits

Gel Purification

DNA bands amplified by PCR were purified from agarose gels using the QIAquick Gel Extraction Kit (Qiagen, Duesseldorf, Germany). All buffers and materials used were provided with the kit. Briefly, after separating DNA by agarose gel electrophoresis, the section containing the desired band was excised from the gel with a scalpel. The gel slices were dissolved by incubation for 10 min at 50 °C in three gel volumes QG buffer. One gel volume isopropanol was added to the dissolved gel and DNA mixture to provide the proper binding conditions. Up to 400 mg agarose was loaded onto a QIAquick spin column and centrifuged at 17,900×g for one min to bind the DNA to the silica membrane in the provided spin columns. Residual agarose was washed from the columns and bound DNA was then washed with 0.5 mL QG buffer. The column was washed with 0.75 mL PE buffer, and DNA was eluted from the column with 50 µL warm (55 °C) water.

PCR Cleanup

When described below, PCR amplified products were separated from the PCR reaction mixture containing DNA template, primers, polymerase, and buffers with the QIAquick PCR Purification Kit (Qiagen). All buffers and materials used were provided in the kit. Five volumes PBI buffer were added to one volume of the PCR sample, and the PCR product was bound to a silica membrane-containing spin column by centrifugation at 17,900×g for one min. After washing the column with 0.75 mL PE buffer, purified PCR product was eluted from the column with 50 µL warm (55°C) water.

Plasmid extraction

Plasmids in *E. coli* cells were extracted and purified with the GeneJET Plasmid Miniprep Kit (Fermentas, Glen Burnie, MD). All buffers and materials used were

provided in the kit. Briefly, cells grown in LB medium were centrifuged at $17,900\times g$ and the supernatant was discarded. After suspending the pellet in 0.25 mL resuspension solution, cells were lysed by addition of 0.25 mL SDS and alkaline lysis solution. Following lysis, 0.35 mL neutralization solution was added in order to precipitate cellular components and SDS and to provide proper binding conditions in the mixture. The formed precipitate was separated from the mixture by centrifugation at $17,900\times g$ for ten min, and the plasmid DNA in the resulting supernatant was bound to a silica membrane in the spin columns by centrifugation for one min. Bound DNA was washed twice with 0.5 mL wash solution and then eluted with 50 μ L warm ($55\text{ }^{\circ}\text{C}$) water.

TA cloning

PCR reaction products were TA-ligated to the pGEM-TEZ vector using the pGEM-TEZ vector system (Promega) for isolation and future amplification of the desired PCR product. A volume of 1-3 μ L PCR reaction mixture was added to 5 μ L 2x T4 ligase buffer, 1 μ L 50 ng/ μ L pGEM-TEZ vector, and 1 μ L T4 DNA ligase, and the reaction was incubated for 16 h at $16\text{ }^{\circ}\text{C}$ unless otherwise noted. Ligation mixture (0.5-2 μ L) was electroporated into 40 μ L JM109 cells, and rescued cells were incubated overnight on LBAXI agar. White colonies were screened for an insert of desired length by colony PCR with primers T7 and SP6 (Table A1) using PCR program 13 described in Table 2.1. A single blue colony was also screened as the negative (empty plasmid) control.

Electroporation

Plasmids were introduced into *E. coli* JM109, *E. coli* BL21(DE3), *E. coli* 10G, or ElectroMAX *E. coli* DH10B electrocompetent cells by electroporation with a GenePulser Xcell electroporation unit (Bio-Rad). Approximately 0.5-3 μ L plasmid stock was added to 40 μ L JM109 cells in a 2-mm electroporation cuvette (Bio-Rad) and subjected to 2.5 kV, 200 Ω , and 25 μ F for 4-5 ms. Alternatively, plasmid stock was added to 20 μ L BL21(DE3), DH10B, or *E. coli* cells in a 1-mm electroporation cuvette

(Bio-Rad) and subjected to 1.8 kV, 200 Ω , and 25 μ F for 4-5 ms. Transformant cells were rescued by incubation in 1 mL SOC medium at 37 °C and 250 rpm rotary shaking for 1 h, plated on LBA or LBAXI agar, and incubated overnight at 37 °C.

PCR

PCR reactions were carried out with an Eppendorf Mastercycler ep gradient S thermocycler (Eppendorf, Hamburg, Germany) in 0.2 mL PCR tubes (RPI). Unless otherwise noted, a typical 25 μ L reaction contained 0.2 μ M forward primer, 0.2 μ M reverse primer, 0.2 mM dNTPs, 2.5 μ L 10x Taq Buffer, 0.5 μ L Taq polymerase, and an appropriate amount of template (2-50 μ g DNA or 0.5 μ L overnight culture).

Table 2.1. Temperatures and times of each step and the number of cycles performed in the different PCR reactions used in this study.

Program	Heating		Melting		Annealing		Extension		Final		Number of cycles
	°C	min	°C	s	°C	s	°C	min	°C	min	
1	95	3	95	30	52	30	72	2.5	72	10	30
2	95	3	95	30	55	30	72	0.5	72	10	35
3	95	3	95	30	55	30	72	0.75	c. b.*		5
		f. p.*	95	30	58	30	72	0.75	72	10	30
4	95	3	95	30	58	30	72	3	72	10	30
5	95	3	95	30	60	30	72	3	72	10	30
6	95	0.5	95	30	55	30	68	8	-	-	18
7	94	2	94	30	62	30	72	2	c. b.		10
		f. p.	94	30	60	30	72	2	72	10	20
8	94	2	94	30	60	30	72	1.16	68	10	30
9	98	0.5	98	10	60	30	72	3.5	72	5	20
10	95	3	95	30	58	30	72	1	72	10	30
11	95	0.5	95	30	55	60	68	7	-	-	15
12	95	3	95	30	58	30	72	0.75	72	10	30
13	95	3	95	30	60	30	72	1/kb	72	10	35

* c. b., continued below; f. p., from previous. Programs 3 and 7 used two different annealing temperatures for different cycles.

Table 2.1 contains a list of all thermocycler programs used for PCR amplification. An initialization, or heating, step was first performed in order to activate the polymerase. This step also served to lyse cells during colony/culture PCR. The temperature was then cycled through multiple melting, annealing, and extension times, followed by a final extension time of 5-10 min. Reactions were held at 4°C or ice for short-term storage. Long-term storage of PCR reactions, including storage overnight, was at -20 °C. Negative controls of the PCR reactions were performed by excluding the forward primer, reverse primer, or template in order to confirm that the PCR products observed in the reaction were due to specific binding of primers to the template. Following PCR, production of amplified DNA was observed by separating between 0.5 to 5 µL reaction *via* agarose gel electrophoresis as described above.

All PCR reactions performed in this study are listed below in Table 2.2. For a comprehensive list of all PCR primers and their sequences, see Table A1.

Colony/Culture PCR

In order to screen transformants for insertion of the desired DNA sequence into the plasmid, colonies or cultures of single colonies were subjected to PCR. A sterile toothpick was used to scrape part of a single colony off of the plate upon which it was growing, and the collected culture was either directly added to the PCR reaction or inoculated to 4 mL LB with antibiotic. After overnight incubation at 37 °C with 250 rpm shaking, 0.5 µL culture was then added to the PCR reaction. Cultures and colonies were screened with PCR program 13, in which cells were lysed and Taq polymerase activated by initial heating to 95 °C for 3 min. Reactions were then cycled 35 times at 95 °C for 30 s, 60 °C for 30 s, and 72°C for 1 min/kb, followed by a final extension at 72 °C for 10 min.

Table 2.2. A comprehensive list of all PCR reactions, and the templates, primers, and time programs used in each reaction, excluding colony/culture screening.

Reaction Name	Template	Forward Primer	Reverse Primer	PCR Program(s)
1A	gDNA	A-degF	B-degR	1
1B	gDNA	B-degF	A-degR	1
1C	gDNA	A-degF	B-degF	1
1D	gDNA	A-degR	B-degR	1
A1	gDNA	A-degF2	RieskeR	2
A2	gDNA	A-degF3	RieskeR	2
B1	gDNA	B-degF2	RieskeR	2
B2	gDNA	B-degF3	RieskeR	2
A1-1	gDNA	A-degF	cdm-R1	3
A1-2	gDNA	A-degF2	cdm-R1	3
A1-2	gDNA	A-degF3	cdm-R1	3
A1-4	gDNA	A-speF	cdm-R1	3
B1-1	gDNA	B-degF	cdm-R1	3
B1-2	gDNA	B-degF2	cdm-R1	3
B1-3	gDNA	B-degF3	cdm-R1	3
B1-4	gDNA	B-speF	cdm-R1	3
B2-1	gDNA	B-degF	cdm-R2	3
B2-2	gDNA	B-degF2	cdm-R2	3
B2-3	gDNA	B-degF3	cdm-R2	3
B2-4	gDNA	B-speF	cdm-R2	3
B3-1	gDNA	B-degF	cdm-R3	3
B3-2	gDNA	B-degF2	cdm-R3	3
B3-3	gDNA	B-degF3	cdm-R3	3
B3-4	gDNA	B-speF	cdm-R3	3
E1-1	EcoRI library	A-speF2	Marcy	4
E2-1	EcoRI library	A-speF2	pUC19R	4
S1-1	SmaI library	A-speF2	Marcy	4
S2-1	SmaI library	A-speF2	pUC19R	4
E1-2	E1-1	A-speF3	Marcy	5
E2-2	E2-1	A-speF3	pUC19R	5
S1-2	S1-1	A-speF3	Marcy	5
S2-2	S2-1	A-speF3	pUC19R	5

Table 2.2. Continued

Reaction Name	Template	Forward Primer	Reverse Primer	PCR Program(s)
A5'-1	EcoRI library	pUC19R2	cdm-R1	5
A5'-2	A5'-1	pUC19R	A-speR2	5
B1-0	EcoRI library	B-iPCR-F1	B-iPCR-R1	6
B2-0	EcoRI library	B-iPCR-F2	B-iPCR-R2	6
B1-1	B1-0	B-speF3	pUC19R2	7
B2-1	B2-0	B-speF3	pUC19R2	7
B3-1	EcoRI library	B-speF3	pUC19R2	7
B1-2	B1-1	B-speF6	pUC19R	7
B2-2	B2-1	B-speF6	pUC19R	7
B3-2	EcoRI library	B-speF6	pUC19R	7
B5'1-1	SmaI library	Marcy	B-speR10	4
B5'2-1	SmaI library	pUC19R2	B-speR10	4
B5'1-2	B5'1-1	Marcy	B-speR11	5
B5'2-2	B5'2-1	pUC19R2	B-speR11	5
B3'1-1	SmaI library	B-speF7	Marcy	4
B3'2-1	SmaI library	B-speF7	pUC19R2	4
B3'1-2	B3'1-1	B-speF8	Marcy	5
B3'2-2	B3'2-1	B-speF8	pUC19R	5
B3'2-3	B3'2-1	B-DownF1	B-DownR1	5
B3'2-4	B3'2-1	B-DownF2	B-DownR1	5
B3'2-5	B3'2-1	B-DownF3	B-DownR2	5
A-clone	gDNA	pET-ndmA-F	pET-ndmA-R	10
A-His	pET32a/ <i>ndmA</i>	ndmA-sdm-F	ndmA-sdm-R	11
B-clone1	gDNA	B-degF	B-R-XhoI	12
B-clone2	pGEM-TZ/ <i>ndmB</i>	B-F-AseI	B-R-XhoI	12
B-His1	pGEM-TZ/ <i>ndmB</i>	OE-PCR-F2	OE-PCR-R	8
B-His2	pET32a	B-His1 megaprimer		9
B3'3-1	EcoRI library	ROx-F1	Marcy	4
B3'4-1	EcoRI library	ROx-F1	pUC19R2	4
B3'3-2	B3'3-1	ROx-F2	Marcy	5
B3'4-2	B3'4-1	ROx-F2	pUC19R	5

Location of *ndmA* and *ndmB* Relative to Each Other

In order to determine the relative orientation of *ndmA* and *ndmB* to each other, reactions 1A, 1B, 1C, and 1D were carried out with Taq polymerase and using PCR program 1.

Sequencing of *ndmA* and its Flanking Regions

The gene coding for NdmA, *ndmA*, was amplified by traditional PCR with degenerate primers and by nested PCR with specific primers. The 250-bp specific PCR products amplified in reactions A1 and A2 using PCR program 2 were isolated by subjecting 3 μ L both reactions to TA ligation as described above. A volume of 2 μ L TA ligation products were electroporated into 40 μ L JM109 cells, and rescued cells were incubated overnight at 37 °C on LBAXI agar. Five white colonies were chosen from each plate for colony screening using T7 and SP6 primers with PCR program 13. A single blue colony served as the negative (empty plasmid) control. One of the five colonies from both reactions was inoculated into 4 mL LBA broth and cultured overnight at 37 °C and 250 rpm shaking. The plasmids were subsequently extracted from overnight cultures using a plasmid preparation kit (Fermentas) described above and submitted for DNA sequencing.

Reactions A1-1, A1-2, A1-3, and A1-4 were performed to amplify the majority of the *ndmA* sequence from gDNA with Taq DNA polymerase using PCR program 3 and viewed by separation on a 0.8% acrylamide gel as described above. Reaction A1-1 was TA ligated and 1 μ L of ligation reaction was electroporated into 40 μ L JM109 cells. Rescued cells were plated on LBAXI agar and incubated overnight at 37 °C. Three white colonies were grown overnight in 4 mL LBA broth, and their plasmids were extracted and submitted for DNA sequencing with T7 and SP6 primers.

The 3' end of the *ndmA* sequence and the sequences flanking both ends of the gene were determined using a nested PCR approach described by Porter-Jordan *et al.*

(1990) with either Taq or Pfu DNA polymerases. Primary reactions E1-1, E2-1, S1-1, and S2-1 were carried out with PCR program 4. Templates for the primary reactions were EcoRI and SmaI gDNA libraries previously prepared from CBB5 by Dr. Michael Louie. Secondary (nested) PCR reactions E1-2, E2-2, S1-2, and S2-2 were performed with PCR program 5. Reactions E1-1, E2-1, S1-1, and S2-1 were added directly without any cleanup to reactions E1-2, E2-2, S1-2, and S2-2, respectively, to serve as template. The 3-kb PCR product observed in reaction E1-2 was gel purified to 10 ng/ μ L from 120 μ L reaction mixture and submitted for DNA sequencing using A-speF3, Marcy, A-3'1F, A-3'1R, A-3'2F, and A-3'2R primers.

The sequence 5' to *ndmA* was identified using reactions A5'-1 and A5'-2 with Taq polymerase using PCR program 5. A 3-kb PCR product was gel purified from 150 μ L reaction A5'-2 to 50 ng/ μ L and submitted for DNA sequencing with A-speR2, pUC19R, A-5'1F, A-5'1R, A-5'2F1, A-5'2F2, A-5'2R, A-5'3F, and A-5'3R primers.

Sequencing of *ndmB* and its Flanking Regions

The gene coding for NdmB, *ndmB*, was amplified by traditional PCR with degenerate primers and by a combination of site-directed mutagenesis and nested PCR techniques with specific primers. The 250-bp specific PCR products amplified in reactions B1 and B2 with PCR program 2 were viewed on a 0.8% acrylamide gel and isolated by subjecting 3 μ L both reactions to TA ligation as described above. A volume of 2 μ L TA ligation products were electroporated into 40 μ L JM109 cells, and rescued cells were incubated overnight at 37 °C on LBAXI agar. Five white colonies were chosen from each plate for colony screening using T7 and SP6 primers with PCR program 13. A single blue colony served as the negative (empty plasmid) control. One of the five colonies from both reactions was inoculated into 4 mL LBA broth and cultured overnight at 37 °C and 250 rpm shaking. The plasmids were subsequently

extracted from overnight cultures using a plasmid preparation kit (Fermentas) described above and submitted for DNA sequencing with T7 and SP6 primers.

Reactions B1-1, B1-2, B1-3, B1-4, B2-1, B2-2, B2-3, B2-4, B3-1, B3-2, B3-3, and B3-4 were performed in an attempt to amplify 50-90% of the *ndmB* sequence from gDNA with Taq DNA polymerase using PCR program 3. About 2 μ L reaction B3-1 was TA ligated and 1 μ L of ligation reaction was electroporated into 40 μ L JM109 cells. Rescued cells were plated on LBAXI agar and incubated overnight at 37 °C. Three white colonies were grown overnight in 4 mL LBA broth, and their plasmids were extracted and submitted for DNA sequencing with T7 and SP6 primers.

A combination of site-directed mutagenesis and nested PCR approaches were used to determine the complete *ndmB* sequence and flanking regions. Reactions B1-0 and B2-0 were performed to amplify the *ndmB*-containing plasmid in the EcoRI library using PCR program 6. About 1 μ L EcoRI library was added to 5 μ L 10x Pfu ultra buffer, 1.4 μ L 10 μ M forward primer, 1.3 μ L 10 μ M reverse primer, 1 μ L 10 mM dNTP mix, and 1 μ L Pfu ultra polymerase in 50 μ L total volume. Upon completion of PCR, 1 μ L DpnI was directly added to the reaction mixture and incubated 1 h at 37 °C.

Reactions B1-0 and B2-0 were used as templates for reactions B1-1 and B2-1, respectively, in a primary round of nested PCR with PCR program 7 using Taq polymerase. The EcoRI library was also used as a template in reaction B3-1 with PCR program 7 and Taq polymerase. Secondary PCR reactions B1-2, B2-2, and B3-2 were then carried out with Taq polymerase using PCR program 7. The 1.1-kb PCR product in reaction B2-2 was gel purified from 300 μ L reaction and submitted for DNA sequencing using B-speF6 and pUC19R primers.

The region 5' to *ndmB* was amplified from the SmaI library in reactions B5'1-1, B5'1-2, B5'2-1, and B5'2-2. About 3 μ L Reaction B5'1-2 was subjected to TA cloning and 1 μ L of ligation was electroporated into 20 μ L DH10B cells. Rescued cells were plated on LBAXI agar and incubated overnight at 37 °C. Ten colonies were screened for

ligated insert and vector by colony PCR with T7 and SP6 primers using PCR program 13. Two screened cultures containing the ligated plasmid, B5-7-1 and B5-7-5, were grown overnight in 4 mL LBA agar at 37 °C and 250 rpm, and their plasmids were extracted and submitted for DNA sequencing with T7 and SP6 primers. Plasmid B5-7-5 was further submitted for DNA sequencing with primers B-UpF1 and B-UpR1.

Reactions B3'1-1, B3'2-1, B3'1-2, and B3'2-2 were tested to amplify the region immediately 3' to *ndmB* from the *SmaI* library using PCR program 4 (B3'1-1 and B3'2-1) and program 7 (B3'1-2 and B3'2-2). The 4-kb PCR product from 300 µL reaction B3'2-2 was gel purified to 75 ng/µL and submitted for DNA sequencing with B-speF8 and pUC19R primers. Further sequencing of the 4-kb fragment was performed by amplifying the product from reaction B3'2-1 with Taq Select polymerase (Lucigen) using PCR program 5. The major band was purified from 250 µL reaction B3'2-3, B3'2-4, and B3'2-5 and submitted for DNA sequencing with primers B-DownF1/B-DownR1 (reaction B3'2-3), B-DownF2/B-DownR1 (B3'2-4), and B-DownF3/B-DownR2 (reaction B3'2-5).

About 3 µL reaction B3'2-5 was subjected to TA ligation as described previously. The ligation (1 µL) was electroporated into 40 µL JM109 cells, and rescued cells were incubated overnight at 37 °C. Ten colonies were screened for the ligated insert/vector by colony PCR with T7 and SP6 primers using PCR program 13. Two of the colonies, B3-1 and B3-6 were grown overnight in 4 mL LBA broth, and their plasmids were extracted and submitted for DNA sequencing with B-DownF3 and B-DownR2 primers. Further sequencing of the insert was performed on plasmid B3-6 with primers B-DownF4, B-DownF5, and B-DownR3.

An additional 2 kb sequence 3' of the already obtained *ndmB* 3' flanking sequence was determined with Taq polymerase using nested PCR with the *EcoRI* library. Reactions B3'3-1 and B3'4-1 were performed as primary reactions with PCR program 4. Secondary PCR reactions B3'3-2 and B3'4-2 were performed with PCR program 5. The

2 kb major band was gel purified from 100 μL both reactions to 80 $\text{ng}/\mu\text{L}$, and 800 ng were submitted for DNA sequencing with ROx-F2, ROx-F3, ROx-R1, Marcy, and pUC19R primers.

Cloning

Cloning of *ndmA*

The full length *ndmA* gene was amplified from gDNA with Taq polymerase by reaction A-clone (Table 2.2) in 75 μL total volume using PCR program 10. Following amplification, the reaction contents were concentrated to 16 μL with an Eppendorf Vacufuge and incubated at 37 $^{\circ}\text{C}$ for 16 h with 2 μL 10x NEB Buffer 4, 1 μL EcoRI, and 1 μL NdeI restriction enzymes. A heat kill step of 65 $^{\circ}\text{C}$ for 20 min was used to inactivate the restriction enzymes, and the cut *ndmA*/NdeI/EcoRI insert was purified using the PCR cleanup kit described above to a concentration of 5 $\text{ng}/\mu\text{L}$.

Approximately 2 μg pET32a vector was also cut at 37 $^{\circ}\text{C}$ for 16 h with 2 μL NEB Buffer 4, 1.5 μL NdeI, and 1.5 μL EcoRI in 20 μL total volume. Following overnight digestion, 3 μL 10x Antarctic Phosphatase (AP) buffer, 6 μL dH_2O , and 1 μL AP enzyme were added to the digested vector, the reaction mixture was incubated for one h at 37 $^{\circ}\text{C}$, followed by a heat kill step at 70 $^{\circ}\text{C}$ for 15 min, and the pET32a/NdeI/EcoRI/AP vector was gel purified to a concentration of 10 $\text{ng}/\mu\text{L}$.

Ligation of the *ndmA*/NdeI/EcoRI insert to the pET32a/NdeI/EcoRI/AP vector was carried out in a 25 μL reaction containing 70 ng vector, 75 ng insert, 2.5 μL 10x T4 ligase buffer, and 0.5 μL T4 DNA ligase at 16 $^{\circ}\text{C}$ for 16 h. Five separate electroporations of 3 μL ligated pET32a/*ndmA* reaction into 40 μL *E. coli* JM109 electrocompetent cells (15 μL plasmid and 200 μL cells total) were carried out in a 2-mm electroporation cuvette (Bio-Rad) as described previously. The cells were rescued by incubating in 1 mL SOC medium at 37 $^{\circ}\text{C}$ for 1 h with 250 rpm shaking, and each transformation was plated onto LBA agar plates, which were incubated at 37 $^{\circ}\text{C}$ overnight. A total of 33 transformant

colonies grew overnight. These colonies were screened with PCR program 13, using T7 and T7term primers, and an insert of correct size was found in three colonies, colonies A4, A7, and A29.

Colonies A4, A7, and A29 were inoculated into 4 mL LBA broth and incubated overnight at 37 °C with 250 rpm shaking. Following overnight incubation, plasmids were extracted from the three cultures and submitted for sequencing using the T7 and T7term primers. Plasmid A29 (0.5 µL) was subsequently electroporated into 20 µL BL21(DE3) cells as described above and 10 µL rescued cell suspension was spread and incubated overnight on LBA agar. A single colony from the overnight incubation was grown overnight in 4 mL LBA broth, mixed 1:1 (v/v) with 50% glycerol, and then stored at -80 °C.

Cloning of *ndmA-His*

The pET32a/*ndmA* vector was mutated by site-directed mutagenesis (Bauer *et al.*, 2002) by removing the stop codon from *ndmA* (*ndmA-His*) to allow for the fusion of six histidine residues at the C-terminus of NdmA (NdmA-His). PCR of the A-His reaction (Table 2.2) was carried out with PCR program 11 in order to amplify the entire plasmid and add the mutation. After cooling to 4 °C for 2 min, 1 µL DpnI restriction enzyme was added, and the reaction was incubated at 37 °C for 1 h to digest the methylated pET32a/*ndmA* template plasmid, leaving only the amplified pET32a/*ndmA-His* plasmid.

About 0.5 µL pET32a/*ndmA-His* plasmid was electroporated into 40 µL JM109 cells as described previously, and 100 µL rescued cell suspension was spread on LBA agar. Following overnight incubation at 37 °C, a single colony was inoculated into 4 mL LBA agar and incubated overnight at 37 °C and 250 rpm shaking. The pET32a/*ndmA-His* vector was then extracted from the overnight culture and submitted for sequencing using the T7 and T7term primers in order to confirm removal of the stop codon.

Finally, 1 μL 30 ng/ μL pET32a/*ndmA-His* was electroporated into 20 μL BL21(DE3) cells, and 10 μL rescued cell suspension was spread on an LBA plate and incubated overnight at 37 °C. A single resultant colony was inoculated into 4 mL LBA broth and incubated overnight at 37 °C with 250 rpm shaking, whereupon the culture was mixed 1:1 (v/v) with 50% glycerol and stored at -80 °C.

Cloning of *ndmB*

The *ndmB* sequence was amplified in reaction B-clone1 with PCR program 12. Approximately 3 μL reaction B-clone1 was subjected to TA cloning, and 1 μL ligation reaction mixture was added to 20 μL DH10B cells and electroporated as described above. Rescued cells were spread on two LBAXI plates and incubated overnight at 37 °C. Thirty four colonies were randomly selected from over 200 that grew on the LBAXI plates and inoculated into 4 mL LBA broth. Following overnight incubation at 37 °C and 250 rpm, cultures were screened for insertion of *ndmB* with T7 and SP6 primers using PCR program 13. Only one of the 34 colonies, E10, was found to contain a 1-kb insert, and the plasmids were therefore extracted from colony E10. Ligation of *ndmB* with pGEM-TEZ plasmid, creating plasmid pGEM-TEZ/*ndmB*, was confirmed by DNA sequencing of the extracted plasmid with T7 and SP6 primers.

The *ndmB* sequence was amplified from pGEM-TEZ/*ndmB* with AseI and XhoI sequences at the 5' and 3' ends, respectively, in the B-clone2 reaction (Table 2.2) using PCR program 12. The specific 1.1-kb *ndmB* product amplified in the reaction was gel purified from 100 μL reaction B-clone2 and eluted in 50 μL dH₂O. Digestion of the amplified *ndmB* sequence at 37 °C for 16 h was carried out by adding 6 μL 10x NEB Buffer 3, 1.7 μL AseI, and 1.7 μL XhoI to the *ndmB* insert (60 μL total volume of digestion reaction), and the digested 1.1-kb *ndmB*/AseI/XhoI insert was gel purified to a concentration of 25 ng/ μL .

The pET32a vector was digested in two separate steps. First, 40 μL of 37 ng/ μL pET32a was digested in 50 μL total volume with 5 μL 10x NEB Buffer 2, 0.5 μL 100x BSA (NEB), and 2 μL XhoI at 37 °C for 3 h. The pET32a/XhoI cut plasmid was purified with a PCR cleanup column to 42.5 μL , to which 5 μL 10x NEB Buffer 5 and 2.5 μL NdeI were added. This second digestion was incubated for 3 h at 37 °C, followed by dephosphorylation by 1 μL AP and 6 μL 10X AP buffer and 37 °C incubation for another hour. All enzymes in the reaction were subjected to a heat-kill step at 80 °C for 15 min, and the pET32a/XhoI/NdeI/AP was gel purified to 5 ng/ μL .

Ligation of insert to vector was carried out by adding 1.7 μL 10x T4 ligase buffer, 0.5 μL T4 DNA ligase, and 2.5 μL 25 ng/ μL *ndmB*/AseI/XhoI to 12.5 μL 5 ng/ μL pET32a/NdeI/XhoI/AP and incubating at 16 °C for 16 h. A 1 μL aliquot of the ligation containing pET32a/*ndmB* was electroporated into 20 μL DH10B cells as described above. The eight resultant colonies were screened for pET32a/*ndmB* using T7 and T7term with PCR program 13. Four colonies containing pET32a/*ndmB*, B2, B3, B4, and B8 were grown overnight in LBA broth at 37 °C and 250 rpm shaking, mixed 1:1 (v/v) with 50% glycerol, and stored at -80 °C. About 4 mL culture B3 was subjected to plasmid purification, and the presence of a non-mutated *ndmB* sequence in plasmid B3 was confirmed by DNA sequencing with T7 and T7term primers.

Cloning of *ndmB*-His

Over-extension PCR (OE-PCR) described by Bryksin and Matsumura (2010) was used to clone *ndmB* into pET32a with a six histidine tag fused to the 3' end of *ndmB* (*ndmB*-His). Reaction B-His1 and PCR program 8 were used with Taq polymerase to amplify the *ndmB*-His megaprimer by excluding the *ndmB* stop codon from the OE-PCR-R reverse primer. The 1.1-kb *ndmB* megaprimer was gel purified from 100 μL reaction B-His1 to 15 ng/ μL and inserted into pET32a by a second round of PCR, reaction B-His2. About 0.3 μL Phusion HF DNA polymerase was added to 0.4 μL 10 mM dNTP

mix, 4 μL 5x HF buffer, 4.3 μL dH_2O , 10 μL 15 ng/ μL megaprimer, and 1 μL 3 ng/ μL pET32a (20 μL total reaction volume). The reaction was subjected to PCR program 9, following which 1 μL DpnI restriction enzyme was added to the reaction and incubated at 37 °C for 1 h.

An aliquot of 0.5 μL pET32a/*ndmB-His* was electroporated into 25 μL *E. cloni* cells, and the rescued cells were plated onto LBA agar and incubated overnight at 37 °C. Eleven colonies were screened for pET32a/*ndmB-His* plasmid by colony PCR with T7 and T7term primers using PCR program 13. Two colonies containing the pET32a/*ndmB-His* vector, colonies BH4 and BH5, were incubated in 4 mL LBA broth overnight at 37 °C and 250 rpm shaking, and their plasmids were extracted and submitted for DNA sequencing with T7 and T7term primers. A 0.5 μL aliquot of plasmid BH5 was electroporated into 20 μL BL21(DE3) cells as described above, and the rescued cells were plated onto LBA agar and grown overnight at 37 °C. A single colony of BL21(DE3) cells containing the pET32a/*ndmB-His* plasmid was grown overnight in 4 mL LBA broth, mixed 1:1 with 50% glycerol, and stored at -80 °C.

Functional Expression

Functional expression of *ndmA*, *ndmA-His*, *ndmB*, and *ndmB-His* was carried out in the same manner for each enzyme. An inoculum culture of BL21(DE3) cells containing the desired plasmid was prepared by adding a small amount of cells from the frozen glycerol stock to LBA medium. Cultures were incubated in a 250-mL Kimax culture flask at 37 °C with 250 rpm shaking overnight. The cells were added to fresh LBA medium to a final OD_{600} of approximately 0.1 and grown at 37 °C with 250 rpm shaking. When the OD_{600} reached 0.5 (approximately 1-2 h), sterile FeCl_3 was added to a final concentration of 10 μM and the culture was shifted to the induction temperature to be tested (between 18-37 °C). IPTG was added to a final concentration of 0.1 to 1 mM when the OD_{600} reached 0.8-1.0 (approximately 1-2 h after addition of FeCl_3). Induced

cells were then grown between 4.5 to 18 h post-induction and harvested by centrifugation. Harvested cells were suspended in KPGD buffer and lysed by passing twice through a chilled French press. The lysate was centrifuged at $30,000 \times g$ for 20 min in order to separate the soluble protein in the supernatant from the insoluble pellet, and protein preparations were analyzed by SDS-PAGE to determine expression of soluble recombinant enzyme.

Purification of His-Tagged Proteins

The expressed NdmA-His and NdmB-His enzymes were purified on a 1-mL (column volume) Nickel/NTA column (GE Healthcare) at a flow rate of $1 \text{ mL} \cdot \text{min}^{-1}$ and temperature of $4 \text{ }^\circ\text{C}$ using an ÄKTA Purifier FPLC system. The column was pre-equilibrated in binding buffer consisting of 300 mM NaCl and 10 mM imidazole in 25 mM KP_i buffer. Imidazole and NaCl were added to final concentrations of 10 mM and 300 mM, respectively, to the soluble fraction of NdmA-His and NdmB-His cell lysates, and 4 mL of each lysate was passed through the nickel column to bind His-tagged proteins. Unbound protein was washed from the column with 10 mL binding buffer, and the bound protein was then eluted with 10 mL elution buffer consisting of 300 mM NaCl and 250 mM imidazole. Protein eluants were collected in 1 mL fractions, and the bound protein was concentrated to 3 mL using 30k MWCO tubes by centrifugation as described previously. NdmA-His was dialyzed (MWCO of 10k) at $4 \text{ }^\circ\text{C}$ three times against 1 L KPGD for 2 hours, 2 h, and 12 h to remove imidazole. Purified NdmA-His and NdmB-His were stored short-term on ice and at $-80 \text{ }^\circ\text{C}$ for long term storage. *N*-demethylation activity assays of the purified His-tagged proteins were performed as described above for wild-type Ndm.

CHAPTER 3
METABOLISM OF CAFFEINE, THEOPHYLLINE, AND RELATED
METHYLXANTHINES BY *PSEUDOMONAS PUTIDA* CBB5

Introduction

Pseudomonas putida CBB5 was isolated from soil by an enrichment procedure with caffeine as the sole source of carbon and nitrogen. Initial results suggested that caffeine was degraded by sequential *N*-demethylation to form xanthine. Surprisingly, CBB5 was also able to grow on theophylline as the sole source of carbon and nitrogen. Metabolism of theophylline, however, appeared to be initiated by oxidation of theophylline to 1,3-dimethyluric acid, which was then sequentially *N*-demethylated to uric acid. The metabolism of theophylline *via* both C-8 oxidation and *N*-demethylation was curious, as no report of the pathways combining to degrade methylxanthines has been described in the literature.

There have been many studies regarding the degradation of caffeine and related methylxanthines by bacteria *via N*-demethylation (Woolfolk, 1975; Blecher and Lingens, 1977; Middelhoven and Bakker, 1982; Asano *et al.*, 1993; Mazzafera *et al.*, 1996; Madyastha and Sridhar, 1998; and Yu *et al.*, 2008). Although the bacterial metabolism of caffeine has been well documented, no report has been published concerning the metabolism of theophylline by bacteria. Here the metabolism of caffeine and theophylline by *Pseudomonas putida* CBB5 is investigated and reported in detail. Substrate consumption and product formation in growth media, resting cell suspensions, and cell extracts of CBB5 were studied in order to determine the exact degradation pathways for both caffeine and theophylline. This work presents the first detailed characterization of bacterial metabolism of theophylline.

Growth and Degradation of Caffeine and Theophylline by
CBB5

CBB5 grew in M9 medium when caffeine was provided as the sole carbon and nitrogen source (C medium), reaching stationary phase with an OD₆₀₀ of approximately 0.4 after 72 h of incubation. During this period, the caffeine concentration in the medium decreased from 2.5 g·L⁻¹ to 0.2 g·L⁻¹. CBB5 growth rate and final cell density were significantly increased by supplementation of M9-caffeine medium with YNB (CY medium) or with soytone (CS medium) as a second nitrogen source (Figure 3.1).

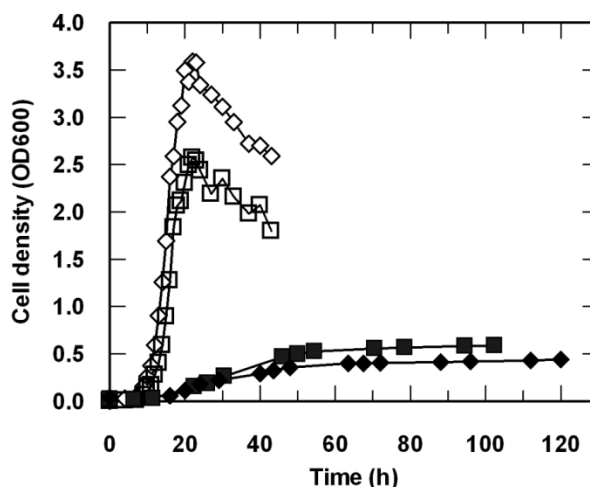


Figure 3.1. Growth curves of *P. putida* CBB5 in soytone-free (closed symbol) and soytone supplemented (open symbol) M9 media with caffeine (◆, ◇) or theophylline (■, □) as carbon and nitrogen sources. Concentration of caffeine in soytone-free and soytone supplemented media was 2.5 g·L⁻¹. Concentration of theophylline in soytone-free media was 1 g·L⁻¹; 2.5 g·L⁻¹ was used in soytone supplemented media.

When grown in CY medium, CBB5 completely utilized 2.5 g·L⁻¹ caffeine and reached an OD₆₀₀ of 1.06 in 53 h. In contrast, it took only 20 h for a culture of CBB5 to consume the same amount of caffeine in CS medium, growing to an OD₆₀₀ of 2.43.

Although YNB contains higher concentrations of various vitamins than does soytone, 18

amino acids are present only in soytone. These differences in composition might account for the increased growth with soytone when compared with YNB.

CBB5 also grew in M9 medium when theophylline was provided as sole source of carbon and nitrogen. A concentration of $2.5 \text{ g}\cdot\text{L}^{-1}$ theophylline almost completely inhibited cell growth. However, CBB5 reached stationary phase with an OD_{600} of 0.56 after 72 h incubation when initial theophylline concentration was $1 \text{ g}\cdot\text{L}^{-1}$ (T medium), degrading approximately 60% of the theophylline. When $4 \text{ g}\cdot\text{L}^{-1}$ soytone was supplemented to the medium (TS medium), $2.5 \text{ g}\cdot\text{L}^{-1}$ theophylline was completely consumed in 30 h, and cells reached a final OD_{600} of 2.5 (Figure 3.1).

The enhanced caffeine degradation in soytone-grown CBB5 was also observed in resting cell suspension experiments. CBB5 resting cell suspensions ($\text{OD}_{600} = 4$) prepared from cells grown in C medium completely degraded 1 mM caffeine in 80 min, while a suspension of cells grown in CS medium degraded the 1 mM caffeine in only 45 min. A resting suspension of CBB5 grown in CY medium took 150 min to degrade the same amount of caffeine.

Table 3.1. Growth of CBB5 on caffeine, with or without nitrogen supplementation.

Growth Media	Final OD_{600}	Time to final OD_{600} (h)	Substrate Consumed (%)	Time to Degrade 1 mM Growth Substrate with Resting Cells (min)
M9-caffeine	0.4	72	92%	80
M9-caffeine + YNB	1.06	53	100%	150
M9-caffeine + soytone	2.43	20	100%	45
M9-theophylline	0.56	72	60%	120
M9-theophylline + soytone	2.5	30	100%	60

CBB5 resting cell suspensions prepared from cells grown in T medium degraded 1 mM theophylline in 120 min. A suspension of resting TS medium-grown CBB5 degraded the same amount of theophylline in 60 min. These results, summarized in Table 3.1 clearly showed that addition of soytone enhanced CBB5 growth and caffeine degradation. Therefore, CBB5 was cultivated in soytone-supplemented M9 medium unless otherwise noted.

Identification of Metabolites Produced from Caffeine

Degradation

Five metabolites were detected by HPLC analyses of spent media removed at different times from CBB5 growing in CS medium (Figure 3.2).

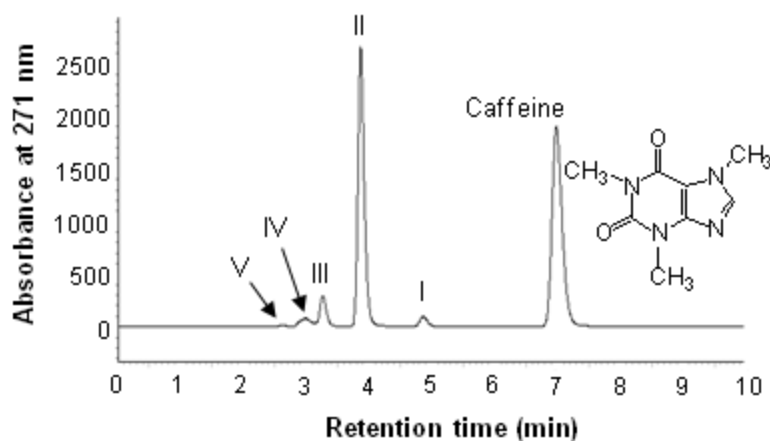


Figure 3.2. HPLC of spent medium of *P. putida* CBB5 grown in soytone-supplemented M9-caffeine medium. A sample was collected 20 h post-inoculation. The identities of the metabolites are as follows: metabolite I, paraxanthine; metabolite II, theobromine; metabolite III, 7-methylxanthine; metabolite IV, xanthine; and metabolite V, uric acid. Physical characteristics of these metabolites are shown in Table 3.2.

The retention times (Rts) and absorption spectra of the major metabolites, II and III (Table 3.2), were identical to those of theobromine and 7-methylxanthine, respectively.

Table 3.2. UV absorption spectra and ESI mass spectral properties of metabolites formed from degradation of caffeine, theophylline, and 3-methylxanthine by *P. putida* CBB5.

Growth Substrate	Metabolite	UV λ_{\max} (nm)	m/z value ^a	Identity of metabolite
Caffeine (UV λ_{\max} , 273 nm; m/z 195)	I	271	ND ^b	Paraxanthine
	II	271	181	Theobromine
	III	269	167	7-Methylxanthine
	IV	196, 267	153	Xanthine
	V	240, 284	169	Uric Acid
Theophylline (λ_{\max} , 271 nm; m/z 181)	VI	231, 287	197	1,3-Dimethyluric acid
	VII	231, 284	183	1-Methyluric acid
	VIII	234, 287	183	3-Methyluric acid
	IX	198, 267	167	1-Methylxanthine
	X	198, 271	167	3-Methylxanthine
	IV	196, 267	153	Xanthine
	V	240, 284	169	Uric Acid
3-Methylxanthine (λ_{\max} , 198 and 271 nm; m/z 167)	VIII	234, 287	183	3-Methyluric acid
	IV	196, 267	153	Xanthine
	V	240, 284	169	Uric Acid

^a m/z values of protonated molecular ions were determined by ESI mass spectrometry operating in positive-ion mode.

^b ND, not detected. No ESI mass spectrum was detected for paraxanthine, possibly because of the low concentration of this metabolite in spent media. Metabolite I was determined to be paraxanthine by comparing its HPLC Rt and UV spectrum with those of an authentic standard.

Ionization of metabolites II and III by ESI in positive-ion mode resulted in M+1 molecular ion m/z values of 181 and 167, respectively, which were identical to the

molecular weights of protonated theobromine and 7-methylxanthine. Similarly, metabolites I, IV, and V were identified as paraxanthine, xanthine, and uric acid based on comparison of Rts, absorption spectra, and ESI mass spectra with authenticated standards (Table 3.2). When CBB5 was grown in C medium, theobromine was still produced as the major metabolite, followed by 7-methylxanthine and xanthine. These results suggested that CBB5 degraded caffeine *via N*-demethylation to theobromine (major metabolite) and paraxanthine (minor metabolite), similar to previous reports for other caffeine-degrading bacteria (Mazzafera *et al.*, 1996; Yamaoka-Yano and Mazzafera, 1999; Mazzafera, 2004; Dash and Gummadi, 2006).

Catabolism of Caffeine and Related Methylxanthines by Caffeine-Grown CBB5 Resting Cells

Resting cell suspensions of CBB5 grown in CS medium ($OD_{600} = 4$) degraded 1 mM caffeine and most related methylxanthines within 60 min without any lag period (Figure 3.3A to E). Of all substrates tested, 3-methylxanthine was most rapidly degraded; 1 mM 3-methylxanthine was completely degraded in 15 min (Figure 3.3F). Addition of caffeine to a cell suspension resulted in detection of theobromine, paraxanthine, 7-methylxanthine, xanthine, and uric acid as metabolites (Figure 3.3A). This result suggested that caffeine is degraded by the *N*-demethylation pathway, as was observed in spent media of CBB5 cultures (Figure 3.2).

When theobromine was added to a resting cell suspension, only 7-methylanthine, xanthine, and uric acid were detected as metabolites (Figure 3.3B). No metabolites were observed when paraxanthine was added to the CBB5 suspension. In order to slow down the reaction, and thus determine the metabolites of paraxanthine, 2 mM paraxanthine was added to the same cell suspension at OD_{600} of 4 and 2. Significant amounts of downstream metabolites did not accumulate (Figure 3.3D), although small amounts of xanthine and uric acid were detected. Thus, paraxanthine appears to be metabolized

more rapidly than theobromine. Xanthine and uric acid were the only detected metabolites when 7-methylxanthine was added to a CBB5 resting cell suspension (Figure 3.3C).

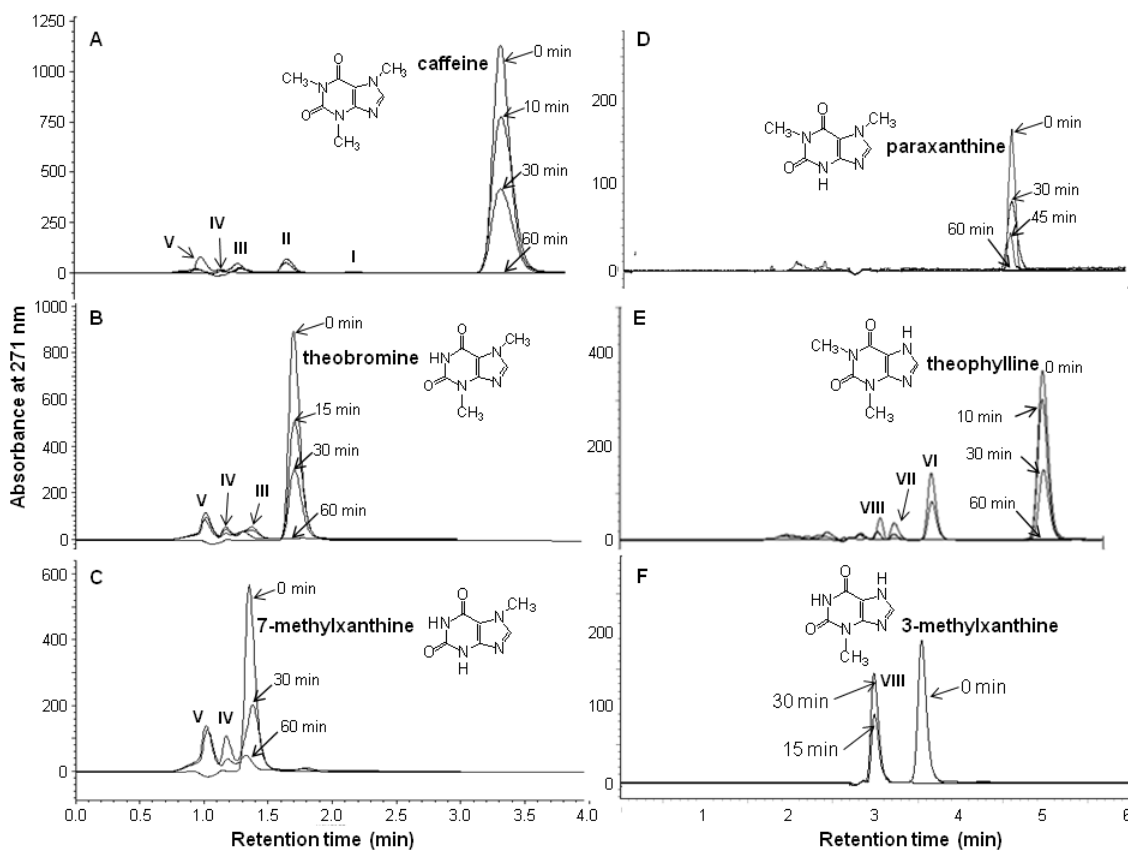


Figure 3.3. HPLC analyses of metabolites produced by *P. putida* CBB5 resting cell suspensions. CBB5 was cultivated in soytone-supplemented M9-medium. The cells were washed and resuspended at an OD_{600} of 4.0. The following compounds (1 mM) were then added to cell suspensions: (A) caffeine, (B) theobromine, (C) 7-methylxanthine, (D) paraxanthine, (E) theophylline, and (F) 3-methylxanthine; metabolite IV, xanthine; metabolite V, uric acid; metabolite VI, 1,3-dimethyluric acid; metabolite VII, 1-methyluric acid; and metabolite VIII, 3-methyluric acid. Physical characteristics of these metabolites are shown in Table 3.2.

The above results indicate that theobromine, paraxanthine, 7-methylxanthine, and xanthine are sequential downstream metabolites of caffeine. In order to cross-check this

conclusion, CBB5 was grown with theobromine, paraxanthine, and 7-methylxanthine as carbon and nitrogen source and with or without soytone supplementation. CBB5 cultures grown on these compounds as the sole carbon and nitrogen source reached OD₆₀₀ values of 0.14 to 0.56. Culturing of CBB5 on theobromine, paraxanthine, and 7-methylxanthine in soytone-supplemented M9 media increased both growth and substrate utilization: cell densities reached an OD₆₀₀ of 2.5 and substrates were completely consumed in 20 to 30 h. In the theobromine- and paraxanthine-grown cultures, 7-methylxanthine, xanthine, and uric acid were detected. Xanthine and uric acid were the only metabolites formed in 7-methylxanthine-grown cultures.

Resting cell suspensions prepared from CBB5 grown in soytone-supplemented M9 media containing theobromine, paraxanthine, or 7-methylxanthine degraded caffeine, theobromine, paraxanthine, or 7-methylxanthine at similar rates without any lag period and produced the same metabolites as observed in spent media. Thus, caffeine is *N*-demethylated to form either paraxanthine or theobromine, both of which are then *N*-demethylated to 7-methylxanthine. Xanthine is formed from *N*-demethylation of 7-methylxanthine, and is subsequently oxidized at the C-8 position to form uric acid.

Catabolism of Theophylline and 3-Methylxanthine by Caffeine-Grown CBB5

Theophylline was metabolized without any lag period when added to a CBB5 resting cell suspension prepared from cells grown in CS medium (Figure 3.3E), just as was observed with caffeine and its metabolites. Three new metabolites not observed during caffeine metabolism (metabolites VI, VII, and VIII) were formed and accumulated in the cell suspension. The absorption spectra of these metabolites (Table 3.2) were similar to those of uric acid, with a λ_{max} at ca. 287 nm, suggesting that they could be either di- or monomethyluric acids.

When preparations of resting cells incubated with theophylline were subjected to HPLC-ESI mass spectrometry analyses, the R_t and the $M+1$ molecular ion of metabolite VI (m/z 197) were identical to those of an authentic 1,3-dimethyluric acid standard. The $M+1$ molecular ions of metabolites VII and VIII were identical, with m/z values of 183, suggesting that they are protonated monomethyluric acids. The R_t of metabolite VII matched that of an authenticated standard of 1-methyluric acid, confirming its identity. Unfortunately, an authentic standard is not available commercially for confirmation of metabolite VIII as 3-methyluric acid. However, when 1 mM 3-methylxanthine was added to a CBB5 resting cell suspension prepared from cells grown in CS medium, only metabolite VIII was detected (Figure 3.3F), which further supports the conclusion that metabolite VII is 3-methyluric acid.

The above data suggest that caffeine-grown CBB5 can oxidize theophylline to 1,3-dimethyl, 1-, and 3-methyluric acids and 3-methylxanthine to 3-methyluric acid. However, these methyluric acids were not metabolized further by resting cell suspensions (Figure 3.3E and F) or crude extracts prepared from caffeine-grown CBB5. Because the detected theophylline metabolites were not further degraded and the expected *N*-demethylated theophylline metabolites (1- and/or 3-methylxanthine) were not detected, degradation of theophylline was reexamined in theophylline-grown cells.

Metabolism of Theophylline by Theophylline-Grown

CBB5

When theophylline was added to resting cell suspensions (OD_{600} , 4.0) prepared from CBB5 cells grown on TS medium, five metabolites were resolved by HPLC. The five peaks were identical in absorption spectra, R_t s, and $M+1$ molecular ions to those formed by theophylline-metabolizing resting suspensions of CBB5 grown on caffeine plus soytone: xanthine (metabolite IV), uric acid (metabolite V), 1,3-dimethyluric acid (metabolite VI), 1-methyluric acid (metabolite VII), and very likely 3-methyluric acid

(metabolite VIII [an authentic standard was not available for confirmation]). Metabolites VI, VII, and VIII again accumulated in the suspension and were not further degraded, consistent with the results for CBB5 resting cells grown in CS medium.

In order to slow the reaction, the OD₆₀₀ of the resting cell suspension was lowered to 2.0. Under this condition, two previously unobserved metabolites (metabolites IX and X) were detected transiently, although at very low concentrations. The physical properties of metabolites IX and X (Table 3.2) were identical to those of 1-methylxanthine and 3-methylxanthine, respectively, indicating that theophylline is *N*-demethylated by CBB5, similar to the caffeine metabolic pathway.

The production of 1- and 3-methylxanthine was more pronounced in CBB5 resting cells (OD₆₀₀, 4.0) grown in T medium (Figure 3.4A). More importantly, 1-methylxanthine, 3-methylxanthine, xanthine, and uric acid did not accumulate in the resting cell suspension and were completely utilized by CBB5 cells within 5 h (Figure 3.4B). Meanwhile, 1,3-dimethyluric acid and 1- and 3-methyluric acids still accumulated in the cell suspension, as observed for metabolism of theophylline by resting cell suspensions prepared from CBB5 grown in either CS (Figure 3.3E) or TS media. These methyluric acids are most likely dead-end metabolites and were estimated to account for 20 to 25% of the total theophylline metabolite pool, based on HPLC analysis with standards of known concentration.

3-Methylxanthine was completely consumed in 3 h when added to the resting cell suspension prepared from CBB5 cells grown on T medium. Only xanthine (metabolite IV), uric acid (metabolite V), and 3-methyluric acid (metabolite VIII) were detected as metabolites of 3-methylxanthine. Xanthine and uric acid accumulated transiently and were completely degraded within 4 h. Consistent with the results for CBB5 grown in C, CS, T, or TS media, 3-methyluric acid (metabolite VII) accumulated in the medium and was not degraded further (Figures 3.3F and 3.4B). When xanthine was added to the same resting cell suspension, it was completely consumed in 1 h. Uric acid was the only

metabolite detected, and it was promptly degraded. These results suggest that 3-methylxanthine, xanthine, and uric acid are sequential downstream metabolites of theophylline.

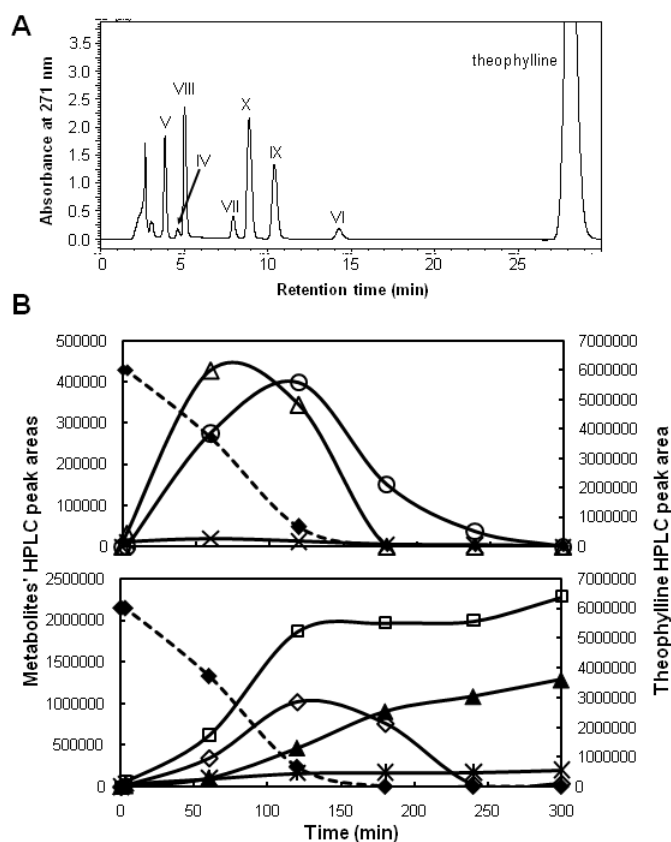


Figure 3.4. Determination of theophylline metabolites. (A) HPLC analyses of metabolites produced from theophylline by a resting cell suspension of *P. putida* CBB5 grown in soytone-free M9-theophylline medium. The identities of metabolites are shown in Table 3.2. (B) Degradation of theophylline and various metabolites by a resting cell suspension of *P. putida* CBB5 grown in soytone-free M9-theophylline medium. Symbols: ◆, theophylline; ○, 1-methylxanthine; △, 3-methylxanthine; ×, xanthine; *, 1,3-dimethyluric acid; ▲, 1-methyluric acid; □, 3-methyluric acid; and ◇, uric acid.

Theophylline *N*-demethylase activity was also detected in crude extracts of CBB5 cells grown on TS medium. Both 1- and 3- methylxanthines were detected when

theophylline was added to the crude extract (Figure 3.5). Moreover, the production of 1- and 3-methylxanthines from theophylline was enhanced by addition of NAD(P)H to the reaction mixture (Figure 3.5), indicating that the theophylline *N*-demethylase is likely an NAD(P)H-dependent enzyme.

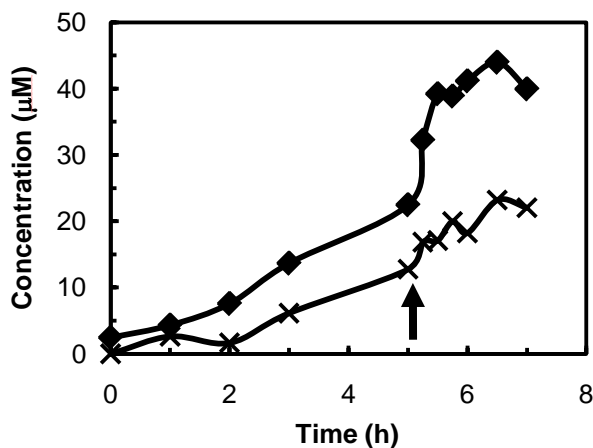


Figure 3.5. Production of 1-methylxanthine (◆) and 3-methylxanthine (×) from theophylline by cell extracts prepared from *P. putida* CBB5 grown in soytone-supplemented M9-theophylline medium. At 5 h, 0.15 mM NADH was added to the enzyme reaction mixture (indicated by the arrow), resulting in increased production of 1- and 3-methylxanthine.

Collectively, these data suggest that theophylline degradation occurred *via* initial *N*-demethylation to 1-methylxanthine and 3-methylxanthine. These two compounds were further *N*-demethylated to xanthine, which was subsequently oxidized to uric acid. 1,3-Dimethyluric and 1- and 3-methyluric acids formed from theophylline were not metabolized further by either resting cell suspensions or cell extracts prepared from CBB5 grown on theophylline or caffeine with or without soytone supplementation.

Growth and Metabolism of 3-Methylxanthine by CBB5

Because a resting cell suspension prepared from theophylline-grown CBB5 could metabolize 3-methylxanthine (Figure 3.4B), the ability of CBB5 to utilize this compound as a sole carbon and nitrogen source was also examined. When grown in soytone-free and soytone-supplemented media containing $1.0 \text{ g}\cdot\text{L}^{-1}$ 3-methylxanthine (media 3 and 3S, respectively), CBB5 cultures reached an OD_{600} of 0.14 (after 72 h) and 2.5 (after 30 h), respectively. 3-Methyluric acid (metabolite VIII) was detected under both conditions and was not metabolized further. Resting cell suspensions prepared from CBB5 grown on 3-methylxanthine degraded this compound at rates comparable to the rates observed for resting cell suspensions prepared from CBB5 grown on caffeine, theophylline, theobromine, paraxanthine, and 7-methylxanthine (Figure 3.6).

Interestingly, a resting cell suspension prepared from 3-methylxanthine-grown CBB5 also degraded theophylline without any lag period. However, theophylline degradation occurred at a rate significantly lower than that of a resting cell suspension prepared from theophylline- or caffeine-grown CBB5 (Figure 3.6), and only 1,3-dimethyluric acid was produced. Caffeine, theobromine, and 7-methylxanthine were not degraded by 3-methylxanthine-grown resting cells incubated for 60 min, while paraxanthine was degraded minimally. A resting cell suspension prepared from CBB5 cells grown in soytone-supplemented M9 medium did not degrade any methylxanthines except theophylline and 3-methylxanthine, which were degraded at significantly lower rates (Figure 3.6). Thus, 3-methylxanthine does not appear to induce the expression of *N*-demethylase enzymes in CBB5.

Co-expression of Theophylline and Caffeine Metabolism in

CBB5

Although caffeine and theophylline are both degraded by CBB5 *via N*-demethylation, the pathways are distinct and their respective metabolites are not present

in the other pathway. In order to determine whether or not the pathways were co-expressed or induced separately, resting cell suspensions of CBB5 grown on soytone-supplemented M9 medium with either caffeine, theobromine, paraxanthine, 7-methylxanthine, theophylline, 3-methylxanthine, or no methylxanthine were assayed with 1 mM caffeine, theobromine, paraxanthine, 7-methylxanthine, theophylline, and 3-methylxanthine (Figure 3.6).

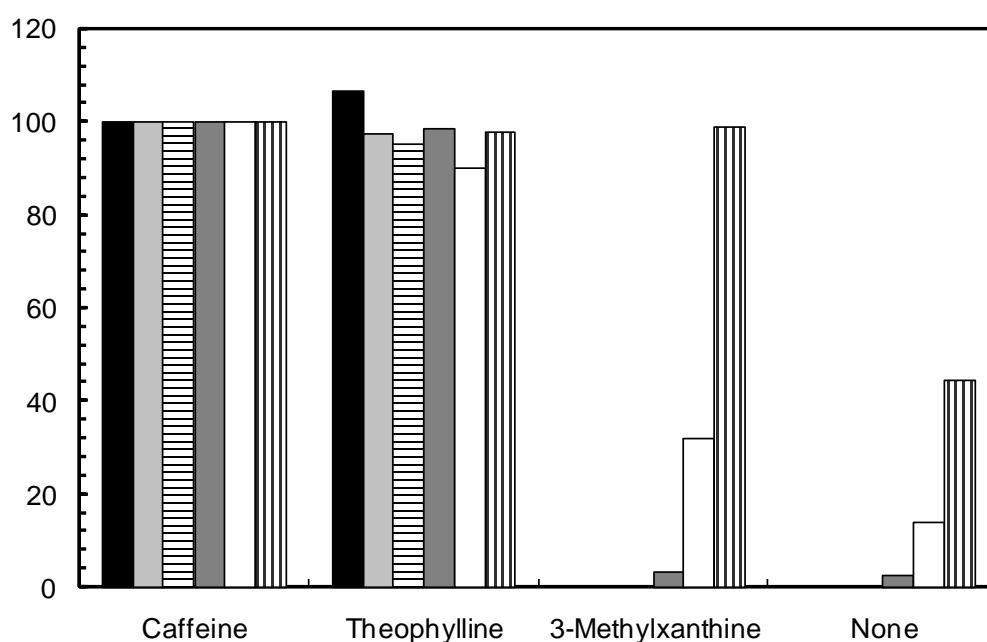


Figure 3.6. Relative degradation rates of caffeine and other methylxanthines (y-axis) by CBB5 resting cells prepared from cultures that were grown in soytone supplemented M9 medium containing $2.5 \text{ g}\cdot\text{L}^{-1}$ caffeine, $2.5 \text{ g}\cdot\text{L}^{-1}$ theophylline, $1.0 \text{ g}\cdot\text{L}^{-1}$ 3-methylxanthine, or without caffeine and any methylxanthines (x-axis). Bars represent degradation of 1 mM of the following substrates in resting cell: (■) caffeine, (■) theobromine, (≡) 7-methylxanthine, (■) paraxanthine, (□) theophylline, and (▨) 3-methylxanthine. Degradation rates of these substrates by resting cells prepared from caffeine grown CBB5 culture were designated as 100%. Resting cells prepared from CBB5 grown on theobromine, paraxanthine, and 7-methylxanthine degraded the test substrates at rates similar to resting cells prepared from CBB5 grown on caffeine.

Resting suspensions of CBB5 grown in CS medium degraded all six compounds within 1 h without lag (Figures 3.3 and 3.6). While most compounds were degraded in approximately 60 min, 3-methylxanthine was degraded in 15 min with only 3-methyluric acid produced as a detectable metabolite. When theophylline was added to the resting cells, only 1,3-dimethyluric acid and 1- and 3-methyluric acids were detected by HPLC, similar to the resting cell suspensions prepared from soytone-supplemented M9-theophylline media.

Resting cell suspensions prepared from TS-medium-grown cells also degraded caffeine, theobromine, paraxanthine, and 7-methylxanthine without any lag in activity (Figure 3.6). Thus, the enzymes involved in *N*-demethylation of caffeine and theophylline are co-expressed in CBB5 cells grown on either compound or the *N*-demethylated metabolites of caffeine.

Suspensions of resting cells grown in 3S medium degraded 3-methylxanthine at rates that were comparable to the suspensions grown on caffeine, theophylline, theobromine, paraxanthine, or 7-methylxanthine. Theophylline was also degraded by this suspension without any lag, but at a much lower rate than suspensions prepared from caffeine- or theophylline-grown CBB5. In this case, only methyluric acids were produced from theophylline. Caffeine, theobromine, and 7-methylxanthine were not degraded by 3-methylxanthine-grown resting cells after 60 min incubation, while paraxanthine was degraded minimally. In resting cell suspensions of CBB5 grown in soytone-supplemented M9-medium without methylxanthines, only theophylline and 3-methylxanthine were degraded to their respective methyluric acids, though at much lower levels.

These results indicate that the caffeine and theophylline metabolic pathways are not constitutive, but are rather induced by the presence of caffeine, theophylline, theobromine, paraxanthine, or 7-methylxanthine. That 3-methylxanthine does not induce the *N*-demethylation of caffeine, its *N*-demethylated derivatives, or theophylline is

another indication that the caffeine and theophylline metabolic pathways might be catalyzed by separate enzymes. This also indicates that the methyluric acids formed from theophylline and 3-methylxanthine are not part of the *N*-demethylation pathways of caffeine and theophylline.

Origin of 1,3-Dimethyluric Acid and 1- and 3-Methyluric

Acids from Theophylline

The C-8 oxidation of methylxanthines has been studied previously. Yamaoka-Yano and Mazzafera (1999) previously reported that caffeine-degrading *P. putida* L possessed a broad substrate range xanthine oxidase which also oxidized theophylline and 3-methylxanthine. In growth media, resting cell assays, and cell extracts of CBB5, oxidation of theophylline and 1- and 3-methylxanthines at the C-8 position was observed (Figures 3.3E and 3.4). Whether the formation of these compounds was due to a xanthine oxidase with a broad substrate range, similar to the enzyme described by Yamaoka-Yano and Mazzafera, was investigated further.

A native PAGE gel activity staining procedure was developed to determine if C-8 oxidation of theophylline and 3-methylxanthine by CBB5 was catalyzed by an enzyme similar to xanthine oxidase from *P. putida* L (Yamaoka-Yano and Mazzafera, 1999) or caffeine dehydrogenase from *Pseudomonas* sp. CBB1 (Yu *et al.*, 2008). Cell extracts from TS medium-grown CBB5 cells were resolved by native PAGE gels (Figure 3.7, lane 1). The gels were stained by incubation with various methylxanthine substrates in the presence of NBT. A single blue band, formed by reduction of NBT, appeared on gels after 10 min when xanthine was used as a substrate in the activity staining solution (Figure 3.7A), indicating the presence of an active xanthine-oxidizing enzyme in CBB5 cell extracts. No band resulted when xanthine was replaced with caffeine, theobromine, theophylline, or 3-methylxanthine (Figure 3.7B), in spite of longer incubation time.

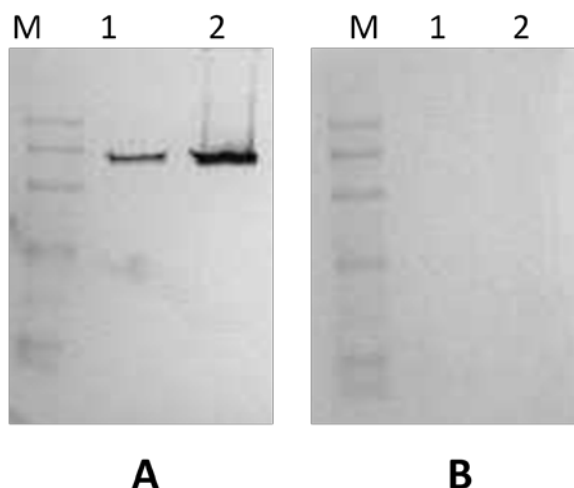


Figure 3.7. Native PAGE gels of crude extracts (lane 1) and partially purified xanthine dehydrogenase (lane 2) prepared from *P. putida* CBB5 cells grown on soytone supplemented M9-theophylline medium were stained by a substrate-dependent nitro blue tetrazolium reduction activity. Substrates used in this staining were (A) xanthine and (B) theophylline. Bio-Rad precision plus protein standards (Kaleidoscope, lane M) were used to monitor progress of electrophoresis. No stained bands were observed in either lane when caffeine, theobromine, and 3-methylxanthine were used as substrates.

Cell extracts prepared from CBB5 cells grown in TS medium were fractionated on a Phenyl Sepharose High Performance liquid chromatography column (Figure 3.8). Enzyme activity assays detected three peaks of xanthine-oxidizing fractions, A, B, and C which were eluted from the column with 0.25 M ammonium sulfate, 0.18 M ammonium sulfate, and water, respectively. In the presence of NBT or NAD^+ , Fraction A oxidized xanthine to uric acid, which was identified by HPLC. A spectrophotometric enzyme activity assay showed that Fraction A coupled oxidation of xanthine to uric acid with concomitant reduction of NAD^+ or NBT. No reduction of NAD^+ or NBT was observed when caffeine, theobromine, theophylline, or 3-methylxanthine was used as a substrate in this spectrophotometric enzyme activity assay. Fraction A was also resolved by native PAGE and subjected to the activity staining procedure (Figure 3.7, lane 2). When incubated with xanthine and NBT, the same band that formed in cell extracts was

observed in Fraction A. Thus, Fraction A was determined to contain a highly specific xanthine dehydrogenase, exhibiting no activity with caffeine, theobromine, theophylline, and 3-methylxanthine. Such an enzyme has been reported previously in literature (Woolfolk and Downard, 1977).

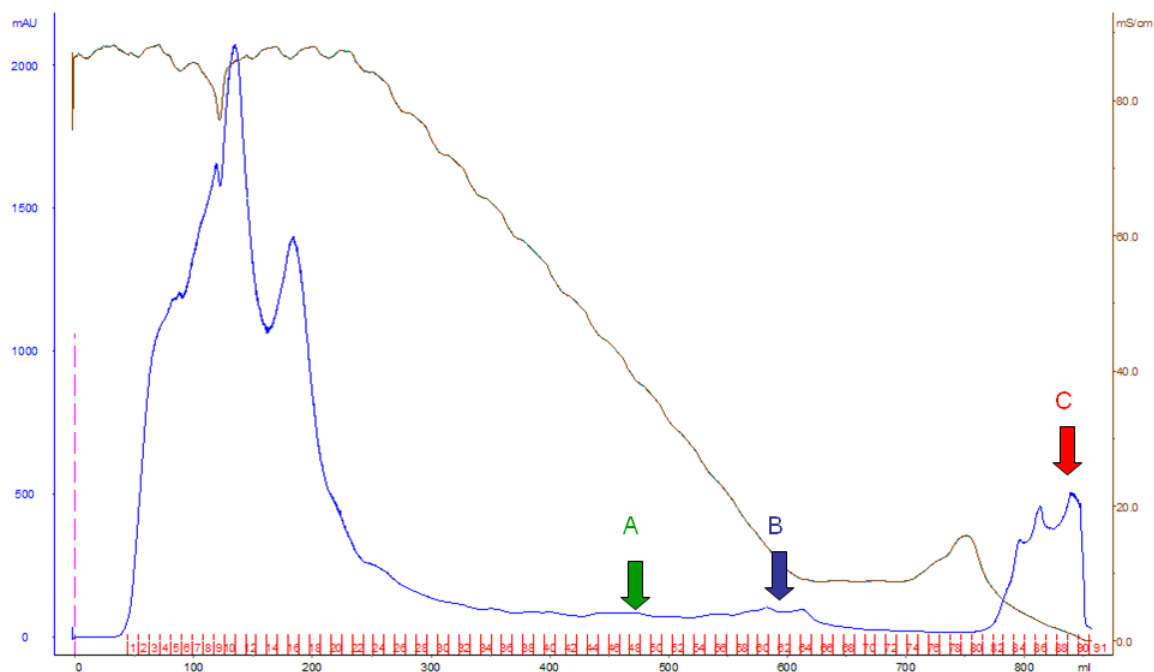


Figure 3.8. Elution profile of CE separated on Phenyl Sepharose. Blue line, A_{280} (mAU, left axis); Brown line, conductivity (mS/cm, right axis). Elution of fractions A, B, and C are indicated by the green, blue, and red arrows, respectively.

Fractions B and C also oxidized xanthine to uric acid with concomitant reduction of NBT. Ferricyanide, but not NAD^+ , could replace NBT as the electron acceptor with Fraction B, although no native electron acceptor was determined. Fraction B was also active with theophylline and 3-methylxanthine, producing 1,3-dimethyluric acid and 3-methyluric acid, respectively. Fraction C also oxidized theophylline and 3-methylxanthine to their respective uric acids in the presence of NBT, but could not use

NAD⁺ or ferricyanide as an electron acceptor. Caffeine and theobromine were not substrates for fraction B or C, however. Production of 1-methyluric acid from 1-methylxanthine was not examined due to lack of the latter. For fraction B, the highest level of activity was observed with 3-methylxanthine; the levels of activity with xanthine and theophylline were 83% and 13%, respectively, relative to activity on 3-methylxanthine. Because the activity with Fraction C was very labile, substrate preference was not determined. Thus, the production of 1,3-dimethyluric acid and 3- and 1- methyluric acids from theophylline and 3- and 1-methylxanthines, respectively (Figures 3.3E and 3.4), is probably due to the activity of the broad-substrate-range xanthine-oxidizing enzyme in Fractions B and C.

Discussion

Caffeine and Theophylline are Metabolized *via N*-Demethylation by *Pseudomonas putida* CBB5

A unique caffeine-degrading bacterium, *P. putida* CBB5, was isolated from the soil, which uses not only caffeine, theobromine, and 7-methylxanthine as sole carbon and nitrogen sources but also theophylline and 3-methylxanthine. The primary mode of purine alkaloid metabolism by CBB5 is *N*-demethylation, however C-8 oxidation of theophylline and 1- and 3-methylxanthines was also observed.

Caffeine was metabolized by CBB5 *via* successive *N*-demethylation steps to xanthine. Theobromine was the major product of the initial *N*-demethylation, although paraxanthine was also detected as a minor metabolite. These two dimethylxanthines were further *N*-demethylated to 7-methylxanthine, which was *N*-demethylated to xanthine before oxidation to uric acid (Figure 3.1). Based on these data, a sequential *N*-demethylation pathway is proposed here for caffeine (Figure 3.9A). This pathway is further supported by the fact that CBB5 metabolized theobromine, paraxanthine, and 7-methylxanthine with the same pathway (Figure 3.3).

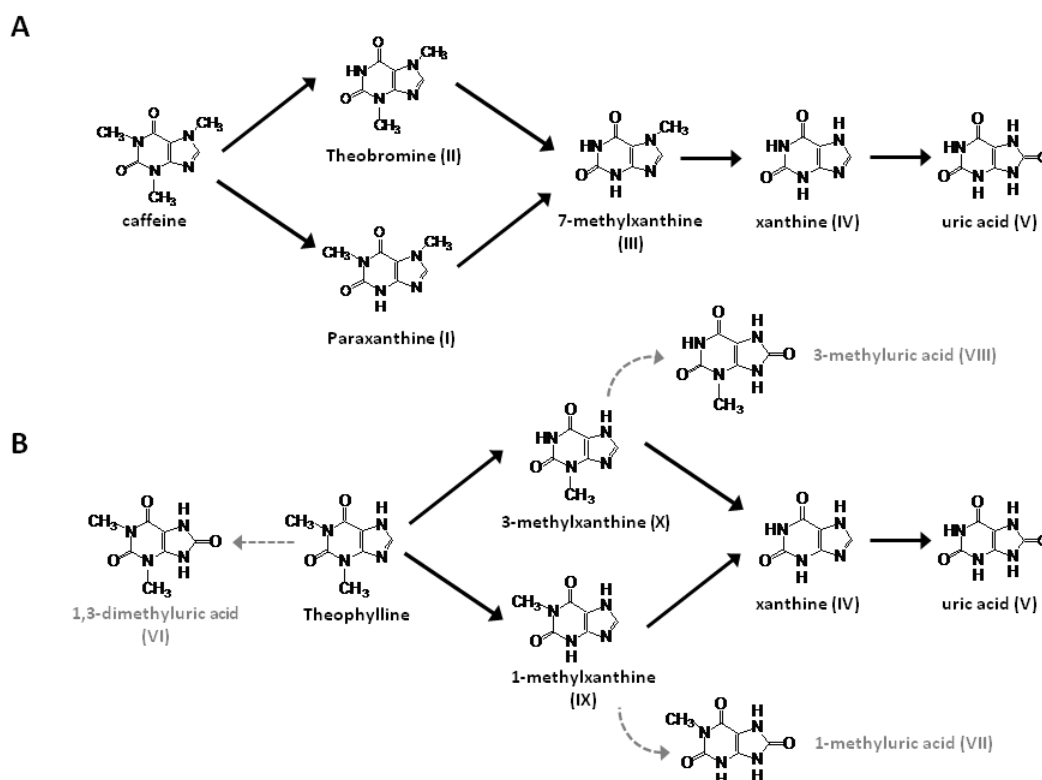


Figure 3.9. Proposed pathway for degradation of (A) caffeine and (B) theophylline by *P. putida* CBB5. The dashed arrows indicate oxidation of theophylline and 1- and 3-methylxanthine to their respective methyluric acids, which were not metabolized further.

The pathway proposed for caffeine *N*-demethylation in CBB5 is similar, but not identical to that in caffeine-degrading *P. putida* L (Yamaoka-Yano and Mazzafera, 1999). In the latter organism, theobromine, paraxanthine, and 7-methylxanthine produced from caffeine were also shown to be oxidized to the corresponding methyluric acids. Although theophylline and 3-methylxanthine were not produced during caffeine metabolism, they were oxidized to 1,3-dimethyluric acid and 3-methyluric acid, respectively, by *P. putida* L. A xanthine oxidase with broad substrate specificity was reported to be responsible for oxidizing all of these purine alkaloids. In the present study, methyluric acids were not

detected when caffeine, theobromine, paraxanthine, and 7-methylxanthine were used as growth substrates for CBB5, in resting cell studies, or in cell extract studies.

Although caffeine metabolism by bacteria has been well characterized and reported in literature, there is very little information on bacterial metabolism of theophylline and 3-methylxanthine. Theophylline has not been proposed as an intermediate in the caffeine degradation pathways of bacteria (Mazzafera *et al.*, 1996; Yamaoka-Yano and Mazzafera, 1999; Mazzafera, 2004; Dash and Gummadi, 2006; Yu *et al.*, 2008). In contrast, caffeine catabolism in plant species and in caffeine-degrading fungi has been reported to proceed *via* theophylline, which is further degraded by *N*-demethylation to 3-methylxanthine (Schwimmer *et al.*, 1971; Hakil *et al.*, 1998; Mazzafera, 2004). Caffeine-degrading *Serratia marcescens* was unable to utilize theophylline or 3-methylxanthine as a growth substrate (Mazzafera *et al.*, 1996). Woolfolk (1975) reported that *Pseudomonas* isolates capable of growth on 0.1% caffeine also grew well on all dimethylxanthines, including theophylline. However, details of theophylline metabolism in these *Pseudomonas* isolates were not elucidated.

As in all other cases reported in literature, theophylline was not produced during *N*-demethylation of caffeine by CBB5. Theophylline was metabolized, however, by a previously unknown *N*-demethylation pathway, forming 1-methylxanthine and 3-methylxanthine (Figures 3.4 and 3.9B). These two intermediates were further *N*-demethylated to xanthine, which was finally oxidized to uric acid. Metabolism of theophylline by this *N*-demethylation pathway was confirmed using CBB5 culture media, resting cell suspensions, and cell extracts. CBB5 also oxidized theophylline to 1,3-dimethyluric acid and 1- and 3-methyluric acids (Figures 3.3E and 3.4). These methyluric acids were not metabolized further by resting cells or crude extracts (Figure 3.4B), and appear to be dead-end metabolites.

Broad-Substrate-Range Xanthine Dehydrogenases Oxidize Theophylline and its Metabolites to Methyluric Acids

Two broad-substrate-range xanthine-oxidizing enzymes that were partially purified from CBB5 appear to be involved in the oxidation of theophylline to the methyluric acids. This hypothesis is supported by the fact that 3-methylxanthine is the best substrate for one of these enzymes, Fraction B, and by the fact that 3-methyluric acid was also produced from 3-methylxanthine (Figure 3.3F) by both of these enzymes. In addition, CBB5 grown on 3-methylxanthine produced only 3-methyluric acid, which was not metabolized further. Based on these results, a new *N*-demethylation pathway is proposed for theophylline degradation in CBB5 (Figure 3.9B). In this pathway, formation of methyluric acids is represented as dead-end metabolites of theophylline and 1- and 3-methylxanthines (Figure 3.9B, dashed arrows).

The formation of methyluric acids from theophylline and 1- and 3-methylxanthines is not unusual. A xanthine oxidase that was active with theophylline and 3-methylxanthine was identified in caffeine-degrading *P. putida* L cell extracts by activity staining of native PAGE gels (Yamaoka-Yano and Mazzafera, 1999). This enzyme was subsequently purified, but theophylline and 3-methylxanthine products were not reported. An NAD⁺-dependent xanthine dehydrogenase activity was also identified in cell extracts of caffeine-degrading *S. marcescens* using a similar activity staining procedure (Mazzafera *et al.*, 1996). This xanthine dehydrogenase was active with caffeine, theobromine, theophylline, 1-methylanthine, 3-methylxanthine, and 7-methylxanthine. Blecher and Lingens (1977) reported oxidation of theobromine, paraxanthine, and 7-methylxanthine by *Pseudomonas putida* C1 when these compounds were formed from degradation of caffeine.

Aside from the reports described above, most xanthine-oxidizing enzymes appear to exhibit high specificity with xanthine and monomethylxanthines. Dikstein *et al.* (1957) studied xanthine oxidase activities in 10 different species of human intestinal

bacteria. None of the enzymes were active with theophylline, while seven were active with 3-methylxanthine. At present, the physiological role of the broad-substrate-range xanthine-oxidizing enzymes in CBB5 is unclear because CBB5 could not metabolize methyluric acids. Hence, further purification of Fractions B and C was not considered in favor of the focus on the main *N*-demethylation pathway. Nevertheless, purification, sequencing, and cloning of these enzymes could be of use in a large-scale production of methyluric acids. There is another example of such an enzyme whose function with respect to the *N*-demethylation pathway is not clear. *S. marcescens*, which can oxidize theophylline, 3-methylxanthine, and 1-methylxanthine (Mazzafera *et al.*, 1996), was also not capable of utilizing methyluric acids as growth substrates.

Multiple *N*-Demethylases Might be Involved in Metabolism of Caffeine and Theophylline by CBB5

The number and nature of *N*-demethylases involved in *N*-demethylation of caffeine and related methylxanthines has not been determined in any organism, however, multiple *N*-demethylases have been implicated in many instances. For example, during purification of a theobromine *N*-demethylase from caffeine-degrading *P. putida* No. 532 that was inhibited by Zn^{2+} , Asano *et al.* (1994) also detected caffeine *N*-demethylase activity in the cell extracts which was not inhibited by Zn^{2+} . Glück and Lingens (1988) partially purified a 7-methylxanthine *N*-demethylase from caffeine-degrading *P. putida* WS which was specific for 7-methylxanthine and had no activity with caffeine and theobromine. Caffeine and theobromine also did not inhibit 7-methylxanthine *N*-demethylation by this enzyme. A recent study by Dash and Gummadi (2008) showed that caffeine and theobromine *N*-demethylases in *Pseudomonas* sp. strain NCIM5235 were inducible by nature, but the caffeine *N*-demethylase activity in theobromine-grown cells was 10-fold lower than that in caffeine-grown cells. These data implied that different *N*-demethylases were responsible for caffeine and theobromine *N*-

demethylation. Previous attempts to purify caffeine *N*-demethylase from NCIM5235 were unsuccessful due to instability of the enzyme.

The only known bacterial *N*-demethylase in the UniProt protein database is *N*-methylproline demethylase (StcD) of *Sinorhizobium meliloti*, which is involved in stachydrine catabolism (Phillips *et al.*, 1998). The biochemical properties of StcD were not studied in detail, but its protein sequence is similar to those of α/β -barrel oxidoreductase flavoproteins. A caffeine *N*-demethylase nucleotide sequence (accession no. E07469) from *P. putida* strain IF-3 was also found in the GenBank database. The deduced protein sequence showed a high degree of similarity with Rieske [2Fe-2S] domain-containing oxygenase subunits of many putative vanillate *O*-demethylases, putative phenylpropionate dioxygenases, and Hpx of *Klebsiella pneumonia*, which is involved in the oxidation of hypoxanthine to uric acid (de la Riva *et al.*, 2008). Present work on purification of an *N*-demethylase from CBB5 and its detailed biochemical characterization, including substrate specificity, is presented in Chapter 4.

The nature of *N*-demethylase enzymes has also not been completely elucidated. Woolfolk (1975) suggested that methyl groups were removed through a hydrolytic mechanism to form methanol in *Pseudomonas putida* strain 40. Many other reports, however, have suggested that caffeine *N*-demethylase is an oxygenase (Hohnloser *et al.*, 1980; Middelhoven and Lommen, 1984; Asano *et al.*, 1994). This suggestion is based on the observation that caffeine *N*-demethylation is NADH-dependent and that formaldehyde is produced from the methyl group that is removed. Finally, Ogunseitan (2002) reported a caffeine-inducible cytochrome P450 enzyme is responsible for degradation of caffeine in *Pseudomonas putida* ATCC 700097, similar to the degradation of caffeine in yeasts (Sauer *et al.*, 1982) and humans (Berthou, 1992). However, this was attributed only to the presence of a P450 in the organism and was not shown with a purified enzyme.

Both Caffeine and Theophylline Metabolic Pathways are Co-Expressed in CBB5

Use of caffeine, *N*-demethylated metabolites of caffeine, or theophylline as the growth substrate for CBB5 resulted in co-expression of both caffeine and theophylline *N*-demethylation pathways proposed in Figure 3.9. CBB5 grown on 3-methylxanthine, however, did not metabolize caffeine, theobromine, or 7-methylxanthine. Additionally, there was much less degradation of theophylline by 3-methylxanthine-grown CBB5, with production of only methyluric acids (Figure 3.6).

There are precedents for differential regulation of caffeine degradation by an alternative carbon or nitrogen source. For instance, when caffeine-degrading *Pseudomonas* sp. Strain NCIM5235 was grown with theobromine as the sole source of carbon and nitrogen, the caffeine *N*-demethylase activity in cell extracts was 10-fold lower and theobromine *N*-demethylase activity was 3- to 4-fold higher than the activities in cell extracts from caffeine-grown cells (Dash and Gummadi, 2008). Caffeine dehydrogenase activity in *Pseudomonas* sp. strain CBB1 was repressed when this organism was grown in the presence of soytone plus caffeine. However, addition of YNB did not suppress activity of this enzyme (Yu *et al.*, 2008). Expression of caffeine oxidase in *Alcaligenes* sp. strain CF8 was completely suppressed by starch, but glucose increased the caffeine oxidase expression two-fold. Caffeine oxidase expression in *Alcaligenes* sp. strain CF8 was also stimulated by addition of sodium nitrate, while ammonium sulfate and ammonium chloride substantially reduced production of this enzyme (Mohapatra *et al.*, 2006).

Although detailed metabolic studies, including induction and inhibition of activity, can provide the basis for hypothesizing the number of *N*-demethylases present in bacteria, they cannot prove the exact number of enzymes required to completely metabolize caffeine *via N*-demethylation. Rather, at least one of two additional methods- a biochemical study or molecular biology study- must be used in order to determine the

number of bacterial methylxanthine *N*-demethylases. Enzyme purification and detailed biochemical characterization, including characterization of substrate specificity will be useful if the activities can be resolved during purification. Conversely, a molecular biology approach might be used. Under this approach, construction and screening of a gDNA library or use of transposon mutagenesis might allow for determination of an enzyme with a single, specific *N*-demethylase activity.

Summary

A new caffeine-degrading bacterium, *Pseudomonas putida* CBB5, was isolated from the soil by enrichment with caffeine as the sole source of carbon and nitrogen. Caffeine was *N*-demethylated by CBB5 to theobromine (major metabolite) and paraxanthine (minor metabolite). These two dimethylxanthines were subsequently *N*-demethylated to 7-methylxanthine and then to xanthine. Theophylline was also metabolized by a novel *N*-demethylation pathway, with production of 1- and 3-methylxanthine, which were further *N*-demethylated to xanthine. The caffeine and theophylline *N*-demethylation pathways are distinct and do not converge until xanthine, which enters the normal purine catabolic pathway. The first step in xanthine catabolism is the oxidation of xanthine to uric acid by a specific, NAD⁺ dependent xanthine dehydrogenase.

Both caffeine and theophylline *N*-demethylation pathways were co-expressed in the presence of caffeine, theophylline, theobromine, paraxanthine, and 7-methylxanthine. Two broad-substrate-range xanthine-oxidizing enzymes were responsible for the formation of 1,3-dimethyluric acid and 1- and 3-methyluric acids from the methylxanthines in the theophylline *N*-demethylation pathway. These enzymes were not active on caffeine or any of its *N*-demethylated metabolites. The physiological role of these enzymes is currently unknown, as the methyluric acids formed are dead-end metabolites and are not degraded further. Although much has been reported regarding

bacterial metabolism of caffeine, this is the first detailed report of theophylline metabolism by a bacterial strain.

CHAPTER 4

PURIFICATION AND CHARACTERIZATION OF A BROAD-SPECIFICITY METHYLXANTHINE *N*-DEMETHYLASE

Introduction

Pseudomonas putida CBB5 is capable of utilizing several natural purine alkaloids as the sole source of carbon and nitrogen (Yu *et. al.*, 2009; Chapter 3 of this document). This organism metabolizes caffeine *via* sequential *N*-demethylation to paraxanthine and theobromine, 7-methylxanthine, and xanthine, which enters the normal purine catabolic pathway. A previously unknown pathway for *N*-demethylation of theophylline was also discovered in CBB5. Theophylline was metabolized to form 1- and 3-methylxanthines, which were further *N*-demethylated to xanthine. Although the pathways for degradation of caffeine and theophylline are co-expressed in the presence of caffeine, theophylline, and related methylxanthines, the intermediates of the two pathways do not overlap until xanthine (Figure 3.9).

While much has been reported concerning bacterial metabolism of caffeine, a detailed characterization of the *N*-demethylase enzyme(s) involved in this pathway has not been published to date. Therefore, little is known regarding the exact nature, number, and mechanism of methylxanthine *N*-demethylase(s) found in bacteria. The activity of bacterial *N*-demethylases has been reported to be very labile, with loss of activity occurring after a single chromatographic purification step (Sideso *et al.*, 1996, Dash and Gummadi, 2006). Many oxygenase systems responsible for the degradation of aromatic and other xenobiotic compounds are composed of at least two different enzymes. A large class of these enzymes, Rieske [2Fe-2S] oxygenases, receives reducing equivalents from NAD(P)H, which are transferred through a reductase, either with or without an additional ferredoxin component (Ferraro *et al.*, 2005). Therefore, for this work it was hypothesized that the loss of activity reported may be due to the chromatographic separation of the *N*-

demethylase component from its partner electron transfer components and/or due to the instability of one or both components.

Because there is little known concerning bacterial *N*-demethylases, four distinct hypotheses were developed regarding the number of *N*-demethylases present in CBB5.

These hypotheses were that:

1. There is only one broad substrate specificity *N*-demethylase that completely degrades both caffeine and theophylline to xanthine,
2. There are three *N*-demethylases present in CBB5, each enzyme active on a specific methyl group of caffeine,
3. There are two *N*-demethylases, one that catalyzes each step in the caffeine degradation pathway, and another responsible for each step in the theophylline metabolic pathway, or
4. There are two *N*-demethylases: one enzyme responsible for removing the *N*-7 methyl group from the five member ring and another enzyme that removes the *N*-1 and *N*-3 methyl groups from the six member ring.

The presence of a single, broad substrate specificity enzyme capable of *N*-demethylating all methylxanthines to xanthine (Hypothesis 1) seems unlikely because the caffeine and theophylline metabolic pathways in CBB5 are very distinct and do not overlap until xanthine (Figure 3.9). However, the presence of multiple *N*-demethylases responsible for caffeine metabolism in bacteria (Hypotheses 2 through 4) has been postulated, but never demonstrated concretely (Glück and Lingens, 1988; Asano *et al.*, 1994; Dash and Gummadi, 2008). Purification of a single bacterial *N*-demethylase and characterization of its substrate specificity may provide answers regarding the number of *N*-demethylases responsible for metabolism of purine alkaloids in bacteria.

This chapter describes the first detailed purification and biochemical characterization of a soluble, broad-specificity methylxanthine *N*-demethylase from *P. putida* CBB5. This enzyme system is composed of a reductase component (Ccr) and a

two subunit *N*-demethylase component (Ndm). Ndm activity is dependent on NAD(P)H oxidation, catalyzed by Ccr. Furthermore, Ndm is predicted to be a Rieske [2Fe-2S]-domain containing non-heme iron oxygenase based on its distinct UV/visible absorption spectrum, its iron content, and analysis of the N-terminal amino acid sequences of its subunits. When coupled with Ccr, Ndm exhibited an oxygen dependent, broad-based activity towards caffeine, paraxanthine, theobromine, theophylline, 7-methylxanthine, and 3-methylxanthine, all of which were converted to xanthine. The methyl groups are converted to formaldehyde with the consumption of one mole of NADH per methyl group removed.

N-Demethylase Activity of CBB5 in Cell Extracts

In order to determine which methylxanthine to use as substrate during enzyme purification, the NADH-dependent *N*-demethylase (Ndm) activity of cell extracts prepared from CBB5 grown on soytone-supplemented M9-caffeine medium was tested on caffeine, theophylline, theobromine, and paraxanthine. Because a compound containing at least two methyl groups was desired in order to test for multiple *N*-demethylases with a single substrate, Ndm activity of cell extracts on monomethylxanthines was not tested. A 0.5 mM solution of paraxanthine was completely utilized by cell extract containing $0.72 \text{ mg}\cdot\text{mL}^{-1}$ protein in approximately 20 min (Figure 4.1). Theobromine, caffeine, and theophylline were degraded at significantly slower rates.

That paraxanthine was most rapidly degraded was not surprising, as it was also metabolized very quickly by resting cell suspensions of CBB5 grown in soytone-supplemented M9-caffeine medium (Figure 3.3D). Because paraxanthine contains a methyl group on each ring (at the *N*-1 and *N*-7 atoms) of the xanthine molecule, it was considered the best substrate to assay for the presence of multiple *N*-demethylases that were either position- or ring-specific (Hypotheses 2 and 4). Thus, paraxanthine was

chosen as the substrate to monitor the *N*-demethylase(s) purification and characterization due to its high rate of degradation, the presence of multiple methyl groups, and the position of the methyl groups attached to the xanthine molecule.

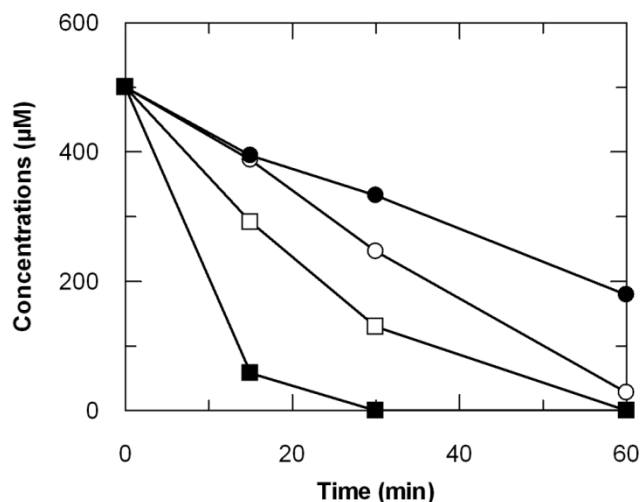


Figure 4.1. Degradation of paraxanthine (■), theobromine (□), caffeine (○), and theophylline (●) by cell extracts prepared from *P. putida* CBB5 grown in soytone-supplemented M9-caffeine medium. All reactions contained 0.5 mM substrate, 0.5 mM NADH, and 7.2 mg·mL⁻¹ protein. This experiment was repeated three times and similar patterns were observed in all replicates.

Purification of Ndm

Ndm was purified from cell extracts of CBB5 grown on soytone-supplemented M9-caffeine medium by traditional protein chromatography techniques (Table 4.1). The three step procedure resulted in a 26-fold purification of Ndm relative to the activity in cell extracts. An NAD(P)H:cytochrome *c* oxidoreductase (Ccr) activity co-eluted with Ndm from the DEAE Sepharose column at 0.23 M KCl in KPGD buffer (Figure 4.2). NADH was determined to be the preferred electron donor for *N*-demethylation of paraxanthine; activity with NADPH was only 22% of that with NADH.

Table 4.1. Purification of methylxanthine *N*-demethylase from *Pseudomonas putida* CBB5.

Purification step	Total protein (mg)	Total activity (mU)*	Specific act (mU·mg ⁻¹)	Purification (fold)	Yield (%)
Cell extract	2361	5053	2.1	1	100
DEAE Sepharose	480.2	1767	3.7	1.7	35
Phenyl Sepharose HP	37.5	962	25.6	12	19
Q Sepharose	7.0	388	55.4	26	7.7

*One unit of activity corresponds to 1 μmol paraxanthine consumed·min⁻¹, in the presence of saturating amounts of Ccr and 50 μM Fe²⁺, as described in Chapter 2.

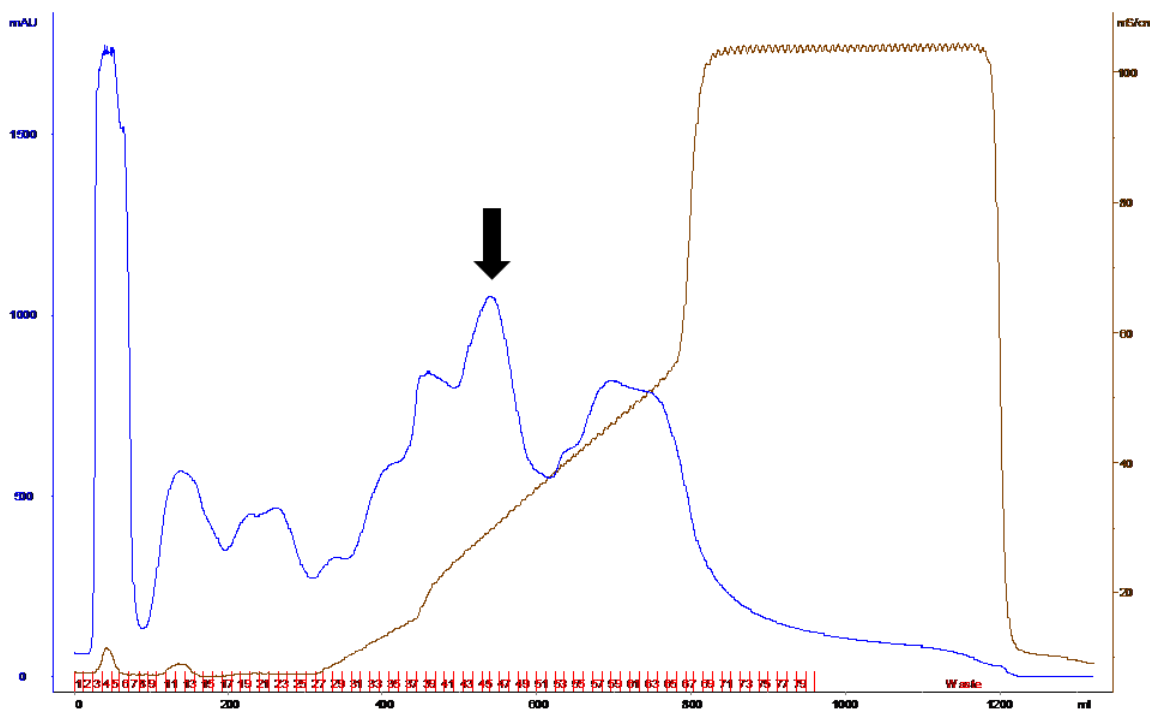


Figure 4.2. Elution profile of CE separated on DEAE Sepharose. Blue line, A_{280} (mAU, left axis); Brown line, conductivity (mS/cm, right axis). Elution of Ccr and Ndm is indicated by the black arrow.

When this DEAE Sepharose eluant was loaded onto a Phenyl Sepharose High Performance column, Ccr eluted from the column under 0.05 M $(\text{NH}_4)_2\text{SO}_4$ and was gold

in color. Ndm was dark red and eluted from the column with water, indicating that it is more hydrophobic (Figure 4.3).

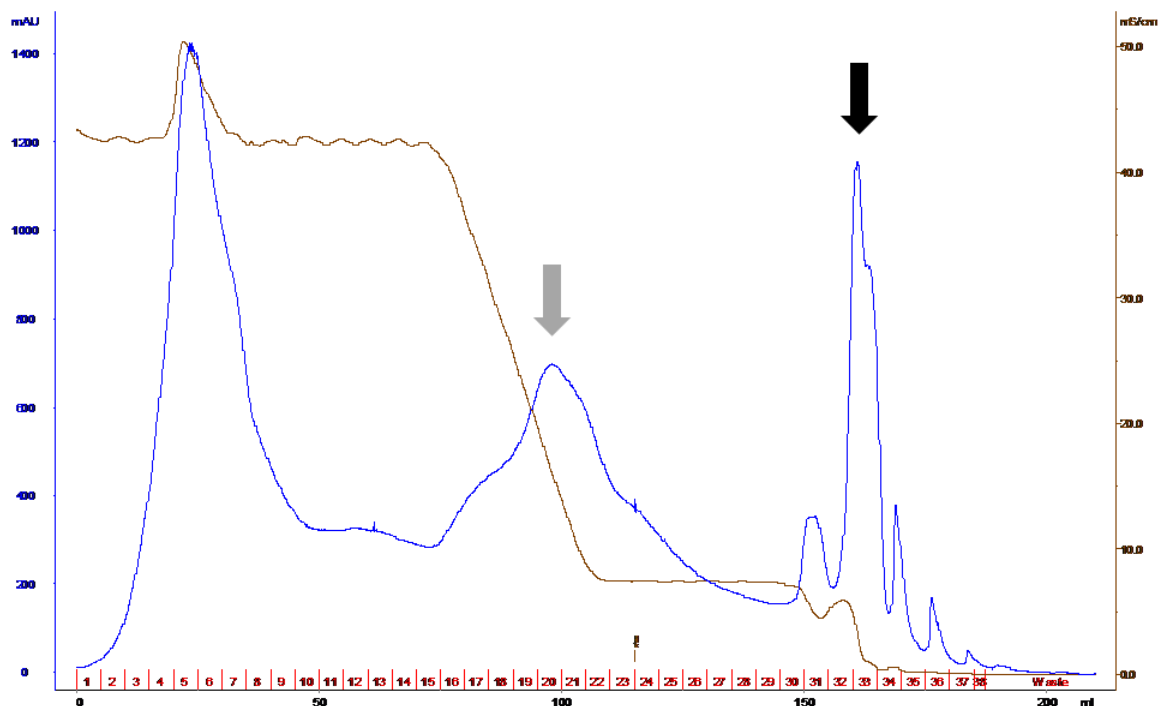


Figure 4.3. Elution profile of DEAE Sepharose-purified Ccr and Ndm separated on Phenyl Sepharose. Blue line, A_{280} (mAU, left axis); Brown line, conductivity (mS/cm, right axis). Elution of Ccr is indicated by the grey arrow, while elution of Ndm is indicated by the black arrow.

Ndm eluted from Phenyl Sepharose did not contain any Ccr activity. Also, neither Ccr, Ndm, nor any other fractions from Phenyl Sepharose exhibited paraxanthine *N*-demethylase activity when assayed singly in the presence of NADH. When Ccr and Ndm fractions were combined in the presence of NADH, *N*-demethylation of paraxanthine was negligible. However, exogenous addition of $50 \mu\text{M Fe}^{2+}$ to the reaction mixture containing both Ccr and Ndm resulted in *N*-demethylation of paraxanthine at $25.6 \text{ mU} \cdot \text{mg}^{-1}$. Addition of Fe^{2+} to either Ndm or Ccr alone did not result in any *N*-demethylation of paraxanthine.

The partially purified Ccr fraction was not purified any further, but was used for assay in the presence of Fe^{2+} and NADH during the further purification of Ndm in a Q Sepharose column (Figure 4.4). The dark red color of Ndm was retained throughout purification. Specific activity of the final purified Ndm, in the presence of a saturating amount of Ccr, was $55.4 \text{ mU}\cdot\text{mg}^{-1}$. 7-Methylanthe and xanthine were detected as products of paraxanthine *N*-demethylation by HPLC.

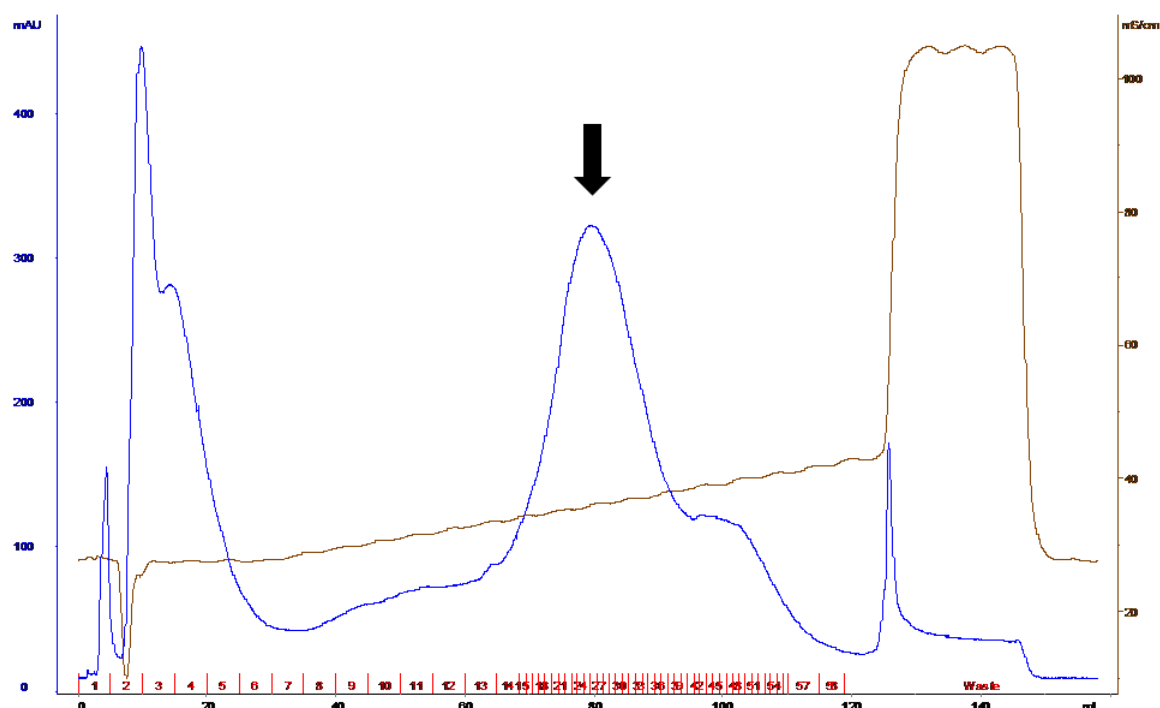


Figure 4.4. Elution profile of Phenyl Sepharose-separated Ndm on Q Sepharose. Blue line, A_{280} (mAU, left axis); Brown line, conductivity (mS/cm, right axis). Elution of Ndm is indicated by the black arrow.

Biochemical Characterization of Ndm

When the Ndm fraction from Q Sepharose was subjected to PAGE under denaturing conditions, two bands were resolved (Figure 4.5) with apparent molecular weights of 40 kDa (NdmA) and 35 kDa (NdmB). However, when loaded onto a

Sephacryl S-300 gel filtration chromatography column, the enzyme eluted as a single, symmetrical peak (Figure 4.6).

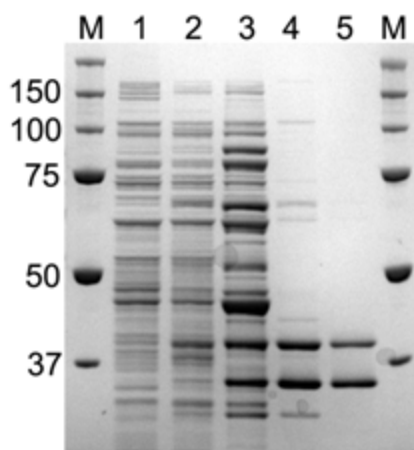


Figure 4.5. SDS-PAGE analysis of *P. putida* CBB5 *N*-demethylase, Ndm, during the purification process. Molecular masses of markers (in kDa) are shown on the left and right (lanes M). Ndm is composed of two subunits with apparent molecular masses of 40 kDa (NdmA) and 35 kDa (NdmB). Lane 1, cell extracts of CBB5 grown on soytone alone; lane 2, cell extracts of CBB5 grown on soytone plus caffeine; lane 3, DEAE Sepharose eluant; lane 4, Phenyl Sepharose eluant; lane 5, Q Sepharose eluant.

The native molecular weight of Ndm was estimated to be about 240 kDa based upon the elution volume (V_e) of Ndm compared with the V_e of various protein standards of known sizes. Other chromatographic methods could not further resolve the NdmA and NdmB, suggesting that the native Ndm was probably composed of the two subunits, possibly in a hexameric configuration. Ndm was stable for at least 5 days at 4°C when stored in KPGD buffer and for over one month at -80°C without significant loss of activity.

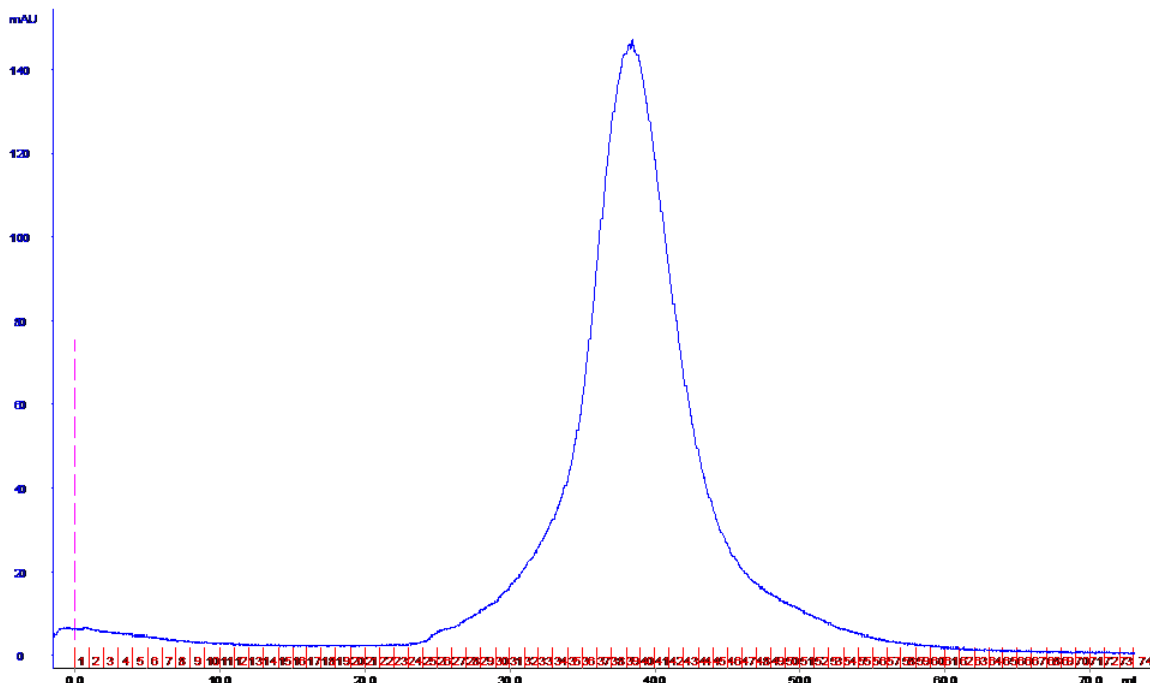


Figure 4.6. Elution profile of purified Ndm on Sephacryl. Blue line, A_{280} (mAU, left axis). Ndm eluted as a single, symmetrical peak with a calculated native molecular weight of 240 kDa, indicating that it is a hexameric enzyme.

The 25 N-terminal amino acid sequence of NdmA, determined by Edman degradation (Edman, 1950), was MEQAIINDEREYLRHFWHPVCTVTE, while that of NdmB was MKEQLKPLLEDKTYLRHFWHPVCTL. A BLASTP (Altschul *et al.*, 1997) search of the Gen Bank database, using NdmA and NdmB N-terminal amino acid sequences as queries, showed that both subunits were substantially similar to the gene product of the *P. putida* strain IF-3 putative caffeine demethylase gene (Cdm, accession number AAB15321) in patent US5550041 (Koide *et al.*, 1996) and a hypothetical protein in *Janthinobacterium* sp. Marseille (mma_0224, accession number YP_001351914). The NdmA and NdmB N-terminal sequences were 84 and 48%, respectively, identical to the first 25 residues of the putative Cdm, and 52 and 64%, respectively, identical to the first 25 residues of mma_0224 (Figure 4.7a).

(a)

```

NdmA      M-EQ-AIINDEREYLRHFWHPVCTVTE 25
Cdm       M-EQ-TINNNDREYLRHFWHPVCTVTE 25
NdmB      MKEQLKPLLEDKTYLRHFWHPVCTL-- 25
mma_0224  MS--FTALLADKSYLRHFWHPVCTLKE 25

```

(b)

```

mma_0224  61-RCHRFAKLSKGCVKQGEAGDRLECPYHGQYDKDGACRTIPACPELPIPKKARSDAFEC-120
Cdm       61-RCHRSAKLSLGTIAN---DRLCCPYHGQYDTEGACKLVPACPNSPIPNRAKVQRFDC 116

mma_0224  121-EVRYDIVVVRDASFGVTEIPVFSWEEEGMRVIVVDSYVWQTTAERRWENFTDFSHFAF-180
Cdm       117-EERYGLIWVRDSSYACTEIPYFSAASDPKLRVVIQEPYWWNATAERRWENFTDFSHFAF-176

mma_0224  181-VHPGTLYDAAYARPPLAPVSRVGGEMRFSIEPPKEMTDQLPDDCPIGAFIYRCTMPYTIN-240
Cdm       177-IHPGTLFDPNNAEPPIVPMDFRNGQFRFVYDTPEDMA--VPDQAPIGSFSYTCSMPFAIN-234

```

Figure 4.7. NdmA and NdmB are similar to other predicted Rieske, non-heme iron proteins. (a) Multiple sequence alignment of the N-terminal protein sequences of NdmA and NdmB with the first 25 amino acid residues of caffeine demethylase (Cdm) of *P. putida* IF-3 and the hypothetical protein mma_0224 in *Janthinobacterium* sp. Marseille. (b) Consensus sequences of the Rieske [2Fe-2S] domain (CXHX₁₆CX₂H, highlighted in black) and the mononuclear ferrous iron domain [(D/E)X₃DX₂HX₄H, highlighted in grey] are identified in Cdm and mma_0224.

The physiological functions of Cdm and mma_0224 have not yet been established, however, sequence analyses predicted both proteins to be Rieske [2Fe-2S]-domain-containing non-heme iron oxygenases (Figure 4.7b). The UV/visible absorption spectrum of oxidized Ndm exhibited maximum absorbance peaks at 318, 440, and 538 nm (Figure 4.8), which is characteristic of proteins with Rieske-type [2Fe-2S] clusters (Capyk *et al.*, 2009; Fee *et al.*, 1984; Subramanian *et al.*, 1979; Yu *et al.*, 2007). Also, the purified protein preparation had an R-value (A_{280}/A_{440}) of 11.1. Based on these results, both NdmA and NdmB appear to contain a Rieske-type [2Fe-2S] cluster, which was further confirmed by determining the gene sequences of both subunits (Chapter 5).

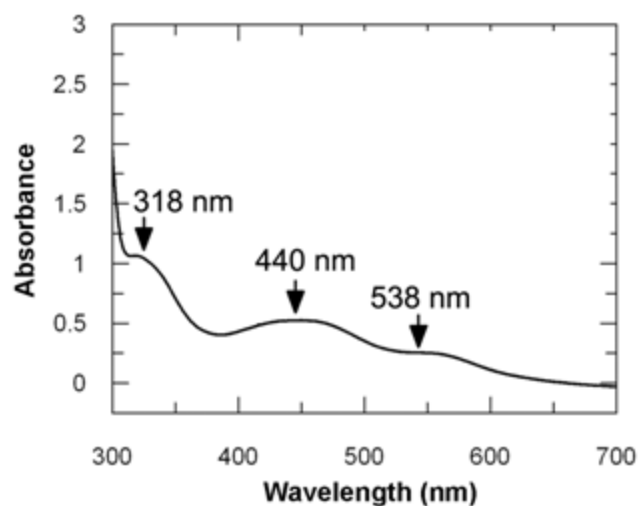


Figure 4.8. UV/visible spectrum of purified Ndm ($1.7 \text{ mg}\cdot\text{mL}^{-1}$) eluted from Q Sepharose. Ndm exhibited three peaks of maximum absorbance, at 318, 440, and 438 nm, characteristic of proteins with Rieske-type [2Fe-2S] clusters.

Table 4.2. Iron is required for *N*-demethylation of paraxanthine by Ndm.

Sample	mol Fe ²⁺ /mol Ndm	Specific Activity* on paraxanthine (mU/mg)	
		With 50 μM Fe ²⁺	Without 50 μM Fe ²⁺
Purified Ndm [†]	$8.5 \pm 0.1^{**}$	55	10
Reconstituted Ndm [#]	$20.1 \pm 0.3^{**}$	161	127

*One unit of activity corresponds to $1 \mu\text{mol}$ paraxanthine consumed $\cdot\text{min}^{-1}$, in the presence of saturating amounts of Ccr and $50 \mu\text{M}$ Fe²⁺, as described in Chapter 2.

[†]Purified Ndm prior to reconstitution of Fe²⁺.

[#]Ndm was reconstituted with Fe²⁺ by incubation with 1 mM Fe(NH₄)₂(SO₄)₂ for 15 min on ice. Excess Fe²⁺ was removed from the enzyme preparation by desalting prior to the assay.

**Values reported as mean \pm one standard deviation.

The purified Ndm preparation contained 8.5 ± 0.1 mol iron per mol hexameric Ndm, with a specific activity of $55 \text{ mU}\cdot\text{mg}^{-1}$ in the presence of $50 \mu\text{M Fe}^{2+}$ in the reaction mixture. If no Fe^{2+} was added to the enzyme reaction, specific activity decreased to $10 \text{ mU}\cdot\text{mg}^{-1}$. When Ndm was pre-incubated with 1 mM Fe^{2+} for 15 min and subsequently passed through a 5-mL desalting column, the iron content increased to 20.1 ± 0.3 mol per mol hexameric Ndm (Table 4.2). This reconstituted Ndm had specific activities to $161 \text{ mU}\cdot\text{mg}^{-1}$ and $127 \text{ mU}\cdot\text{mg}^{-1}$ when $50 \mu\text{M Fe}^{2+}$ was present or absent, respectively, in the enzyme reaction mixture (Table 4.2). Thus, a significant amount of iron appears to be dissociating from Ndm during the purification.

Optimal pH and Temperature of the *N*-demethylation reaction

Ndm was tested for activity in the range of 25°C to 40°C . Maximum Ndm activity was observed at 30°C (Figure 4.9A), with 67.9, 74.5, 59.4, and 7.0% of activity retained at 25, 33, 35, and 40°C .

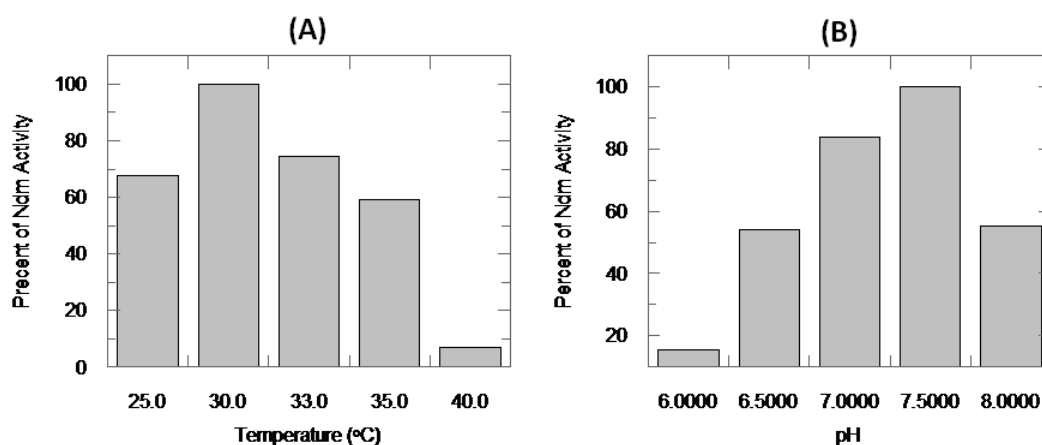


Figure 4.9. Relative activity of *N*-demethylation of paraxanthine by Ndm at different temperature (A) and pH (B). Values are reported as the percent of activity relative to those at which Ndm was most active, which were 30°C and a pH of 7.5.

Similarly, optimum pH for Ndm was tested between pH 6.0 to 8.0. Ndm exhibited optimal activity at a pH of 7.5 in 50 mM KP_i buffer (Figure 4.9B). Ndm activity was reduced to 15.5, 54.2, 83.9, and 55.1% at pH 6.0, 6.5, 7.0, and 8.0, respectively, in 50 mM KP_i buffer. Therefore, all reactions for Ndm activity, in the presence of saturating amount of Ccr and 50 μ M Fe^{2+} , were determined at 30°C in 50 mM KP_i (pH 7.5) buffer.

Oxygen Requirement and Stoichiometric Analysis of Ndm

Reaction

No *N*-demethylation of paraxanthine was observed when Ndm was added to a reaction mixture in a sealed container pre-flushed with N_2 gas (see chapter 2 for experimental set-up). After one hour, the anaerobic reaction was exposed to air, and Ndm activity was immediately restored (Figure 4.10A), indicating that *N*-demethylation by Ndm could be oxygen dependent.

The stoichiometric consumption of oxygen during *N*-demethylation of paraxanthine was demonstrated by monitoring the reaction with a Clark-type oxygen electrode in a sealed chamber. After 13 min of reaction, 79.5 μ M oxygen was consumed, while 60.2 μ M paraxanthine was *N*-demethylated (Figure 4.10B). Approximately 39.9 μ M 7-methylxanthine and 20.3 μ M xanthine were present in the reaction products, revealing that 80.5 μ M methyl groups were removed during the reaction (two are removed for each xanthine molecule formed from paraxanthine). These results indicate that approximately 1 molecule of O_2 was consumed per methyl group removed from paraxanthine. Also, these results indicate that Ndm can remove both the *N*-1 and *N*-7 methyl groups from paraxanthine.

Woolfolk (1975) reported that caffeine is *N*-demethylated through a hydrolytic mechanism in *Pseudomonas putida* strain 40. Since that report, however, several studies have attributed bacterial *N*-demethylation of caffeine to oxygenases due to the formation

of formaldehyde and water during *N*-demethylation reactions (Blecher and Lingens, 1977; Hohnloser *et al.*, 1980; Middelhoven and Lommen, 1984; Asano *et al.*, 1994). Because Ndm is predicted to be a Rieske [2Fe-2S] oxygenase, a simple method to detect the presence of formaldehyde in *N*-demethylation reactions was developed based on the method of Jones *et al.* (1999). Nash reagent (ammonium acetate, acetic acid, and 2,4-pentanedione) was added to aliquots taken from paraxanthine *N*-demethylation assay mixtures and heated at 51 °C for 12 min. Formaldehyde derivatized with ammonia and 2,4-pentanedione, resulting in the formation of 3,5-diacetyl-1,4-dihydrolutidine, which was detected by HPLC as described in Chapter 2.

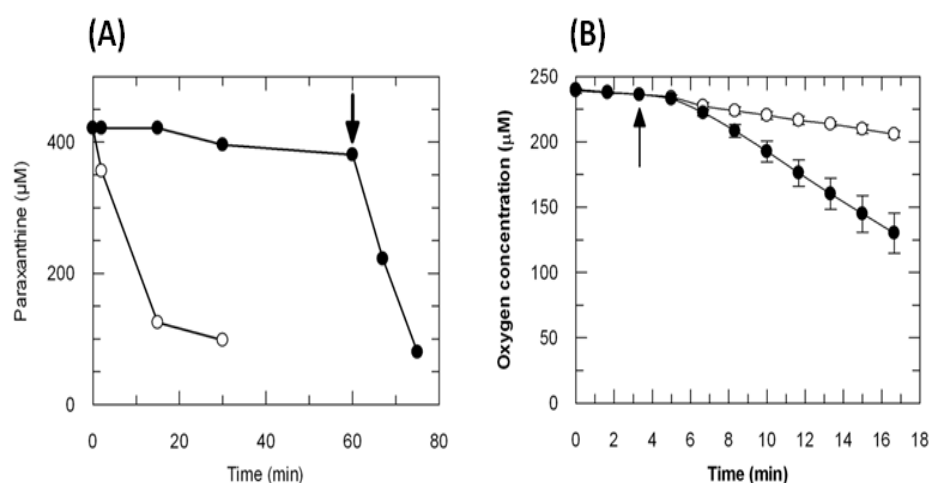


Figure 4.10. Oxygen is required for *N*-demethylation. (A) Degradation of 400 μM paraxanthine under aerobic (○) and anaerobic (●) conditions. After one hour, the anaerobic enzyme reaction mixture was exposed to ambient air (indicated by arrow), and paraxanthine was rapidly degraded. This experiment was repeated twice and a similar pattern was observed in both replicates. (B) Oxygen consumption by Ndm plus Ccr with (●) or without (○) 100 μM paraxanthine in the reaction mixture. The reactions were carried out in air-saturated buffer and equilibrated at 30 °C for 3.3 min before addition of Ndm plus partially purified Ccr to initiate the reactions (indicated by the arrow). The oxygen concentrations reported are means of four replicates with standard deviations (error bars).

After 90 min of incubation, $338.5 \pm 7.7 \mu\text{M}$ paraxanthine was *N*-demethylated by 7.4 units of Ndm, resulting in the production of $126.9 \pm 6.4 \mu\text{M}$ 7-methylxanthine and $193.7 \pm 14.0 \mu\text{M}$ xanthine, or $514.3 \pm 34.4 \mu\text{M}$ methyl groups removed. Simultaneously, $540.6 \pm 20.9 \mu\text{M}$ formaldehyde was formed (Figure 4.11). Thus, approximately one molecule of formaldehyde was formed per methyl group removed.

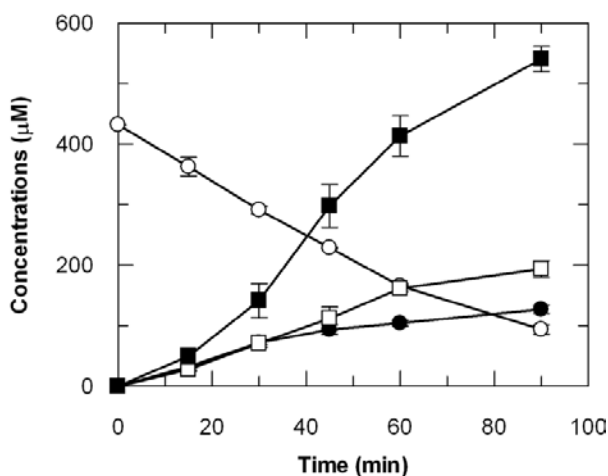


Figure 4.11. Stoichiometric *N*-demethylation of paraxanthine (○), via 7-methylxanthine (●) to xanthine (□) by purified Ndm with concomitant production of formaldehyde (■). The concentrations reported are means of triplicates with standard deviations (error bars).

Substrate Specificity of Ndm

The apparent K_M and k_{cat} values for Ndm were determined using paraxanthine and 7-methylxanthine as substrates over a range of $25 \mu\text{M}$ to $500 \mu\text{M}$ substrate (Figure 4.12). Ndm was most active on 7-methylxanthine, with apparent K_M and k_{cat} values of $63.8 \pm 7.5 \mu\text{M}$ and $94.8 \pm 3.0 \text{ min}^{-1}$, respectively (Figure 4.12A). With paraxanthine as substrate, the apparent K_M and k_{cat} values were $50.4 \pm 6.8 \mu\text{M}$ and $16.2 \pm 0.6 \text{ min}^{-1}$ (Figure 4.12B), respectively. The k_{cat}/K_M value for paraxanthine was nearly six-fold lower than that of 7-methylxanthine.

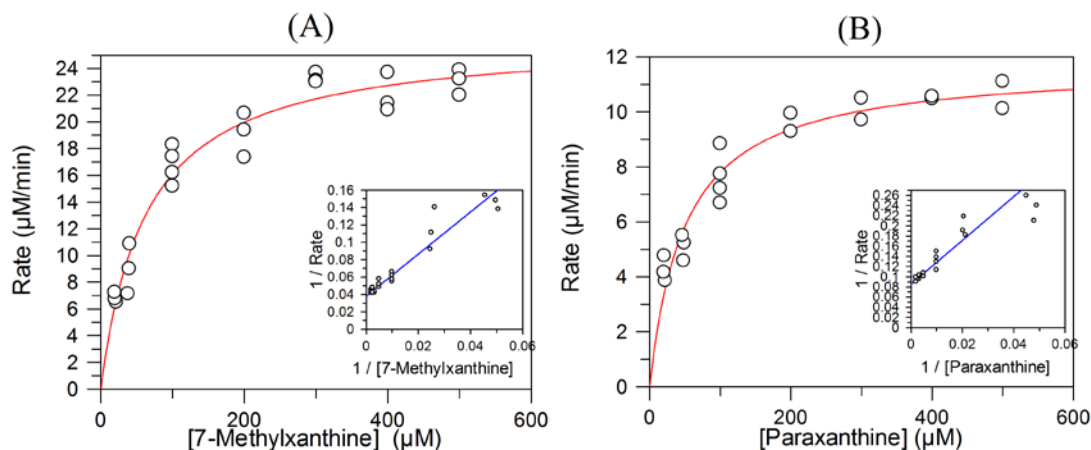


Figure 4.12. Rate of *N*-demethylation of 7-methylxanthine (A) and paraxanthine (B) by Ndm at concentrations of 20 μM to 500 μM substrate for determination of apparent K_M and k_{cat} .

Ndm was also active on caffeine, theophylline, theobromine, and 3-methylxanthine. The activities of Ndm on each substrate relative to paraxanthine are reported in Table 4.3. Xanthine was formed from all substrates tested, indicating that Ndm, in conjunction with the partially purified Ccr, is able to remove the methyl group from all three positions of the caffeine molecule. Ndm was most active on 7-methylxanthine, followed by paraxanthine, theobromine, 3-methylxanthine, caffeine, and theophylline. Because of the similarity of the N-terminal sequence of NdmA and NdmB with those of dicamba and vanillate *O*-demethylases, *O*-demethylation activity of Ndm was also examined. Ndm did not catalyze *O*-demethylation of either vanillate or vanillin, even after prolonged incubation. Thus, Ndm appears to be a broad-specificity *N*-demethylase capable of removing the methyl groups from all methylxanthines that were previously shown to serve as growth substrates (Table 4.3).

Table 4.3. Substrate preference of Ndm towards methylxanthines, relative to paraxanthine.

Substrate	Relative <i>N</i> -demethylase activity** at various substrate conc. (μ M)		Products identified*
	500	200	
Paraxanthine	100.0 \pm 3.1	100.0 \pm 3.7	7-methylxanthine, xanthine
7-Methylxanthine	455.7 \pm 17.6	664.2 \pm 61.1	xanthine
Theobromine	59.8 \pm 1.9	80.2 \pm 7.8	3- & 7-methylxanthine, xanthine
3-Methylxanthine	55.2 \pm 6.0	68.9 \pm 2.6	xanthine
Theophylline	17.6 \pm 1.0	14.2 \pm 1.6	1- & 3-methylxanthine, xanthine
Caffeine	30.8 \pm 1.7	48.2 \pm 4.8	paraxanthine, theobromine, 7-methylxanthine, xanthine

*The same products were identified at both concentrations of substrates.

**Relative activities are listed as the mean \pm one standard deviation from three replicates.

Reductase Requirement of Ndm

When the purified Ndm was assayed without the partially purified reductase component, no *N*-demethylase activity on caffeine, paraxanthine, theophylline, or theobromine was observed. Ndm is predicted to be a Rieske [2Fe-2S] non-heme iron oxygenase, and oxygenases of this type often exhibit promiscuity in terms of partner reductases (Subramanian *et al.*, 1979; Yu *et al.*, 2007). Therefore, Ndm was assayed with reductase plus ferredoxin or with reductase alone from either spinach or *Pseudomonas* sp. 9816 naphthalene dioxygenase system (Haigler & Gibson, 1990a, b). However, Ndm did not couple with any reductase, with or without ferredoxin, aside from the reductase present in the partially purified Ccr fraction. Thus, Ndm appears to be specific for coupling to the Ccr reductase component from CBB5 for the *N*-demethylation reaction.

Discussion

Ndm is a Broad-Specificity Methylxanthine *N*- Demethylase

This work represents the first purification and characterization of a broad-specificity, soluble *N*-demethylase from CBB5. The enzyme system is composed of a reductase component (Ccr) and an *N*-demethylase oxygenase component (Ndm). Ndm itself is a two-subunit enzyme with broad substrate specificity, capable of removing the *N*-methyl groups from the *N*-1, *N*-3, and *N*-7 positions of the xanthine molecule. Thus, Ndm can completely convert caffeine, all three natural dimethylxanthines, 3-methylxanthine, and 7-methylxanthine (Table 4.3) to xanthine. The ability of Ndm to *N*-demethylate 1-methylxanthine to xanthine was not tested due to lack of a purified stock of 1-methylxanthine. 1-Methylxanthine accumulated only transiently when theophylline was incubated with Ndm plus Ccr; hence, Ndm is proposed to carry out each *N*-demethylation step in both the caffeine and theophylline metabolic pathways shown in Figure 3.9.

7-Methylxanthine was the best substrate for Ndm, with a k_{cat}/K_M value almost six-fold higher than that for paraxanthine. No *O*-demethylation was observed when vanillate and vanillin were provided as the substrates for Ndm. Enzyme activity of Ndm was absolutely dependent on oxygen as a co-substrate. One molecule of O₂ was consumed for each *N*-methyl group removed from paraxanthine (Figure 4.10). *N*-Methyl groups removed from methylxanthines were stoichiometrically oxidized to form formaldehyde (Figure 4.11). Formation of formaldehyde from bacterial *N*-demethylation of caffeine has been reported previously (Blecher and Lingens, 1977; Asano *et al.*, 1994), but the stoichiometry of the reaction was not established. Whether the formaldehyde produced is utilized by CBB5 has yet to be determined.

Ndm Appears to be a Rieske [2Fe-2S] Non-Heme Iron Oxygenase

The N-terminal protein sequences of both Ndm subunits were substantially identical to the gene product of an uncharacterized caffeine demethylase gene in *P. putida* IF-3 (Koide *et al.*, 1996) and a hypothetical protein in *Janthinobacterium* sp. Marseille. Although the physiological functions of neither of these proteins have been established, both were predicted to be Rieske [2Fe-2S]-domain-containing non-heme iron oxygenases based on their gene sequences analysis. Besides sequence information, the UV/visible absorption spectrum of Ndm was characteristic of that of a protein with a Rieske [2Fe-2S] cluster (Figure 4.7b).

Exogenous addition of 50 μM Fe^{2+} to the Ndm enzyme reaction mixture stimulated Ndm enzyme activity 16-fold. This stimulation of activity has been observed in a number of Rieske [2Fe-2S]-domain-containing non-heme iron oxygenases, such as toluene, naphthalene, and biphenyl dioxygenases (Subramanian *et al.*, 1979; Ensley & Gibson, 1983; Yu *et al.*, 2007). It has been well documented that the mononuclear ferrous iron in Rieske oxygenases is not tightly bound and often dissociates during protein purification. However, iron could be reconstituted to the enzyme by incubating the oxygenase with excess Fe^{2+} . In fact, after incubating Ndm with 1 mM Fe^{2+} , the iron content of Ndm increased from 8.5 to 20.1 mol per mol hexameric Ndm (approximately 3 iron atoms per subunit). Furthermore, Ndm specific activity also increased from 55 $\text{mU}\cdot\text{mg}^{-1}$ to 161 $\text{mU}\cdot\text{mg}^{-1}$. Additional exogenous Fe^{2+} in the enzyme reaction mixture was not absolutely necessary for high Ndm activity. These results indicate that Ndm contains non-heme iron, probably one per subunit, which dissociates during purification. Therefore, Ndm is predicted to be a Rieske [2Fe-2S]-domain containing non-heme iron oxygenase based on the UV/visible absorption spectrum, N-terminal amino acid sequences of NdmA and NdmB, and the uptake of and stimulation of activity by exogenous Fe^{2+} .

The native molecular weight of Ndm was estimated to be 240 kDa by gel filtration chromatography. Both subunits of Ndm, NdmA and NdmB, were approximately 40 kDa (Figure 4.5), suggesting that Ndm is a hexameric protein. Because 20.1 iron atoms were present per molecule of reconstituted Ndm, it is very likely that each NdmA and NdmB subunit contains three iron atoms, in agreement with the presence of a [2Fe-2S] cluster and a mononuclear ferrous iron in each subunit. This finding is intriguing, however, because the mononuclear ferrous iron is known to be the catalytic center of Rieske oxygenases (Ferraro *et al.*, 2005). Both NdmA and NdmB are proposed to contain a mononuclear ferrous iron, which may suggest that there are two catalytic centers in native Ndm. However, the iron content of each subunit will need to be determined *via* cloning and testing the activity of NdmA and NdmB individually.

Some Rieske oxygenases are known to be assembled in a hexameric $\alpha_3\beta_3$ configuration (Kauppi *et al.*, 1998; Dong *et al.*, 2005; Friemann *et al.*, 2005; Yu *et al.*, 2007). In these cases, however, only the α subunits contain the [2Fe-2S] cluster and the mononuclear ferrous iron, while the β subunits are mainly for structural purposes (Ferraro *et al.*, 2005). The 2-oxo-1,2-dihydroquinoline 8-monooxygenase of *P. putida* 86 was reported to be in an α_6 configuration, determined by gel filtration chromatography (Rosche *et al.*, 1995), but the crystal structure showed that it is actually a homotrimer (Martins *et al.*, 2005). The proposed presence of two catalytic centers in Ndm raises some important questions, such as

1. How reducing equivalents generated from the reductase component are distributed between these two catalytic centers,
2. Whether both catalytic centers are functional, and
3. If they have different or overlapping substrate specificities which, in combination, account for the substrate preferences of Ndm.

The present data also does not completely exclude the possibility that NdmA and NdmB are individual Rieske oxygenases that co-purify or agglomerate together during

purification. In this case, each enzyme could have different or overlapping substrate specificity. Heterologous expression of each subunit separately will answer some of these questions.

Ndm Receives Electrons from a Specific Reductase

Ndm enzyme activity was dependent on the presence of a reductase component, Ccr. This reductase component exhibited NAD(P)H-dependent cytochrome *c* reductase activity *in vitro*, and was thus designated Ccr (cytochrome *c* reductase component). The purified reductases of several well-characterized Rieske non-heme iron oxygenases are also known to reduce cytochrome *c in vitro* (Subramanian *et al.*, 1979; Haigler and Gibson, 1990b; Yu *et al.*, 2007). In the present case, partially purified Ccr was used in order to purify the Ndm component, and the Ccr requirement for *N*-demethylation by Ndm was specific. Ferredoxins and/or reductases of either spinach or the *Pseudomonas* sp. 9816 naphthalene dioxygenase system (Haigler and Gibson, 1990a, b) did not support the *N*-demethylase reaction by Ndm. In contrast, the reductase components of toluene dioxygenase of *P. putida* (Subramanian *et al.*, 1979) and biphenyl dioxygenase of *Sphingobium yanoikuyae* B1 (Yu *et al.*, 2007) are easily substituted by spinach ferredoxin reductase and the reductase of naphthalene dioxygenase, respectively.

A proposed reaction scheme for *N*-demethylation of paraxanthine (and other methylxanthines) by Ccr plus Ndm is presented in Figure 4.13. This scheme is similar to those of other known microbial mono- and dioxygenases; however, none of the other oxygenases is known to catalyze *N*-demethylation. Here, a specific Ccr is hypothesized to function in the transfer of electrons to Ndm, the oxygenase component exhibiting broad-based *N*-demethylation activity on purine alkaloids. This enzyme system accounts for the ability of CBB5 to utilize these substrates for growth. Molecular oxygen is incorporated into formaldehyde and water, with one molecule of oxygen consumed per methyl group removed.

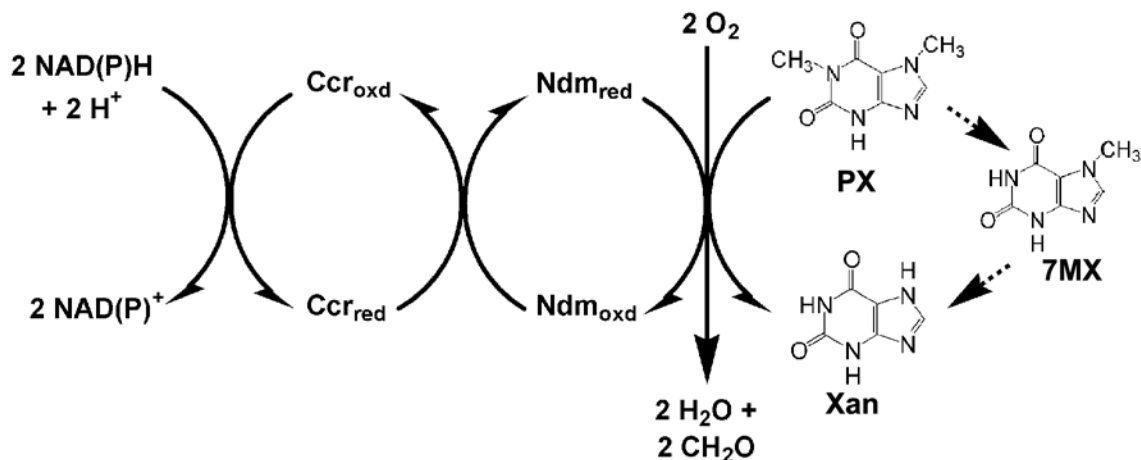


Figure 4.13. Proposed reaction scheme for paraxanthine *N*-demethylation by the *P. putida* CBB5 two-component *N*-demethylase. Reducing equivalents are transferred from NAD(P)H to the two-subunit *N*-demethylase component (Ndm) by a specific reductase (Ccr). One mole of paraxanthine (PX) is *N*-demethylated to xanthine (Xan) through 7-methylxanthine (7MX) as an intermediate (dashed arrow).

The Number of *N*-demethylases in *P. putida* CBB5 is Still

Unknown

Whether Ndm is the only *N*-demethylase responsible for methylxanthine metabolism in CBB5 is currently unclear. Some indirect experiments reported in the literature indicate the presence of specific, and most likely multiple, *N*-demethylases in caffeine-metabolizing bacteria. Glück and Lingens (1988) partially purified a specific 7-methylxanthine *N*-demethylase from caffeine-degrading *P. putida* WS. This enzyme was not active on caffeine, theobromine, or paraxanthine. Also, *N*-demethylation of 7-methylxanthine by the partially purified enzyme was not inhibited by caffeine or theobromine. These results imply multiple *N*-demethylases in *P. putida* WS for degradation of caffeine. A recent report by Dash and Gummadi (2008) showed that caffeine and theobromine *N*-demethylases in *Pseudomonas* sp. NCIM 5235 were inducible in nature, but that caffeine *N*-demethylase activity in theobromine-grown cells

was 10-fold lower than that of caffeine grown cells. This also implies different *N*-demethylases for caffeine and theobromine *N*-demethylation.

Finally, the presence of multiple *N*-demethylases was also implicated in caffeine-degrading *P. putida* no. 352 (Asano *et al.*, 1994). Three distinct fractions exhibiting caffeine *N*-demethylase activity were partially purified by DEAE Sepharose. One of the fractions was reported as a theobromine *N*-demethylase, and was capable of producing 7-methylxanthine from theobromine. This activity was inhibited by addition of Zn^{2+} to the reaction mixture, while caffeine *N*-demethylation in all three fractions was not inhibited. The theobromine *N*-demethylase was subsequently purified to homogeneity and reported to have a native molecular weight of 250 kDa and a subunit molecular weight of 41 kDa (theorized as a homohexamer). This enzyme was brown in color and exhibited an absorbance maximum of 415 nm; however, it has not been well characterized. Based on the previously published data described above, the presence of multiple *N*-demethylases involved in caffeine metabolism appears likely. However, Ndm is distinct from the above *N*-demethylases in terms of substrate specificity, UV/visible absorption spectrum, subunit structure, and requirement of a reductase component.

The *P. putida* CBB5 methylxanthine Ndm provides the first concrete example of a Rieske non-heme iron oxygenase with broad-based *N*-demethylase activity on a number of purine alkaloids. Although the caffeine demethylase gene in *P. putida* IF-3 (Koide *et al.*, 1996) was predicted to encode a Rieske non-heme iron oxygenase, the gene function was assigned solely based on reversion to a caffeine-negative phenotype of a mutated strain of *P. putida* IF-3. There are no direct enzymological data to substantiate this claim. Also, the physiological function of this enzyme with respect to the ability of bacteria to utilize purine alkaloids as a sole source of carbon and nitrogen is unknown. The *N*-demethylation of *N*-methylaniline and *N,N*-dimethylaniline to aniline by naphthalene dioxygenase of *Pseudomonas* sp. Strain 9816 was reported by Lee (1995). This reaction is not well characterized and indicates only the promiscuity of naphthalene dioxygenase,

not its physiological role in *N*-demethylation. This enzyme, in fact, enables the utilization of naphthalene by converting it to *cis*-dihydroxy-1,2-dihydronaphthalene (Ensley and Gibson, 1983).

N-Demethylation (or *N*-dealkylation) reactions in eukaryotes and prokaryotes are known to be catalyzed only by cytochrome P450s (Tassaneeyakul *et al.*, 1994; Cha *et al.*, 2001; Guengerich, 2001; Abel *et al.*, 2003; Caubet *et al.*, 2004; Asha and Vidyavathi, 2009), various flavo-enzymes (Wagner, 1982; Kvalnes-Krick and Jorns, 1986; Nishiya and Imanaka, 1993; Phillips *et al.*, 1998; Meskys *et al.*, 2001; Shi *et al.*, 2004; Chang *et al.*, 2007), and a ketoglutarate-dependent non-heme iron oxygenase (Tsukada *et al.*, 2005). The present study therefore broadens the understanding of the possible enzymatic mechanism for *N*-demethylation and will aid the discovery of new microbial *N*-demethylases in the future.

Summary

Pseudomonas putida CBB5 uses a broad-specificity, two component *N*-demethylase system to initiate biotransformation of caffeine and related natural purine alkaloids. The *N*-demethylation of these compounds is catalyzed by the terminal *N*-demethylase (Ndm), a two-subunit oxygenase. A specific Ccr component with cytochrome *c* reductase activity is involved in the transfer of electrons from NADH to Ndm. The methyl groups are liberated stoichiometrically to form formaldehyde, utilizing one molecule of NADH per methyl group removed. The N-terminal protein sequences of Ndm subunits were significantly homologous to two proteins predicted to the Rieske [2Fe-2S]-domain containing, non-heme iron oxygenases. Also, the hypothesis that Ndm is a Rieske [2Fe-2S] non-heme iron oxygenase is further supported by the iron content and UV absorbance spectrum of the enzyme. This is the first report and detailed characterization of a bacterial *N*-demethylase responsible for the degradation of caffeine. Future research will focus on isolation of the gene sequences coding for NdmA and

NdmB, their cloning, and heterologous expression as a means to confirm the results from this biochemical investigation of Ndm.

CHAPTER 5
CLONING, HETEROLOGOUS EXPRESSION, AND ACTIVITY OF
NDMA AND NDMB

Introduction

A novel methylxanthine *N*-demethylase (Ndm) was purified from *Pseudomonas putida* CBB5 (Summers *et al.*, 2011; Chapter 4 of this document). This heterohexameric enzyme was composed of two subunits, NdmA and NdmB, which could not be separated by protein chromatographic methods. Ndm consumed oxygen and removed the *N*-1, *N*-3, and *N*-7 methyl groups from caffeine to form xanthine with stoichiometric production of formaldehyde and water. Ndm received reducing equivalents from NAD(P)H *via* a partially purified reductase component (Ccr). The enzyme was capable of *N*-demethylating caffeine, theophylline, and all of their methylxanthine metabolites shown in Figure 3.9.

Based on its reductase requirement, iron content, and the 25 N-terminal amino acid sequences of both NdmA and NdmB, Ndm was predicted to be a Rieske [2Fe-2S] non-heme iron monooxygenase. Cloning and heterologous expression of Ndm may be of interest in many biotechnological applications, including pharmaceutical production, bioremediation, and wastewater treatment. In order to utilize Ndm in these applications, the genes coding for NdmA and NdmB- *ndmA* and *ndmB*, respectively- would need to be determined.

The expected sizes of *ndmA* and *ndmB* were determined to be approximately 1.1 kb and 0.95 kb, respectively, based on the Equation 5.1:

$$G_{\text{size}} = 27.27 * P_{\text{size}}, \quad (5.1)$$

where G_{size} is the size of the gene, in bp, and P_{size} is the apparent molecular weight of the protein subunit, in kDa (40 and 35 kDa, respectively).

Because NdmA and NdmB appeared to form a single enzyme, it was hypothesized that the genes coding for them are in close proximity on the genome.

Figure 5.1 illustrates the four potential orientations of these two genes.

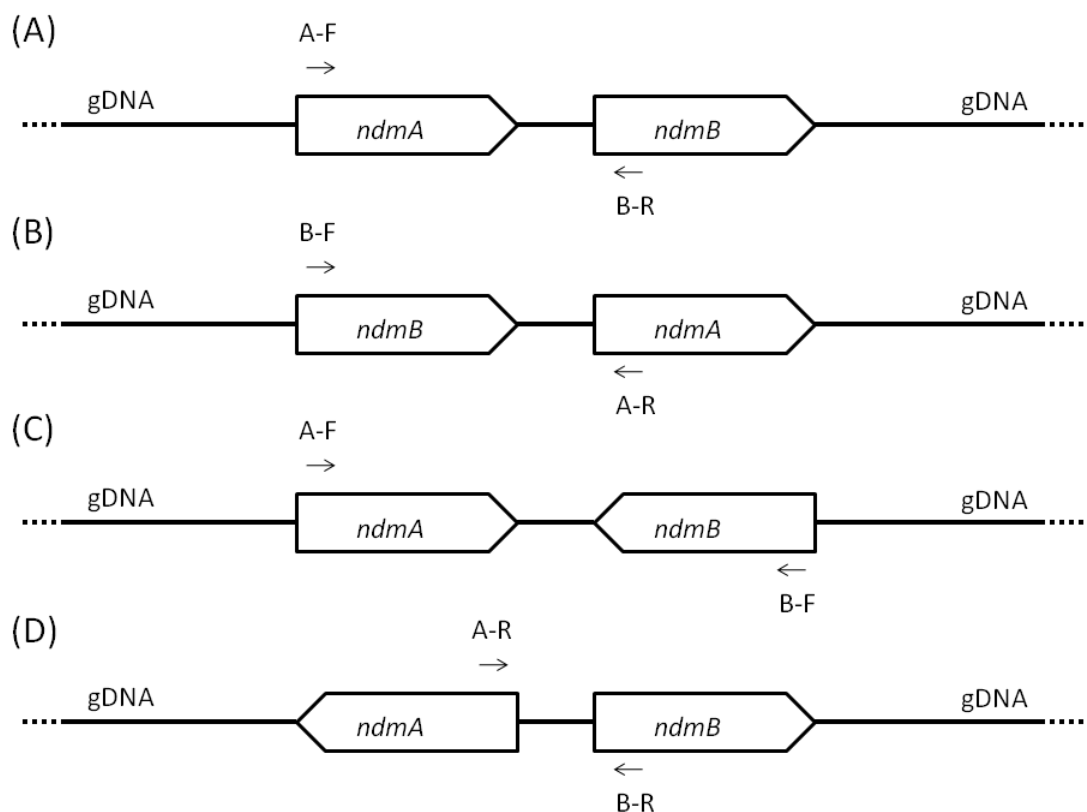


Figure 5.1. The four potential arrangements for *ndmA* and *ndmB* where both are proximal on the genome of CBB5. The *ndmA* and *ndmB* genes could be in the same direction as each other with either *ndmA* 5'-to *ndmB* (A) or *ndmB* 5'-to *ndmA* (B). The genes could also be in opposite directions, with their respective 3' ends (C) or 5' ends (D) nearest each other. Degenerate forward (A-F and B-F) and reverse (A-R and B-R) primers designed from the N-terminal amino acid sequences of NdmA and NdmB are also depicted.

As shown above, *ndmA* and *ndmB* could lie in either the same or opposite directions on the genome. In the example shown in Figure 5.1A, *ndmB* is downstream of (3'- to) *ndmA*. Using a degenerate forward primer (A-F) designed from the N-terminal

amino acid sequence of NdmA and a degenerate reverse primer (B-R) designed from the N-terminal amino acid sequence of NdmB, the *ndmA* sequence and region between the two genes could be amplified by polymerase chain reaction (PCR). Conversely, *ndmB* could be upstream of (5'- to) *ndmA* (Figure 5.1B), in which case the degenerate forward and reverse primers (B-F and A-R) would be generated from the N-terminal amino acid sequences of NdmB and NdmA, respectively, to amplify *ndmB*.

The *ndmA* and *ndmB* genes could also lie in opposite directions on the genome. If the 3'-regions of both genes are nearest each other (Figure 5.1C) and within 4 kbp of each other, the sequence for both might be amplified by PCR using degenerate forward primers for each gene (A-F and B-F). In the last scenario (Figure 5.1D), the 5'-regions of both genes would be nearest each other, with the genes oriented in opposite directions. In this case, the region between both genes could be amplified using degenerate reverse primers from both genes (A-R and B-R). However, the sequences of both *ndmA* and *ndmB* could not be amplified by PCR using degenerate reverse primers designed from the N-terminal sequences of NdmA and NdmB in this final scenario.

Previous Work

Two CBB5 genomic DNA (gDNA) libraries were created by Dr. Michael Louie. These libraries were prepared by partially digesting gDNA with EcoRI or SmaI restriction enzymes and ligating the digested DNA to a pUC19kan vector. The pUC19kan vector was created by replacing the ampicillin marker on the pUC19 vector with a kanamycin marker. The pUC19kan vector also contains a *lacZa* gene for β -galactosidase blue/white screening.

Determination of 5'-Sequences of *ndmA* and *ndmB*

Degenerate forward and reverse primers were designed based on the N-terminal amino acid sequences of NdmA (MEQAIIN, primers A-degF, A-degR) and NdmB (MKEQLKP, primers B-degF, B-degR). For a complete list of primers used in this study

and their sequences, see Appendix A. The forward and reverse primers were used in different combinations during PCR (reactions 1A-1D) to determine if *ndmA* and *ndmB* were near each other on the genome (Table 5.1). Taq DNA polymerase was used in the reactions with an extension time of 2.5 min. A complete list of each PCR reaction is given in Table 2.2. A non-specific product approximately 3 kb in size due to the A-degF primer was amplified in reactions 1A and 1C (Figure 5.2). In reactions 1B and 1C, three bands (3, 1.8, and 1.4 kb) due to the B-degF primer were observed. A specific 2.5-kb PCR product was detected in reaction 1D that was not present in either single primer or no template controls.

Table 5.1. PCR set-up to determine if *ndmA* and *ndmB* were near each other on the genome using degenerate primers derived from the N-terminal amino acid sequences of NdmA and NdmB.

Reaction	Forward Primer	Reverse Primer	Template	Observed Product
1A	A-degF	B-degR	gDNA	Non-specific PCR product from A-degF
1B	B-degF	A-degR	gDNA	Non-specific PCR product from B-degF
1C	A-degF	B-degF	gDNA	Non-specific PCR product from both primers
1D	A-degR	B-degR	gDNA	2.5-kb specific PCR product

These results indicate that *ndmA* and *ndmB* lie in opposite directions on the genome, with their respective 5'-regions nearest each other (scenario D in Figure 5.1) and are approximately 2.5 kb apart. Given the N-terminal amino acid sequences of both NdmA and NdmB, the region between *ndmA* and *ndmB* could be amplified and sequenced. However, the sequences for either *ndmA* or *ndmB* cannot be amplified by PCR given the information available. Therefore, a new method was developed in order to obtain the sequences of *ndmA*, *ndmB*, and their flanking regions.

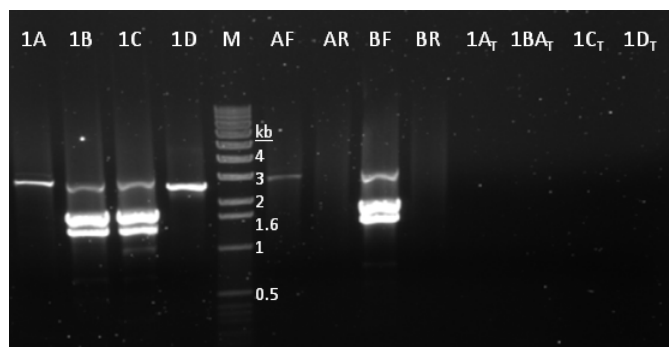


Figure 5.2. Agarose gel electrophoresis of reactions 1A, 1B, 1C, 1D, and their controls to determine the orientation of *ndmA* and *ndmB* relative to each other. M, kb marker; AF, A-degF primer only; AR, A-degR primer only; BF, B-degF primer only; BR- B-degR primer only; 1A_T, 1B_T, 1C_T, 1D_T, no template controls of reactions 1A, 1B, 1C, and 1D, respectively.

Two new forward degenerate primers were designed from the N-terminal amino acid sequences of NdmA (AIINDERE, primers A-degF2 and A-degF3) and NdmB (KPLLEDKT, primers B-degF2 and B-degF3). Because Ndm was predicted to be a Rieske [2Fe-2S]-type oxygenase, a single reverse primer was designed from the most conserved region (CX[Y/F]HGW, Rieske-R primer) of many Rieske [2Fe-2S]-type oxygenase conserved domains (Table 5.2).

Table 5.2. PCR set-up to amplify approximately 250 bp of *ndmA* and *ndmB* using degenerate primers derived from the N-terminal amino acid sequences of NdmA and NdmB.

Reaction	Forward Primer	Reverse Primer	Expected Product Size	Observed Product
A1	A-degF2	Rieske-R	250 bp	250 bp
A2	A-degF3	Rieske-R	250 bp	250 bp
B1	B-degF2	Rieske-R	250 bp	270 bp
B2	B-degF3	Rieske-R	250 bp	270 bp

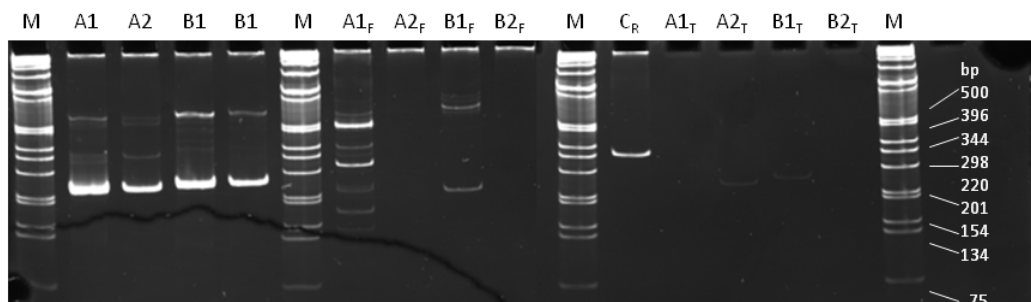


Figure 5.3. Acrylamide gel electrophoresis of reactions A1, A2, B1, B2, and their controls. M, kb marker; XY_F, forward primer only controls; C_R, reverse primer only control; XY_T, no template controls. A product of approximately 250 bp was amplified in each reaction, but was not observed in the control reactions.

PCR of the Rieske-R primer with each of the forward degenerate primers using gDNA as a template resulted in the production of DNA segments approximately 240-270 bp in length, as determined by PAGE (Figure 5.3). Single primer and no-template controls did not yield the major DNA fragments from the PCR reactions. Therefore, the PCR products were subjected to TA ligation with the pGEM-TEZ vector.

The TA-ligated clones were electroporated into JM109 electrocompetent cells as described in Chapter 2, plated on LBAXI agar, and incubated overnight at 37 °C. Five white colonies from each plate were screened for insertion of the DNA fragment by PCR using T7 and SP6 primers on either side of the cloning site of the pGEM-TEZ vector. A single blue colony was used as the negative control. All clones contained inserts of approximately expected size (Figure 5.4), therefore, colonies A1₄, A2₃, B1₃, and B2₃ were grown overnight in LB broth with 100 µg/mL ampicillin (LBA broth) at 37 °C. The plasmids of all colonies were extracted and submitted for sequencing. Sequencing results from the plasmids matched the N-terminal sequences of NdmA and NdmB. The *ndmA* sequence was 258 bp, while that of *ndmB* was 276 bp. Thus, approximately 25% of each sequence was determined (see Appendix B for full gene sequences). These results also

indicate that both *ndmA* and *ndmB* contain Rieske [2Fe-2S] domains, as predicted by the biochemical characterization of Ndm.

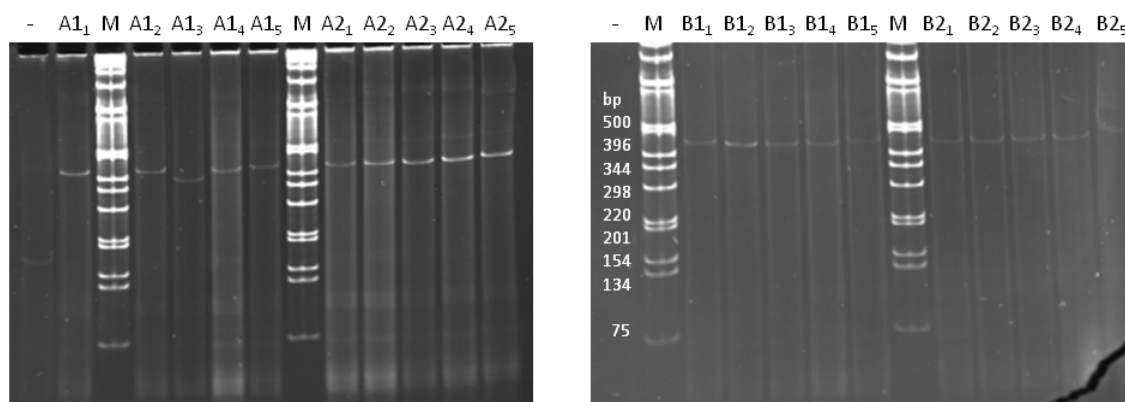


Figure 5.4. Screening of JM109 colonies containing the TA-ligated 250 bp PCR product from reactions A1, A2, B1, and B2. Five colonies of each ligation were screened. Inserts of approximately the correct size were found in all lanes.

Further Sequencing of *ndmA* and *ndmB*

A BLASTN search revealed that the 0.25-kb nucleotide sequences coding for both *ndmA* and *ndmB* were most similar to the sequences of a hypothetical caffeine demethylase gene (*cdm*, accession number AAB15321) and an uncharacterized gene from the *Janthinobacterium* sp. Marseille genome (*mma_0224*, YP_01355314). The hypothetical gene products of these two genes were also the two most similar protein sequences to NdmA and NdmB, as determined by a BLASTP search. Alignment of the *cdm* and *mma_0224* predicted protein sequences revealed two conserved regions, one approximately in the middle of the peptide sequence, and one nearly 10% from the C-terminus of both enzymes. Two degenerate reverse primers, *cdm*-R3 and *cdm*-R2, were designed from the two respective conserved regions. Furthermore, a conserved

nucleotide region at the 3'-end of both genes was detected, from which a specific reverse primer, cdm-R1 was designed.

Table 5.3. PCR set-up to amplify *ndmA* and *ndmB* using the cdm-R1 reverse primer.

Reaction	Forward Primer	Reverse Primer	Expected Product Size	Observed Product
A1-1	A-degF	cdm-R1	1 kb	0.95 kb
A1-2	A-degF2	cdm-R1	1 kb	0.9 kb
A1-3	A-degF3	cdm-R1	1 kb	1 kb
A1-4	A-speF	cdm-R1	1 kb	1 kb
B1-1	B-degF	cdm-R1	0.9 kb	No product
B1-2	B-degF2	cdm-R1	0.9 kb	Non-specific PCR product
B1-3	B-degF3	cdm-R1	0.9 kb	Non-specific PCR product
B1-4	B-speF	cdm-R1	0.9 kb	No product

Four PCR reactions (reactions A1-1, A1-2, A1-3, and A1-4) were set up using cdm-R1 with the specific and degenerate primers for *ndmA* and *ndmB* (Table 5.3). An approximately 1-kb product was produced from all *ndmA* primers (Figure 5.5A). The product was slightly smaller when A-speF was used than with A-degF1, A-degF2, or A-degF3, which was expected since A-speF is 66 bp downstream of the start codon. No specific product was detected when any of the primers for *ndmB* were used. A weak band, approximately 0.9 kb was detected when B-degF2 was combined with cdm-R1. However, the same 0.9-kb band was also present in the B-degF2 single primer control (Figure 5.5B), indicating that it was amplified due to non-specific binding of primer B-degF2.

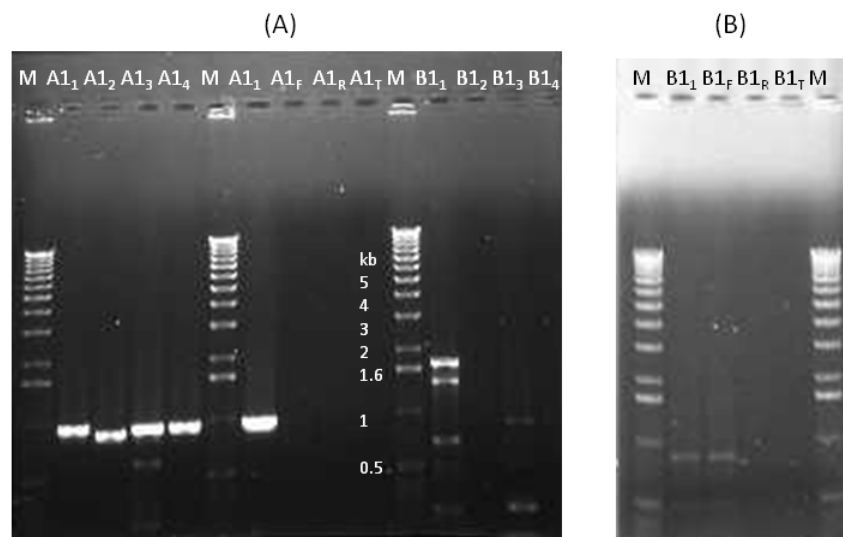


Figure 5.5. PCR of *ndmA* and *ndmB* using the *cdm-R1* reverse primer. (A) An approximately 1-kb *ndmA* product was amplified in each reaction ($A1_1$ - $A1_4$) and not observed in the control reactions ($A1_F$, forward only primer; $A1_R$, reverse only primer; $A1_T$, no template). (B) Products observed in reaction $B1_1$ ($B1_1$) were due to non-specific amplification from the *B-degF1* primer ($B1_F$). No specific *ndmB* products were amplified with the *cdm-R1* primer.

Table 5.4. PCR set-up to amplify *ndmB* using the *cdm-R2* and *cdn-R3* reverse primers.

Reaction	Forward Primer	Reverse Primer	Expected Product Size	Observed Product
B2-1	B-degF	<i>cdm-R2</i>	0.9 kb	Non-specific PCR product
B2-2	B-degF2	<i>cdm-R2</i>	0.9 kb	Non-specific PCR product
B2-3	B-degF3	<i>cdm-R2</i>	0.9 kb	Non-specific PCR product
B2-4	B-speF	<i>cdm-R2</i>	0.9 kb	Non-specific PCR product
B3-1	B-degF	<i>cdm-R3</i>	0.5 kb	0.45 kb
B3-2	B-degF2	<i>cdm-R3</i>	0.5 kb	0.5 kb
B3-3	B-degF3	<i>cdm-R3</i>	0.5 kb	0.5 kb
B3-4	B-speF	<i>cdm-R3</i>	0.5 kb	0.5 kb

Only weak, non-specific bands were produced from PCR using the *ndmB* primers with *cdm-R2* (Figure 5.6A), as observed with the *cdm-R1* primer. PCR using *cdm-R3* as

the reverse primer resulted in amplification of a DNA band approximately 500 bp in size with any of the four *ndmB* primers (Figure 5.6A, Table 5.4). Although the B-degF1 single primer control reaction produced many bands, none was 500 bp in size, thus confirming that the 500 bp DNA fragment was produced due to specific annealing of the primers (Figure 5.6B).

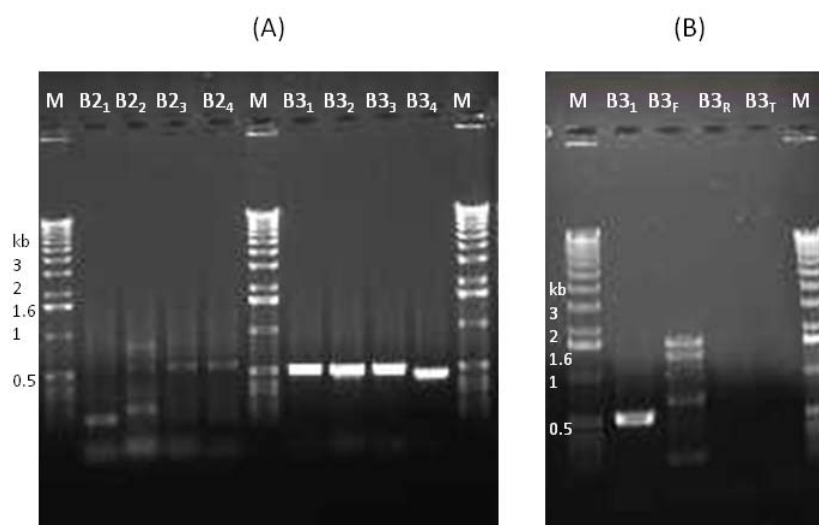


Figure 5.6. PCR of *ndmB* using the cdm-R2 and cdm-R3 reverse primers. (A) About 500 bp *ndmB* were amplified using cdm-R3 reverse primer (B3₁-B3₄). No specific products were observed using cdm-R2 primer (B2₁-B2₄). (B) The 500 bp product in reaction B3-1 (B3₁) was not produced in the forward primer only (B3_F), reverse primer only (B3_R), and no template (B3_T) controls.

The reaction mixtures containing the 1-kb product amplified from *ndmA* and the 500-bp product amplified from *ndmB* were subjected to TA ligation to the pGEM-TEZ vector and electroporated into *E. coli* JM109. The transformants were plated onto LBAXI agar and incubated at 37 °C overnight. Three transformants were subsequently grown overnight in LBA broth, and their plasmids were then extracted and submitted for sequencing. Sequencing results revealed that the inserted DNA matched both the 250-bp products originally sequenced and the N-terminal amino acid sequences for NdmA and

NdmB. The *ndmA* and *ndmB* sequences were 963 bp (321 amino acids) and 528 bp (176 amino acids) in length, respectively, and neither contained a stop codon. Thus, based on predicted gene length, approximately 95% of *ndmA* and 55% of *ndmB* sequences were obtained.

Isolation of the Complete *ndmA* Gene

The complete *ndmA* gene was isolated by adapting the nested PCR approach (Figure 5.7) described by Porter-Jordan *et al.* (1990).

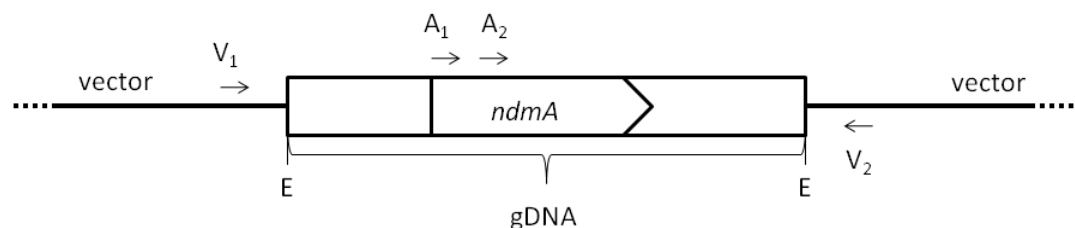


Figure 5.7. Scheme for a nested PCR approach to amplify *ndmA* from a CBB5 gDNA library. E, restriction enzyme site; V₁, pUC19R primer; V₂, Marcy primer; A₁, A-speF2 primer; A₂, A-speF3 primer.

In this approach, two sequential specific primers (A-speF2 and A-speF3) were designed from the *ndmA* sequence already obtained. Because the insert can ligate with the vector in either direction, reverse vector primers were designed on either side of the inserted gDNA (Marcy and pUC19R primers). A list of primers and templates used in the nested PCR approach is given in Table 5.5.

A primary PCR reaction was effected using A-speF2 forward primer and Marcy or pUC19R reverse primers. Taq polymerase was used to amplify DNA; Pfu polymerase could not generate a product. The EcoRI or SmaI gDNA libraries were used as template DNA. A second round of PCR was then performed with the amplified DNA from the

primary PCR reactions serving as template. A-speF3 forward primer and Marcy and pUC19R reverse primers were used to amplify the desired sequence from the primary reaction as described in Table 2.2. Analysis by agarose gel electrophoresis revealed a dominant PCR product band of approximately 3 kb in reaction E1-2, which was originally amplified from the EcoRI library using the Marcy reverse primer (Figure 5.8). No other specific band was detected in any of the reactions. The 3-kb DNA product was gel purified and submitted for sequencing.

Table 5.5 Primers and templates used to amplify the *ndmA* DNA from gDNA libraries using a nested PCR approach.

Reaction Number	Forward Primer	Reverse Primer	Template
E1-1	A-speF2	Marcy	EcoRI library
E2-1	A-speF2	pUC19R	EcoRI library
S1-1	A-speF2	Marcy	SmaI library
S2-1	A-speF2	pUC19R	SmaI library
E1-2	A-speF3	Marcy	E1-1
E2-2	A-speF3	pUC19R	E2-1
S1-2	A-speF3	Marcy	S1-1
S2-2	A-speF3	pUC19R	S2-1

The 5' sequence of the 3-kb DNA product from E1-2 matched the 1 kb *ndmA* already obtained and also contained the remaining 3'-end of *ndmA*. The complete gene sequence and predicted peptide sequence can be found in Appendix B. The sequence for *ndmA* contains both Rieske [2Fe-2S] and non-heme iron domains, as predicted by the biochemical characterization of purified protein described in Chapter 4. The complete gene includes 1,056 bp, or 351 amino acids. Predicted size of the encoded peptide, based on sequence length and an average amino acid size of 110 Da, was 40.2 kDa, similar to the 40 kDa predicted by SDS-PAGE of the purified enzyme.

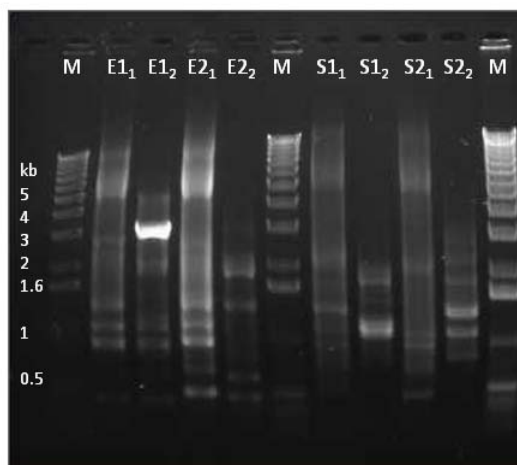


Figure 5.8. A 3-kb PCR product containing the 3' end of *ndmA* was observed in the nested PCR reaction E1-2 (E1₂). No other dominant PCR products were amplified using the PCR approach.

Isolation of the Complete *ndmB* Gene

Although many different specific forward primers were used, the nested PCR approach used to isolate the complete *ndmA* gene did not work alone for isolation of *ndmB* gene. Instead, this approach was combined with a site-directed mutagenesis approach (Bauer *et al.*, 2002) in order to sequence the complete *ndmB* gene as described in Chapter 2. Two pairs of complimentary primers (B-iPCR-F1/B-iPCR-R1 and B-iPCR-F2/BiPCR-R2) were designed approximately 300 bp from the known 5' end of *ndmB*. These two pairs of primers were used to enrich the *ndmB*-containing clones from the EcoRI gDNA library by PCR with Pfu polymerase. Following PCR, DpnI restriction enzyme was added to the reaction mixtures to degrade the methylated gDNA library template.

A nested PCR approach using DpnI-treated reactions B1-0 and B2-0 was performed according to Table 5.6 to isolate the complete *ndmB* sequence. Analysis of the reactions by agarose gel electrophoresis revealed the presence of a major DNA band

amplified in reaction B2-2 (Figure 5.9), which was not produced in the single primer and no template controls.

Table 5.6. Primers and templates used in the site directed mutagenesis and nested PCR approaches used to isolate *ndmB*.

Reaction Number	Forward Primer	Reverse Primer	Template
B1-0	B-iPCR-F1	B-iPCR-R1	EcoRI library
B2-0	B-iPCR-F2	B-iPCR-R2	EcoRI library
B1-1	B-speF3	Marcy	B1-0
B2-1	B-speF3	pUC19R2	B2-0
B3-1	B-speF3	Marcy	EcoRI library
B1-2	B-speF6	Marcy	B1-1
B2-2	B-speF6	pUC19R	B2-1
B3-2	B-speF6	Marcy	B3-1

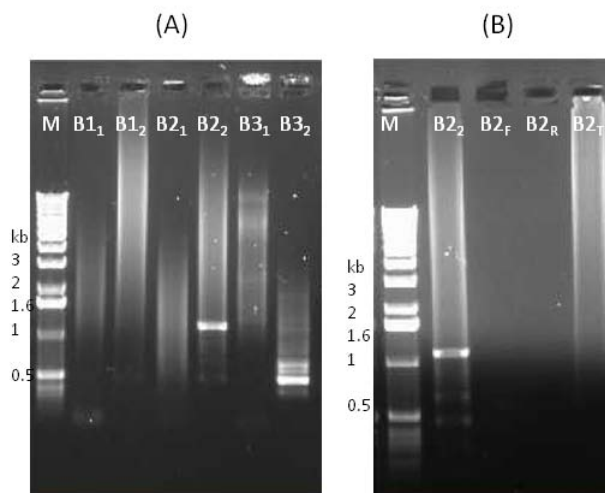


Figure 5.9. A combination of site-directed mutagenesis and nested PCR approaches was used to sequence the complete *ndmB* gene. (A) Amplification of DNA containing *ndmB* resulted in a 1.1-kb product in reaction B2-2 (B2₂). (B) The 1.1-kb product was not amplified in the forward primer only (B2_F), reverse primer only (B2_R), or no template (B2_T) controls.

The 1.5-kb PCR product in about 300 μ L reaction B2-2 was gel purified and submitted for DNA sequencing. The 5' portion of the resulting sequencing data matched the known *ndmB* sequence, and the remaining, unknown, 3' portion of the *ndmB* sequence was also present. The complete gene and peptide sequence of *ndmB* can be found in Appendix B.

As with the sequence for *ndmA*, *ndmB* contains both Rieske [2Fe-2S] and non-heme iron domains. This was also predicted by the biochemical characterization of the purified protein described in Chapter 4. The complete *ndmB* gene includes 1,068 bp which is higher than the expected 950 bp based on apparent molecular weight of 35 kDa determined by SDS-PAGE of the purified peptide. Similarly, the predicted size of the encoded peptide (355 amino acids) was 39.2 kDa, which was somewhat higher than the 35 kDa observed by SDS-PAGE of the purified enzyme.

There are a few possible explanations for the difference in the predicted versus observed molecular weight of NdmB. Error during any of the three PCR steps used to isolate *ndmB* could lead to deletion of the stop codon, thus giving a larger sequence than really exists. Similarly, an error in DNA sequencing could have led to removal of the stop codon in the correct location. Finally, it is possible that NdmB contains secondary structures that are not completely denatured during SDS-PAGE, thus causing the peptide to appear smaller than it really is. Confirmation that the full-length *ndmB* gene encodes the NdmB peptide observed during purification of Ndm was obtained by cloning, heterologous expression, and subsection of the recombinant peptide to SDS-PAGE, as described later in this chapter.

Sequencing of the Regions Flanking *ndmA* and *ndmB*

The regions flanking *ndmA* on the genome were also sequenced in an attempt to locate and sequence either *ndmB* and/or the gene coding for the reductase in the Ccr fraction. The 3-kb band in approximately 120 μ L reaction E1-2 was gel purified and

submitted for sequencing. The resulting sequencing data contained overlapping sequence with the 3' end of *ndmA* and the pUC19R sequence 5' of the Marcy primer. Hence, the 3-kb band was determined to contain the correct DNA fragment and was completely sequenced.

Table 5.7. Primers and templates used to amplify the region 5' to *ndmA* for sequencing.

Reaction Number	Forward Primer	Reverse Primer	Template
A5'-1	pUC19R2	cdm-R1	EcoRI library
A5'-2	pUC19R	A-speR2	A5'-1

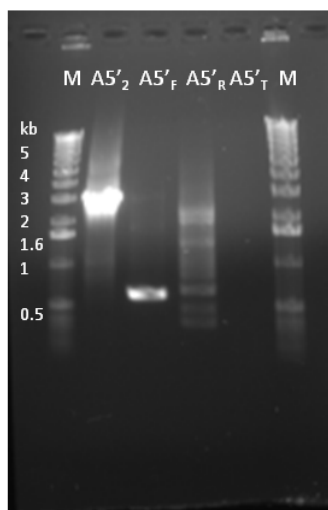


Figure 5.10. A 3-kb PCR product was amplified in the nested PCR reaction A5'-2 (A5'₂) which was not observed in the forward primer only (A5'_F), reverse primer only (A5'_R), or no template (A5'_T) controls.

The sequence 5' to *ndmA* was also identified using nested PCR with the EcoRI library (Table 5.7). A third vector primer, pUC19R2 was designed further than the pUC19R primer from the cloning site on the pUC19 vector. A primary PCR reaction

(A5'-1) was carried out using pUC19R2 and cdm-R1 primers to amplify the region 5' to *ndmA* in the EcoRI library.

A complimentary primer to A-speF2, A-speR2 was designed as the reverse primer in the second round of nested PCR (A5'-2). This primer was used with the pUC19R primer to further amplify the PCR product in A5'-1. Agarose gel electrophoresis of the PCR products in both reactions revealed a strong DNA band of approximately 3 kb which was not present in the single primer and no template controls (Figure 5.10). Thus, the 3-kb band from approximately 50 μ L reaction A5'-2 was gel purified and submitted for DNA sequencing.

The regions both 5' and 3' to *ndmB* were amplified from both SmaI and EcoRI libraries using nested PCR with Taq polymerase. As with *ndmA*, the sequences were amplified with Taq polymerase, gel purified, and submitted for DNA sequencing. Each primer used to amplify sequences and to sequence the DNA was designed from the sequencing data obtained previously.

The region 5' to *ndmB* was amplified using nested PCR according to Table 5.8 from the CBB5 SmaI library with Taq polymerase. Agarose gel electrophoresis revealed a dominant PCR product approximately 1.8 kb in size in reaction B5' 1-2. A faint band of the same size was detected in the forward-primer-only control, but was not present in the other controls. However, the extreme difference in band intensity between reaction and control indicated that the 1.8 kb band was most likely a specific PCR product containing the sequence 5' to *ndmB*.

Reaction B5' 1-2 was subjected to TA ligation with the pGEM-TEZ vector and electroporated into JM109 cells, which were incubated overnight on LBAXI agar. Ten white colonies were grown overnight in LBA broth and screened for insertion of the 1.8 kb band by PCR with T7 and SP6 primers. Two of the 10 cultures (labeled 7-1 and 7-5) were found to contain an insert of the correct size. The plasmids were extracted from both cultures and submitted for DNA sequencing. Both plasmids identically matched the

5' sequence of *ndmB* and the pUC19 sequence 5' of the insertion site, indicating that both plasmids contained the sequence 5' to *ndmB*.

Table 5.8. Primers and templates used during the nested PCR approach to sequence the regions both 5' and 3' to *ndmB*.

Reaction Number	Forward Primer	Reverse Primer	Template
B5' 1-1	Marcy	B-speR10	SmaI library
B5' 2-1	pUC19R2	B-speR10	SmaI library
B5' 1-2	Marcy	B-speR11	B5' 1-1
B5' 2-2	pUC19R	B-speR11	B5' 2-1
B3' 1-1	B-speF7	Marcy	SmaI library
B3' 2-1	B-speF7	pUC19R2	SmaI library
B3' 1-2	B-speF8	Marcy	B3' 1-1
B3' 2-2	B-speF8	pUC19R	B3' 2-1
B3' 2-3	B-DownF1	B-DownR1	B3' 2-1
B3' 2-4	B-DownF2	B-DownR1	B3' 2-1
B3' 2-5	B-DownF3	B-DownR2	B3' 2-1
B3' 3-1	ROx-F1	Marcy	EcoRI library
B3' 4-1	ROx-F1	pUC19R2	EcoRI library
B3' 3-2	ROx-F2	Marcy	B3' 3-1
B3' 4-2	ROx-F2	pUC19R	B3' 4-1

The region 3' to *ndmB* was also amplified with Taq polymerase from the CBB5 SmaI library using nested PCR according to Table 5.8. A major PCR product approximately 4 kb in size was detected in reaction B3'2-2. This band was not produced in any of the single primer or no template controls, and thus most likely contained the sequence 3' to *ndmB*.

TA cloning of reaction B3'2-2 with pGEM-TEZ vector was unsuccessful. Therefore, the 4-kb band from 250 μ L reaction B3'2-2 was gel purified and submitted for DNA sequencing. The sequencing data matched the 3' sequence of *ndmB* and the pUC19

vector sequence 3' of the insertion site, indicating that the 4-kb band contains the sequence 3' to *ndmB* on the genome. Reaction B3'2-1 was further used as a template for additional nested PCR reactions as described in Chapter 2.

An additional 2-kb 3' to the 4-kb region described above was obtained using the nested PCR approach with the EcoRI library as described in Table 5.8. A 2-kb PCR product was detected in both B3'3-2 and B3'4-2 that was not produced in the negative control reactions. Thus, the 2-kb fragment was gel purified from 100 μ L each reaction and submitted for DNA sequencing as described in Chapter 2.

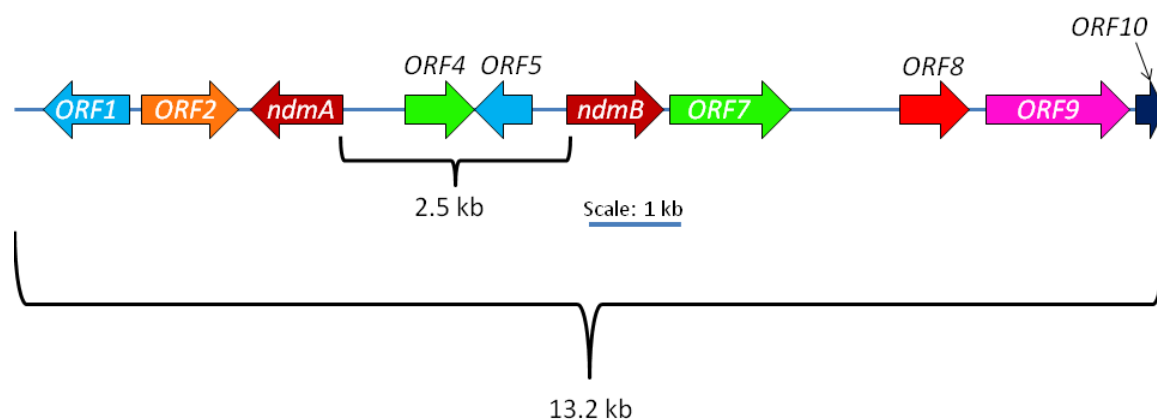


Figure 5.11. Arrangement and orientation of *ndmA*, *ndmB*, and the genes surrounding them on the genome of *P. putida* CBB5.

The EcoRI- and SmaI-cut gDNA fragment containing *ndmA* and *ndmB* and their flanking genes was 13.2 kb in length and can be seen in Appendix B. Nine complete open reading frames (ORFs) and the 5' end of one partial ORF were identified over the length of the fragment, designated as ORF1 through ORF10 (Figure 5.11). ORF1 and ORF5 lie in the same direction as *ndmA*, while all others are oriented in the same direction as *ndmB*. The translated peptide sequences of each ORF were analyzed by BLASTP (Benson *et al.*, 2008) using either the non-redundant (BLASTP_{NR}) or SwissProt

(BLAST_{SP}) protein sequence databases in order to determine possible function of each gene (Table 5.9).

ORF1 lies in the same direction as *ndmA*, belongs to the *araC* family of transcriptional regulators, and most closely matched *mma_0222* from *Janthinobacterium* sp. Marseille (accession number YP_001355312; Audic *et al.*, 2007) and *glxA* from *Sinorhizobium melliloti* (O87389; Capela *et al.*, 2001) by BLAST_{NR} and BLAST_{SP} analysis. ORF2, which was co-directional with *ndmB*, was most similar to the formaldehyde dehydrogenase genes *mds_2843* from *Pseudomonas mendocina* NK-01 (YP_004380626; Guo *et al.*, 2011) and *frmA* from *Synechocystis* sp. PCC 6803 (P73138; Kaneko *et al.*, 1996). ORF3 encoded *ndmA* and ORF6 was *ndmB*. Both genes were closest to *mma_0224* from *J.* sp. Marseille (YP_001355314; Audic *et al.*, 2007) and *cbaA*, 3-chlorobenzoate-3,4-dioxygenase from *Comomonas testosteroni* (Q44256; Nakatsu *et al.*, 1995) as determined by BLAST_{NP} and BLAST_{SP}, respectively.

ORF4 is similar to *GIE_06918* from *Pseudomonas putida* TJI-51 (ZP_08139013; Benson *et al.*, 2008) and *ompK* from *Vibrio parahaemolyticus* (P51002; Inoue *et al.*, 1995), both of which belong to the *tsx* family of outer membrane proteins. ORF5 was most homologous to *gntR* family transcriptional regulators *mma_3679* from *J.* sp. Marseille (YP_001355369; Audic *et al.*, 2007) and *ydhC* from *Bacillus subtilis* (O05494; Sadaie *et al.*, 1997). ORF6 most closely matched xanthine permeases *pbuX7* from *J.* sp. Marseille (YP_001355365; Audic *et al.*, 2007) and *ygfU* from *Escherichia coli* K-12 (Q46821; Blattner *et al.*, 1997).

ORF8 was most similar to *GIE_06898* in *P. putida* TJI-51 (ZP_08139009; Benson *et al.*, 2008) and *caoI* in *Chlamydomonas reinhardtii* (Q9ZWM5; Tanaka *et al.*, 1998). The second-most similar gene to ORF8 determined by BLAST_{NR} was *mma_3678* in *J.* sp. Marseille (YP_001355368, E-value of 2e-88; Audic *et al.*, 2007). ORF8, its most similar proteins as determined by BLAST_{NR} and BLAST_{SP}, *ndmA*, *ndmB*, and the C-terminal catalytic domains of the alpha subunit of Rieske [2Fe-2S] non-heme iron

Table 5.9. Genes containing the highest identity to ORFs 1-10 as determined by BLASTP search.

ORF	Non-Redundant Protein Sequences Database				SwissProt Protein Sequences Database			
	Homolog	Organism	Accession Number	E-Value	Homolog	Organism	Accession Number	E-Value
1	<i>mma_0222</i>	<i>J. sp. Marseille</i>	YP_001355312	1e-93	<i>glxA</i>	<i>S. melliloti</i>	O87389	9e-20
2	<i>mds_2843</i>	<i>P. mendocina</i> NK-01	YP_004380626	0.0	<i>frmA</i>	<i>S. sp. PCC 6803</i>	P73138	4e-160
<i>ndmA</i>	<i>mma_0224</i>	<i>J. sp. Marseille</i>	YP_001355314	4e-109	<i>cbaA</i>	<i>C. testosteroni</i>	Q44256	2e-16
4	<i>G1E_06918</i>	<i>P. putida</i> TJI-51	ZP_08139013	3e-82	<i>ompK</i>	<i>V. parahaemolyticus</i>	P51002	9e-6
5	<i>mma_3679</i>	<i>J. sp. Marseille</i>	YP_001355369	6e-74	<i>ydhC</i>	<i>B. subtilis</i>	O05494	2e-9
<i>ndmB</i>	<i>mma_0224</i>	<i>J. sp. Marseille</i>	YP_001355314	8e-122	<i>cbaA</i>	<i>C. testosteroni</i>	Q44256	4e-15
7	<i>pbuX7</i>	<i>J. sp. Marseille</i>	YP_001355365	3e-169	<i>ygfU</i>	<i>E. coli</i> K-12	Q46821	6e-132
8	<i>G1E_06898</i>	<i>P. putida</i> TJI-51	ZP_08139009	2e-94	<i>caoI</i>	<i>C. reinhardtii</i>	Q9ZWM5	4e-3
9	<i>mma_3677</i>	<i>J. sp. Marseille</i>	YP_001355367	5e-127	<i>vanB</i>	<i>P. putida</i>	O54037	1e-59
10	<i>gst9</i>	<i>J. sp. Marseille</i>	YP_001355366	5e-47	<i>gstA</i>	<i>R. leguminosarum</i>	Q52828	2e-13

oxygenases belong to the START/RHO_alpha_C/PITP/Bet_v1/CoxG/CalC (SRPBCC) superfamily, which is composed of enzymes with deep hydrophobic ligand-binding pockets (Marchler-Bauer *et al.*, 2005). Although ORF8 is similar to *ndmA* and *ndmB*, it does not contain a Rieske [2Fe-2S] domain. It could, however, potentially be involved in some part of methylxanthine metabolism by CBB5.

ORF9 contains three conserved domains: a Rieske [2Fe-2S] domain, a reductase (flavin binding) domain, and a plant-type ferredoxin domain, and was most similar to the hypothetical gene *mma_3677* in *J. sp. Marseille* (YP_001355367; Audic *et al.*, 2007) and *vanB* in *Pseudomonas putida* (O54037; Venturi *et al.*, 1998). Although there are many putative gene sequences similar to ORF9, with fused Rieske [2Fe-2S], reductase, and plant-type ferredoxin domains, no purification and/or characterization of such an enzyme has been reported in the literature. The proximity of ORF9 to *ndmB* suggests that it might code for the specific Ccr required for *N*-demethylation activity of Ndm. However, cloning, expression, and assaying of ORF9 have yet to be performed. ORF10, of which only the 632 bp (120 amino acids) of the 5' end was obtained, was similar to the glutathione *S*-transferases *gst9* in *J. sp. Marseille* (YP_001355366; Audic *et al.*, 2007) and *gstA* in *Rhizobium leguminosarum* (Q52828; Benson *et al.*, 2008).

Cloning of *ndmA* into the pET32a Expression Vector

Cloning of *ndmA*

The full length *ndmA* gene was amplified by Taq polymerase from gDNA using pET-A-F and pET-A-R2 primers. Both *ndmA* insert and pET32a vector were digested with NdeI and EcoRI and ligated together as described in Chapter 2. Following electroporation of pET32a/*ndmA* ligation into JM109 cells, ten transformant colonies containing the pET32a/*ndmA* vector were detected by colony PCR. Three colonies, A4, A7, and A29, were grown overnight in LB-broth with 100 µg/mL ampicillin. Insertion of *ndmA* into pET32a was confirmed by extracting and sequencing plasmids from each

culture. Plasmids from A4 and A7 contained single point mutations, while the plasmid from A29 completely matched the *ndmA* sequence. Therefore, plasmid A29 was electroporated into BL21(DE3) cells, and a glycerol stock of BL21(DE3) cells containing pET32a/*ndmA* vector was prepared as described in Chapter 2.

Mutagenesis of *ndmA* to Produce *ndmA-His*

The stop codon was removed from the *ndmA* sequence on the pET32a vector by site-directed mutagenesis (see Chapter 2 for details) in order to create an *ndmA-His* fusion gene, which would result in addition of a 6-histidine tag at the C-terminus of NdmA (NdmA-His). The mutated plasmid, pET32a/*ndmA-His*, was recovered by electroporation into JM109. Following overnight incubation on LBA agar, a single colony (AH1) was grown overnight in LBA broth. Sequencing of plasmids extracted from the AH1 culture confirmed removal of the stop codon from *ndmA* to form *ndmA-His*. The remaining sequence was identical to *ndmA*. Therefore, the pET32a/*ndmA-His* plasmid was electroporated into BL21(DE3) cells and a glycerol stock was prepared as described in Chapter 2.

Cloning of *ndmB* into the pET32a Expression Vector

Two primers, B-F-AseI and B-R-XhoI, were designed to clone *ndmB* into the pET32a expression vector. Because *ndmB* contains an internal NdeI site, the forward primer was designed with an AseI sequence. Although AseI and NdeI cut different sequences, they leave the same cut overhang. However, *ndmB* was not amplified by PCR when these two primers were used; only a 700 bp product was formed due to non-specific binding of B-F-AseI. Therefore, the *ndmB* sequence was amplified by PCR using B-degF as the forward primer and B-R-XhoI as the reverse primer. Agarose gel electrophoresis of the amplified DNA revealed six bands, one of which was approximately 1.1 kb (Figure 5.12).

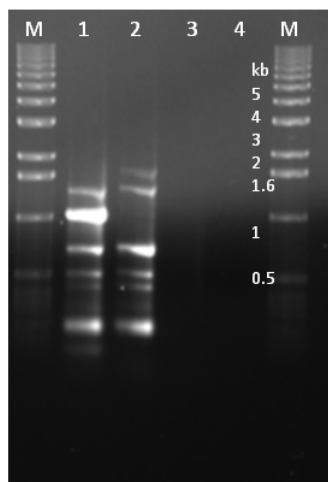


Figure 5.12. The 1.1-kb *ndmB* gene product amplified with B-degF and B-R-XhoI primers (lane 1) was not produced in the negative controls. M, kb marker; 2, forward primer only control; 3, reverse primer only control; 4, no template control.

The PCR products were TA ligated to a pGEM-TEZ vector and electroporated into JM109 cells. Overnight incubation on LBAXI agar resulted in growth of over 200 colonies. Thirty four colonies were randomly picked from the plate, grown overnight in LBA broth, and screened for the presence of *ndmB* insert by PCR with T7 and SP6 primers. Only one colony, colony E10, contained a vector with a ligated insert, as revealed by PCR using T7/SP6 and B-degF/B-R-XhoI primer pairs. Sequencing of plasmid E10 confirmed that the inserted sequence was *ndmB*.

Cloning of *ndmB*

PCR using B-F-AseI and B-R-XhoI primers with plasmid E10 as the template resulted in the production of a 1.1-kb product. The PCR product and pET32a vector were digested by AseI or NdeI and XhoI and ligated together as described in Chapter 2. The ligated pET32a/*ndmB* was electroporated into DH10B cells and incubated on LBA agar overnight, resulting in growth of eight transformant colonies on LBA agar.

PCR screening of the eight PCR colonies with T7 and T7term primers resulted in a 1.2-kb signal in four colonies, suggesting the presence of a 1.1-kb insert in the plasmid. The four colonies, B2, B3, B4, and B8 were grown overnight in LBA broth, mixed 1:1 with 50% glycerol, and stored at -80 °C. DNA sequencing of plasmid B3, extracted from colony B3, confirmed the presence of *ndmB* in the vector.

Cloning of *ndmB-His*

Cloning of *ndmB* with a 6-histidine tag at the 3' end of the gene (*ndmB-His*) into the pET32a expression vector was performed by over-extension PCR (OE-PCR) (Bryskin and Matsumura, 2010). Chimeric primers containing 30 bp of pET32a sequence and 30 bp of the 5' and 3' ends of *ndmB* were used in PCR to amplify the *ndmB* sequence. The stop codon was removed from the reverse primer, which was designed so that OE-PCR would result in addition of a histidine tag at the C-terminus of NdmB (NdmB-His). Taq polymerase was used to amplify *ndmB* from plasmid E10. The resulting 1.1 kb PCR product was gel purified and used as a megaprimer in OE-PCR. Because each end of the megaprimer contained the sequence for both sides of the insertion part on pET32a, it was used as the only primer and pET32a was used as the vector.

Following OE-PCR, DpnI was added to the reaction to digest the unamplified pET32a. The vectors were electroporated into *E. coli* electrocompetent cells, and cells were plated onto LBA agar. Following overnight incubation at 37 °C, the pET32a/*ndmB* vector was found in four colonies, BH4 – BH7, by colony PCR with T7 and T7term primers. Two colonies, BH4 and BH5, were inoculated into 4 mL LBA broth and grown overnight at 37 °C. Plasmids were extracted from both cultures and submitted for sequencing. DNA sequencing confirmed integration of *ndmB* into pET32a with no mutations by OE-PCR. Therefore, the plasmid from culture BH5 was electroporated into BL21(DE3) cells, and a glycerol stock was prepared as described in Chapter 2.

Functional Expression and of *ndmA* and *ndmB*

Biochemical characterization of Ndm (Chapter 4) concluded that NdmA and NdmB were subunits of a single *N*-demethylase enzyme. In order to confirm this finding, *ndmA* and *ndmB* were expressed individually in BL21(DE3) cells to determine the presence of soluble recombinant protein prior to assaying for activity. All procedures for growth of cells are listed in Chapter 2.

Expression of NdmA

BL21(DE3) cells containing pET32a/*ndmA* plasmid were induced at OD₆₀₀ of 0.844 by addition of IPTG to a final concentration of 0.4 mM. Cells were cultured at 30 °C for 4.5 h to a final OD₆₀₀ of 3.135 (Table 5.10). Another culture of BL21(DE3) containing the empty pET32a plasmid was also induced under the same conditions, growing to an OD₆₀₀ of 1.710.

Table 5.10. OD₆₀₀ of *E. coli* BL21(DE3) containing either pET32a/*ndmA* or pET32a empty plasmid induced at 30 °C for 4.5 h.

Plasmid	Starting OD ₆₀₀	OD ₆₀₀ at Induction	Final OD ₆₀₀	IPTG (mM)	Induction Temp (°C)	Induction Time (h)
pET32a/ <i>ndmA</i>	0.106	0.844	3.135	0.4	30	4.5
pET32a	0.082	0.768	1.710	0.4	30	4.5

SDS-PAGE of culture lysates revealed the production of a 40-kDa peptide in the pET32a/*ndmA*-containing cells that was not expressed in the cells containing the empty plasmid (Figure 5.13). Approximately 90-98% of NdmA was insoluble, as estimated from band intensities on the gel; however, a distinct soluble band can be seen.

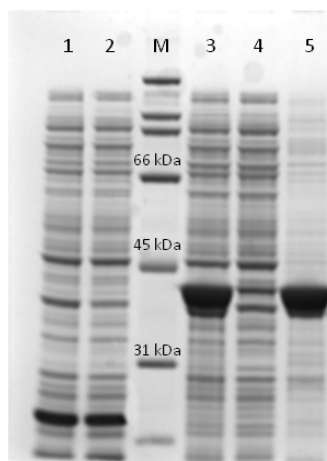


Figure 5.13. A soluble, 40-kDa NdmA was expressed in BL21(DE3) cells. Lanes 1 and 2, lysate and soluble fraction of empty pET32a vector control; M, molecular weight marker; 3, lysate containing expressed NdmA; 4, soluble fraction containing soluble NdmA; 5, insoluble fraction containing insoluble NdmA.

Expression and Purification of NdmA-His

BL21(DE3) cells containing pET32a/*ndmA-His* plasmids were induced at either 30 or 23 °C with 0.1-0.4 mM IPTG (Table 5.11).

Table 5.11. OD₆₀₀ of *E. coli* BL23(DE3) containing pET32a/*ndmA-His* induced at 30 or 23 °C with IPTG concentrations from 0.1-0.4 mM.

Plasmid	Starting OD ₆₀₀	OD ₆₀₀ at Induction	Final OD ₆₀₀	IPTG (mM)	Induction Temp (°C)	Induction Time (h)
pET32a/ <i>ndmA-His</i>	0.105	0.854	3.05	0.4	30	4.5
pET32a/ <i>ndmA-His</i>	0.104	0.840	3.02	0.2	30	4.5
pET32a/ <i>ndmA-His</i>	0.103	0.957	7.11	0.1	23	18

Similar to the expressed NdmA, approximately 90-98% of NdmA-His was produced as insoluble protein, as observed by SDS-PAGE (Figure 5.14). Although soluble NdmA-His could be seen under all three conditions as a 41 kDa peptide,

induction with 0.1 mM IPTG at 23 °C resulted in the highest ratio of soluble to insoluble enzyme.

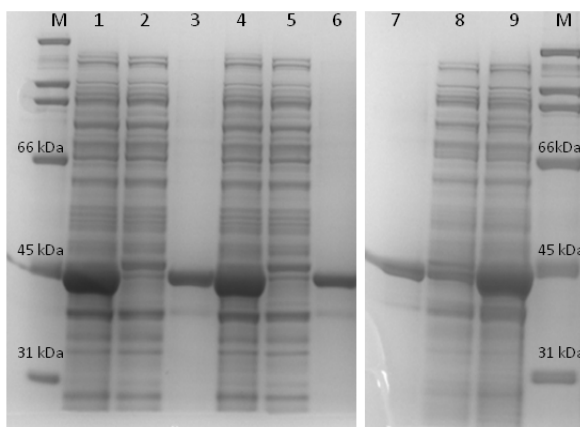


Figure 5.14. The lysate, soluble, and insoluble fractions of ndmA-His induced at 0.4 mM IPTG, 30 °C (lanes 1-3); 0.2 mM IPTG, 30 °C (lanes 4-6); 0.1 mM IPTG, 23 °C (lanes 7-9A); lane M, MW marker. The induction at 0.1 mM IPTG and 23 °C provided the highest ratio of soluble:insoluble NdmA-His.

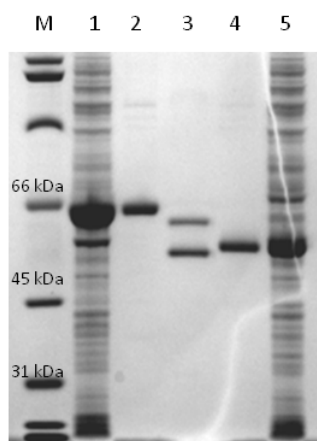


Figure 5.15. NdmA-His and NdmB-His were purified to about 95-99% purity with a nickel column. Lane M, molecular weight marker; 1, NdmA-His lysate; 2, purified NdmA-His; 3, purified Ndm; 4, purified NdmB-His; 5, NdmB-His lysate. A slight increase in molecular weight was observed for the histidine-tagged subunits (lanes 2 and 4) compared with their native molecular weight (lane 3).

The soluble fraction containing NdmA-His was separated on a nickel column as described in Chapter 2. Bound NdmA-His was eluted under 250 mM imidazole, concentrated, and dialyzed overnight to remove imidazole. Purity of the enzyme was observed to be very high (approximately 95-99%) by SDS-PAGE (Figure 5.15). Also, a slight increase in the molecular weight of NdmA-His over NdmA, due to the addition of the histidine tag, was clearly observed.

Expression of NdmB

BL21(DE3) cells with the pET32a/*ndmB* plasmid were induced at either 25 or 18 °C with 1 mM IPTG (Table 5.12).

Table 5.12. Growth and induction of BL21(DE3) cells containing pET32a/*ndmB*.

Plasmid	Starting OD ₆₀₀	OD ₆₀₀ at Induction	Final OD ₆₀₀	IPTG (mM)	Induction Temp (°C)	Induction Time (h)
pET32a/ <i>ndmB</i>	0.105	0.748	n.d.	1	18	18
pET32a/ <i>ndmB</i>	0.104	1.076	n.d.	1	25	18

*Final OD₆₀₀ was not recorded prior to cell harvesting.

SDS-PAGE of the lysate prior to centrifugation and the soluble and insoluble fractions revealed a band with an apparent molecular weight of 35 kDa, similar to the molecular weight of purified NdmB (Figure 5.16). This result confirmed that *ndmB* is the gene coding for the NdmB subunit observed during purification, and that the gene length was not extended due to PCR or DNA sequencing errors. The smaller apparent molecular weight compared to the estimated molecular weight could be due to secondary structures in the peptide that are not denatured completely during SDS-PAGE.

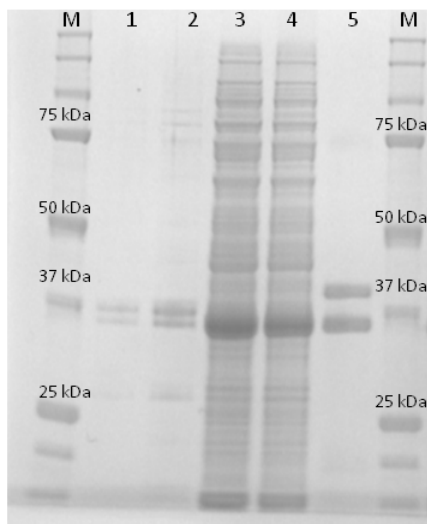


Figure 5.16. SDS-PAGE analysis of expressed NdmB. Lane M, molecular weight marker; lanes 1-2, insoluble fraction of 18 °C-induced cells; 3 and 4, soluble fraction and lysate of 18 °C induced cells; 5, purified Ndm.

Expression and Purification of NdmB-His

BL21(DE3) cells containing pET32a/*ndmB-His* plasmid were induced at either 25 or 18 °C with 1 mM IPTG (Table 5.13). Over 50% of NdmB-His was expressed as soluble protein (Figure 5.17).

Table 5.13. Growth and induction of BL21(DE3) cells containing pET32a/*ndmB-His*.

Plasmid	Starting OD ₆₀₀	OD ₆₀₀ at Induction	Final OD ₆₀₀	IPTG (mM)	Induction Temp (°C)	Induction Time (h)
pET32a/ <i>ndmB-His</i>	0.107	0.804	n.d.	1	18	18
pET32a/ <i>ndmB-His</i>	0.108	0.988	n.d.	1	25	18

*Final OD₆₀₀ was not recorded prior to cell harvesting.

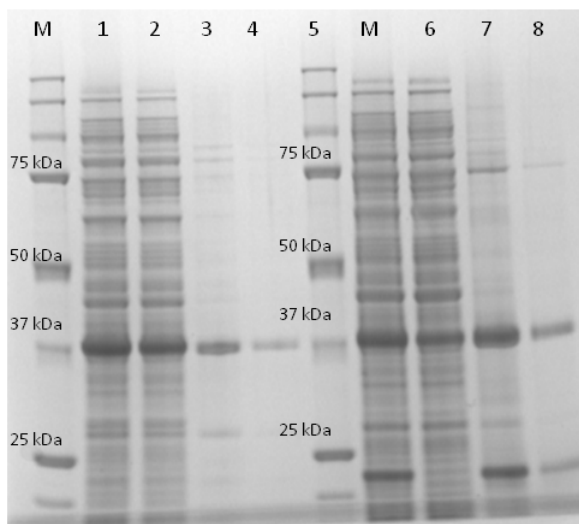


Figure 5.17. SDS-PAGE analysis of expressed NdmB-His induced at 18 °C (lanes 1-4) and 25 °C (lanes 5-8). Lanes 1 and 5, lysate; 2 and 6, soluble fraction; 3, 4, 7, and 8, insoluble fraction.

NdmB-His was separated from the soluble enzymes by passing through a nickel column and eluted with 250 mM imidazole. The purified enzyme was concentrated using 30 kDa MWCO filter tubes and visualized by SDS-PAGE. An increase in apparent molecular weight from 35 to 36 kDa was observed for NdmB-His (Figure 5.15) due to addition of the histidine tag, and the purified enzyme was approximately 95-99% pure.

Activity Assay of NdmA-His and NdmB-His

In order to determine whether NdmA and NdmB were subunits of the same enzyme or two different enzymes that co-purified, NdmA-His and NdmB-His were assayed individually with partially purified Ccr (Chapter 4) for methylxanthine *N*-demethylase activity. No *N*-demethylation activity was detected when NdmA-His or NdmB-His was assayed without addition of Ccr. Surprisingly, NdmA-His plus Ccr and NdmB-His plus Ccr both degraded caffeine to either theobromine or paraxanthine, respectively (Tables 5.14 and 5.15). NdmA-His plus Ccr also converted theophylline to 3-methylxanthine, paraxanthine to 7-methylxanthine and xanthine, and 1- and 7-

methylxanthine to xanthine, but did not *N*-demethylate 3-methylxanthine or theobromine (Table 5.14). Controls using boiled NdmA-His plus Ccr were unable to degrade any methylxanthine but 7-methylxanthine, which was *N*-demethylated to xanthine at the same rate with which it was *N*-demethylated when incubated with active NdmA-His.

Table 5.14. Substrate specificity of NdmA-His plus Ccr.

Enzyme	Substrate	Product(s)
NdmA-His	Caffeine	Theobromine
NdmA-His	Theophylline	3-methylxanthine
NdmA-His	Paraxanthine	7-methylxanthine, xanthine
NdmA-His	Theobromine	No activity
NdmA-His	1-methylxanthine	Xanthine
NdmA-His	3-methylxanthine	No activity
NdmA-His	7-methylxanthine	Xanthine
Boiled NdmA-His	Caffeine	No activity
Boiled NdmA-His	Theophylline	No activity
Boiled NdmA-His	Paraxanthine	No activity
Boiled NdmA-His	Theobromine	No activity
Boiled NdmA-His	1-methylxanthine	No activity
Boiled NdmA-His	3-methylxanthine	No activity
Boiled NdmA-His	7-methylxanthine	Xanthine

NdmB-His plus Ccr degraded caffeine to paraxanthine, theophylline to 1-methylxanthine, theobromine to 7-methylxanthine and xanthine, and 3- and 7-methylxanthines to xanthine, but did not *N*-demethylate paraxanthine or 1-methylxanthine (Table 5.15). Boiled NdmB-His controls plus Ccr degraded 7-methylxanthine to xanthine, but did not *N*-demethylate any other methylxanthine.

Table 5.15. Substrate specificity of NdmB-His plus Ccr.

Enzyme	Substrate	Product(s)
NdmB-His	Caffeine	Paraxanthine
NdmB-His	Theophylline	1-methylxanthine
NdmB-His	Paraxanthine	No activity
NdmB-His	Theobromine	7-methylxanthine, xanthine
NdmB-His	1-methylxanthine	No activity
NdmB-His	3-methylxanthine	Xanthine
NdmB-His	7-methylxanthine	Xanthine
Boiled NdmB-His	Caffeine	No activity
Boiled NdmB-His	Theophylline	No activity
Boiled NdmB-His	Paraxanthine	No activity
Boiled NdmB-His	Theobromine	No activity
Boiled NdmB-His	1-methylxanthine	No activity
Boiled NdmB-His	3-methylxanthine	No activity
Boiled NdmB-His	7-methylxanthine	Xanthine

These results indicate that NdmA-His can remove the *N*-1 methyl group from caffeine and related methylxanthines, while NdmB-His was active on the *N*-3 methyl group. *N*-7 demethylation of 7-methylxanthine was also observed with both enzymes, but also occurred at the same rate in the boiled enzyme controls, as well. Incubation of the Ccr fraction alone with 0.5 mM 7-methylxanthine resulted in complete *N*-demethylation of substrate to xanthine. However, the Ccr fraction alone did not exhibit *N*-7-demethylation activity toward caffeine, theobromine, or paraxanthine. Therefore, NdmA-His appears to be an *N*-1 specific *N*-demethylase and NdmB-His is a specific *N*-3-demethylase. A third *N*-demethylase with 7-methylxanthine specific *N*-7-demethylation activity (putative NdmC) appears to have co-eluted with the Ccr fraction and has yet to be further purified.

Percent Identity of NdmA and NdmB to Other Enzymes

The NdmA and NdmB peptide sequences were checked for percent identity to each other and to the Cdm and mma_0224 peptide sequences (Table 5.16) by multiple sequence alignment using clustalw (Chenna *et al.*, 2003). The two most similar enzymes were NdmA and Cdm, which were 89% identical. Both enzymes also contained the same number of amino acids. NdmA was 53% and 49% identical to mma_0224 and NdmB, respectively. The mma_0224 sequence was most similar to NdmB, at 58% identity. The two sequences with the least similarity were NdmB and Cdm, which were 48% identical.

Table 5.16. Percent Identity of NdmA, NdmB, Cdm, and mma_0224 peptide sequences.

Sequence A	Name	Length	Sequence B	Name	Length	Score*
1	NdmA	351	2	NdmB	355	49.0
1	NdmA	351	3	Cdm	351	89.0
1	NdmA	351	4	mma_0224	365	53.0
2	NdmB	355	3	Cdm	351	48.0
2	NdmB	355	4	mma_0224	365	58.0
3	Cdm	351	4	mma_0224	365	53.0

* Pairwise scores were calculated by comparing sequences using Clustalw2 Multiple Sequence Alignment software.

A radial phylogram was constructed in order to determine the phylogenetic relationships between NdmA, NdmB, and the catalytic (alpha) subunits of 75 well-characterized Rieske oxygenases (Figure 5.18). A complete list of the sequences used in construction of the phylogenetic tree can be found in Appendix C. NdmA and NdmB clustered with Cdm and mma_0224 to form a new family of Rieske oxygenases. This family was most identical to a family of *O*-demethylases, including vanillate *O*-demethylases (VanA, accession numbers CAA72287 and AAA26019), dicamba *O*-

demethylase (DdmC, AAV53699), and *p*-toluenesulfonate methyl-monooxygenase (TsaM, AAC44804).

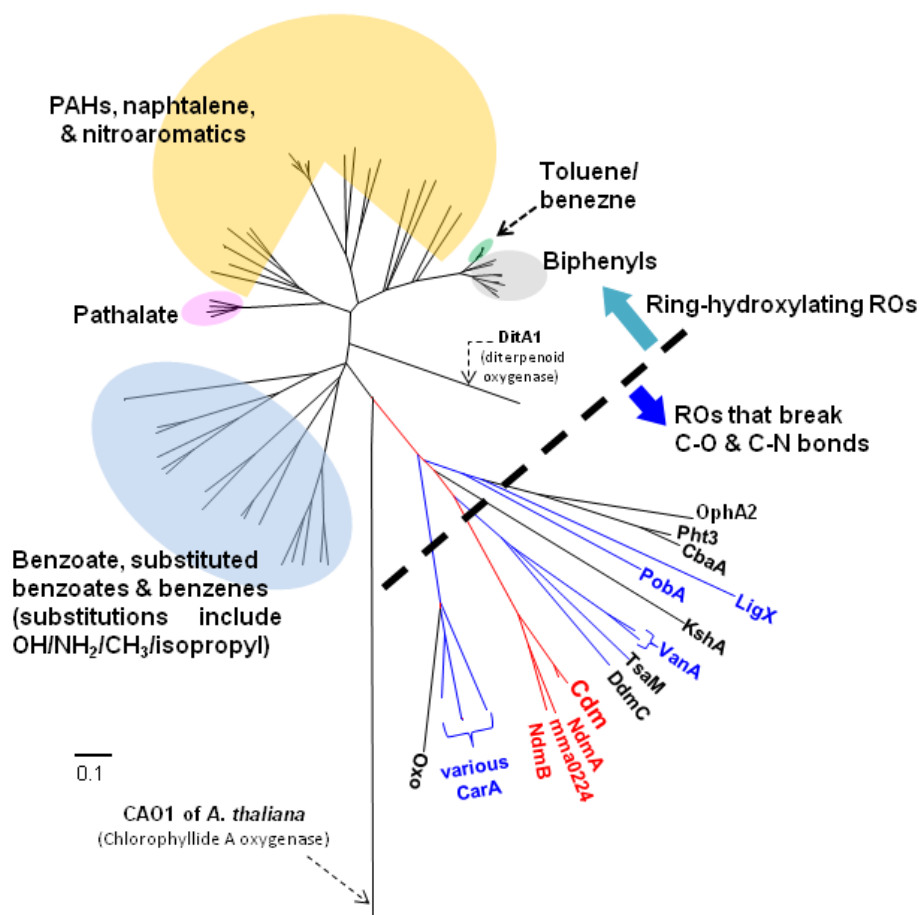


Figure 5.18. Radial phylogram showing the similarity of NdmA and NdmB to the catalytic subunits of 75 other well-characterized Rieske [2Fe-2S] oxygenases. Phylogenetic analyses were conducted using *MEGA* version 4.0.2 (Tamura *et al.*, 2007). The evolutionary history was inferred using the Neighbor-Joining method with bootstrap values of 5,000. The tree is drawn to scale, and distance correlates to the number of amino acids substituted per site.

Many other genes that clustered nearby *ndmA* and *ndmB* are also involved in breaking C/N and C/O bonds. The carbazole 1,9a-dioxygenases (CarA) from *P. resinovorans* CA10 (BAA21729 and BAA21728), *Pseudomonas* sp. XLDN4-9

(AA56339), *Janthinobacterium* sp. J3 (gene ID 75765412), *Sphingomonas* sp. KA1 (YP_717981), and *Nocardiodes aromaticivorans* (BAE79498) catalyze the oxidation of carbazole to 2'-aminobiphenyl-2,3-diol (Nam *et al.*, 2002) through cleavage of a C/N bond. Also, 5,5'-dehydrodivanillate demethylase (LigX, BAA36168) from *Sphingomonas paucimobilis* SYK-6 is responsible for breaking a C/O bond in 5,5'-dehydrodivanillic acid to form its *O*-demethylated product, 2,2',3-trimethoxy-3'-methoxy-5,5'-dicarboxybiphenyl (Sonoki *et al.*, 2000).

Discussion

Pseudomonas putida CBB5 uses at least two positional-specific *N*-demethylases, NdmA and NdmB, to degrade caffeine to 7-methylxanthine and theophylline to xanthine. NdmA and NdmB co-purified from wild-type and could not be separated by chromatographic techniques. Thus, they were assumed to be subunits of a single enzyme, Ndm, which was capable of *N*-demethylating caffeine, theophylline, and all of their methylated metabolites to xanthine (Chapter 4). Isolation of the gene sequences *ndmA* and *ndmB* confirmed that both enzymes are Rieske [2Fe-2S] non-heme iron oxygenases, which was predicted by biochemical analysis of the co-purified enzymes. The peptide sequences of NdmA and NdmB are very similar (49% identity), which explains why the two enzymes could not be separated by biochemical methods.

Cloning, expression, and purification of histidine-tagged enzymes individually allowed for assaying of substrate specificities of each enzyme with the partially purified reductase, Ccr, described in Chapter 4. NdmA-His was shown to be a specific *N*-1-demethylase by production of theobromine from caffeine. No other products were formed during *N*-demethylation of caffeine by NdmA-His plus Ccr (Table 5.14). Similarly, theophylline, paraxanthine, and 1-methylxanthine were *N*-demethylated by NdmA-His plus Ccr to 3-methylxanthine, 7-methylxanthine, and xanthine, respectively.

No *N*-demethylation was observed when NdmA-His plus Ccr was assayed with theobromine or 3-methylxanthine, neither of which contain an *N*-1 methyl group.

Assaying of *N*-demethylation activity of NdmB-His plus Ccr on caffeine revealed that NdmB-His is an *N*-3-demethylase by formation of paraxanthine as the only product (Table 5.15). Theophylline, theobromine, and 3-methylxanthine were likewise *N*-demethylated by NdmB-His plus Ccr to 1-methylxanthine, 7-methylxanthine, and xanthine, respectively. No *N*-demethylation of theophylline or 1-methylxanthine, which do not have an *N*-3 methyl group, was observed with NdmB-His plus Ccr.

N-7-demethylation was also observed when NdmA-His plus Ccr or NdmB-His plus Ccr were assayed with 7-methylxanthine. Similarly, 7-methylxanthine produced by *N*-demethylation of paraxanthine or theobromine by NdmA or NdmB, respectively, was degraded to xanthine. Using boiled NdmA/B with active Ccr as controls, no *N*-7-demethylation of paraxanthine, theobromine, or caffeine was observed. However, 7-methylxanthine was *N*-demethylated by the boiled controls at the same rate as with the active NdmA/B. Hence, *N*-7-demethylation observed was attributed to a putative NdmC in the partially purified Ccr fraction. This was not determined during biochemical characterization (Chapter 4) because only paraxanthine was used to screen fractions for activity. Ccr was not active on paraxanthine, theobromine, or caffeine, all of which contain an *N*-7 methyl group. Thus, the putative NdmC appears to be specific only for 7-methylxanthine. Further purification of both Ccr and NdmC will allow for improved characterization of all enzymes in the caffeine and theophylline metabolic pathways.

An ORF downstream of *ndmB* on the CBB5 genome, ORF8, contains a deep hydrophobic ligand binding pocket, similar to *ndmA* and *ndmB*, suggesting that it could be a putative NdmC. However, no Rieske [2Fe-2S] domain was observed in ORF8. The lack of a Rieske [2Fe-2S] domain could explain why this enzyme is separated from NdmA and NdmB during purification. Also, ORF9, which was immediately 3' to the putative NdmC, contained Rieske [2Fe-2S], flavin, and ferredoxin domains, and was

classified as a possible Ccr. Future cloning, heterologous expression, and assaying of these enzymes may provide another means of characterizing NdmC and Ccr if purification proves unsuccessful.

The presence of multiple *N*-demethylases in CBB5 was confirmed by cloning and heterologous expression of *ndmA* and *ndmB*. However, the exact number of enzymes involved in both caffeine and theophylline degradation pathways is yet unknown. *N*-demethylation by co-purified NdmA and NdmB was shown to require a specific reductase found in the partially purified Ccr (Chapter 4). Whether a single reductase can partner with all *N*-demethylases or whether each *N*-demethylase requires a specific reductase has not been established. Also, NdmA, NdmB, and NdmC may not be the only *N*-demethylases present in CBB5. Gene knockout studies may provide further answers concerning the exact number of enzymes involved in *N*-demethylation of caffeine and related methylxanthines.

The presence of iron in NdmA and NdmB should come as no surprise, as iron-sulfur clusters have been implicated as some of the earliest cofactors in enzyme catalysis (Rees and Howard, 2003). NdmA and NdmB are similar to other iron-sulfur cluster-containing oxygenase enzymes that have been found to degrade a broad range of natural and xenobiotic compounds, such as vanillate, dicamba, toluene, naphthalene, biphenyls, and polycyclic aromatic hydrocarbons (Parales and Gibson, 2000).

The sequences of *ndmA*, *ndmB*, and many of the ORFs at their 3' and 5' ends are similar to those of *Janthinobacterium* sp. Marseille. This organism is a mobile, waterborne bacterium isolated from ultrapure water in hemodialysis units in France (Audic, *et al.*, 2007). However, *J.* sp. Marseille contains only one gene (*mma_0224*) that is homologous to both *ndmA* and *ndmB*. Because the gene product has not been characterized, the function and activity of *mma_0224* are unknown. It is possible that *J.* sp. Marseille can perform only one *N*-demethylation or that *mma_0224* codes for a broad-specificity *N*-demethylase. The high similarity between the genes in CBB5 and *J.* sp.

Marseille is curious and presently unclear. An estimated 17% of the genes found in *J. sp.* Marseille originated from lateral transfer, thus the presence of genes coding for *N*-demethylation of methylxanthines may be more common than originally believed (Dash and Gummadi, 2006).

Summary

The gene sequences of positional-specific methylxanthine *N*-demethylases have been isolated, cloned, and expressed, and the enzymes were purified in order to characterize their substrate specificity. The *ndmA* and *ndmB* sequences were obtained using degenerate primers designed from the N-terminal amino acid sequences of both enzymes and the conserved domains of similar genes.

NdmA is a specific *N*-1-demethylase, and can remove the *N*-1 methyl group from caffeine, theophylline, paraxanthine, and 1-methylxanthine. NdmA was not active on theobromine, 3-methylxanthine, or 7-methylxanthine. Conversely, NdmB is a specific *N*-3-demethylase, capable of removing the *N*-3 methyl group from caffeine, theophylline, theobromine, and 3-methylxanthine. NdmB cannot *N*-demethylate paraxanthine, 1-methylxanthine, or 7-methylxanthine.

Both NdmA and NdmB are Rieske [2Fe-2S] non-heme iron oxygenases and require the transfer of electrons from an NAD(P)H-dependent cytochrome *c* reductase (Ccr). The partially purified Ccr fraction used in this chapter and in Chapter 4 contains 7-methylxanthine-specific *N*-7-demethylation activity (putative NdmC). Neither Ccr nor NdmC has been purified to homogeneity; however, two ORFs downstream of *ndmB* are hypothesized to code for the Ccr and NdmC. Cloning and functional expression of these two ORFs, along with continued purification of the Ccr fraction to separate the two activities will need to be performed in order to completely characterize the enzymes and genes responsible for caffeine and theophylline *N*-demethylation pathways in CBB5.

CHAPTER 6
SUMMARY OF COMPLETED RESEARCH AND SUGGESTIONS
FOR FUTURE WORK

A novel caffeine-degrading organism, *Pseudomonas putida* CBB5, was isolated from the soil behind the Center for Biocatalysis and Bioprocessing in Coralville, IA, by enrichment with caffeine as the sole source of carbon and nitrogen. CBB5 degraded caffeine *via* sequential *N*-demethylation to theobromine (major product) and paraxanthine (minor product), 7-methylxanthine, and xanthine. This pathway is similar to other reports of bacterial metabolism of caffeine. A new pathway for metabolism of theophylline, which had not previously been reported as a growth substrate in bacteria, was also discovered in CBB5. Theophylline was also sequentially *N*-demethylated, first to 1- and 3-methylxanthine, and then to xanthine. Curiously, theophylline and 1- and 3-methylxanthines were not intermediates during degradation of caffeine. However, these compounds were oxidized to their respective methyluric acids, which were not further degraded by CBB5. This oxidation to dead-end metabolites was catalyzed by two broad-specificity xanthine dehydrogenases, which were partially purified and characterized with respect to their substrate specificities.

Further research was focused on the degradative pathway of caffeine, theophylline, and their methylxanthine metabolites. Two *N*-demethylase enzymes, NdmA and NdmB, which are Rieske [2Fe-2S] non-heme iron monooxygenases, were responsible for degradation of these methylxanthines. NdmA and NdmB were co-purified from wild-type using paraxanthine as a substrate to screen for active *N*-demethylase fractions. These two *N*-demethylases could not be resolved by traditional purification methods, probably due the extreme similarity between the enzymes. Both enzymes are absolutely dependent on an NAD(P)H-dependent cytochrome *c* reductase (Ccr) for *N*-demethylation activity. Ccr was partially purified to support detailed studies

of NdmA & B. The electrons from Ccr are transferred to NdmA/B, which catalyzed an oxygen-dependent *N*-demethylation of methylxanthines. The methyl groups were stoichiometrically removed as formaldehyde and water. NdmA & B appear to be specific to the reductase from CBB5 since Ccr could not be replaced by reductase and reductase plus ferredoxin from other well-characterized Rieske oxygenase systems.

The presence of multiple *N*-demethylases was demonstrated by cloning and heterologous expression of *ndmA* and *ndmB* genes. NdmA was characterized as a specific *N*-1-demethylase, converting caffeine to theobromine, theophylline to 3-methylxanthine, paraxanthine to 7-methylxanthine, and 1-methylxanthine to xanthine. Similarly, NdmB was shown to be a specific *N*-3-demethylase by conversion of caffeine to paraxanthine, theophylline to 1-methylxanthine, theobromine to 7-methylxanthine, and 3-methylxanthine to xanthine. Both NdmA and NdmB require Ccr reductase for activity. A third *N*-7 specific *N*-demethylase, putative NdmC, has also been hypothesized. This protein was found to co-purify Ccr and catalyzed *N*-demethylation of 7-methylxanthine to xanthine. No *N*-7-demethylation activity towards caffeine, theobromine, or paraxanthine was detected in the partially purified Ccr fraction, indicating that the putative NdmC is a specific 7-methylxanthine *N*-7-demethylase. Thus, there are at least three highly specific *N*-demethylases involved in the degradation of caffeine in CBB5.

This work demonstrates the synergistic power of using both biochemistry and molecular biology to identify and characterize novel bacterial *N*-demethylases involved in the degradation of methylated xanthines. All *N*-demethylases were shown to be NAD(P)H- and oxygen-dependent. One molecule of oxygen was used in the formation of one molecule of formaldehyde for each methyl group removed. The reductase requirement, oxygen requirement, and iron content of purified methylxanthine *N*-demethylases indicated that they were most likely Rieske [2Fe-2S] non-heme iron oxygenases. However, biochemical characterization was unable to determine the number of methylxanthine *N*-demethylases present in CBB5.

Molecular biology revealed that the subunits designated as NdmA and NdmB from biochemical characterization were actually separate enzymes that were co-purifying. That both enzymes are Rieske [2Fe-2S] non-heme iron oxygenases was confirmed by observing the domains in the nucleotide and peptide sequences. Also, NdmA and NdmB were determined to be *N*-1- and *N*-3-specific *N*-demethylases *via* cloning and heterologous expression. However, a molecular-biology-only approach also has limitations that would be difficult to overcome without the biochemical research performed in this work. Because the exact type of enzyme that catalyzes bacterial *N*-demethylation was not known, many different types of enzymes would need to be assumed by annotation alone. Primers designed from known sequences of other enzymes might not anneal specifically to amplify the correct sequence. The *ndmA* and *ndmB* sequences would have been grouped most closely to *O*-demethylases, and thus the “new” microbial enzyme catalyzing *N*-demethylation may have been overlooked. Also, the activity of an *N*-demethylase gene may never have been achieved by cloning alone, due to the requirement of the reductase partner for activity. Thus, forward biochemistry and reverse molecular biology approaches contributed to a completely new class of genes and enzymes, the *N*-demethylases in CBB5.

Much work has been performed in order to characterize *N*-demethylation of caffeine and theophylline by CBB5; however, there is much work that has yet to be performed. Although the substrate specificity of NdmA and NdmB was established, complete characterization was not. The iron content, oxygen requirement, and reaction stoichiometry and kinetics of both enzymes will need to be established, similar to the characterization of the co-purified enzymes in Chapter 4.

Only two (NdmA and NdmB) of at least four enzymes responsible for *N*-demethylation have been purified and heterologously expressed. The reductase and putative NdmC still have not been purified. Also, whether only one or multiple reductases in CBB5 can partner with NdmA, NdmB, and NdmC is presently unknown.

Complete purification of the reductase(s) and NdmC will allow for N-terminal amino acid sequencing and eventual heterologous expression of these enzymes.

Two open reading frames downstream of *ndmB*, ORF B5 and ORF B6, have been identified as putative genes for reductase and NdmC enzymes. Functional cloning and expression of these ORFs will allow for testing of this hypothesis. Also, expression of a recombinant reductase that can partner with at least one of the *N*-demethylases has many potential applications, including

1. Ease in preparation of a large quantity of reductase for kinetic testing of both reductase and *N*-demethylase,
2. Cloning and heterologous expression of a complete *N*-demethylase system,
3. Production of high-value methylxanthines from caffeine for ease of synthesis of different xanthine derivatives, and
4. Scale up of the *N*-demethylase system for industrial applications.

Expression of either the reductase or NdmA, NdmB, and NdmC, or all four, is induced by caffeine, theophylline, theobromine, paraxanthine, and 7-methylxanthine. Regulation of enzymes involved methylxanthine *N*-demethylation by CBB5 has not yet been investigated. Gene knockout studies may assist in determining the mechanism for *N*-demethylation regulation. Also, knockout studies of individual genes will provide added confirmation of the enzyme activities determined in Chapter 5.

The work performed and described here is the first detailed biochemical characterization, cloning, and expression of bacterial methylxanthine *N*-demethylases. There are many potential uses of this technology, such as (i) production of methylxanthines as pharmaceutical intermediates, (ii) removal of xanthine derivative pollutants from wastewater, coffee and tea processing plants, and contaminated soils in coffee and tea fields, and (iii) regulation control of heterologously expressed enzymes in metabolic engineering. The metabolism of caffeine, theophylline, and their methylated metabolites by *P. putida* CBB5 was shown to be catalyzed by Rieske [2Fe-2S] non-heme

iron *N*-demethylases (oxygenases). Another putative *N*-7-specific alkylxanthine *N*-demethylase has been identified. This study has opened a new clade of genes and enzymes; many more are yet to be discovered. There are many *N*-methylated xenobiotics, including pharmaceuticals and chemicals for protection of agricultural crops. The environmental fate of these compounds will depend on several microbial *N*-demethylases yet to be discovered. While the work described herein provides insight into bacterial degradation of caffeine and related methylxanthines, this study will serve as the basis for discovery and characterization of a plethora of new *N*-demethylases involved in degradation of natural products and xenobiotics.

APPENDIX A
PRIMERS USED IN THIS STUDY

Table A1. A complete list of primers used in this study and their sequences. Sequences are listed from 5' to 3' end of each primer.

Primer Name	Sequence (5'-N _x -3')
A-degF	ATGGARCARGCNATYATYAA
A-degR	TTRATRATNGCYTGYTCCAT
A-degF2	GCSATYATYAAAYGAYGARCGNGA
A-degF3	GCSATYATYAAAYGAYGARAGRGA
B-degF	ATGAARGARCARCTSAARCC
B-degR	GGYTTSAGYTGTYTCYTTCAT
B-degF2	AARCCSCTSCTBGARGAYAARAC
B-degF3	AARCCSTTRTTRGARGAYAARAC
A-speF	TAAGTGAAGCTTGAAAAGGC
A-speF2	TACAGTAAGTGGAAACCGCC
A-speF3	CAATGTGTCATGTCCGGTAG
A-speR2	GGCGGTTTCCACTTACTGTA
B-speF	CCTTAATGAATTTCGAACGC
B-speF3	ACAAAAGCATCTCTCCTCGG
B-speF6	GGCTGGATAACAGCTTCGAT
B-speF7	TGTGGAAAGATGACTCACGT
B-speF8	CGCTAGCCCTGTCGATAACA
B-speR10	TTCCGGCGTTGCTGCAAAC
B-speR11	CCAACACCAATTTCTCGCCT
RieskeR	CCANCCRTGRWANGGRCA
cdm-R1	CAGCCATTTTCTATACTGGATCGA
cdm-R2	GGYTTRTCYTCNGCRAASAC
cdm-R3	AARTCNGTRAARTTYTCCCA
Marcy	CAGGAAACAGCTATGACC
puC19R	CATTCAGGCTGCGCAACTGT
pUC19R2	GCAGATTGTAAGTGTGAGAGTGC
B-iPCR-F1	GTCAACTGATCCCTGCTTGCCCTGAC
B-iPCR-R1	GTCAGGGCAAGCAGGGATCAGTTGAC

Table A1. Continued

Primer Name	Sequence (5'-N _x -3')
B-iPCR-F2	CTGACAAAAGCATCTCTCCTCGGGCC
B-iPCR-R2	GGCCCGAGGAGAGATGCTTTTGTTCAG
B-DownF1	GCCTAAGGATCAAATCGCGT
B-DownR1	CGCAACTCGTTACCGGTATT
B-DownF2	CCATTTTGTGGGCATGGCA
B-DownR2	ACACCTTTCTCACGCAGCCA
B-DownF3	GTCTCTGGCCTATTGTTGCA
B-DownF4	AGAAGGATGCAAGGGAGTCA
B-DownF5	AAATCGCGGTGCGCCAATTG
B-DownR3	CGAACATCTCACTGGGTTTG
B-UpF1	GTATGGGAGGATGGCAAGTT
B-UpR1	ATCTGATGCGATCTACCACC
pET-ndmA-F	GCACGGCATATGGAGCAGGCGATCATCAATGATGA
pET-ndmA-R	GCGCGCGAATTCTTATATGTAGCTCCTATCGCTTT
ndmA-sdm-F	GCGATAGGAGCTACATATAAGAATTCGAGCTCCGT
ndmA-sdm-R	ACGGAGCTCGAATTCTTATATGTAGCTCCTATCGC
B-F-AseI	CGCTGGATTAATGAAGGAGCAACTGAAGCCG
B-R-XhoI	CGCCGGCTCGAGTTACTGTTCTTCTTCAATAACATT
OE-PCR-F2	GAAGGAGATATACATATGAAGGAGCAGCTCAAGCCG
OE-PCR-R	GTGGTGGTGGTGGTCTCGAGTTACTGTTCTTCTTCAATAAC
ROx-F1	TAGAGGATTGCGGTTGACAC
ROx-F2	AACGAGTTGCGGTGTCAGTA
ROx-F3	AGAAGCTGTAGCTACCGACT
ROx-R1	CCTCACAGATCGAGAACGAT
SP6	CGATTTAGGTGACACTATAG
T7	TAATACGACTCACTATAGGG
T7term	GCTAGTTATTGCTCAGCGG
A-5'1F	GACGATGCCTTCGAGCTT
A-5'1R	GTGCACAGCATTCAAGAC
A-5'2R	TCCGAATACTCGCCTAGA
A-5'2F1	GTACTIONGAAAGCGGTGTG
A-5'2F2	AGGAACATACTGCACATC

Table A1. Continued

Primer Name	Sequence (5'-N _x -3')
A-5'3F	CCCGTACTTATCACCTAT
A-5'3R	TTCTACTATCGGAAACCC
A-3'1F	GGTCAAGCCCCATCGTAT
A-3'1R	GCAGATCACCTCCGCTTA
A-3'2F	CGGTGCTCTTTAGGAAC
A-3'2R	GGTCAACCTTCTGTGCGT

APPENDIX B
DNA AND PROTEIN SEQUENCES

DNA sequence

The sequenced EcoRI- and SmaI-digested gDNA fragments containing *ndmA* and *ndmB* and their flanking sequences were combined to form the 13.2-kb sequence below.

For better visualization, start codons have been **bolded**, stop codons are *italicized*, and untranslated regions are highlighted in grey.

```

GAATTCAGGAGTAAAGGAGCGGCGTTGTTTGGTCATCTGACACCTCGA
TCTGGCGAGCATTCTCGCCTAAATGGGTGTCCGGTTTCATTAGACCACTACAT
TTATGTTCTCCCTGTTTTTCCTACTGGGAAGCATCTAGACGCCCGCAGCCTGG
CCTCTCAACGGCCATTATTTGTCAATACCGGTTGAAAACAGACCCACCCCGGC
GCTATTTAAATTGTGCATTTTCATCGCGATGTAGTATTAGCAGCTTGGTGATC
AAAATTCTCGTAAAAACATTTTGTAATTTTCATGATCGTATTGTATTAGTTAG
GTTTGTATTAGAGATTTATCCATGGCTTTTAACAAAGCGGCTACGGTATTCCTT
AGGGGTTACTGAGAGATGCTTCTTGAATGTTAGTCGCATGTGGTCAGAAGTGTG
GTGAACCCGGCTTTGAAGGCTATCGTTTTGAGAGGCAGATCACCTCCGCTTAA
CAAGCGCCTTGCGAAATCAATACGAGATTTCTCCAGAACTCTGAAGGGCAC
ATACCAACCTCCTTCTGAAATAATCGAGTGAAATGTCGTGTGCTCATTGAGGC
GCGATCTGCCATCATCGAAACATTAATTTTTTTTTCTAAATTTTCAAATACCCA
TTCTTGTGTCTGCCGAAGACTTGATAGTTGTGTTTTTTGAGTCATCAAGTTTGT
GCTGAATTGCGACTGGCCACCTGGACGTTTGAGAAAAATTACGAGGTCTTGT
GCCACCTCAAGGGCGAGTTTATGTCCATGATCCTCTTCTACGAATGCTAGAGC
CAGATCTATAGATGCACTGACTCCAGCGGAAGTCCATAGATTTCCGTCGCGA
ATAAAAATCGAATCTATATCCATGATTACATGAGGAAAAC TAGATTGGAAC
CACCTGCCATTCGCCAATGAGTAGTGGCTCGACGGCCATCCAATAGGCCAGT
TGCCGCTAGAAAAAAGCCCCAGAACATAATGCGGCAAACGGTCAACCTTC
TGTGCGTTATTAGTAATCCACTGTTTAAGCTCAGTGTTCATACACAAGTCT
CTGTATGTCATGAGCACCAACAAGAACAAGAGTTTGAGGCTTCAATGCTA
TCGAGGGACTCCGTCGCTTGGAACGATATTTCTGTGTCAGAAATTACTGGGCC
AATAGTAGTTGAACGAAGAGTGAGATGATAGCGGTCAAGTGATCCACTGGCC
TGGAGGATTTTGTTTGCATAAGTGAAGACGGTCATCGGGCCAATAGCCTCAA
ATGACTTAAATTCAGGGTAGATTATAATGTCAATTTTCTTTGTATTGCCGAGT
TCTTCGAACATTTTTGTATTCTCCTCGATGTCTGATATTGACGTCATTTTGTCC
GCATTTACGCTTCTTTGAACACCCAATCCTTTCTTATGGAGATAAAAATGAGA
CCTCCGAATCATAAAAAATACGGTAACTATAATGATAAAAATCACGCGCTGCT
GTAGCGTTCGCGCCAATCAGCCCCTGACGATTGTTGAGGTCGATGTTTCAGCC
ACCTCAGGCTGGTGAAGTATTGGTTCGAGTGGTGGCCACCGGTGTTTGTGATA
CGGATGCCTATACACTTTCTGGGCAAGATTCTGAAGGCGTATTTCCATGCATT
TTGGGGCATGAAGGTGGCGGGATTGTTGAAGCGGTAGGTGAAGGAGTTACTT
CTCTTAAGGTGCGCGATCATGTCATCCCTCTCTATACCGCAGAATGTGGAGAG

```


TGTAATTTTGCAGTCAGGTAAAACCAACTTATGCCAAGCTGTGAGAGCAA
 CGCAAGGCAAGGGGCTAATGCCAGACGGCAGACCCGTTTTAGTTACAAAGG
 TGAGCCTATCTACCATTACATGGGCTGCTCCACATTTTCTGAATACACAGTGT
 TGCCTGAAATTAGTTTGGCTAAAGTTCCTAAAGAAGCACCGCTTGAAAAAGT
 ATGTTTGCCTGGTTGCGGTGTAACAACGGGAATCGGCGCGGTACTCAATACA
 GCTAAGGTAGAAAAAGGTGCTACCGTGGCGGTGTTTGGCCTGGGAGGCATCG
 GGCTCGCGGCTATTATTGGTGCGAAGATGGCGGAAGCCAGTCGTATCATTGC
 GATAGATATAAACCCCTCTAAGTTTCAAATCGCACGAGATTTGGGTGCTACT
 GATTCATTAATCCCAAAGAGTACGATCGTCCTATCCAAGACGTTATTGTCGA
 TCTTACGGAAGGAGGGGTTGACTATTCCTTCGAATGCATCGGAAATGTCAAC
 CTTATGCGAGCTGCGCTTGAGTGCTGCCATAAAGGTTGGGGAGAGTCTGTAA
 TCATCGGCGTAGCACCTGCAGGAGCCGAAATCACTACTCGCCCATTCCAATT
 GGTTACGGGCGGAGTCTGGCGCGGCTCCGCGTTTGGTGGGGTTAAAGGCAGG
 AGTGAGCTGCCGAGCTATGTGCGAAAGAGCTGAGAGGGGAGATATTCCACTCG
 ACAAATTCATCACCCATACGATGGGGCTTGACCAAATCAATGATGCATTTGA
 TCTGATGCATGAGGGTAAGAGCATTGCAACGGTAATTCATTATTAATTCCTAT
 CTGCCCAAGAAGTCAAAATTTCCACATCGTTCGCGACCTTGACGGCAACAAG
 CTAGCTGGTTACACATTCGACTCCCATAGCAGCGAGTTTACGGCCTCTTTTGA
 GGCCGTCTTTTTACATCAAAAAAAGGTGGCGTTGAAAACGCCACCTAGTGC
 TTTATGAAGTTATATGTAGCTCCTATCGCTTTCATGACTGGGTCTAACAAG
 CACTTCGGAAGGCTTGTGAACCTTCTTTATGAGCTTCTTTTAGTTCCCGCAGC
 CATTTTCTATATTGTATCGATACCTTATCTGCGACTACTGAGACCTCATCTGCT
 GGCGCGTCTTTAGGCCATTGGGACTCAATTACTGGTTTGTCTTCAGCGAAGAC
 GAGATCATTAAATGCAATGTGCAAGATAATCCGAGTCGTCCGATTGCTCCCTA
 GCGAAGATCAGAAAGTTTTTCGTGGTGTGGCTGTCTACCGGACATGACACAT
 TGAATAACACATGCAGCGAACTGCTGGAGTATTTGGATACTTCAAGGTTAAT
 AGCAAACGGCATGCTGCAAGTATACGAAAATGAACCAATTGGAGCCTGATTT
 GGGACAGCCATATCTTCTGGCGTGTGCTAGACAAACCGAAACTGACCATTGA
 ATCGATCCATCGGAACAATTGGAGGTTTCAGCATTATTTGGATCGAAAAGCGT
 GCCTGGGTGAATGAATGCAAAGTGAGAAAAATCTGTAAAATTTTCCCATCTA
 CGTTCTGCAGTCGCATCCCACCAGTAAGGTTCTTGTATAACAATACGCAACCT
 AGGATCGTTGGCTGCACTAAAGTAGGGAATTTCAAGTGCAGTCAAACTAGAG
 TCCAATCGAATCCAAATCAATCCATAGCGTTCCTTCGCAATCGAAGCGATCAA
 CTTTAGCCTTGTGGGTATTGGGCTGTTGGGGCACGCTGGTACGAGCTGGCAA
 GCGCCATGCGTATCATATTGCCATCCGTGATAGGGGCACTGTAGGCGGTTTCC
 ACTTACTGTACCCAAGGAAAGCTTAGCTGATCGATGAGCGCATCTATCACGC
 ATCGCGACGTAATCATCGCCTAGCTTGGCGACAACGAGCTGTTTATTAGCA
 GCTTAACGGCCAGGGGGCCGAGGCTGGAAGGATGCGCCTTTTCAAGCTCAGT
 TACAGTACATACGGGATGCCAGAAATGGCGAAGATACTCCCGTTCATCATT
 ATGATTGCCTGTTCCATGTATGTAGCCTTTGTGGATGACGTTGTTATGTTTGA
 AGCAGTTGGATTACCCGCCTGCCATGTCTCCTACTTCTACTCACAGAAAGGGT
 AAACACTAGATACATCTTGTATTTACACCAATCAAACCGCTGGTACTTCAGGT
 TTCTAATCTGGTACACCAGAAAGGTAGGCTATTTTTGAGAACGGTGTCAACC
 ATTAGCCGCCAGAAGGAACAGCAATAACATTTACAGATACGAGGCCACTATT
 TTTAGAGTATTAGCTAAGTAAGTTGCGCATTAGCTCTAGATTGCAGCTAAGAG
 CGTGTCCGATTGCTATTGGTGGAAAAGAAACAGGAGGTTCCGGGAGCCGCGCA

CCAATTCGTTACATTAAGTGGTACCCCTGGTGCGGTTTTAGTGCACAGCATT
 AAGACTGGTCAATAGGTTTGATGAGATCTTTGAAAGAAAGCACAAATTTCTT
 AAGCGGGGCAATGATTATTTTCTGACTTTTGGAGGGATAAGTTACATGCCA
 AGGTAAGTAGATTGACATATCTCTAATCTGACAAGAGTTCCTGAGAATTTAA
 GTAGCAAAGTAGACTTGTATACAATTTCAATTTGTATAGCTAACGAATTTGTAG
 ATTTGATTTTGGCTCACATCTTGCTTAGGGATCACCCACCTGACTTCTGGGT
 CAGGTTATTAGGAGAGAGT**GAGTG**AAAAACAAGATAATAAACACATGCCTG
 CTTCTATCCGCTGCAGTCGTAGCGCCAACAAGCCAAGCCGATGGCAAGCTGT
 TATGGCATCAGGAAAGCATTAGCTATCAATATGGTAAAGACTTCAAAGTAGA
 TCCCGGGCGGATGCAGATCATTACGTTCGAACATACGAGTGCATGGGGGTGG
 GGGACTTCTTCTTTCATCGACAATTTGGTATCCTGGCGCGCAAACAGC
 ATATGACGGGCACCATGGAATGTATCCGAATACTCGCCTAGATTTTCATTT
 CAAAATTACAGGGAGTAATTATAGCTGGGGGATAGTAAAAGATGTGCTTGT
 CGCAACTGCAATTGAGTGGGATAACAATAGGAGCAGCGGGCGTGATGATCA
 GGTAATTATTTGGTTGGGCCAGGGTTTGATCTCTCTTTACCAGGCTTCGATT
 ACTTCATGCTTAATTTCTACTATCGGAAACCCGAGGGTGGGGAAGGTATGGG
 AGGATGGCAAGTTACACCCGTTTGGTTCGTATACAGTCCCAGTTGGGAAAAGT
 AATGTTGTGGTTGATGGCTATATTGATTGGGTTATAGGTGATAAGTACGGGT
 AAAGCATAACTTCCATTTAATCCGCAAATTAAGTACGATATCGGTAAGGCA
 TTTTGGAGTGCGCCAGGTAAATTTATGTTGGAATTGAGTACGATTATTGGTC
 TAATAAATATGGGATTGAAAATACAAGTGCATATGATACAAATCAGAATGTA
 ACAAGTGCAATAGTAAATATTATTTCTGA**ATG**AGGGGTGGGGGCTATGCCCC
 CTTTTTTTGTTCAGACCCTTAGGGCAAATTT**CAG**ATTTATATCAGGAGATCGG
 GTGGTGTCAAATTTATAACCTTTAATCACCAAGTTGTAATGTGACGCAAGAA
 GCTCTTTAGCCGACACAGCATCCCTACGCTCTAAGCATGTACAGAGTTGTGTG
 TGTTCAATCCTGAGCTTGCAGTAGCCGAACCCA**ACT**CGGTATAGGGCATTAT
 CAACGCTTCACGGCGTCGGAGTTGGGGGTGAATCTGATTGATGGTATTATTT
 CAAGAAAGGAAATAAGAAGCGAATGAAAGCCCTCCCTAATTTATCTCCTTC
 ATCATCCAATCCGCATTGATGTGCAGTATGTTCCTTTTGAGTGTGGATTCTTA
 GTTCTTCTAACTGTTGTT**CAG**TGATGCACTGAATTAATTGATCAATCACACCG
 CTTTCGAGTACCAAGAGCATTGGTAAAGCTCGAAGGCATCGTCAAATGTAG
 GACACCAAACGCTTGTGAGCGTTGGGTGAGATTTCCACCAGCTTGTCTTGA
 GATAGTCGGATGAGGGCTTGGCGGACGACTGTGCGGCTAACGTTGAATAGCT
 CTGCGATCTCTCGCTCATT**CAG**CTTCGTTCCGGGTGGAAGCCTGCGGTGGTAG
 ATCGCATCAGATATGGCTGCAACGATTGTCTGGGT**CAGCA**TTGATTTACCTTT
 GGCGCCTTT**CGG**CTCTAAGAGCTGTCATGGTGATCGAACACGGCACCAAAT
 GTAACACGGCCGTGGCTGGTGT**CAC**CGTTAGAAACAGCCTTGGTGCACAAAA
 CATCTTTGCCTTGATACACTTT**CAT**GC**GG**CTTTCTGTCCTTTTCCAAAAAAA
 TATGCCGATTTTCAATGGTATAGCATGCCGGGGAATTGTAGTACCTCCATTT
 TGGCACGAATTCTGCTGTTCAA**AA**T**CAT**CCAGTCCACCTATCCGGCGGGCA
 GCGAAAAAGCGCTGCTCGTCAA**AAAA**ACCGACTATGGTGGTATAACCAGTTAT
 CTATTCTGGTAAACCTTGTAGGCGCTTTTGGTTTAGAACAATAAGACCAGCAA
 TCCCCAGCCCTGAGGACACTCAA**GTG**AAAGAACAGCTCAAGCCGCTGCTAG
 AAGACAAGACTTACCTTCGCCACTTCTGGCATCCCGTGTGTACCCTTAATGAA
 TTCGAACGCGCCAACGCCAGTGGGCACGGCCCATGGGCGTCACCTTGCTAG
 GCGAGAAATTGGTGTGGCCAGGTTAAATTCAAAGATCATTGCGGCTGCTGA

CCGATGTGCTCATCGATCGGCACAGCTCTCCATCGGTTCGCGTTTGCAGCAACG
 CCGGAAAGGACTATCTCGAATGCCCGTATCACGGCTGGCGCTACGATGAGGC
 TGGGGCCTGTCAACTGATCCCTGCTTGCCCTGACAAAAGCATCTCTCCTCGGG
 CCAAGATTTCTCATTTCGATTGTGAGGTGAAATACGACATCGTGTGGGTACG
 GCTGGATAACAGCTTCGATTGCACTCAGATTCCATAACCTCAGCGATTTTCGATA
 ATCCCGACATGCAGGTAATCGTTGCCGATTTCGTATATTTGGGAGACTGTTGCC
 GAGCGGCGGTGGGAGAACTTTACAGATTTTTTCGCACTTTGCCTTCGTACACCC
 AGGGACGCTCTATGATCCGTTTTTCGCTAGCCACCCAAGTGTACGTGAATC
 GCGTTGATGGTGAGTTGCAATTCAAACTCGCTCCGCCGCGTGAAATGAAAGG
 CATCCCGCCAGAAGCACCGATGGGTGACTTCACCTACCGCTGCACAATGCCG
 TATTCAGTAAATCTTGAAATCAAATTGTGGAAAGATGACTCACGTTTCGTTCT
 TTGGACTACCGCTAGCCCTGTCGATAACAAGTCTTGCCGGAATTTTATGATTA
 TTGTGCGTGAGAAGGATAATCAACCTGATCATATGCACCTGGCTTTCCAGAA
 GCGGGTGCTTGACGAAGACCAGCCTGTTATCGAATCGCAATGGCCTCTCGAA
 ATACAGACCTCGGAAGTCTCCGTTGCAACCGATAAAAATTTCCGTCCAGTTCGG
 CAAATGGCATAAAGAGCTATCTCTGTCAGCCGTTGAAGGACGGGAGGCGTTC
 CGCGATTCCGTCTTGACGAATGTTATTGAAGAAGAACAGTAAGAGTCCGCCA
 AGTGGAATTCAGTGCCGACCTGATGAGGACGGCACGCGTATTTGAGATGT
 CTGGTGCAGACTCTTTCGGTCACTAATACTTATTAGTTTAGGTGCTTCTCATG
 CAATCACTAGCCTTGCAGAAGAAAACAAGCATTGGAAGGTCATTTTCATGG
 GATGGCAGCACGTGCTTGTGATGTACGCCGGTGTGTCGCCGTCCCTTTGATA
 CTTGGCGCCGCACTCAAGTTGCCTAAGGATCAAATCGCGTCTTAATCAATGC
 AGATCTTTTTGCCTGTGGGATCGCAACATTAATTCAGTGTGTTGGCTTTGCAA
 ATGTAGGCATTAGGTTGCCTGTCATGATGGGCGTAACTTTTACGGCAATTGGG
 CCGCTGATTGCGATCGGGACAGATCCTCAAGCTGGATTGCTTCAAGTCTTTGG
 TTCTACCATTGCTGCCGGGATCTTTGGGTTTCTGGTTCGCCCCCTTCATCGGAA
 AACTTATAAGATTCTTTCCCTCCCGTTGTAACCGGTACGGAAATTTTGGCGGTT
 GGTTTGTGCTGATGGTAGTAGCTGCAAGCTGGTCAGCGGGAGGATACGGCA
 ATCCTGATTTTGGTAATCCGCTGTATCTAACTATTGCTGCCTCCGTTTTGGTTCG
 TAATCTTATTCAATTGTGAGATTTGCAAAAGGTTTCATTTTCGAACATTTCCATTT
 TGTTGGGCATGGCATTGTTGGGTTTCGCTTTAGCTTTTCAGTGCCTGGCATATTAAT
 TTCGATGATGTGAGCGCAGCCCCCTGGTTTGGACTGGTTTTGCCTTTCCATTTT
 GGAGTGCCTTCATTTAGTCTCTGGCCTATTGTTGCAATGTGCATTGTTATGCTG
 GTTACCTTTATTGAATCCACAGGCATGTTCTTGGCTCTGGGCGAGTTGGTTGA
 AAAACCCGTAAGCGAAAAAGACCTCGTGCGTGGGTTTAGAGCTGATGGGTTT
 GGAACAATGTTAGGTGGTGTGTTCAATACATTCCTTATACGTCATATGCTCA
 GAATATTGGTCTCATTAGCATCACAGGTGTTAAGAGCAGATGGGTGTGTGCT
 CTCGCCGGCCTCTTCTTGGTAGGATTGGCATTGTTTCTAAAGTTGCAATGAT
 TATCGCCTCAACACCACCATACGTCTTGGGGGGGGCCGGTTTGGTAATGTTTG
 GGATGGTTCGAGCTAGCGGCATCAAAGTTTTATCCAGGGTCAGCTTTGCCGA
 TAGTAAAAATCTTTACGTAGTAGCAATTAGTGTATCCATAGGAATGATTCCGG
 CCGTGTACCCCAGTTCTTCGCAAAACTGCCAAAGGATTTGTCTCCGTTGCTA
 GAAAGCTCTGTATTGCTCACTGCGATATGCGCGGTCGTTTTGAATGTCTTCTT
 CAATGGCTTTGGAAGTGAGAAGGATGCAAGGGAGTCACTTCTGACGGCAGCA
 AAAGAAGCAGAGGTTTGAATTTTACAATTCGGTCTAAGAGAGAAAAACAAT
 GAAAAAGATGTTCTTGCTTGGTTGTGCAGGTCGTGGCGTTCAACCCCCATCCA

TCAGTAAACCGGTTTCTGATCGCGAACTTCCGATTATGGAGCAGTTTCGTCTT
 CAAAAGGAATCGGGGTTGTGGGATTTTGTGATCGAATTCCCGTAGGCACAG
 AAGAGTTGGATGAGTACATCAAGGCAAGTCAGCGATACTCCTTGCCAGTTTA
 CAGTGGAAGTTGGACTTACACTCTCGGTGCCGATGAGTAACGCATTTCGGGAA
 AATATTGATCAGACCCTGGCTGTGGGTGCTAAATACCATAATCTTATGGTGTG
 GGCGAAGCACGCTGACGGTCACTACATTACTGATGAAGAGGTAGCGATTTCCG
 TATCTAAACGCCTTTGAATATGCGGACAAACAAGGCGTAATTATTACCTATG
 AGAATCACGTTGATATGTGGTCTGAGGATCCGAGGCGTGTGCAAAGGTTGC
 GAATATCGTAGAGCGACACGGTATTCCATTTAACATTTGCATGGATTACAGTC
 ACTGCATCTTCAAAGTAGAAAACGAAGTTGAAATCGCGGTGCGCCAATTGTG
 AGGTGACCAAGATGGTATTCGACGCCTCGACCCCTTCAATGATGATAGCTAC
 GCAGACGATTGGTTGGCTCGCAACACTGTCCACTGGGCGCAAGTACGTCCAG
 CTGTACCTAACGGGCCCGCAATTGGTGGGCTGGCGAAACTGGCCCTTGGGA
 TGGATTAGGGTATGACCGACCAGGGCGTTCATCCAATATCCATTTAGCAATC
 CAAAACCAGGCGAATGGCATAACGATTTTTGGCATGCACATAAACTCGCCCC
 CACCAAGAGTTAATTCGTAAAGCAATTGACAGCTACATCCAGGAAGACAAA
 TCCAGTCTTCGGCTGATGACGATCGACAATATCAACCTCGCTGCGTACGGTAC
 AGGTGGAAGTGCGACATGTTTGTCTGATAGCTGTTTGGTGGCCAAGTTTGTGC
 GGGAGCTTTATGCGGAGCGAGTAGCTGTGCGCGAAGCTAGGAAGTCTCTAGG
 GGCTGATTTTGTAAATCAACACCGTAATCAACTGTAATTTTTGGATCTCGCCA
 TCTGTTGCCTCTGAGAGGGGCAAGAGATTTTACTCAAAAATCAGCTTAAGAA
 TTGCTGGCCAATCTTAATAGGTTTGTAGTCAGTAGTTCTTGGGCTATTATC
 TAGTATAACCAGATAGATAAGCTGAATGGCCAGAGGGGATTATAATGTCTACT
 GACCAAGTAATTTTTAACGACTGGCATCCAGTCGCTGCTTTGGAAGATGTATC
 TCTCGATAAACGATACCGCTGTCGACTACTAGGTCGTACAGTTAGTTATGTGA
 AAACATCTGATGCTGTTAATGCTCATTGGGAAGAAAGTGCAGATGGAATTA
 GACCATCCGCGCTAAAGAAATCTATGGTCTTCTGTGGCTCTCCTTTGCCGACA
 AACCCAGTGAGATGTTTCGATATTGCAGAGTTCAAGGAACCTGATCGCCGAAT
 CGTCAGCGCTGGATCTGTGCGCGTAAATGTCTCAGGACTGCGTGCTATCGAA
 AACTTTCTGGACATGGCTCATTTCCTTTTGTTCATACGGATATTTTGGGTGCA
 GAGCCACTGACGGAAGTTGGGCCGTATAACGTCAACTATGTTGAAACTGTTG
 ATGAGATCTTCGCTACTGAGTGTAAGTTCCCGCAACCTAAAGGCTCAGCTACT
 GCTGTGAGCCAATTGATATGCAGTATATATACCGCATTACACGGCCATATTC
 CGCCATTTTATATAAACTTGCCCCGCCGAACCGCATAGATGGGATGCCCTC
 GGTCTGTTTATTCAACCTGTAGACGAAGATTGGTGCATAGCGCATAACAATTAT
 GTGCTATGTGGATGACGTTAACTCAGATCAACAACCTTCGCCATTTCCAGCAGA
 CGATTTTTGGCCAGGACTTGATGATTCTTATCAACCAAGTTCCAAAGCGTCTT
 CCCCTGGCTGCAAGTCGAGAGAGCCAGTCCGGGCGGATGTGCTTGCAACAG
 CTTATCGTCGCTGGCTGCGTGAGAAAGGTGTGCAATATGGTGTCTGCGGGA
 CTAATAACAAGAATTGCTAAGAGGGTATGTGCCGTGAACAAACTTGACGTCA
 ACCAGTGGTTTCTATTGCTACCACTGAAGATCTCCCGAAGCGCCATGTCTTT
 CATGCCACGTTGTTGGGGCAAGAAATGGCCATCTGGCGCGATGACTCTGGTT
 CAGTTAATGCTTGGGAGAACCGCTGCCCGCATAGAGGATTGCGGTTGACACT
 GGGTGCTAATAACCGTAACGAGTTGCGGTGTCAGTATCATGGATGGACTTAT
 GAAAGCGGGACTGGTGGCTGCACTTTTGTCCCAGCCCATCGCGATGCACCAC
 CCCCAATGCCGCGCGGGTTAATACTTTTCTGTCCGCGAAAAGCACGGCTTT

ATCTGGACGACATTAGGTCAGCCGCCAGGAGAGCCCATTTCAATCCTCGATG
 ACGCTCAGCTTGTAACGCTGTAAAAACAAATCTGCATAGCGTAGTTATAGA
 TGCTGATATTGACGGAGTTGTCAGCGTCCTACGTCAGAATCTTTCAGCGTTCA
 TCGATGTGTTTGGTGCGGCCAGCGCTGAAGATCTGCATTTGAAATCCATGCTG
 CAAGATCGAGGGATTCTGGTAACAAGATCAGGCTCTATTGCTATTCATTTTTA
 TATGCAGCGCTCAACCATTAGTAAATGCGTGTGTACATGCGCAAGTACTTACTC
 CGGGACGTCCAGGATACGAACTTCAAAGAACTACTCGTATGCCATGAACGT
 TATCCGCAGGGCAGCAGAAGCTGTAGCTACCGACTTGATTAGCATTACAGAT
 ATCAGCGATCAGACTATCGAAAAGCTTGAAGTCGTTAGAGAAAACATGACTA
 AGGCTCCTCCAACCCACTATATCTGCGAAGTGGTTACGCGTACTCAAGAGAC
 AGGTGATATTAACCTACTGGCTGAAGCCTATCGGCTACCCACTACCAGCAT
 TCAGTCCAGGGATGCACATCAGCATCACACGCCGGAGGGTAGCATTTCGACA
 ATATTCCCTCGTGAACGGGCTGACGAGCGTGAATCCTTCATCATCGGTGTGA
 AGAAAGAGATTCAGTCCCGTGGCGGCTCCAGATCAATGCACGAAGATGTGAA
 GGTTGGAACGCAACTAAAAGTTACACTTCCGAGGAACGGTTTTTCCACTCGTC
 CAAACCAGAAAACACCCGATTCTCGTAGCAGGTGGCATCGGTATCACCCCAA
 TTTTGTGTATGGCACAGGCTCTGGATCAGCAAGGTTTCATCGTATGAAATACAT
 TATTTTGTCTCGTGCATTTGAGCATGTTCCATTCCAGGATCGACTGACTGCGTT
 GGGCGATCGTTTGAATGTGCATCTTGGCCTCGGCCAGACGAGACTAGAGCA
 AAACCTCCCGACATCATGGAGATTCATAACGCCCAAGACGTAGATGTTTACA
 CTTGCGGCCCGCAACCAATGATCGAAACTGTATCTGCTGTGCTCTTGGCTCAT
 GGCATCGCTGAAGAGTCCATCCGATTTGAATTTTTTCAGTAAAAAGAACGATG
 TTCCCGTTTCTGATGAAGAATATGAGGTTGAGCTCAAAAAAACTGGTCAAAT
 ATTCACTGTCTCGCCTGGCTCTACGTTGTTGCAAGCTTGTTTGGACAACGATG
 TTCGTATCGAAGCTTCTTGTGAGCAGGGTGTATGCGGGACTTGTATAACTCCA
 GTCGTATCCGGCGATCTCGAGCATCATGACACTTACCTTTCTAAGAAAGAAA
 GGGAAAGCGGTAAGTGGATCATGCCGTGTGTTTCGCGCTGCAAGTCCAAAAA
 AATCGTTCTCGATCTGTGAGGCCCTAAAACCGTGTATTACACTCTATGACTATGA
 GCTTTCCGGGAAGTACTGCTACAAGATCAGGCTTTTTTTTGTCCATTCTGAATATGG
 GATACCAAAGTACTGAGCCTGTAGAGTTCTATCCGTCGCGTGAGCATAAATCTGA
 AGCGTTCCTGAAAATCAATCCTCTCGGCCAACTTCTGCTTTGAAGGATGGTG
 ATCTCGTGCTGAGGGACGCACAGGCAATTCTCGTCTATCTGGCCACTCAGTAT
 GATAAGAGCTGCTACTGGTACCCGACCGCCCGCCGGATCTGATGGCTGAGG
 TCAACATGTGGATGGCCTTTGCTGATAGCCTGACCAGCACCATTTCTTCCGCG
 CGATTACATGACTTGTTTTTCTATGAATTC

Peptide Sequences

Open reading frames in the 6-kb region were translated to their corresponding peptide sequences using FastPCR software and are listed below.

ORF1 (*araC* family transcriptional regulator homolog)

mtsisdieentkmfeelgntkkidiiipefksfeaigpmtvftyankilqasgsldryhltrsttigpvisdteisfq
atesldsieasnsvllvgahdiqrlvyentelkqwitnaqkvdrfaalcsgafflaatgldgrratthwrmagefqssfphvi
mdidsifirdgnlwtsagvsasidlalafveedhghklalevaqdlviflkrpggqsqfstnlmtqktqlsslrtqewvfenle
kkinvsmmadrasmsrthfrlfqkevqgmcpsefleksridfarrllsggdplktiafkagftssdhmrlltfkkhlsvtpkey
rsrfvkshg

ORF2 (*frmA* formaldehyde dehydrogenase homolog)

miksraavafapnqpltivevdvppqagevlrvvatgvchtdaytlsgqdsegvfpcilghegggiveavge
gvtslkvgdhviptyaecgeckfcksgktnlcqavratqgkglmpdgtrfsykgepiyhymgcstfseytvlpeislakvp
keaplekvcllgcgvttgigavIntakvek gatvavfllggiglaaiigakmaeasriiainpskfeiardlgatdfinkey
drpiqdvivdlteggvdysfecignvnlmraalecchkgwgesviigvapagaeittrpfqlvtgrvwrgsafggvkgrsel
psyveraergdipldkfithmglqdindafdlmhegksirtvihy

ORF3 (*ndmA*)

meqaiindereylrhfwphvctvtelekahpsslglavkllneqlvvaklgdeyvamrdcahrsakslgtvsg
nrlqcpyhgwqydhgacqlvpacpnspipnkakvdrfdceerygliwirdssfdteipyfsaandprlriqiqepyww
dataerrwenftdfshfafihipgtlfdpnnaeppivpmdrfngqfrfvydtpedmavpnqapigsfsytcsmpfainlevsk
ysssslhvlfnvscpvdshhtknflifareqsddsyhliafndlvfaedkpviesqwpkdapadevsvvadkvsiqyrkw
relkeahkegsqafrsalldpviesdrsyi

ORF4 (*tsx* family channel protein homolog)

mqiitfehtsawgwgdfffidnywypgaqtaydghhgmyseysprfskitgsnyswgivkdvlvataiew
dnnrsgrrddqvnylvpgfdlslpgfdyfmInfyirkpeggegmggwqvtpvwsytpvgksnvvdgyidwvig
dkyglkhnfhfnpqikydidgkafwsapgkyfygieydywsnkygientsaydtnqnvtasivkyyf

ORF5 (*gntR* family transcriptional regulator homolog)

mltqtivaaisdaiyhrrlppgklnereiaelfnvsrtvvrqalirlsqdklveispkrstsvwcptfddafelyqml
vlesgvidqliqciteqqleelrihtqkehtahqcgldegdkgfghsllisflgnntinqihpqlrrealinalyrvfggyckl
rnehtqlvtclerrdavsakellashynlvikgykfdttrspdinlkfalrv

ORF6 (*ndmB*)

mkeqlkplledktylrhwhpvctlnferanasghgpmgvllgeklvlarlnskiaaadrcahrsaqlsigrv
snagkdylecphygwrydeagacqlipacpdkisprakissfdcevkydivwvrlndsfctqipylsdfndpdmqviv
adsyiwetvaerrwenftdfshfafvhpgtlydpffashptvyvnrvdgelqfklappremkgippeapmgdftyrcmp
ysvnleiklwkdssrflwttaspvdknscrnmiiivrekdnqpdhmlafqkrvldedqpvesqwpleiqtsevsvatd
kisvqfrkwhkelsavegreafdrsvltnvieeeq

ORF7 (xanthine permease homolog)

mqsalalqkktiwiwvifmgwqhvlvmyagavavplilgaalkpkdqiaflinadlfacgiatliqcvgfanvgi
rlpvmmgvftaigpliaigtqpqagllqvfgstiaagifgflvapfigklirffppvvtgteilavglslmvvaaswsaggygn
pdfgnplyltiaasvlvvilfivrfakgfisnisillgmafgalafasawhinfddvsapwfglvlpfhfgvpsfslwpivamc
ivmlvtfiestgmflalgelvekpvsedlvrgfradgfgtmllggvntfpytsyaqnilisitgvksrwvcalagflvlgalf
pkvamiiastpppylvggaglvmfgmvaasgikvlsvsfadsknlyvvaisvsigmipavspqffaklpkdlsplessvllt
aicavvlnvffngfgsekdareslltaakeav

ORF8 (SRPBCC superfamily, possible *NdmC*)

mstdqvifndwhpvaaledvsldkryrcrllgrtvsyvktsdavnahweesadgiktirakeiygllwlsfadkps
emfdiaefkepdrriivsagsvrvnvsglraiEnfIDmaHfpfvHtdilgaepktevgpynvnyvetvdeifateckfpqpk
gsatavepidmqiyirtrpysailyktcppephrwdalglfiqpvedwciahtimcyvddvnsdqqlrhfqqtifgqdl
milinqvprkrlplaasrespvradvlatayrrwlrkvgvqyalrd

ORF9 (*vanB* homolog, possible *Ndm* system reductase)

mnkldvnqwfpiattedlpkrhvfhatllgqemaiwrddsgsvnawenrcphrglrlltgantgnelrcqyhgw
tyesgtggctfvpahrdappnaarvntfpvrekghfiwttlgppgepisilddaqlvnavktnlshsvvidadidgvsvlr

qnlafidvfgaasaedlhklsmlqdrgilvtrsgsiaihfymqrstiskcvvhaqvltpgrpgyelqknysyamnvirrae
 avatdlisitdisdqieklevvrenmtkapthycevvtrtqetgdinsywlkpiigyplpafspgmhisittpegsirqyslv
 ngpderesfiigvkkeiqsrggsrsmhedvkvtqlkvtlprngfplvqtrkhpilvaggiitpilcmaqaldqqgssyeih
 yfarafehvpfqdriltalgdrlnvhlglgpdetraklpdimeihnaqdvdvytcgppmietetvsavalahgiaeesirfeffsk
 kndvpsdeeyevelkktgqiftvspgstllqaclndvrieasceqgvcgtcitpvvsgdlehdtylskkesgkwimp
 cvsckskkivldl

ORF10 (partial *gst* homolog)

mitlydyelsgncykirlflsilnmgyqtepvfypsrehkseafkinplgqlpalkdgdvlrdaqailvylatqy
 dkscywyptarpdlmaevnmwmafadststissarlhdlff...

APPENDIX C
SEQUENCES USED TO CREATE THE RADIAL PHYLOGRAM

Table C1. Names and accession numbers of the genes used to create the radial phylogram in Figure 5.18.

Enzyme (Original Organism)	Accession No.	Gene Name
Carbazole 1,9a-dioxygenase (<i>P. resinovorans</i> CA10)	BAA21729	CarAb
3-chlorobenzoate dioxygenase (<i>Alcaligenes</i> sp. BR60)	AAC45716	CbaA
Phenoxybenzoate dioxygenase (<i>P. pseudoalcaligenes</i> POB310)	CAA55400	PobA
Phthalate dioxygenase (<i>B. cepacia</i> DBO1)	AAD03558	OphA2
<i>p</i> -Toluenesulfonate methyl-monooxygenase (<i>C. testosterone</i> T-2)	AAC44804	TsaM
Aniline dioxygenase (<i>Acinetobacter</i> sp. YAA)	BAA13012	AtdA
Aniline oxygenase (<i>P. putida</i> UCC22)	BAA12807	TdnA1
2-Halobenzoate 1,2-dioxygenase (<i>P. cepacia</i> 2CBS)	CAA55681	CbdA
Benzoate 1,2-dioxygenase (<i>Acinetobacter</i> . sp. ADP1)	AAC46436	BenA
Anthranilate dioxygenase (<i>Acinetobacter</i> . sp. ADP1)	AAC34813	AntA
Phenanthrene dioxygenase (<i>Nocardioides</i> sp. KP7)	BAA94708	PhdA
Phthalate dioxygenase (<i>Terrabacter</i> sp. DBF63)	BAC54156	PhtA1
Phthalate dioxygenase (<i>A. keyseri</i> 12B)	AAK16534	PhtAa_12B
Phthalate dioxygenase (<i>M. vanbaalenii</i> PYR-1)	AAQ91914	PhtAa_PYR1
Phthalate dioxygenase (<i>Rhodococcus</i> sp. RHA1)	BAD36800	PadAa2
3,4-Dihydroxyphenanthrene dioxygenase (<i>A. faecalis</i> AFK2)	BAA76323	PhnAc
Naphthalene dioxygenase (<i>Pseudomonas</i> sp. 9816-4)	AAA92141	NahAc
PAH dioxygenase (<i>P. putida</i> OUS82)	BAA20391	PahAc

Table C.1. Continued

Enzyme (Original Organism)	Accession No.	Gene Name
Carbazole dioxygenase (<i>Sphingomonas</i> sp. CB3)	AAC38616	CarAa_CB3
Dioxin dioxygenase (<i>Sphingomonas</i> sp. RW1)	CAA51365	DxnA1
Biphenyl dioxygenase (<i>Rhodococcus</i> sp. RHA1)	BAA06868	BphA1
Toluene dioxygenase (<i>P. putida</i> F1)	AAA26005	TodC1
Biphenyl dioxygenase (<i>Pseudomonas</i> sp. KKS102)	BAA04137	BphA1_KKS102
Biphenyl 2,3-dioxygenase (<i>B. xenovorans</i> LB400)	AAB63425	BphA
Biphenyl dioxygenase (<i>P. pseudoalcaligenes</i> KF707)	AAA25743	BphA1_KF707
biphenyl dioxygenase (<i>Sphingobium</i> yanoikuyae B1)	ABM79814	BphA1e
Aniline dioxygenase (<i>D. acidovorans</i> 7N)	BAD61049	Orf7NC
Phthalate dioxygenase (<i>P. putida</i>)	BAA02511	Pht3
Vanillate <i>O</i> -demethylase oxygenase (<i>Pseudomonas</i> sp. HR199)	CAA72287	VanA_HR199
Vanillate <i>O</i> -demethylase oxygenase (<i>Pseudomonas</i> sp. strain ATCC 19151)	AAA26019	VanA
Anthranilate 1,2-dioxygenase (<i>P. resinovorans</i> CA10)	BAB32747	AntA_CA10
Naphthalene dioxygenase (<i>Ralstonia</i> sp. U2)	AAD12610	NagAc
Salicylate 5-hydroxylase (<i>Ralstonia</i> sp. U2)	AAD12607	NagG
Salicylate 5-hydroxylase (<i>P. aeruginosa</i> JB2)	AAC69484	HybB
Naphthalene dioxygenase (<i>P. aeruginosa</i> Pak1)	BAA12240	PahA3
Cumene dioxygenase (<i>P. fluorescens</i> IP01)	BAA07074	CumA1
Naphthalene dioxygenase (<i>Rhodococcus</i> sp. NCIMB12038)	AAD28100	NarAa
Carbazole 1,9a-dioxygenase (<i>Pseudomonas</i> sp. XLDN4-9)	AAY56339	CarAa
PAH dioxygenase (<i>R. erythropolis</i> TA421)	BAA25623	BphA1_TA421
Nitrobenzene dioxygenase (<i>Comamonas</i> sp. strain JS765)	AAL76202	NbzAc

Table C.1. Continued

Enzyme (Original Organism)	Accession No.	Gene Name
2-Nitrotoluene dioxygenase (<i>Pseudomonas</i> sp. JS42)	AAB40383	NtdAc
Dinitrotoluene dioxygenase (<i>B. cepacia</i>)	AAL50021	DntAc
PAH dioxygenase (<i>M. vanbaalenii</i> PYR-1)	AAF75991	NidA
PAH dioxygenase (<i>M. vanbaalenii</i> PYR-1)	AAV85176	NidA3
PAH dioxygenase (<i>Pseudomonas abietaniphila</i> BKME-9)	AAD21063	DitA1
<i>p</i> -Cumate dioxygenase (<i>R. palustris</i> No.7)	BAA82116	PsbAb
<i>p</i> -Cumate dioxygenase (<i>P. putida</i> F1)	AAB62285	CmtAb
Dicamba O-demethylase (<i>Pseudomonas maltophilia</i> DI-6)	AAV53699	DdmC
Caffeine demethylase	AAB15321	Cdm
<i>Janthinobacterium</i> sp. Marseille (mma_0224)	YP_001351914	Mma0224
2-oxo-1,2-dihydroquinoline 8-monooxygenase (<i>P. putida</i> 86)	CAA73203	Oxo
5,5'-dehydrodivanillate demethylase (<i>P. paucimobilis</i> SYK-6)	BAA36168	LigX
Chlorophyllide a oxygenase isoform 1 (<i>Arabidopsis</i>)	BAA82484	CAO1
3-Ketosteroid-9-Alpha-Hydroxylase (<i>Mycobacterium Tuberculosis</i>)	GI:224510546	KshA
Carbazole dioxygenase (<i>Janthinobacterium</i> sp. J3)	GI:75765412	CarAa_J3
3-phenylpropionate dioxygenase (<i>E. coli</i> K12)	P0ABR5	HcaE
Toluate-1,2-dioxygenase (<i>P. putida</i>)	P23099	XylX
Salicylate 1-hydroxylase (<i>Sphingomonas</i> sp. CHY-1)	Q65AS5	PhnA1b
PAH dioxygenase (<i>Sphingomonas</i> sp. CHY-1)	Q65AT1	PhnA1a
Salicylate 1-hydroxylase (<i>Sphingomonas</i> sp. P2)	Q83VL2	AhdA1c
Salicylate 1-hydroxylase (<i>Sphingomonas</i> sp. P2)	Q83VK6	AhdA1d
Salicylate 1-hydroxylase (<i>Sphingomonas</i> sp. P2)	Q83VI7	AhdA1e
PAH dioxygenase (<i>Mycobacterium</i> sp. 6PY1)	Q84EU3	PdoA1
PAH dioxygenase (<i>Mycobacterium</i> sp. 6PY1)	Q84EU7	PdoA2

Table C.1. Continued

Enzyme (Original Organism)	Accession No.	Gene Name
Chlorobenzene dioxygenase (<i>Pseudomonas</i> sp. P51)	Q52383	TcbAa
PAH dioxygenase (<i>Cycloclasticus</i> sp. A5)	Q7WUA0	PhnA1
Carbazole dioxygenase (<i>Spingomonas</i> sp. KA1)	YP_717981	CarAa1
Carbazole dioxygenase (<i>Nocardioides aromaticivorans</i>)	BAE79498	CarAa
Biphenyl dioxygenase (<i>Bacillus</i> sp. JF8)	BAC79226	BphA1
Biphenyl dioxygenase (<i>Comamonas testosteroni</i>)	BAC01052	BphA1
Biphenyl dioxygenase (<i>Comamonas testosteroni</i>)	Q46372	BphA
isopropylbenzene dioxygenase (<i>P. putida</i>)	AAC03436	IpbAa
Benzene dioxygenase (<i>P. putida</i> ML2)	Q07944	BedC1
Chlorobenzene dioxygenase (<i>Burkholderia</i> sp. PS12)	AAC46390	TecA1
Biphenyl dioxygenase (<i>Rhodococcus</i> sp. M5)	AAB07750	BpdC1
Dibenzofuran dioxygenase (<i>Terrabacter</i> sp. YK3)	BAC06602	DfdA1
PAH dioxygenase (<i>Sphingomonas</i> sp. A4)	BAD34447	ArhA1

APPENDIX D
PUBLICATIONS AND PRESENTATIONS

Publications

Summers, R. M., Louie, T. M., Yu, C. L., & Subramanian, M. (2011). Characterization of a Broad-Specificity Non-Haem Iron *N*-Demethylase from *Pseudomonas putida* CBB5 Capable of Utilizing Several Purine Alkaloids as Sole Carbon and Nitrogen Source. *Microbiology* **157**(2): 583-592.

Yu, C. L., Louie, T. M., Summers, R., Kale, Y., Gopishetty, S., & Subramanian, M. (2009). Two Distinct Pathways for Metabolism of Theophylline and Caffeine Are Coexpressed in *Pseudomonas putida* CBB5. *Journal of Bacteriology* **191**(14): 4624-4632.

Presentations

Summers, R. M., Yu, C. L., Louie, T. M., & Subramanian, M. (2011). Purification, Cloning, and Functional Expression of NdmA and NdmB, Two Positional-Specific Methylxanthine *N*-Demethylases from *Pseudomonas putida* CBB5. American Society of Microbiology Conference, New Orleans, LA.

Summers, R. M., Yu, C. L., Louie, T. M., & Subramanian, M. (2011). Purification, Cloning, and Functional Expression of NdmA and NdmB, Two Positional-Specific Methylxanthine *N*-Demethylases from *Pseudomonas putida* CBB5. University of Iowa College of Engineering Research Open House, Iowa City, IA.

Summers, R. M., Yu, C. L., Louie, T. M., & Subramanian, M. (2010). A Broad Specificity Non-Heme Iron *N*-Demethylase Enables *Pseudomonas putida* CBB5 to

Metabolize Several Purine Alkaloids. Center for Biocatalysis and Bioprocessing Conference, Iowa City, IA.

Louie, T. M., Summers, R. M., Yu, C. L., & Subramanian, M. (2010). Cloning and Functional Expression of NdmA and NdmB, Two Positional-Specific Methylxanthine *N*-Demethylases from *Pseudomonas putida* CBB5. Center for Biocatalysis and Bioprocessing Conference, Iowa City, IA.

Summers, R. M., Yu, C. L., Louie, T. M., & Subramanian, M. (2010). Partial Purification of a Two-Component Methylxanthine *N*-Demethylase from *Pseudomonas putida* CBB5. American Society of Microbiology Conference, San Diego, CA.

Summers, R. M., Yu, C. L., Louie, T. M., & Subramanian, M. (2010). Partial Purification of a Two-Component Methylxanthine *N*-Demethylase from *Pseudomonas putida* CBB5. University of Iowa College of Engineering Research Open House, Iowa City, IA.

Summers, R. M., Yu, C. L., Louie, T. M., & Subramanian, M. (2009). Partial Purification of a Two-Component Methylxanthine *N*-Demethylase from *Pseudomonas putida* CBB5. Center for Biocatalysis and Bioprocessing Conference, Iowa City, IA.

Summers, R. M., Yu, C. L., & Subramanian, M. (2009). Characterization of Methylxanthine-Oxidizing Enzymes in *Pseudomonas putida* CBB5. American Society of Microbiology Conference, Philadelphia, PA.

Summers, R. M., Yu, C. L., & Subramanian, M. (2009). Characterization of Methylxanthine-Oxidizing Enzymes in *Pseudomonas putida* CBB5. University of Iowa College of Engineering Research Open House, Iowa City, IA.

Summers, R. M., Yu, C. L., & Subramanian, M. (2008). Characterization of Methylxanthine-Oxidizing Enzymes in *Pseudomonas putida* CBB5. Center for Biocatalysis and Bioprocessing Conference, Iowa City, IA.

REFERENCES

- Abel, A. M., Carnell, A. J., Davis, J. A., & Paylor, M. (2003). The synthesis of buprenorphine intermediates by regioselective microbial *N*- and *O*-demethylation reactions using *Cunninghamella echinulata* NRRL 1384. *Enzyme and Microbial Technology* **33**(5): 743-748.
- Altschul, S. F., Madden, T. L., Schäffer, A. A., Zhang, J., Zhang, Z., Miller, W., & Lipman, D. J. (1997). Gapped BLAST and PSI-BLAST: A new generation of protein database search programs. *Nucleic Acids Res* **25**(17): 3389-3402.
- Anaya, A. L., Cruz-Ortega, R., & Waller, G. R. (2006). Metabolism and ecology of purine alkaloids. *Frontiers in Bioscience* **11**: 2354-2370.
- Anderson, L. E., & Gibbs, M. (1962). The biosynthesis of caffeine in the coffee plant. *Journal of Biological Chemistry* **237**(6): 1941-1944.
- Asano, Y., Komeda, T., & Yamada, H. (1993). Microbial production of theobromine from caffeine. *Bioscience, Biotechnology, and Biochemistry* **57**(8): 1286-1289.
- Asano, Y., Komeda, T., & Yamada, H. (1994). Enzymes involved in theobromine production from caffeine by *Pseudomonas putida* No. 352. *Bioscience, Biotechnology, and Biochemistry* **58**(12): 2303-2304.
- Asha, S., & Vidyavathi, M. (2009). *Cunninghamella*-A microbial model for drug metabolism studies-A review. *Biotechnology Advances* **27**(1): 16-29.
- Ashihara, H., Monteiro, A. M., Moritz, T., Gillies, F. M., & Crozier, A. (1996). Catabolism of caffeine and related purine alkaloids in leaves of *Coffea arabica* L. *Planta* **198**: 334-339.
- Ashihara, H., & Crozier, A. (1999). Biosynthesis and metabolism of caffeine and related purine alkaloids in plants. *Advances in Botanical Research* **30**: 117-205.
- Ashihara, H. & Suzuki, T. (2004). Distribution and biosynthesis of caffeine in plants. *Frontiers in Bioscience* **9**: 1864-1876.
- Audic, S., R. C., Campagna, B., Parinello, H., Claverie, J. M., Raoult, D., & Drancourt, M. (2007). Genome analysis of *Minibacterium massiliensis* highlights the convergent evolution of water-living bacteria. *PLoS Genetics* **3**(8): 1454-1463.
- Barone, J. J., & Roberts, H. R. (1996). Caffeine consumption. *Food and Chemical Toxicology* **34**(1): 119-129.
- Bauer, J. C., Wright, D. A., Braman, J. C., & Geha, R. S. (2002). Circular Site-Directed Mutagenesis. United States Patent US6391548B1.

- Baumann, T. W., Koetz, R., & Morath, P. (1983). *N*-methyltransferase activities in suspension cultures of *Coffea arabica* L. *Plant Cell Reports* **2**: 33-35.
- Bayer, T. S., & Smolke, C. D. (2005). Programmable ligand-controlled riboregulators of eukaryotic gene expression. *Nature Biotechnology* **23**(3): 337-343.
- Beltrán, J. G., Leask, R. L., & Brown, W. A. (2006). Activity and stability of caffeine demethylases found in *Pseudomonas putida* IF-3. *Biochemical Engineering Journal* **31**(1): 8-13.
- Benson, D. A., Karsch-Mizrachi, I., Lipman, D. J., Ostell, J., & Wheeler, D. L. (2008). GenBank. *Nucleic Acids Research* **36**: D25-D30.
- Berry, N. E., & Walters, R. H. (1943). Process of decaffeinating coffee. United States Patent US2309092.
- Berthou, F., Flinois, J. P., Ratanasavanh, D., Beaune, P., Riche, C., & Guillouzo, A. (1991). Evidence for the involvement of several cytochromes P-450 in the first steps of caffeine metabolism by human liver microsomes. *Drug Metabolism and Disposition* **19**(3): 561-567.
- Berthou, F., Guillois, B., Riche, C., Dreano, Y., Jacqz-Aigrain, E., Beaune, P. H. (1992). Interspecies variations in caffeine metabolism related to cytochrome P4501A enzymes. *Xenobiotica* **22**(6): 671-680.
- Bhat, V. B., & Madyastha, K. M. (2001). Antioxidant and radical scavenging properties of 8-oxo derivatives of xanthine drugs pentoxifylline and lisofylline. *Biochemical and Biophysical Research Communications* **288**: 1212-1217.
- Blattner, F. R., Plunkett, G., Bloch, C. A., Perna, N. T., Burland, V., Riley, M., Collado-Vides, J., Glasner, J. D., Rode, C. K., & Mayhew, G. F. (1997). The complete genome sequence of *Escherichia coli* K-12. *Science* **277**(5331): 1453-1462.
- Blecher, R., & Lingens, F. (1977). The metabolism of caffeine by a *Pseudomonas putida* strain. *Hoppe-Seyler's Zeitschrift für Physiologische Chemie* **358**: 807-817.
- Bradford, M. M. (1976). A rapid and sensitive method for the quantitation of microgram quantities of protein utilizing the principle of protein-dye binding. *Analytical Biochemistry* **72**: 248-254.
- Brand, D., Pandey, A., Roussos, S., & Soccol, C. R. (2000). Biological detoxification of coffee husk by filamentous fungi using a solid state fermentation system. *Enzyme and Microbial Technology* **27**(1-2): 127-133.
- Bryksin, A., & Matsumura, I. (2010). Overlap extension PCR cloning: A simple and reliable way to create recombinant plasmids. *BioTechniques* **48**: 463-465.

- Buchanan, J. M., Sonne, J. C., & Delluva, A. M. (1948). Biological precursors of uric acid. *Journal of Biological Chemistry* **173**(1): 81-98.
- Buerge, I. J., Poiger, T., Muller, M. D., & Buser, H. R. (2003). Caffeine, an anthropogenic marker for wastewater contamination of surface waters. *Environmental Science & Technology* **37**(4): 691-700.
- Burnette, W. N. (1981). "Western blotting": Electrophoretic transfer of proteins from sodium dodecyl sulfate-polyacrylamide gels to unmodified nitrocellulose and radiographic detection with antibody and radioiodinated protein A. *Analytical Biochemistry* **112**(2): 195-203.
- Butler, M. A., Iwasaki, M., Guengerich, F. P., & Kadlubar, F. F. (1989). Human cytochrome P-450_{PA} (P-450IA2), the phenacetin *O*-deethylase, is primarily responsible for the hepatic 3-demethylation of caffeine and N-oxidation of carcinogenic arylamines. *PNAS USA* **86**: 7696-7700.
- Campbell, M. E., Grant, D. M., Inaba, T., & Kalow, W. (1987). Biotransformation of caffeine, paraxanthine, theophylline, and theobromine by polycyclic aromatic hydrocarbon-inducible cytochrome (s) P-450 in human liver microsomes. *Drug Metabolism and Disposition* **15**(2): 237-249.
- Capela, D., Barloy-Hubler, F., Gouzy, J., Bothe, G., Ampe, F., Batut, J., Boistard, P., Becker, A., Boutry, M., & Cadieu, E. (2001). Analysis of the chromosome sequence of the legume symbiont *Sinorhizobium meliloti* strain 1021. *PNAS USA* **98**(17): 9877-9882.
- Capyk, J. K., D'Angelo, I., Strynadka, N. C., & Eltis, L. D. (2009). Characterization of 3-ketosteroid 9 α -hydroxylase, a Rieske oxygenase in the cholesterol degradation pathway of *Mycobacterium tuberculosis*. *Journal of Biological Chemistry* **284**(15): 9937-9946.
- Carrillo, J. A., & Benitez, J. (2000). Clinically significant pharmacokinetic interactions between dietary caffeine and medications. *Clinical Pharmacokinetics* **39**(2): 127-153.
- Caubet, M. S., Comte, B., & Brazier, J. L. (2004). Determination of urinary ¹³C-caffeine metabolites by liquid chromatography-mass spectrometry: The use of metabolic ratios to assess CYP1A2 activity. *Journal of Pharmaceutical and Biomedical Analysis* **34**(2): 379-389.
- Cha, C. J., Doerge, D. R., & Cerniglia, C. E. (2001). Biotransformation of malachite green by the fungus *Cunninghamella elegans*. *Applied Environmental Microbiology* **67**(9): 4358-4360.
- Chang, B., Chen, Y., Zhao, Y., & Bruick, R. K. (2007). JMJD6 is a histone arginine demethylase. *Science* **318**(5849): 444-447.

Chenna, R., Sugawara, H., Koike, T., Lopez, R., Gibson, T. J., Higgins, D. G., & Thompson, J. D. (2003). Multiple sequence alignment with the clustal series of programs. *Nucleic Acids Research* **31**(13): 3497-3500.

Coulter T. P. (2009). Food: the chemistry of its components. The Royal Society of Chemistry, Cambridge, UK.

Daly, J. W., Butts-Lamb, P., & Padgett, W. (1983). Subclasses of adenosine receptors in the central nervous system: Interaction with caffeine and related methylxanthines. *Cellular and Molecular Neurobiology* **3**(1): 69-80.

Daly, J. W. (2007). Caffeine analogs: Biomedical impact. *Cellular and Molecular Life Sciences* **64**(16): 2153-2169.

Dash, S. S., & Gummadi, S. N. (2006). Catabolic pathways and biotechnological applications of microbial caffeine degradation. *Biotechnology Letters* **28**: 1993-2002.

Dash, S. S., & Gummadi, S. N. (2007). Degradation kinetics of caffeine and related methylxanthines by induced cells of *Pseudomonas* sp. *Current Microbiology* **55**: 56-60.

Dash, S. S., & Gummadi, S. N. (2008). Inducible nature of the enzymes involved in catabolism of caffeine and related methylxanthines. *Journal of Basic Microbiology* **48**: 227-233.

de la Riva, L., Badia, J., Aguilar, J., Bender, R. A., & Baldoma, L. (2008). The *hpx* genetic system for hypoxanthine assimilation as a nitrogen source in *Klebsiella pneumoniae*: Gene organization and transcriptional regulation. *Journal of Bacteriology* **190**(24): 7892-7903.

Desai, S. K., & Gallivan, J. P. (2004). Genetic screens and selections for small molecules based on a synthetic riboswitch that activates protein translation. *Journal of the American Chemical Society* **126**: 13247-13254.

Dikstein, S., Bergmann, F., & Henis, Y. (1957). Studies on uric acid and related compounds: IV. The specificity of bacterial xanthine oxidases. *Journal of Biological Chemistry* **224**(1): 67-77.

Dong, X., Fushinobu, S., Fukuda, E., Terada, T., Nakamura, S., Shimizu, K., Nojiri, H., Omori, T., Shoun, H., & Wakagi, T. (2005). Crystal structure of the terminal oxygenase component of cumene dioxygenase from *Pseudomonas fluorescens* IP01. *Journal of Bacteriology* **187**(7): 2483-2490.

Edman, P. (1950). Method for determination of the amino acid sequence in peptides. *Acta Chemica Scandinavica* **4**: 283-293.

Ensley, B. D., & Gibson, D. T. (1983). Naphthalene dioxygenase: Purification and properties of a terminal oxygenase component. *Journal of Bacteriology* **155**(2): 505-511.

Essayan, D. M. (2001). Cyclic nucleotide phosphodiesterases. *Journal of Allergy and Clinical Immunology* **108**: 671-680.

Eugster, H. P., Probst, M., Würigler, F. E., & Sengstag, C. (1993). Caffeine, estradiol, and progesterone interact with human CYP1A1 and CYP1A2: Evidence from cDNA-directed expression in *Saccharomyces cerevisiae*. *Drug Metabolism and Disposition* **21**(1): 43-49.

Fee, J. A., Findling, K. L., Yoshida, T., Hille, R., Tarr, G. E., Hearshen, D. O., Dunham, W. R., Day, E. P., Kent, T. A., & Münck, E. (1984). Purification and characterization of the Rieske iron-sulfur protein from *Thermus thermophilus*. Evidence for a [2Fe-2S] cluster having non-cysteine ligands. *Journal of Biological Chemistry* **259**(1): 124-133.

Feldman, J. R., & Katz, S. M. (1976). Caffeine. In *Encyclopedia of Chemical Processing and Design: Blowers to Calcination*. Edited by J. J. McKetta. Marcel Dekker, New York, NY, p. 424-440.

Ferraro, D. J., Gakhar, L., & Ramaswamy, S. (2005). Rieske business: Structure-function of Rieske non-heme oxygenases. *Biochemical and Biophysical Research Communications* **338**(1): 175-190.

Friemann, R., Ivkovic-Jensen, M. M., Lessner, D. J., Yu, C. L., Gibson, D. T., Parales, R. E., Eklund, H., & Ramaswamy, S. (2005). Structural insight into the dioxygenation of nitroarene compounds: The crystal structure of nitrobenzene dioxygenase. *Journal of Molecular Biology* **348**(5): 1139-1151.

Fujimori, N., Suzuki, T., & Ashihara, H. (1991). Seasonal variations in biosynthetic capacity for the synthesis of caffeine in tea leaves. *Phytochemistry* **30**(7): 2245-2248.

Gibson, D. T., & Parales, R. E. (2000). Aromatic hydrocarbon dioxygenases in environmental biotechnology. *Current Opinion in Biotechnology* **11**: 236-243.

Glück, M., & Lings, F. (1988). Heteroxanthinedemethylase, a new enzyme in the degradation of caffeine by *Pseudomonas putida*. *Applied Microbiology and Biotechnology* **28**: 59-62.

Gokulakrishnan, S., Chandraraj, K., & Gummadi, S. N. (2005). Microbial and enzymatic methods for the removal of caffeine. *Enzyme and Microbial Technology* **37**: 225-232.

Gopishetty, S. R., Louie, T. M., Yu, C. L., & Subramanian, M. V. (2011). Microbial degradation of caffeine, methylxanthines, and its biotechnological applications. Narosa Publishing House, *In Press*.

- Grant, D. M., Tang, B. K., & Kalow, W. (1983). Variability in caffeine metabolism. *Clinical Pharmacology & Therapeutics* **33**(5): 591-602.
- Grant, D. M., Campbell, M. E., Tang, B. K., & Kalow, W. (1987). Biotransformation of caffeine by microsomes from human liver: Kinetics and inhibition studies. *Biochemical Pharmacology* **36**(8): 1251-1260.
- Guengerich, F. P. (2001). Common and uncommon cytochrome P450 reactions related to metabolism and chemical toxicity. *Chemical Research in Toxicology* **14**(6): 611-650.
- Guo, W., Wang, Y., Song, C., Yang, C., Li, Q., Li, B., Su, W., Sun, X., Song, D., & Yang, X. (2011). Complete genome of medium-chain-length polyhydroxyalkanoates and alginate oligosaccharides synthesis strain *Pseudomonas mendocina* NK-01. *Journal of Bacteriology*, JB.05068-11v1.
- Haigler, B. E., & Gibson, D. T. (1990a). Purification and properties of NADH-ferredoxinNAP reductase, a component of naphthalene dioxygenase from *Pseudomonas* sp. strain NCIB 9816. *Journal of Bacteriology* **172**(1): 457-464.
- Haigler, B. E., & Gibson, D. T. (1990b). Purification and properties of ferredoxinNAP, a component of naphthalene dioxygenase from *Pseudomonas* sp. strain NCIB 9816. *Journal of Bacteriology* **172**(1): 465-468.
- Hakil, M., Denis, S., Viniegra-Gonzalez, G., & Augur, C. (1998). Degradation and product analysis of caffeine and related dimethylxanthines by filamentous fungi. *Enzyme and Microbial Technology* **22**: 355-359.
- Heckman, M. A., Weil, J., & De Mejia, E. G. (2010). Caffeine (1, 3, 7-trimethylxanthine) in foods: A comprehensive review on consumption, functionality, safety, and regulatory matters. *Journal of Food Science* **75**(3): R77-R87.
- Henderson, J. F., & Paterson, A. R. P. (1973). Nucleotide metabolism: An introduction. Academic Press, New York, NY.
- Hille, R., & Nishino, T. (1995). Flavoprotein structure and mechanism 4. Xanthine oxidase and xanthine dehydrogenase. *The FASEB Journal* **9**: 995-1003.
- Hohnloser, W., Osswald, B., & Lingens, F. (1980). Enzymological aspects of caffeine demethylation and formaldehyde oxidation by *Pseudomonas putida* C1. *Hoppe-Seyler's Zeitschrift für Physiologische Chemie* **361**: 1763-1766.
- Hollingsworth, R. G., Armstrong, J. W., & Campbell, E. (2002). Pest control: Caffeine as a repellent for slugs and snails. *Nature* **417**(6892): 915-916.

- Inoue, T., Matsuzaki, S., & Tanaka, S. (1995). Cloning and sequence analysis of *Vibrio parahaemolyticus ompK* gene encoding a 26-kDa outer membrane protein, OmpK, that serves as receptor for a broad-host-range vibriophage, KVP40. *FEMS Microbiology Letters* **134**(2-3), 245-249.
- Jones, S. B., Terry, C. M., Lister, T. E., & Johnson, D. C. (1999). Determination of submicromolar concentrations of formaldehyde by liquid chromatography. *Analytical Chemistry* **71**(8): 4030-4033.
- Juliano, L. M., & Griffiths, R. R. (2005). Caffeine. In *Substance Abuse: A Comprehensive Textbook*, 4th ed., Edited by J. H. Lowinson, P. Ruiz & R. B. Millman. Lippincott Williams & Wilkins, Philadelphia, PA.
- Kaneko, T., Sato, S., Kotani, H., Tanaka, A., Asamizu, E., Nakamura, Y., Miyajima, N., Hirosawa, M., Sugiura, M., & Sasamoto, S. (1996). Sequence analysis of the genome of the unicellular *Cyanobacterium synechocystis* sp. strain PCC6803. II. Sequence determination of the entire genome and assignment of potential protein-coding regions. *DNA Research* **3**(3): 109-136.
- Kauppi, B., Lee, K., Carredano, E., Parales, R. E., Gibson, D. T., Eklund, H., & Ramaswamy, S. (1998). Structure of an aromatic-ring-hydroxylating dioxygenase-naphthalene 1, 2-dioxygenase. *Structure* **6**(5): 571-586.
- Koide, Y., Nakane, S., & Imai, Y. (1996). Caffeine demethylase gene-containing DNA fragment and microbial process for producing 3-methyl-7-alkylxanthine. United States Patent US5550041.
- Kvalnes-Krick, K., & Jorns, M. S. (1986). Bacterial sarcosine oxidase: Comparison of two multisubunit enzymes containing both covalent and noncovalent flavin. *Biochemistry* **25**(20): 6061-6069.
- Ladenson, R. C., Crimmins, D. L., Landt, Y., & Ladenson, J. H. (2006). Isolation and characterization of a thermally stable recombinant anti-caffeine heavy-chain antibody fragment. *Analytical Chemistry* **78**(13): 4501-4508.
- Lee, K. (1995). *Biochemical studies on toluene and naphthalene dioxygenases*. Ph.D. Thesis, University of Iowa.
- Lee, C. (2000). Antioxidant ability of caffeine and its metabolites based on the study of oxygen radical absorbing capacity and inhibition of LDL peroxidation. *Clinica Chimica Acta* **295**: 141-154.
- Lelo, A., Miners, J. O., Robson, R. A., & Birkett, D. J. (1986). Quantitative assessment of caffeine partial clearances in man. *British Journal of Clinical Pharmacology* **22**: 183-186.

- Libragen (2011). Sveltam: Green Innovation for Organic Slimming Cosmetics. p. 6. <http://www.libragen.com/files/Leaflet-Sveltam.pdf>, Accessed 23/06/2011.
- Lumb, J. R., Sideropoulos, A. S., & Shankel, D. M. (1968). Inhibition of dark repair of ultraviolet damage in DNA by caffeine and 8-chlorocaffeine. Kinetics of inhibition. *Molecular and General Genetics* **102**: 108-111.
- Lunell, E., Svedmyr, N., Andersson, K. E., & Persson, C. (1982). Effects of enprofylline, a xanthine lacking adenosine receptor antagonism, in patients with chronic obstructive lung disease. *European Journal of Clinical Pharmacology* **22**(5): 395-402.
- Madyastha, K. M., & Sridhar, G. R. (1998). A novel pathway for the metabolism of caffeine by a mixed culture consortium. *Biochemical and Biophysical Research Communications* **249**: 178-181.
- Madyastha, K. M., & Sridhar, G. R. (1999). Highly efficient C-8 oxidation of substituted xanthines with substitution at the 1-, 3-, and 7-positions using biocatalysts. *Journal of the Chemical Society, Perkin Transactions 1* **1999**(6): 677-680.
- Madyastha, K. M., Sridhar, G. R., Vadiraja, B. B., & Madhavi, Y. S. (1999). Purification and partial characterization of caffeine oxidase- A novel enzyme from a mixed culture consortium. *Biochemical and Biophysical Research Communications* **263**: 460-464.
- Marchler-Bauer, A., Anderson, J. B., Cherukuri, P. F., DeWeese-Scott, C., Geer, L. Y., Gwadz, M., He, S., Hurwitz, D. I., Jackson, J. D., & Ke, Z. (2005). CDD: A conserved domain database for protein classification. *Nucleic Acids Research* **33**(Suppl 1): D192-D196.
- Martins, B. M., Svetlitchnaia, T., & Dobbek, H. (2005). 2-Oxoquinoline 8-monooxygenase oxygenase component: Active site modulation by Rieske-[2Fe-2S] center oxidation/reduction. *Structure* **13**(5): 817-824.
- Mazzafera, P. (2002). Degradation of caffeine by microorganisms and potential use of decaffeinated coffee husk and pulp in animal feeding. *Scientia Agricola* **59**(4): 815-821.
- Mazzafera, P. (2004). Catabolism of caffeine in plants and microorganisms. *Frontiers in Bioscience* **9**: 1348-1359.
- Mazzafera, P., Olsson, O., & Sandberg, G. (1996). Degradation of caffeine and related methylxanthines by *Serratia marcescens* isolated from soil under coffee cultivation. *Microbial Ecology* **31**: 199-207.
- McCusker, R. R., Goldberger, B. A., & Cone, E. J. (2006). Caffeine content of energy drinks, carbonated sodas, and other beverages. *Journal of Analytical Toxicology* **30**: 112-114.

- Meskys, R., Harris, R. J., Casaitė, V., Basran, J., & Scrutton, N. S. (2001). Organization of the genes involved in dimethylglycine and sarcosine degradation in *Arthrobacter* spp. *European Journal of Biochemistry* **268**(12): 3390-3398.
- Middlehoven, W. J., & Bakker, C. M. (1982). Degradation of caffeine by immobilized cells of *Pseudomonas putida* C3024. *European Journal of Applied Microbiology and Biotechnology* **15**:214-217.
- Middelhoven, W. J., & Lommen, A. (1984). Degradation of caffeine by *Pseudomonas putida* C3024; the effect of oxygen concentration. *Antonie Van Leeuwenhoek* **50**: 298-300.
- Mizuno, K., Kato, M., Irino, F., Yoneyama, N., Fujimura, T., & Ashihara, H. (2003). The first committed step reaction of caffeine biosynthesis: 7-methylxanthosine synthase is closely homologous to caffeine synthases in coffee (*Coffea arabica* L.). *FEBS Letters* **547**(1-3): 56-60.
- Mohapatra, B. R., Harris, N., Nordin, R., & Mazumder, A. (2006). Purification and characterization of a novel caffeine oxidase from *Alcaligenes* species. *Journal of Biotechnology* **125**: 319-327.
- Nakatsu, C. H., Straus, N. A., & Wyndham, R. C. (1995). The nucleotide sequence of the Tn5271 3-chlorobenzoate 3, 4-dioxygenase genes (cbaAB) unites the class IA oxygenases in a single lineage. *Microbiology* **141**(2): 485-495.
- Nam, J., Nojiri, H., Noguchi, H., Uchimura, H., Yoshida, T., Habe, H., Yamane, H., & Omori, T. (2002). Purification and characterization of carbazole 1,9a-dioxygenase, a three-component dioxygenase system of *Pseudomonas resinovorans* strain CA10. *Applied and Environmental Microbiology* **68**(12): 5882-5890.
- Nathanson, J. A. (1984). Caffeine and related methylxanthines: Possible naturally occurring pesticides. *Science* **226**(4671): 184-187.
- Negishi, O., Ozawa, T., & Imagawa, H. (1985). Methylation of xanthosine by tea-leaf extracts and caffeine biosynthesis. *Agricultural and Biological Chemistry* **49**: 887-890.
- Negishi, O., Ozawa, T., & Imagawa, H. (1988). N-methyl nucleosidase from tea leaves. *Agricultural and Biological Chemistry* **52**(1): 169-175.
- Nishiya, Y., & Imanaka, T. (1993). Cloning and sequencing of the sarcosine oxidase gene from *Arthrobacter* sp. TE1826. *Journal of Fermentation and Bioengineering* **75**(4): 239-244.
- Ogunseitan, O. A. (1996). Removal of caffeine in sewage by *Pseudomonas putida*: Implications for water pollution index. *World Journal of Microbiology and Biotechnology* **12**: 251-256.

- Ogunseitan, O. A. (2002). Caffeine-inducible enzyme activity in *Pseudomonas putida* ATCC 700097. *World Journal of Microbiology and Biotechnology* **18**: 423-428.
- Petermann, J. B., & Baumann, T. W. (1983). Metabolic relations between methylxanthines and methyluric acids in *Coffea* L. *Plant Physiology* **73**: 961-964.
- Phillips, D. A., Sande, E. S., Vriezen, J., de Bruijn, F. J., Le Rudulier, D., & Joseph, C. M. (1998). A new genetic locus in *Sinorhizobium meliloti* is involved in stachydrine utilization. *Applied and Environmental Microbiology* **64**(10): 3954-3960.
- Porter-Jordan, K., Rosenberg, E. I., Keiser, J. F., Gross, J. D., Ross, A. M., Nasim, S., & Garrett, C. (1990). Nested polymerase chain reaction assay for the detection of cytomegalovirus overcomes false positives caused by contamination with fragmented DNA. *Journal of Medical Virology* **30**: 85-91.
- Proiser, E., & Serenkov, G. P. (1963). Caffeine biosynthesis in tea leaves. *Biokhimiya* **28**: 857-861.
- Rees, D. C., & Howard, J. B. (2003). The interface between the biological and inorganic worlds: iron-sulfur metalloclusters. *Science* **300**(5621): 929-931.
- Reissig, C. J., Strain, E. C., & Griffiths, R. R. (2009). Caffeinated energy drinks- A growing problem. *Drug and Alcohol Dependence* **99**: 1-10.
- Rizvi, S. J. H., Mukerji, D., & Mathur, S. N. (1981). Selective phyto-toxicity of 1, 3, 7-trimethylxanthine between *Phaseolus mungo* and some weeds. *Agricultural and Biological Chemistry* **45**(5): 1255-1256.
- Roberts, M. F., & Wallert, G. R. (1979). *N*-methyltransferases and 7-methyl-*N*⁹-nucleoside hydrolase activity in *Coffea arabica* and the biosynthesis of caffeine. *Phytochemistry* **18**(3): 451-455.
- Rosche, B., Tshisuaka, B., Fetzner, S., & Lingens, F. (1995). 2-oxo-1, 2-dihydroquinoline 8-monooxygenase, a two-component enzyme system from *Pseudomonas putida* 86. *Journal of Biological Chemistry* **270**(30): 17836-17842.
- Sadaie, Y., Yata, K., Fujita, M., Sagai, H., Itaya, M., Kasahara, Y., & Ogasawara, N. (1997). Nucleotide sequence and analysis of the *phoB-rnE-groESL* region of the *Bacillus subtilis* chromosome. *Microbiology* **143**(6): 1861-1866.
- Sambrook J., Fritsch E. F., & Maniatis T. (1989). Molecular cloning : a laboratory manual, 2nd ed. Cold Springs Harbor Laboratory, Cold Spring Harbor, N.Y.
- Sankar, J., Lodha, R., & Kabra, S. K. (2008). Doxofylline: The next generation methylxanthine. *Indian Journal of Pediatrics* **75**(3): 251-254.

- Sauer, M., Kappeli, O., & Fiechter, A. (1982). Comparison of the cytochrome P450-containing monooxygenases originating from two different yeasts. In *Cytochrome P-450, Biochemistry, Biophysics, and Environmental Implications* pp. 453-457. Edited by E. Hietanen, M. Laitinen & O. Hanninen. Amsterdam.
- Schwabe, U., Ukena, D., & Lohse, M. J. (1985). Xanthine derivatives as antagonists at A₁ and A₂ adenosine receptors. *Naunyn-Schmiedeberg's Archives of Pharmacology* **330**: 212-221.
- Schwimmer, S., & Kurtzman, R. H. (1971). Caffeine metabolism by *Penicillium roqueforti*. *Archives of Biochemistry and Biophysics* **147**(1): 109-113.
- Seiler, R. L., Zaugg, S. D., Thomas, J. M., & Howcroft, D. L. (1999). Caffeine and pharmaceuticals as indicators of waste water contamination in wells. *Ground Water* **37**(3): 405-410.
- Shamim, M. T., Ukena, D., Padgett, W. L., & Daly, J. W. (1989). Effects of 8-phenyl and 8-cycloalkyl substituents on the activity of mono-, di, and trisubstituted alkylxanthines with substitution at the 1-, 3-, and 7-positions. *Journal of Medicinal Chemistry* **32**(6): 1231-1237.
- Shemin, D., & Rittenberg, D. (1947). On the utilization of glycine for uric acid synthesis in man. *Journal of Biological Chemistry* **167**(3): 875-876.
- Shi, Y., Lan, F., Matson, C., Mulligan, P., Whetstine, J. R., Cole, P. A., Casero, R. A., & Shi, Y. (2004). Histone demethylation mediated by the nuclear amine oxidase homolog LSD1. *Cell* **119**(7): 941-953.
- Sideso, O. F. P., Marvier, A. C., Katerelos, N. A., & Goodenough, P. W. (2001). The characteristics and stabilization of a caffeine demethylase enzyme complex. *International Journal of Food Science and Technology* **36**: 693-698.
- Smyth, D. A. (1992). Effect of methylxanthine treatment on rice seedling growth. *Journal of Plant Growth Regulation* **11**(2): 125-128.
- Sonoki, T., Obi, T., Kubota, S., Higashi, M., Masai, E., & Katayama, Y. (2000). Coexistence of two different *O*-demethylation systems in lignin metabolism by *Sphingomonas paucimobilis* SYK-6: cloning and sequencing of the lignin biphenyl-specific *O*-demethylase (LigX) gene. *Applied and Environmental Microbiology* **66**(5):2125-2132.
- Stavric, B. (1988a). Methylxanthines: Toxicity to humans. 1. Theophylline. *Food and Chemical Toxicology* **26**(6): 541-565.
- Stavric, B. (1988b). Methylxanthines: Toxicity to humans. 2. Caffeine. *Food and Chemical Toxicology* **26**(7): 645-662.

- Stavric, B. (1988c). Methylxanthines: Toxicity to humans. 3. Theobromine, paraxanthine and the combined effects of methylxanthines. *Food and Chemical Toxicology* **26**(8): 725-733.
- Strappaghetti, G., Corsano, S., Barbaro, R., Giannaccini, G., & Betti, L. (2001). Structure-activity relationships in a series of 8-substituted xanthines as A₁-adenosine receptor antagonists. *Bioorganic & Medicinal Chemistry* **9**(3): 575-583.
- Stryer L. (1995). *Biochemistry*, 4th ed. WH Freeman and Co., New York, NY.
- Subramanian, V., Liu, T. N., Yeh, W., & Gibson, D. (1979). Toluene dioxygenase: Purification of an iron-sulfur protein by affinity chromatography. *Biochemical and Biophysical Research Communications* **91**(3): 1131-1139.
- Summers, R. M., Louie, T. M., Yu, C. L., & Subramanian, M. (2011). Characterization of a broad-specificity non-haem iron *N*-demethylase from *Pseudomonas putida* CBB5 capable of utilizing several purine alkaloids as sole carbon and nitrogen source. *Microbiology* **157**(2): 583-592.
- Suzuki, T., & Waller, G. R. (1984). Biosynthesis and biodegradation of caffeine, theobromine, and theophylline in *Coffea arabica* L. fruits. *Journal of Agricultural and Food Chemistry* **32**: 845-848.
- Suzuki, T., & Waller, G. R. (1987). Allelopathy due to purine alkaloids in tea seeds during germination. *Plant and Soil* **98**: 131-136.
- Suzuki, T., & Takahashi, E. (1975). Biosynthesis of caffeine by tea-leaf extracts. Enzymic formation of theobromine from 7-methylxanthine and of caffeine from theobromine. *Biochemical Journal* **146**(1): 87-96.
- Tamura, K., Dudley, J., Nei, M., & Kumar, S. (2007). MEGA4: Molecular evolutionary genetics analysis (MEGA) software version 4.0. *Molecular Biology and Evolution* **24**(8): 1596-1599.
- Tanaka, A., Ito, H., Tanaka, R., Tanaka, N. K., Yoshida, K., & Okada, K. (1998). Chlorophyll *a* oxygenase (CAO) is involved in chlorophyll *b* formation from chlorophyll *a*. *PNAS USA* **95**(21): 12719-12723.
- Tang, B. K., Grant, D. M., & Kalow, W. (1983). Isolation and identification of 5-acetylamino-6-formylamino-3-methyluracil as a major metabolite of caffeine in man. *Drug Metabolism and Disposition* **11**(3): 218-220.
- Tassaneeyakul, W., Birkett, D. J., McManus, M. E., Tassaneeyakul, W., Veronese, M. E., Andersson, T., Tukey, R. H., & Miners, J. O. (1994). Caffeine metabolism by human hepatic cytochromes P450: Contributions of 1A2, 2E1 and 3A isoforms. *Biochemical Pharmacology* **47**(10): 1767-1776.

- The UniProt Consortium. (2011). Ongoing and future developments at the universal protein resource. *Nucleic Acids Research* **39**(Suppl 1): D214-D219.
- Trier, K., Olsen, E. B., Kobayashi, T., Ribel-Madsen, S. M. (1999). Biochemical and ultrastructural changes in rabbit sclera after treatment with 7-methylxanthine, theobromine, acetazolamide, or L-ornithine. *British Journal of Ophthalmology* **83**(12): 1370-1375.
- Tsukada, Y., Fang, J., Erdjument-Bromage, H., Warren, M. E., Borchers, C. H., Tempst, P., & Zhang, Y. (2005). Histone demethylation by a family of JmjC domain-containing proteins. *Nature* **439**, 811-816.
- Udayasankar, K., Manohar, B., & Chokkalingam, A. (1986). A note on supercritical carbon dioxide decaffeination of coffee. *Journal of Food Science and Technology* **23**(6): 326-328.
- Ueda, T., Lode, E. T., & Coon, M. J. (1972). Enzymatic ω -oxidation. VI. isolation of homnogeneous reduced diphosphopyridine nucleotide-rubredoxin reductase. *Journal of Biological Chemistry* **247**(10): 2109-2116.
- Venturi, V., Zennaro, F., Degrassi, G., Okeke, B. C., & Bruschi, C. V. (1998). Genetics of ferulic acid bioconversion to protocatechuic acid in plant-growth-promoting *Pseudomonas putida* WCS358. *Microbiology* **144**(4): 965-973.
- Wagner, C. (1982). Cellular folate binding proteins; function and significance. *Annual Review of Nutrition* **2**: 229-248.
- Waller, G. R. (1989). Biochemical frontiers of allelopathy. *Biologia Plantarum* **31**(6): 418-447.
- Wang, X., Li B., Herman, P. L., & Weeks, D. P. (1997). A three-component enzyme system catalyzes the O demethylation of the herbicide dicamba in *Pseudomonas maltophilia* DI-6. *Applied and Environmental Microbiology* **63**(4): 1623-1626.
- Wang, Y., Chackalamannil, S., Hu, Z., Boyle, C. D., Lankin, C. M., Xia, Y., Xu, R., Asberom, T., Pissarnitski, D., & Stamford, A. W. (2002). Design and synthesis of xanthine analogues as potent and selective PDE5 inhibitors. *Bioorganic & Medicinal Chemistry Letters* **12**(21): 3149-3152.
- Wang, Y., Yang, X., Zheng, X., Li, J., Ye, C., & Song, X. (2010). Theacrine, a purine alkaloid with anti-inflammatory and analgesic activities. *Fitoterapia* **81**: 627-631.
- Ward, A., & Clissold, S. P. (1987). Pentoxifylline. A review of its pharmacodynamic and pharmacokinetic properties, and its therapeutic efficacy. *Drugs* **34**(1): 50-97.

- White, P. A., & Rasmussen, J. B. (1998). The genotoxic hazards of domestic wastes in surface waters. *Mutation Research* **410**: 223-236.
- Woolfolk, C. A. (1975). Metabolism of *N*-methylpurines by a *Pseudomonas putida* strain isolated by enrichment on caffeine as the sole source of carbon and nitrogen. *Journal of Bacteriology* **123**(3): 1088-1106.
- Woolfolk, C. A., & Downard, J. S. (1977). Distribution of xanthine oxidase and xanthine dehydrogenase specificity types among bacteria. *Journal of Bacteriology* **130**(3): 1175-1191.
- Woolfolk, C. A. (1985). Purification and properties of a novel ferricyanide-linked xanthine dehydrogenase from *Pseudomonas putida* 40. *Journal of Bacteriology* **163**(2):600-609.
- Yamaoka-Yano, D. M., & Mazzafera, P. (1999). Catabolism of caffeine and purification of a xanthine oxidase responsible for methyluric acids production in *Pseudomonas putida* L. *Revista de Microbiologia* **30**: 62-70.
- Yanisch-Perron, C., Vieira, J., & Messing, J. (1985). Improved M13 phage cloning vectors and host strains: Nucleotide sequences of the M13mpl8 and pUC19 vectors. *Gene* **33**(1): 103-119.
- Yu, C. L., Liu, W., Ferraro, D. J., Brown, E. N., Parales, J. V., Ramaswamy, S., Zylstra, G. J., Gibson, D. T., & Parales, R. E. (2007). Purification, characterization, and crystallization of the components of a biphenyl dioxygenase system from *Sphingobium yanoikuyae* B1. *Journal of Industrial Microbiology and Biotechnology* **34**(4): 311-324.
- Yu, C. L., Kale, Y., Gopishetty, S., Louie, T. M., & Subramanian, M. (2008). A novel caffeine dehydrogenase in *Pseudomonas* sp. strain CBB1 oxidizes caffeine to trimethyluric acid. *Journal of Bacteriology* **190**(2): 772-776.
- Yu, C. L., Louie, T. M., Summers, R., Kale, Y., Gopishetty, S., & Subramanian, M. (2009). Two distinct pathways for metabolism of theophylline and caffeine are coexpressed in *Pseudomonas putida* CBB5. *Journal of Bacteriology* **191**(14): 4624-4632.
- Zavialov, I. A., Dahanukar, V. H., Nguyen, H., Orr, C., & Andrews, D. R. (2004). New and practical method for synthesis of 1- and 1, 3-substituted xanthines. *Organic Letters* **6**(13): 2237-2240.